Université de Montréal

The Nuclear Pore Complex and its Transporters:

From Virus-Host Interactors to Subverting the Innate Antiviral Immunity

par

Bridget Gagné

Programmes de biologie moléculaire

Faculté de Médecine

Mémoire présenté à la Faculté de Médecine

en vue de l'obtention du grade de maîtrise en sciences (M.Sc.)

en biologie moléculaire

option générale

Mai, 2015

Résumé

Les virus ont besoin d'interagir avec des facteurs cellulaires pour se répliquer et se propager dans les cellules d'hôtes. Une étude de l'interactome des protéines du virus d'hépatite C (VHC) par Germain et al. (2014) a permis d'élucider de nouvelles interactions virus-hôte. L'étude a également démontré que la majorité des facteurs de l'hôte n'avaient pas d'effet sur la réplication du virus. Ces travaux suggèrent que la majorité des protéines ont un rôle dans d'autres processus cellulaires tel que la réponse innée antivirale et ciblées pas le virus dans des mécanismes d'évasion immune.

Pour tester cette hypothèse, 132 interactant virus-hôtes ont été sélectionnés et évalués par silençage génique dans un criblage d'ARNi sur la production interferon-beta (IFNB1). Nous avons ainsi observé que les réductions de l'expression de 53 interactants virus-hôte modulent la réponse antivirale innée. Une étude dans les termes de gène d'ontologie (GO) démontre un enrichissement de ces protéines au transport nucléocytoplasmique et au complexe du pore nucléaire. De plus, les gènes associés avec ces termes (CSE1L, KPNB1, RAN, TNPO1 et XPO1) ont été caractérisé comme des interactant de la protéine NS3/4A par Germain et al. (2014) et comme des régulateurs positives de la réponse innée antivirale. Comme le VHC se réplique dans le cytoplasme, nous proposons que ces interactions à des protéines associées avec le noyau confèrent un avantage de réplication et bénéficient au virus en interférant avec des processus cellulaire tel que la réponse innée.

Cette réponse innée antivirale requiert la translocation nucléaire des facteurs transcriptionnelles IRF3 et NF-κB p65 pour la production des IFNs de type I. Un essai de microscopie a été développé afin d'évaluer l'effet du silençage de 60 gènes exprimant des protéines associés au complexe du pore nucléaire et au transport nucléocytoplasmique sur la translocation d'IRF3 et NF-κB p65 par un criblage ARNi lors d'une cinétique d'infection virale.

En conclusion, l'étude démontre qu'il y a plusieurs protéines qui sont impliqués dans le transport de ces facteurs transcriptionnelles pendant une infection virale et peut affecter la production IFNB1 à différents niveaux de la réponse d'immunité antivirale. L'étude aussi suggère que l'effet de ces facteurs de transport sur la réponse innée est peut être un mécanisme d'évasion par des virus comme VHC.

Mots-clés: Virus d'hépatite C, VHC, interactants virus-hôte, immunité innée antivirale, complexe du pore nucléaire, transport nucléocytoplasmique, criblage ARNi, translocation nucléaire, IRF3, p65, microscopie, cinétique

Abstract

Viruses interact with cellular factors in order to successfully replicate and propagate in host cells. Germain et al. (2014) performed a proteomics analysis to elucidate viral-host interactors of hepatitis C virus (HCV). They found that the majority of host factors did not have an effect on viral replication, suggesting that these host proteins may be beneficial to the virus by affecting other cellular processes such as evading the innate antiviral immunity.

To test that hypothesis, 132 virus-host interactors were selected and silenced by RNAi for their effect on inteferon-beta (IFNB1) production as a readout of the innate antiviral response. 53 were found to modulate the response with enrichment in the gene ontology (GO) terms related to nucleocytoplasmic transport and the nuclear pore complex. An interesting point is that the genes associated with these terms (CSE1L, KPNB1, RAN, TNPO1, and XPO1) were previously elucidated as HCV NS3/4A interactors by Germain et al. (2014), as well as positive regulators of the innate antiviral response. Although it is surprising that a cytoplasmic-replicating virus like HCV would interact with proteins associated with the nucleus, we proposed that viruses interact with these proteins for their benefit to interfere with the innate immune response.

The innate antiviral response requires the nuclear translocation of IRF3 and NF-κB p65 for the production of type I interferons. As it is unclear which transporters or nucleoporins are involved, 60 genes associated with the nuclear pore complex and nucleocytoplasmic transport were studied for their effect on the nuclear translocation of IRF3 and NF-κB p65 via a microscopy-based RNAi screen during a 10-hour viral infection time course.

Overall, the study revealed that many of these proteins are involved in the trafficking of these transcription factors during a viral infection, and can affect the production of IFNB1 at different levels of the innate antiviral response. The study also suggests that the effect of these transport factors on the immune response may be an evasion mechanism for viruses such as HCV.

Keywords: Hepatitis C virus, HCV, virus-host interactors, innate antiviral immunity, nuclear pore complex, NPC, nucleocytoplasmic transport, RNAi screen, nuclear translocation, IRF3, p65, microscopy, time course, kinetic

Table of Contents

List of Tables

List of Figures

List of Abbreviations & Acronyms

CARD	Caspase-recruitment domain
CD81	Cluster of differentiation 81
cGAMP	cyclic-GMP-AMP
cGAS	cGAMP synthase
CLDN1	Claudin-1
CLR	C-type lectin receptor
cNLS	Classical NLS
CSE1L	Chromosome segregation 1-like
DNA	Deoxyribonucleic acid
dsRNA	Double-stranded RNA
EBV	Epstein-Barr virus
EMCV	Encephalomyocarditis virus
ER	Endoplasmic reticulum
FG	Phenylalanine-Glycine
fLuc	Firefly luciferase
GDP	Guanosine diphosphate
GTP	Guanosine triphosphate
HBV	Hepatitis B virus
HCV	Hepatitis C virus
HCMV	Human cytomegalovirus
HIV-1	Human immunodeficiency virus type 1
HPV	Human papillomavirus
HSV-1	Herpes simplex virus Type 1
IAV	Influenza A virus
IFN	Interferon
IKKε	IκB kinase-ε
IRES	Internal ribosome entry site
IRF3	Interferon regulatory factor 3

ISG	Interferon-stimulated gene
ISRE	IFN-stimulated response element
JAK1	Janus kinase 1
JFH-1	Japanese patient with fulminant hepatitis
Kapα	Karyopherin-α
Kapβ	Karyopherin-β
kDa	kiloDalton
KPNB1	Karyopherin (importin) beta 1
LD	Lipid droplet
MAVS	Mitochondrial antiviral signaling
MDa	MegaDalton
MDA5	Melanoma differentiation-associated gene 5
mRNA	messenger RNA
NES	Nuclear export signal
NLR	NOD-like receptor
NLS	Nuclear localization signal
NOD	Nucleotide oligomerization domain
NP	Nucleoprotein
NPC	Nuclear pore complex
NS	Non-structural
NTR	Non-translated region
NUTF2	Nuclear transport factor 2
Nup	Nucleoporin
NXF1	Nuclear RNA export factor 1
NXT1	Nuclear transport factor 2-like export factor 1
OCLN	Occludin
PAMP	Pathogen-associated molecular pattern
PI4K-IIIα	Phosphatidylinositol 4-kinase III α
PI4P	Phosphatidylinositol-4-phosphate
PIC	Pre-integration complex
POM121	Pore membrane protein of 121 kD

PPIase	Prolyl-peptidyl isomerase
PRD	Positive regulatory domain
PRR	Pattern-recognition receptor
PRRSV	Porcine reproductive and respiratory syndrome virus
PY	Proline-Tyrosine
RAN	RAN, member RAS oncogene family
RANGAP	Ran GTPase-activating protein
RCC1	Regulator of chromosome condensation 1
RIG-I	Retinoic acid-inducible gene 1
RLR	RIG-I-like receptor
RNA	Ribonucleic acid
RNAi	RNA interference
SARS-CoV	Severe acute respiratory syndrome coronavirus
SCID	Severe combined immunodeficiency
SeV	Sendai virus
SR-BI	Scavenger receptors class B type I
ssRNA	Single-stranded RNA
STAT	Signal transducer and activator of transcription
STING	Stimulator of IFN genes
TBK1	TANK-binding kinase 1
TLR	Toll-like receptor
TNPO1	Transportin 1
TPR	Translocated promoter region
TYK2	Tyrosine kinase 2
uPA	Urokinase-type plasminogen activator
VACV	Vaccinia virus
VLDL	Very low density lipoprotein
VSV	Vesicular stomatitis virus
VZV	Varicella-Zoster virus
XPO1	Exportin 1

This is dedicated to everyone who believed in me,

supported me, and pushed me to my limits,

so that I could achieve great things in life.

Acknowledgements

I would first like to thank Dr. Daniel Lamarre for giving me the opportunity to pursue my Master's degree in an amazing laboratory, filled with innovative research projects and inspiring colleagues. He paved the foundation for the solid understanding I now have of my field of study, and a greater appreciation for the world of academic research. Most importantly, his guidance, support and patience were key in completing my memoir, and I cannot thank him enough for the time he spent in making me a better scientist.

I would next like to thank Martin Baril, the research associate and colleague I admired most as he taught me everything I needed to know to do good research in a lab from day one. I will remember his patience and support as a mentor and his enthusiasm as a researcher. He has left a deep impression in my scientific career, as I pushed myself to work hard and produce good results in the hope that someday I will make him proud.

To Nicolas Tremblay, my partner-in-crime and caring friend, I will definitely miss the good times we had in the lab, as well as your personal and professional advice which helped me grow and become a better person during my journey as a Master's student. To Michael Meloche and Alex Park, my lab brothers who always know how to lighten up my day, and were always fun to work with in the lab. To Salwa Es-Saad, I will always remember your wisdom and kindness. To Bassim Mohammed, I am sure that you will cure HCV one day. To former lab members Laurent Chatel-Chaix and Marie-Anne Germain, also known as Team HCV, your focus, dedication, and commitment to doing good research is definitely not forgotten.

Last, but not least, I would not have gotten this far without the constant support of my family, friends and my special someone through early mornings, late nights and even weekends to further the knowledge of the scientific world by at least one step. I thank them all from the bottom of my heart.

This journey was an emotional rollercoaster for me, and I have learned more about myself and about science than I ever thought possible. Thank you all for this experience.

Chapter 1: Introduction

1.1 Hepatitis C Virus

1.1.1 Epidemiology

Hepatitis C virus (HCV) currently infects over 185 million individuals around the world [1]. The virus primarily infects hepatocytes, and only 20-30% of those individuals are able to clear the virus during the acute infection [2]. Persistence of the virus causes infected individuals to enter the chronic phase where their condition can lead to several different outcomes of liver disease such as cirrhosis and even hepatocellular carcinoma [2]. Therapies to counteract the virus have become more efficient in recent years, but there is still no cure for HCV globally due to treatment costs and the multiple genotypes of the virus that exist around the world (Figure 1.1) [1].

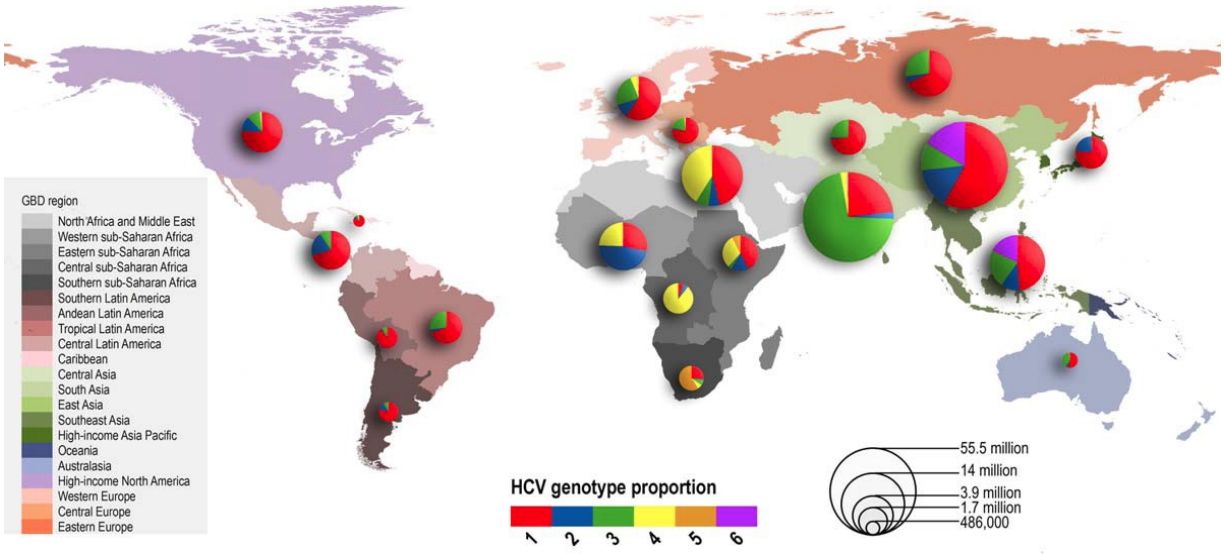

Figure 1.1: HCV Genotype Prevalence by WHO GBD Region

This figure visually represents the amount of individuals affected by HCV per Global Burden of Disease (GBD) region, as well as which genotypes are most common in each area. Overall, genotype 1 is found in all regions, while the occurrence of the other genotypes varies. (Figure from Messina JP, et al., *Hepatology*, 2015) [1]

1.1.2 Virology

1.1.2.1 Genome

HCV, a member of the *Flaviviridae* family, is a positive-sense RNA virus, in which its single-stranded genome can be directly translated into a single polyprotein via the internal ribosome entry site (IRES) located on the 5' end of the virus coding sequence. This polyprotein is composed of 10 viral proteins, where the first cleavage by cellular proteases liberates core, E1, E2 and p7 proteins (Figure 1.2). The viral protein NS2 autocleaves itself from NS3, thus allowing the protease function of NS3 to then cleave the rest of the non-structural (NS) proteins: NS4A, NS4B, NS5A, and NS5B [2-4].

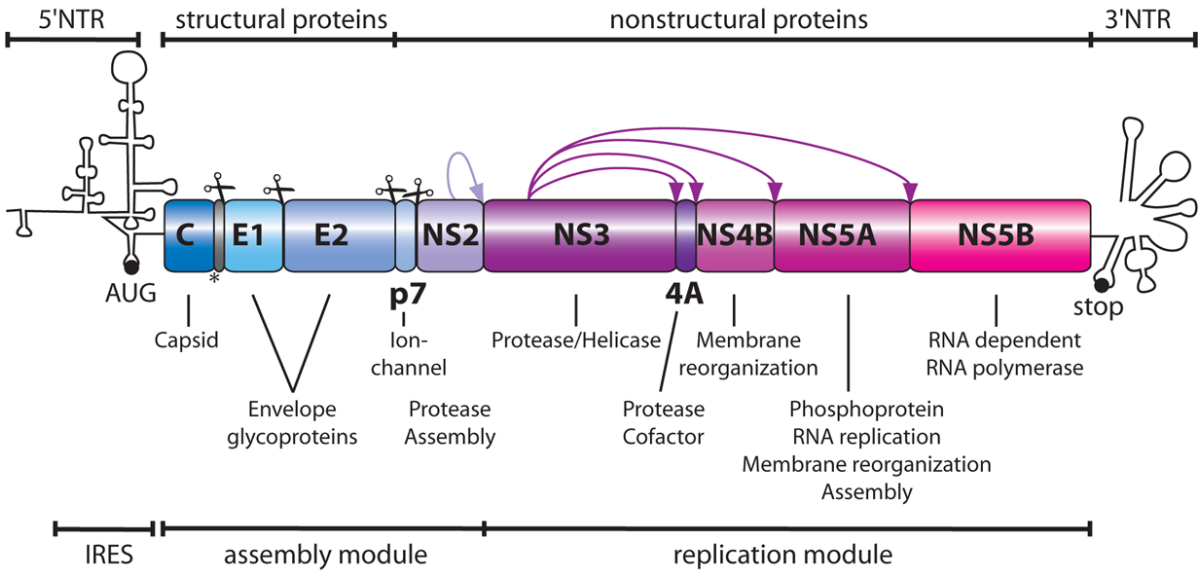

Figure 1.2: HCV Genome

This figure shows the HCV genome, as well as which regions encode which proteins. Scissors depict cleavage by cellular proteases, while the purple arrows depict cleavage by the viral proteins. The role of each viral protein in the HCV life cycle is also indicated. (Reprinted with permission from Lohmann V, et al., *J Med Chem*., 2014. Copyright 2014 American Chemical Society.) [4].

1.1.2.2 Life Cycle

1.1.2.2.1 Viral Entry and Viral RNA Release

Upon viral infection, HCV interacts with SR-BI, CD81, CLDN1 and OCLN on the surface of host cells via the envelope protein E2 and, through a pH-dependent mechanism, the virus is incorporated into the cell via clathrin-mediated endocytosis. Once the virus has entered the cell, its envelope fuses with an acidic endosomal compartment, releasing the viral RNA into the cytoplasm. (Figure 1.3) [3, 5].

1.1.2.2.2 HCV RNA Translation and Polyprotein Processing

The translation of HCV RNA is controlled by the IRES structure at the 5' non-translated region (NTR) of the genome, recruiting the factors necessary for cap-independent translation. The viral RNA is translated into a single polyprotein, which is then cleaved into 10 viral proteins by cellular and viral proteases. The mature proteins associate with ER membranes, as well as the region formed by NS4B called the membranous web, a compartment dedicated to HCV replication [3-5].

1.1.2.2.3 Viral Replication

HCV replication occurs within the membranous web, where the RNA polymerase NS5B will create negative RNA strands from the original positive RNA strand. The negative RNA strands will serve as template to further synthesize more positive-strand HCV RNA, which can then be translated into additional viral proteins or be packaged into newly-formed virions [3, 5].

1.1.2.2.4 Virion Assembly and Egress

Virion assembly is initiated via the interaction between the core protein and HCV RNA. The core protein induces lipid droplet (LD) formation and associates with these structures, which serve as the platform for virus assembly [3, 5]. NS5A binds to the 3' NTR of HCV RNA and transports it from the membranous web to the lipid droplets, where NS5A also plays a role in infectious particle formation [6, 7]. NS2 is also thought to play a role in viral assembly by interacting with multiple HCV proteins, such as E2, p7, NS3 and NS5A, to properly orchestrate their roles in the vicinity of LDs [8, 9]. The newly-assembled virions, composed of HCV RNA, core, E1, and E2, bud from the cells using a mechanism similar to the VLDL secretion machinery. However, it is thought that while the viral particles go through this secretory pathway, p7 protects them by neutralizing acidic compartments in the cell for successful virion release [3, 5, 10].

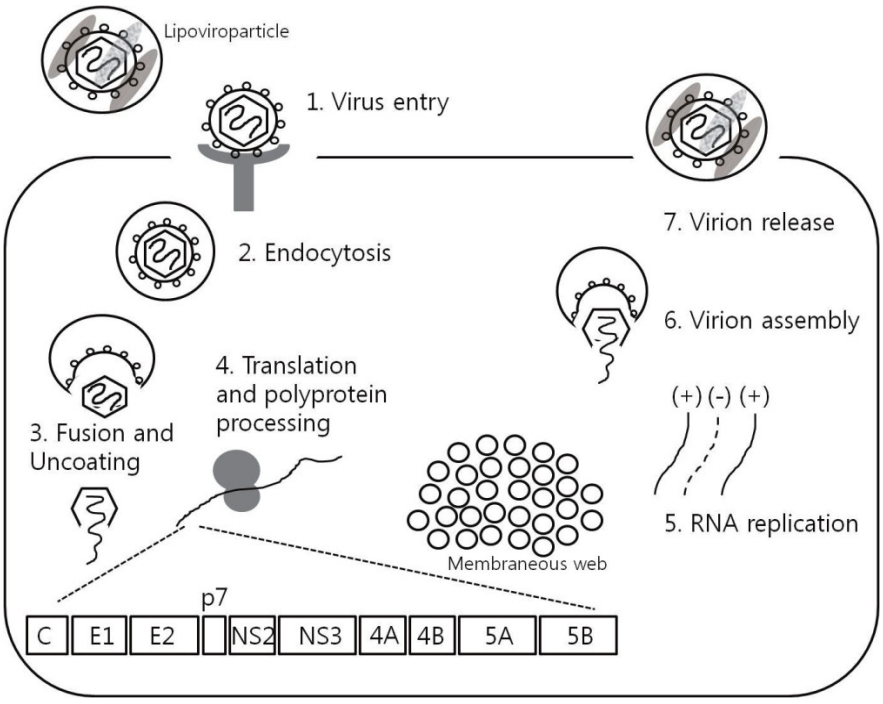

Figure 1.3: HCV Life Cycle

This figure outlines the major steps of the HCV life cycle from viral entry to viral particle budding from the cell. (Figure from Kim CW, et al., *Clin. Mol. Hepatol.,* 2013) [3].

1.1.3 Models for the Study of HCV

1.1.3.1 Replicon System

The replicon system encodes the viral proteins NS3 to NS5B of the HCV genome for the study of HCV replication. The translation of the replicon is mediated by two IRES sequences on the 5' end of the replicon: the first IRES is from HCV which drives the expression of the neomycin selection marker that is resistant against the cytotoxic compound G418, while the second IRES is from Encephalomyocarditis virus (EMCV) which drives the expression of the five viral proteins necessary for viral replication. The replicon also includes the firefly luciferase (fLuc) gene, whose expression is driven by the HCV IRES, to measure HCV replication by quantifying the luminescence produced. Having a quantifiable readout makes the replicon the model of choice for high-throughput RNAi and chemical screens to identify potential replication co-factors/restriction factors and stimulators/inhibitors, respectively. The replicon system known as Con1b signifies the replicon which contains the HCV 1b genotype. There are variations to the replicon system such as a monocistronic system, and an additional GFP within the NS3 to NS5B region to visually identify cells containing replication complexes in immunofluorescence microscopy. However, the replicon does not represent a complete viral infection [4].

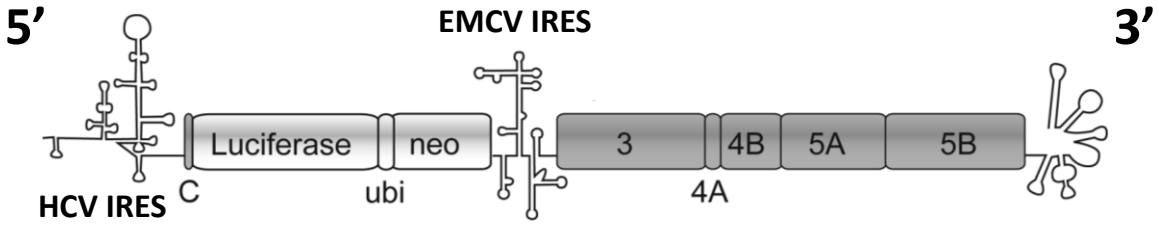

Figure 1.4: Replicon System for the Study of HCV

This figure shows an example of a bicistronic replicon with two viral IRES: the first from HCV encoding the firefly luciferase promoter and selection marker, and the second from EMCV encoding NS3 to NS5B, the non-structural proteins of HCV important for viral replication. (Adapted with permission from Lohmann V, et al., *J Med Chem*., 2014. Copyright 2014 American Chemical Society.) [4].

1.1.3.2 JFH-1 System

JFH-1 is a full-length virus that is able to replicate in cell lines, based on the HCV 2a genotype derived from a Japanese patient with fulminant hepatitis. To increase infectivity, multiple chimeras were created, one of which is JC1. JC1 is a chimeric HCV genome composed of J6 (encoding core to NS2 from another genotype 2a isolate), and JFH-1 (encoding NS3 to NS5B), which yields a viral titer 1000 times more efficient than the original JFH-1 genome [4]. Just like in the replicon, JC1 has also been modified to contain a luciferase gene, in this case renilla luciferase (RLuc), to measure the effects on the entire HCV genome, which can be used in high-throughput RNAi and chemical compound screens, as well as other constructs containing fluorescent proteins for visualization in microscopy [4].

There have been many mutations in the JFH-1 system in order to boost viral titers, but permissive cell lines such as Huh-7.5 can also increase viral replication due to a point mutation in RIG-I, a cytoplasmic RNA sensor, which disrupts the activation of IRF3 for the production of ISGs to induce an antiviral state in the cell [11, 12].

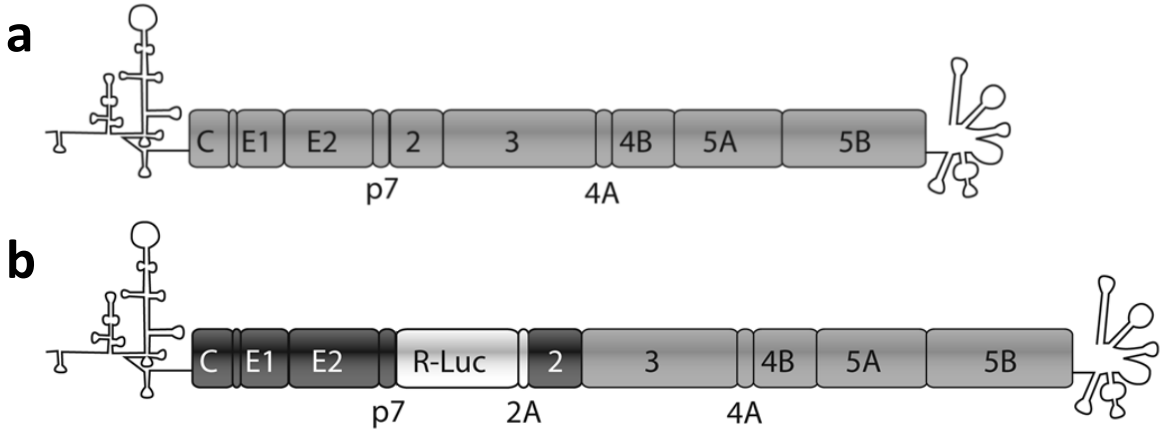

Figure 1.5: JFH-1 System for the Study of HCV

Figure 1.5.a shows the original JFH-1 genome. Figure 1.5.b shows one of the many chimeric versions of JC1 with the viral proteins from J6 and JFH-1 in dark grey and grey, respectively. The particular JC1 chimera shown in (b) is called J6/JFH-1/p7RLuc2a due to the inclusion of a RLuc promoter between viral proteins p7 and 2a. (Adapted with permission from Lohmann V, et al., *J Med Chem*., 2014. Copyright 2014 American Chemical Society.) [4].

1.1.3.3 Mouse Models

Mice have been used as a model to study HCV infection *in vivo*. The first method, viral adaptation, exposes the virus to mouse cells, which causes mutations in E1 and E2 in order to adapt to the murine version of entry factors CD81 and OCLN. This mouse-adapted virus was then tested on immortalized mouse liver cell lines, where the entire life cycle of the virus successfully occurs. However, these were in cell lines with an impaired innate antiviral immunity. Since this method involves the virus adapting to murine cell entry factors, studying viral entry in this model may be influenced by the mutations required to effectively enter mouse cells [13].

The second method uses mice transgenically-expressing HCV or human proteins in the liver. This type of study was used to understand the interactions between viral proteins and the effects on the host cell in an *in vivo* model. Expression of single viral proteins did not have an effect, but the expression of multiple proteins together caused hepatocellular carcinoma. The most well-known transgenic mice is the FL-N/35 mouse expressing the entire HCV polyprotein at close to physiological levels, where hepatic steatosis, increased liver fibrosis and increased risk of developing hepatocellular carcinoma was described. Another transgenic mice is the genetically-humanized mouse model, which involves the expression of human entry factors, such as CD81 and OCLN, delivered to the mouse via an adenoviral vector. The human wild-type virus is unable to replicate properly in murine liver cells unless the mouse is immune deficient, which then allows for a persistent infection. It is not yet known what kind of liver disease this mice develop due to this persistent infection [13].

The third method to study HCV in mice is the xenotransplantation model, which involves immunodeficient mice suffering from a liver injury. The immunodeficiency is required to prevent the rejection of the primary human hepatocyte transplantation, and the damaged liver is required for the human hepatocytes to have a growth advantage over the murine ones. This specific mouse model is the most used to study HCV, but this human-liver mouse chimera can only support the infection of HCV clones that are not based on JFH-1 [13]. Another mice model utilizing a human-liver chimera was the uPA-SCID mouse, which was homozygous for the uPA-transgene, the overexpression of which results in liver dysfunction. It was found that these mice were susceptible to HCV infection [14], whether it be based on

the JFH-1 system or from viruses derived from patients of all genotypes [15], allowing for the study of the entire HCV life cycle, as well as a model to test antiviral therapies. One method tries to overcome the immunodeficiency aspect of these mice models by engrafting human hepatocytes with human $CD34^+$ hematopoietic stem cells. However, even though one group was able to demonstrate a T-cell response to HCV infection, viral RNA could not be detected and the immune activity of $CD34^+$ hematopoietic stem cells is suboptimal, thus making it too early to say whether this model will allow for the study of the adaptive immune response to HCV infection [13].

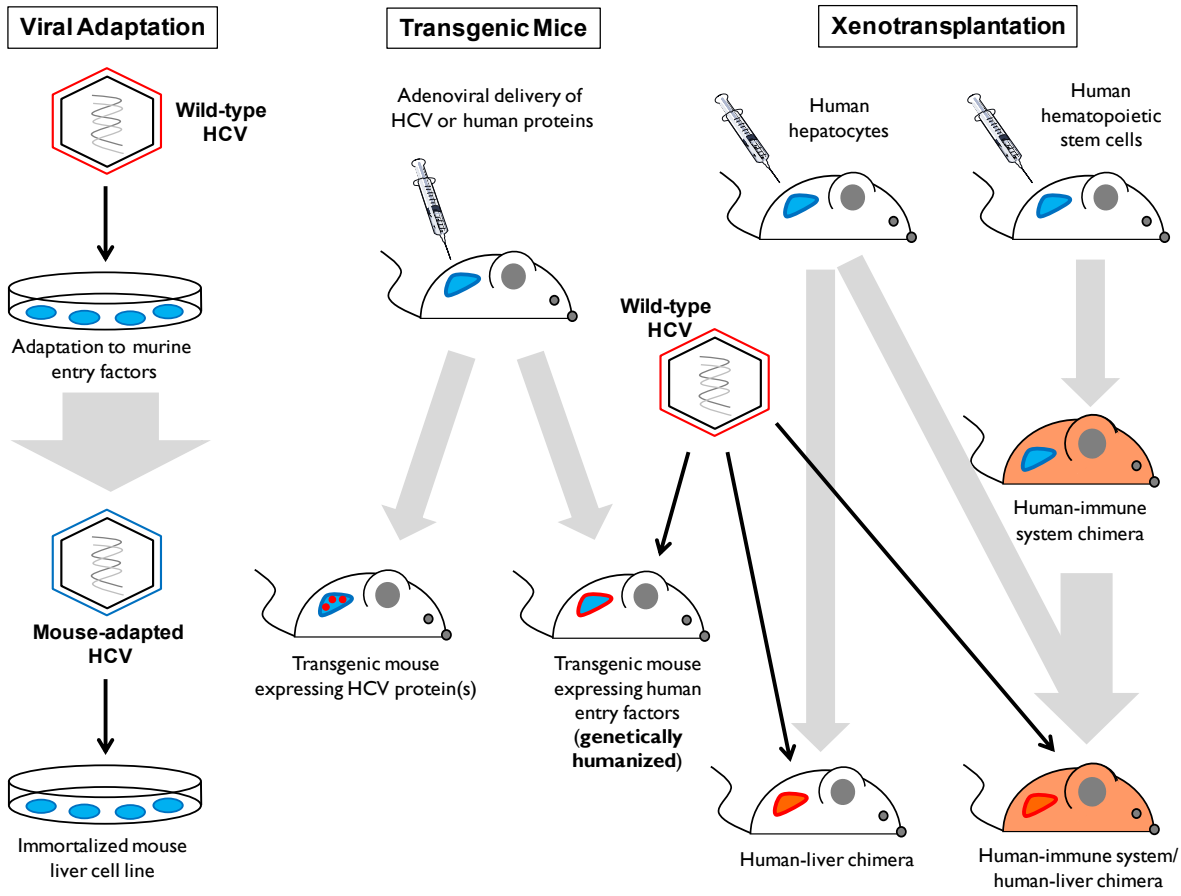

Figure 1.6: Mouse Models for the Study of HCV

This figure shows the three different mouse models: viral adaptation, transgenic mice and xenotransplantation. Viral adaptation involves the wild-type HCV to adapt to murine entry factors in order to successfully replicate in immortalize mouse cell lines. Transgenic mice involve the expression of HCV proteins. One method involves the transmission of human

entry factors, delivered by an adenovirus, to support wild-type HCV infection. The third model involves the transplantation of human hepatocytes in immunodeficient mice with a damaged liver to favour the growth of human hepatocytes in the mouse liver. Mouse models using human immune cells and the human-liver chimera are still not well-characterized for the study of HCV infection and the adaptive immunity [13]. Blue indicates murine cells or liver, while red and orange indicates human liver or human immune system.

1.1.4 HCV-Host Interactors

HCV requires cellular factors in order to effectively replicate, assemble, and propagate to other host cells for its infection. Several RNAi studies have implicated a multitude of host proteins to be pro-viral factors or restriction factors for the different steps of the HCV life cycle [16, 17], but not many have addressed whether these host factors interact with viral proteins to do so. Other studies have identified HCV-host interactors, but have not yet elucidated the importance of all identified interactions to the HCV life cycle [18, 19].

Step of the Life Cycle	HCV Genome	Host Factor	Effect of the Interaction
Cell Entry	E1 & E2	CD81 CDLN1 OCLN SR-BI	The E1E2 heterodimer interacts with cell surface receptors and tight junction proteins for HCV particle binding and entry into host cells [20]
IRES-mediated translation	5' NTR	miR-122	miR-122 interacts with the 5' NTR of HCV to stimulate translation through the enhanced association of ribosomes with the viral RNA [21]
Replication	3' NTR	miR-122	miR-122 interaction with the 3' NTR of HCV reduces viral RNA expression [22]
Replication	5' NTR	miR-122	miR-122 interacts with the 5' NTR of the HCV genome to facilitate replication [23]
Replication	NS3/4A	YBX1	YBX1 interacts with NS3/4A and associates with viral RNA for replication [24, 25]
Replication	NS4B	ATF6	ATF6, part of the unfolded protein response, is induced by NS4B and limits viral replication [18]
Replication	NS5A	Cyclophilin A	Cyclophilin A interacts with NS5A for its PPIase activity [26, 27]

Replication	NS5A	FKBP8	NS5A interacts with FKBP8 and Hsp90 to form a complex that is important for RNA replication [28]
Replication	NS5A	Hsp90	
Replication	NS5A	PI4K-IIIα	NS5A interacts with PI4K-IIIα for proper membranous web formation by increasing levels of PI4P in this region [29-31]
Replication	NS5A	Raf-1	NS5A interacts with Raf-1, causing Raf-1 to phosphorylate. Inhibition of Raf-1 reduced viral replication [32]
Replication	NS5A	TIP47	NS5A interacts with TIP47 for efficient viral replication [33]
Replication	NS5A	VAPA	VAPA interacts with NS5A to positively regulate viral RNA replication [34]
Replication	NS5B	Cyclophilin A	Cyclophilin A is recruited to the replication complex by NS5B for its PPIase activity [35]
Replication	NS5B	HNRNPA1	HNRNPA1 interacts with NS5B, as well as the 5' and 3' NTR of HCV RNA for viral replication [36]
Viral Particle Assembly	Core NS3/4A	YBX1	In a complex with DDX6, C1QBP, IGF2BP2 and LARP1, YBX1, a NS3/4A interactor, is re-localized to LDs by core to regulate the assembly of viral particles [24, 25]
Viral Particle Assembly	HCV RNA	HNRNPK	HNRNPK interacts with HCV RNA and co-localizes with core protein and LDs for regulating viral RNA incorporation into virions [37]
Viral Particle Assembly	NS5A	Rab18	NS5A interacts with Rab18 to associate with LDs [38]

Table 1.1: HCV-Host Interactors and their Effect on the HCV Life Cycle

The above table is a non-exhaustive list of characterized HCV-host interactors and their implication at various stages of the viral life cycle.

1.1.4.1 HCV and the Nuclear Pore Complex and its Transporters

Recent findings have implicated a relationship between the nuclear pore complex (NPC) and nucleocytoplasmic transporters with HCV proteins and viral replication. The first evidence of this is the existence of a nuclear localization signal and a XPO1-dependent nuclear export signal in the core protein, suggesting that the nucleocytoplasmic shuttling of core early in the HCV life cycle is important for viral replication [39, 40].

Neufeldt et al. demonstrated an increase in nucleoporins (Nups), components of the NPC, accumulating at infected areas in the cytoplasm during a HCV infection, which was supported by the overall increase in the mRNA levels of certain Nups during the infection. Several Nups, nucleocytoplasmic transporters and adaptors were identified to interact with HCV proteins, and elucidated to be important for viral infection. It was hypothesized that NPCs and nucleocytoplasmic transporters are beneficial to a cytoplasmic-replicating virus like HCV as it acts as a gate to different viral compartments, and protect the virus from being detected by cytoplasmic sensors, such as the pattern-recognition receptor RIG-I, of the innate antiviral immune response, and it would provide an explanation as to why several HCV proteins, such as core, NS2, NS3 and NS5A all encode nuclear localization signals [41]. This group then went on to demonstrate that the nuclear localization signals found in core and NS2 were found to be important for early stages of viral replication, while those found in NS3 and NS5A were important for later stages of viral replication such as viral particle assembly and egress. These signals may either serve to allow these viral proteins to enter NPC-gated viral compartments or to hijack nucleocytoplasmic transporters as a mode of facilitated transport within the cytoplasm [42].

Germain et al. (2014) identified several nucleocytoplasmic transporters, most of which were elucidated to interact with the NS3/4A protein of HCV such as KPNB1, RAN and TNPO1, which decreased viral replication when their individual gene expression was silenced. It was also suggested that NS3/4A can prevent the nuclear localization of STAT1 through its interaction with KPNB1, which is the main import carrier for STAT1, a novel viral immune evasion mechanism which supports the beneficial relationship between HCV and the NPC and its nucleocytoplasmic transporters [19].

1.2 Nuclear Pore Complex and Nucleocytoplasmic Transporters

1.2.1 Nucleocytoplasmic Transport

The nuclear pore complex (NPC) is the main gateway between the nucleus and the cytoplasm. Small molecules and proteins less than 60 kDa can passively diffuse through the pore, while larger proteins require the help of transporters for active transport to enter the nucleus. In order to enter or exit the nucleus, these larger proteins must contain a nuclear localization signal (NLS) or a nuclear export signal (NES), respectively [43, 44].

1.2.1.1 Protein Import

In order to be imported into the nucleus, a protein is bound by a Karyopherin-α (Kapα) adaptor protein via its NLS, and both of these proteins are then bound by a Karyopherin-β (Kapβ) carrier protein, which mediates the nuclear transport. Once this import complex enters the nucleus, Ran-GTP binds to the Kapβ to dissociate the complex and release both the NLS-containing protein and Kapα (Figure 1.7) [44].

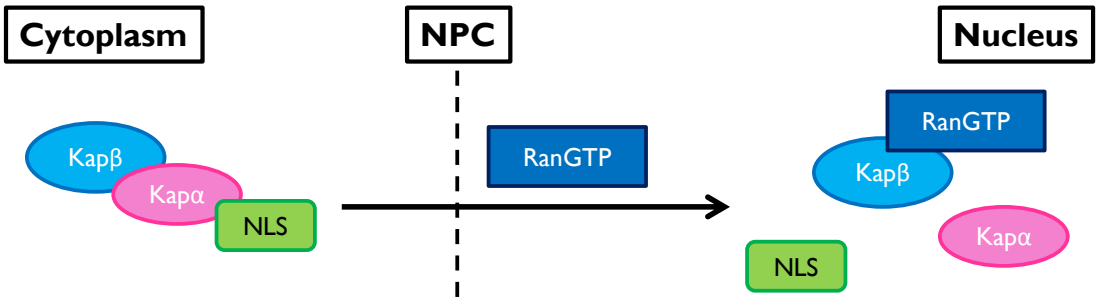

Figure 1.7: Protein Import

The general principle of nuclear import of proteins is that a protein must contain a NLS, which will then be recognized by the Karyopherin-α (Kapα) adaptor protein. The Karyopherin-β (Kapβ) carrier protein forms a complex with the Kapα and its cargo to mediate the translocation of this import complex to the nucleus. The import complex is dissociated upon binding of RanGTP to the Kapβ import carrier.

1.2.1.1.1 Karyopherin-α Adaptors

There exists seven different Kapα adaptor proteins, split into 3 subfamilies (α1, α2, and α3) based on their sequence homology. The α1 subfamily is composed of KPNA2 (importin-α1) and KPNA7 (importin-α8); the α2 subfamily is composed of KPNA3 (importin-α4) and KPNA4 (importin-α3); and the α3 subfamily is composed of KPNA1 (importin-α5), KPNA5 (importin-α6), and KPNA6 (importin-α7). The subfamilies range from α1, α3 to α2 in terms of lowest to highest sequence homology within each subfamily [45].

In the literature, these Kapα adaptor proteins exist under a multitude of different names for each, such as in the case of KPNA1, previously known as NPI-1 due to its interaction with the nucleoprotein (NP) of the Influenza virus. The Kapα proteins are the most associated with nuclear import as over fifty cargoes have been identified over the years, whether it be for the nuclear translocation of transcription factors during an innate antiviral response or for entry into the nucleus by nuclear-replicating viruses like HIV-1 or Influenza virus [45].

1.2.1.1.2 Karyopherin-β Import Carriers

There are several Kapβ carriers involved in nuclear import (Figure 1.7) with the main one being KPNB1, also known as Importin-β. It is known to bind to classical NLSs (cNLSs) such as the monopartite-cNLS and the bipartite-cNLS, which contain one or two stretches of basic amino acids, respectively [46]. In the absence of Kapα, KPNB1 can mediate the nuclear transport of proteins containing an arginine-rich NLS [47].

Another Kapβ import carrier is transportin 1 (TNPO1), which is known to bind to a non-classical NLS known as the PY-NLS, where the proline-tyrosine (PY) amino acids are preceded by either a hydrophobic or basic stretch of amino acid residues for binding by TNPO1 [48]. TNPO1 and TNPO2 are thought to be redundant transporters, as they both can interact and mediate the nuclear import of HNRNPA1 and HUR [49]. However, TNPO2 has been implicated in mRNA export with NXF1 [50]. TNPO3 is known to import serine/arginine-rich (SR) proteins to the nucleus, hence its other name TRN-SR2 [51]. TNPO3 is also heavily implicated in HIV-1 replication such as interaction with the integrase protein for the nuclear import of the pre-integration complex [52, 53].

As shown in Figure 1.10, there are a variety of import carriers, which can specifically bind to certain cargoes. IPO4 has been noted to mediate FANCD2 nuclear import by interacting with C/EBPδ [54]. IPO7 is able to import supercoiled plasmid DNA (exogenous) and human mitochondrial DNA (endogenous) [55], as well as facilitate nuclear import of HIV-1 viral DNA [56]. It can also act as an adaptor in the KPNB1/IPO7 complex for Histone H1 nuclear import [57]. IPO8 is known for the import of the signal recognition particle 19 [58]. IPO8 also interacts with Argonaute 2 (Ago2) for cytoplasmic miRNA-guided gene silencing and the nuclear localization of Ago2 [59]. This IPO8-Ago2 is also important for the nuclear translocation of mature miRNAs [60]. IPO13, related to TNPO3 [61], is one of the few Kapβ carriers involved in both import and export, as it can import RBM8, but can also export translation initiation factor eIF1A [62, 63]. IPO13 can also interact with a sumoylated E2-conjugating enzyme, Ubc9, to suppress auto-sumoylation of this complex [64].

Import carriers can also have common cargo to transport to the nucleus, such as in the case of several ribosomal proteins which can interact with KPNB1, TNPO1, IPO5 and IPO7 for nuclear import [65]. However, some ribosomal proteins like RPL7 and RPL12 can only be imported by IPO5 and IPO11, respectively [66, 67].

Once the Kapβ import carriers have completed their function, they can automatically export back to the cytoplasm, independently of RanGTP, such as in the case of KPNB1 as part of its recycling mechanism to renew the formation of import complexes in the cytoplasm [68].

1.2.1.2 Protein Export

A protein containing a nuclear export signal (NES) can be exported to the cytoplasm when it is bound to a Kapβ export carrier. The Kapβ carrier, bound by RanGTP, can then mediate the translocation of the export complex to the cytoplasm, where RanGTP will be hydrolyzed to RanGDP, with the help of RANBP1 and RANGAP1 (their functions explained in section 1.2.1.3 RAN Gradient), for the dissociation of the complex (Figure 1.8) [44].

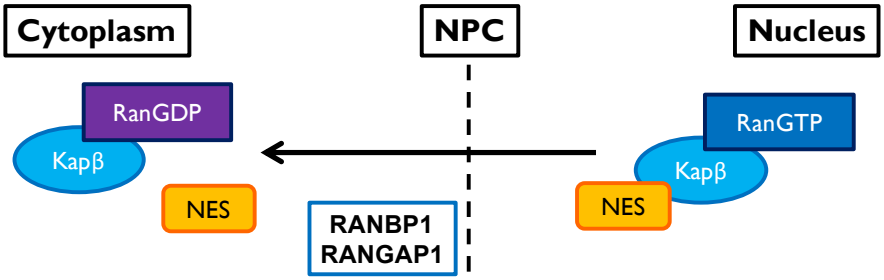

Figure 1.8: Protein Export

The general principle of protein export is that a protein must contain a NES and be bound by a Kapβ export carrier. Once the Kapβ carrier is bound to RanGTP, it can then mediate the translocation of the protein from the nucleus to the cytoplasm. Once in the cytoplasm, the export complex is dissociated upon hydrolyzation of RanGTP to RanGDP, causing the Kapβ carrier to release its cargo.

The main Kapβ export carrier is Exportin 1 (XPO1), also known as CRM1 (chromosome region maintenance protein), which specifically recognizes leucine-rich NES [44]. Many studies have used the XPO1 inhibitor, Leptomycin B, to determine whether the export of a protein is dependent on XPO1 function [69]. One co-factor that can interact with XPO1 for XPO1-mediated protein export is RAN binding protein 3 (RANBP3) [70, 71], which can act as a scaffold for efficient export complex assembly as RANBP3 can interact with the guanine nucleotide exchange factor RCC1, responsible for the exchange of RanGDP to RanGTP that is necessary to complete the export complex and provide the energy to drive this transport mechanism [72].

Another export carrier is XPO6, which is known to specifically export profilin-actin complexes. These complexes are important for the proper cytoplasmic localization of NUTF2, a carrier which is responsible for recycling RanGDP back to the nucleus in order to restore RanGTP levels, via RCC1, for the formation of export complexes [73, 74].

XPO7 is known to export proteins in a XPO1-independent manner, as it recognizes short linear sequences and folded motifs, where it interacts with basic residues for export [75]. XPOT is involved in the export of tRNAs [76], and can interact with the nucleoporins RANBP2 and NUP153, located on the cytoplasmic and nuclear side of the nuclear pore complex, respectively, as part of its ability to shuttle when bound to RanGTP [77].

XPO4 is another Kapβ carrier known to function in both export and import as it can export eukaryotic translation initiation factor 5A and Smad 3 [78, 79], and can import the Sox family of transcription factors [80]. XPO5 is a Kapβ carrier that is also thought to be involved in both import and export of proteins, but has primarily been characterized in export as it can export dsRNA-binding proteins [81, 82], elongation factor 1A for translation [83], 60S subunit of the ribosome complex [84], and the export of pre-miRNA for regulating gene expression [85].

After the dissociation of multiple import complexes in the nucleus, the accumulated Kapα adaptors are recycled back to the cytoplasm by CSE1L, also known as XPO2 or CAS, to renew the formation of import complexes (Figure 1.9) [44].

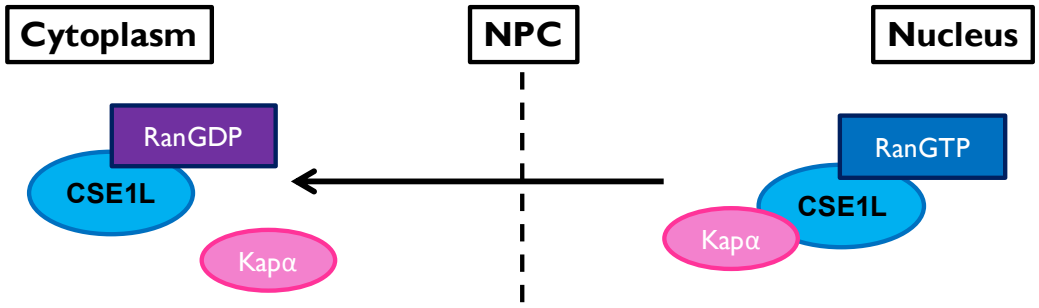

Figure 1.9: Kapα Recycling

Kapα adaptors are recycled back to the cytoplasm by CSE1L. RanGTP is hydrolyzed to RanGDP to dissociate CSE1L and the Kapα adaptor.

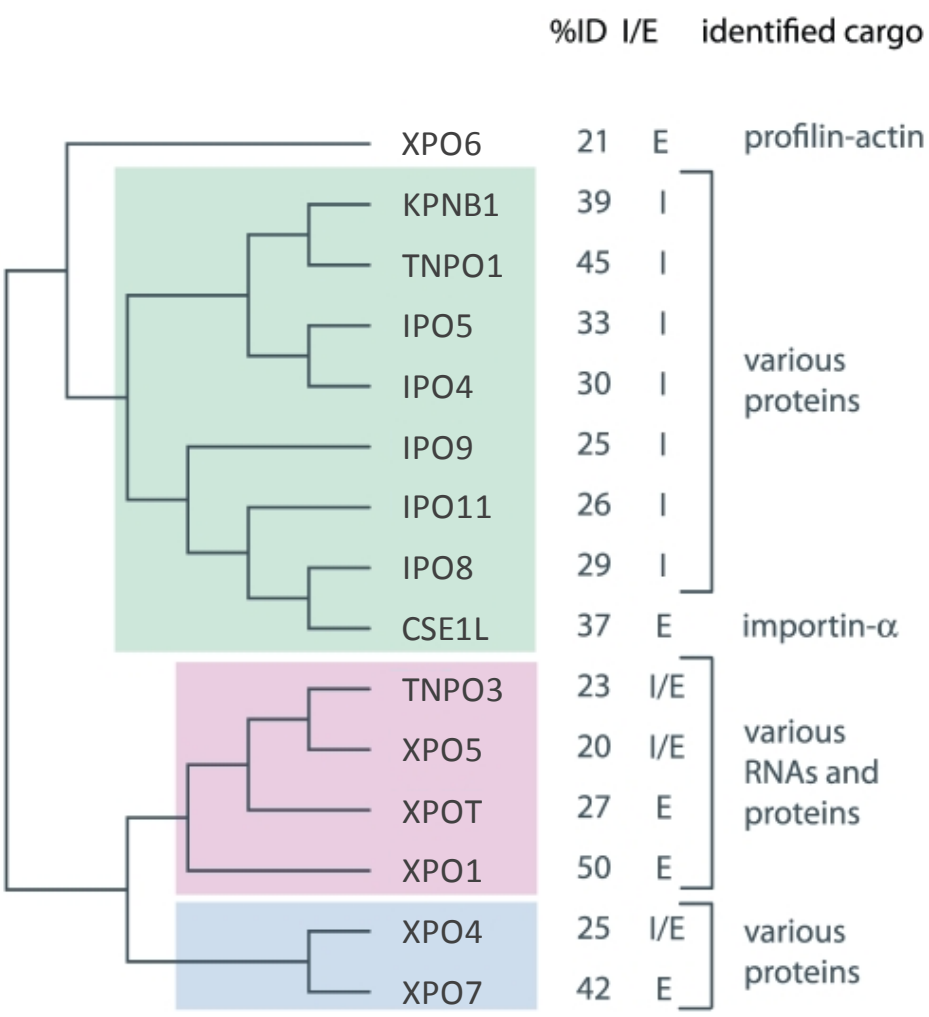

Figure 1.10: Phylogeny of Karyopherin-β subfamilies

The above figure shows the evolution of the Karyopherin-β (Kapβ) carrier proteins with each colour (white, green, pink and blue) representing a different subfamily. The percent identity (%ID) column lists the sequence similarity of each member in comparison to their subfamily. The I/E column identifies which carriers are involved in import (I) and export (E). Some Kapβ proteins are so similar in multiple aspects of their sequences, such as domains, length and composition, that they are considered as paralogous pairs: **TNPO1**-TNPO2, **IPO5**-RANBP6, IPO7-**IPO8**, **TNPO3**-IPO13, and **XPO7**-RANBP17 [61, 86, 87] (with the bolded protein of each pair corresponding to the figure above). (Figure adapted from O'Reilly AJ, et al., *PLoS One*, 2011) [86].

1.2.1.3 RAN Gradient

The RAN gradient is what determines the directionality of transport through the nuclear pore complex, where the nucleus contains a high concentration of RanGTP for export complexes, and the cytoplasm contains a high concentration of RanGDP waiting to be recycled by the carrier, nuclear transport factor 2 (NUTF2). Once in the nucleus, the GDP bound to RAN is exchanged for a GTP by the guanine nucleotide exchange factor RCC1 to renew the formation of export complexes (Figure 1.11), and the dissociation of import complexes [44].

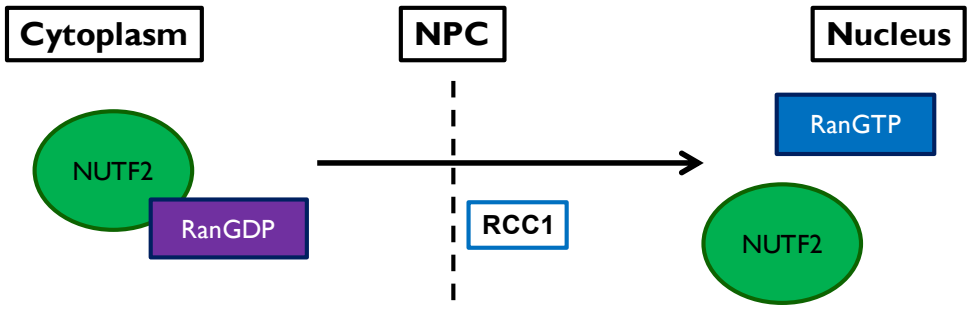

Figure 1.11: Recycling of RanGDP and the Renewal of RanGTP

To prevent the accumulation of RanGDP after the dissociation of export complexes, NUTF2 binds to RanGDP and transports it back to the nucleus, where RCC1 can exchange the GDP to a GTP to continue the formation of export complexes and the dissociation of import complexes in the nucleus.

The Ras-like nuclear protein (RAN) is the only member of the Ran family, which is part of the superfamily of GTP-binding proteins. This superfamily of proteins is known for their intrinsic GTPase activity, converting their GTP-bound active form to a GDP-bound inactive form [88, 89]. However, RAN is a weak GTPase and requires co-factors such as RAN binding protein 1 (RANBP1) and RAN GTPase-activating protein 1 (RANGAP1) to successfully hydrolyze RAN's GTP-bound form into a GDP-bound form for processes such as the dissociation of export complexes in the cytoplasm (Figure 1.8) [44, 90].

When import complexes are dissociated by the binding of RanGTP to Kapβ import carriers, these carriers can only be released from RanGTP when bound to RANBP1 such as in the case of CSE1L and TNPO1. KPNB1 requires the addition of a Kapα adaptor in order to be released from RanGTP. RANGAP1 prevents RanGTP from re-binding to these import carriers in the nucleus by hydrolyzing it to RanGDP [91].

RANBP1 and RANGAP1 are both considered as nucleocytoplasmic shuttling proteins, as they both function in the dissociation of export complexes in the cytoplasm, and the release of Kapβ from RanGTP in the nucleus [92, 93].

1.2.1.4 mRNA Export

Messenger RNAs (mRNAs) are other macromolecules which require an export pathway from the nucleus to the cytoplasm for the translation of mRNAs into mature proteins. The main carrier for mRNA export is nuclear RNA export factor 1 (NXF1), also known as TAP, specifically binds and exports RNA containing a constitutive transport element (CTE), originally found in the Mason Pfizer monkey virus [94]. The majority of mRNA is exported through the NXF1 pathway, where NXF1 forms a heterodimer with NUTF2-like export factor 1 (NXT1) to interact with the phenylalanine-glycine (FG) repeats of several NPC proteins for proper mRNA export [95-97], and this heterodimer also functions to promote the translation of unspliced mRNA [98]. NXT2, a homologue of NXT1, is localized at the nuclear rim and can interact with NXF1 for mRNA export as well [99]. NXF1 can also export mRNA through a TNPO2-mediated pathway, which has a higher export rate than the NXF1 binding to Nups for mRNA export [50].

The transcription-export (TREX) complex is important for mRNA export as the component ALY/REF can interact with NXF1 to expose its RNA-binding domain to increase the amount of mRNA that is bound, therefore increasing NXF1's RNA-binding affinity and increasing the amount of mRNA exported by NXF1. If components of the TREX complex are silenced, then the amount of mRNA bound is reduced, which will ultimately result in a mRNA export block [100, 101].

Other mRNA export factors are NXF2 and NXF3, where NXF2 can export cytoplasmic mRNAs by interacting with the cytoplasmic motor protein KIF17 [102]. NXF2 can also form a heterodimer with NXT1 in order to interact with Nups, similar to NXF1 [103]. NXF3 is another nuclear mRNA export protein related to NXF1 and NXF2, but lacks the domain to bind to Nups. However, it does contain an XPO1-dependent nuclear export signal, so it can still export mRNA via XPO1 function [104].

XPO1 can also mediate the export of certain mRNAs, but is not able to bind to mRNAs directly, such as in the case of the HIV-1 protein Rev which exports unspliced and partially spliced HIV-1 mRNA through its interaction with XPO1 [100]. NXT1 can also interact with XPO1 as a co-factor and is part of the terminal step of XPO1-mediated nuclear export for the release of XPO1 cargo to the cytoplasm, whether it be for mRNA or protein [105].

DDX19B, the DEAD-box helicase also known as DBP5, is another important mRNA export factor, and requires GLE1L, bound to inositol hexakisphosphate, to increase DDX19B's RNA binding and ATPase activity [106, 107], while NUP214 can interact with DDX19B to regulate those same activities [108]. GLE1L is localized to the NPC by the cytoplasmic FG-Nup NUPL2, and can also interact with NUP155 for mRNA export such as the export of HSP70 mRNA [109, 110].

1.2.2 Structure of the Nuclear Pore Complex

The nuclear pore complex (NPC) is a 125 MDa structure, and is embedded in the nuclear envelope (NE), a bilayer made up of the outer nuclear membrane and the inner nuclear membrane. Composed of 30 proteins known as nucleoporins (Nups), the NPC is made up of seven different parts: the cytoplasmic FG-Nups and filaments, the transmembrane-ring Nups, the outer-ring Nups, the linker Nups, the inner-ring Nups, the central FG-Nups, and the nuclear FG-Nups and the nuclear basket (Figure 1.12). These groups function in either the structural integrity of the NPC or in the regulation of macromolecular transport [43, 111-113].

1.2.2.1 Cytoplasmic FG-Nups and Filaments

The cytoplasmic phenylalanine-glycine (FG)-Nups and filaments are composed of NUPL2, RANBP2 (also known as NUP358), and NUP214 [112]. NUPL2 can bind to XPO1 to promote XPO1-dependent nuclear export, such as in the case of HIV-1 Rev export [114, 115].

RANBP2 acts a docking site, promoting nucleocytoplasmic transport for specific transporters and cargos [116], such as TNPO1 nuclear import [117], KPNB1 nuclear import of cNLS-containing cargo [118, 119], and XPO1 nuclear export [120]. RANBP2 can also interact with NXF1, in complex with NXT1, for mRNA export [95], as well as interact with mRNAs part of the alternative mRNA nuclear export (ALREX) pathway to promote their translation [121]. RANBP2 is also thought to play a role in presenting misfolded and ubiquitinated proteins for proteasomal degradation [122], as its cyclophilin-like domain acts as a modulator for the ubiquitin-proteasome system and may contribute to the compartmentalization of properly-folded protein for turnover [123].

RANBP2, part of the cytoplasmic filaments, is linked to the cytoplasmic side of the NPC by the NUP214/NUP88 complex [124], due to the association of NUP214 with the cytoplasmic ring [125]. NUP214 can also be found in the nucleus for its role in XPO1-mediated protein export [126], when in complex with NUP88, such as the export of the pre-ribosomal 60S subunit [127-129].

1.2.2.2 Transmembrane-ring Nups

The transmembrane-ring Nups, composed of NDC1, NUP210 and POM121, are all responsible for the anchoring of the NPC to the NE [130, 131]. NDC1 is important for NPC assembly as it can interact with Nups from different parts of the NPC such as NUP93 (linker Nup), NUP53 (central FG-Nup), and NUP205 (inner-ring Nup) [132, 133]. Out of the transmembrane-ring Nups, NDC1 is the one responsible for the targeting of ALADIN, a Nup thought to be associated with the outer-ring, to the NPC, where this interaction may be important for nuclear import selectivity [134, 135].

In comparison to POM121, NUP210 is thought to be redundant in the function of NE formation [136]. POM121 is thought to be the most important of the transmembrane-ring Nups for NPC assembly at the membrane [137, 138]. POM121 is important for recruiting RANBP2 (cytoplasmic FG-Nups) and NUP62 (central FG-Nups) to the NPC for assembly [130]. POM121 is also important for linking the NUP160 (outer-ring Nup) subcomplex and the NUP155 (inner-ring Nup) subcomplex together for nuclear pore formation and attachment to the NE [139]. POM121 is also thought to interact with KPNA/KPNB1 import complex and several nucleoporins in a NLS-dependent manner, which is important for NPC assembly at the NE and structural integrity of the NPC [140].

1.2.2.3 Outer-ring Nups

The outer-ring Nups are composed of ALADIN, NUP37, NUP43, NUP75, NUP96, NUP107, NUP133, NUP160, SEC13 and SEH1 [112]. ALADIN is targeted to the NPC by the transmembrane-ring Nup NDC1, where this interaction may be important for nuclear import selectivity [134, 135]. The NUP107-160 complex, composed of all the outer-ring Nups, with the exception of ALADIN, is important for nuclear import of NLS-containing cargos, as well as the organization of other complexes of the NPC such as the transmembrane-ring Nups [112, 141]. The NUP107 complex also plays a role in the diameter of the NPC, as it assembles into two reticulated rings, to accommodate the nucleocytoplasmic transport of large cargoes [142]. NUP107 itself is important for the proper assembly of multiple Nups to the NPC such as RANBP2, NUP214, NUP133, NUP153, and TPR [143, 144].

1.2.2.4 Linker Nups

The linker region of the NPC is composed of NUP88 and NUP93, which can be found on both sides of the NPC [112]. NUP88 can interact with lamin A, and NUP214 for XPO1-mediated export on the nuclear and cytoplasmic side of the NPC, respectively [128, 145]. NUP93 acts as a backbone to connect both the cytoplasmic and nuclear sides of the NPC, and in addition interacts with NUP205, NUP155 and NUP53 for proper NPC assembly, while recruiting NUP62 for nucleocytoplasmic transport-competent NPCs [146, 147]. The interaction between NUP93, NUP155 and NUP205 is known as the NUP93 subcomplex [148].

1.2.2.5 Inner-ring Nups

The inner ring of the NPC is composed of NUP155, NUP188 and NUP205 [112]. NUP155 interacts with NUP53 and NDC1 for NPC assembly [133, 149]. NUP188 is thought to regulate the movement of membrane proteins across the NPC [150], and can interact with FG-repeats and move through the NPC [151]. NUP155 and NUP205 interact with NUP93 and NUP53 for proper NPC assembly [146, 147].

1.2.2.6 Central FG-Nups

The central FG-Nups, composed of NUP53, NUP54, NUP58/NUP45, NUP62 and NUP98 [112]. NUP53 interacts and anchors the NUP93 subcomplex and interacts with NDC1 for proper NPC assembly at the NE [133, 148]. NUP98 is a mobile Nup, and is important for RNA export as it can interact with RAE1, a mRNA export factor [152-155]. During TNPO1 import, NUP98 competes for TNPO1 binding via its M9 motif, releasing the import cargo into the nucleus, and RanGTP bound to NUP98 dissociates it from TNPO1 [156]. NUP98, in complex with RANBP3, can act as a co-factor for XPO1-mediated export [157].

Within the central FG-Nups is the NUP62 complex made up of NUP62, NUP58/NUP45 and NUP54, which are all implicated in nuclear import as they all encode for FGs. NUP58/NUP45 complex is responsible for adjusting the diameter of the central channel [158], increasing in size to allow for nucleocytoplasmic transport to pass through the NPC [159]. NUP58 can complex with KPNB1 for SRP1α nuclear import, while NUP62 can interact with NUTF2 for RanGDP nuclear import [160-163]. NUP62 can also interact with TNPO3 for

TNPO3-mediated nuclear import of serine/arginine-rich proteins [51]. NUP62 is also involved in export via interacting with NXT1 for NXF1-mediated mRNA export [97].

1.2.2.7 Nuclear FG-Nups and the Nuclear Basket

The nuclear FG-Nups and the nuclear basket are composed of NUP50, NUP153 and TPR [112]. Despite residing on the nuclear side of the NPC, NUP50 mediates XPO1-dependent export [164]. NUP50, depending on its isoform, can regulate the speed of NLS-cargo nuclear import, allowing CSE1L to properly dissociate the cargo from NUP50 for Kapα export [165, 166], such as in the case of KPNA1 and its cargo PB2 of influenza virus [167].

NUP153 interacts with NUP50 as a scaffold, supporting the NUP50/Kapα for efficient nuclear import [168]. NUP153 interacts with KPNA2 for nuclear export [169], and it is also responsible for the export of multiple classes of RNAs (snRNA, mRNA and 5S rRNA), as well as XPO1-dependent export for viral proteins such as HIV-1 Rev and its dependent RNA export, without affecting tRNA export and KPNB1 recycling to the cytoplasm [170]. Due to NUP153's involvement in export, it is thought to be mobile within the NPC, as it also plays a role in import through interacting with TNPO1 via NUP153's M9 shuttling domain [171]. NUP153 facilitates cNLS-mediated import by interacting with Kapα in the classical Kapα/Kapβ nuclear import pathway [172].

NUP153 interacts with TPR to localize it to the nuclear side of the NPC for the formation of the nuclear basket [173, 174]. TPR restricts the export of unspliced mRNAs via the NXF1-mediated mRNA export pathway [175, 176]. TPR is also thought to be involved in XPO1-dependent protein export [177].

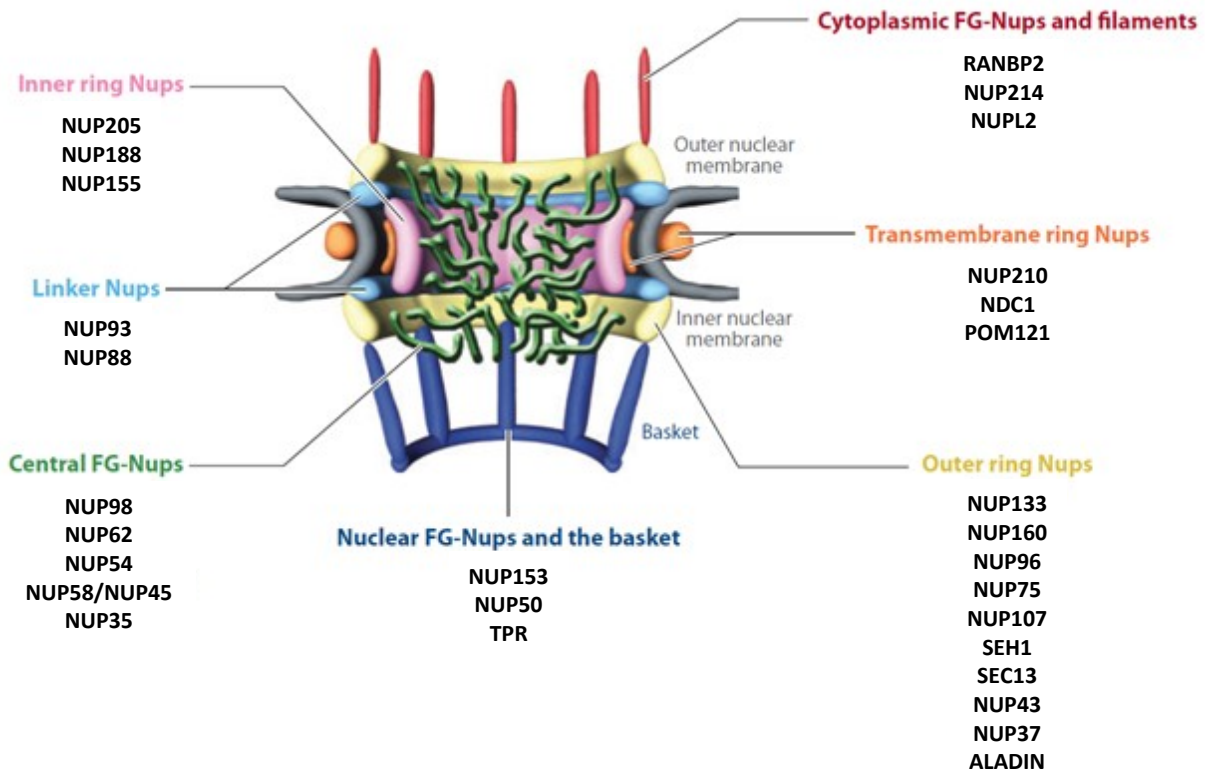

Figure 1.12: Structure of the Nuclear Pore Complex

The nuclear pore complex (NPC) is composed of roughly 30 proteins known as nucleoporins (Nups), which are divided into 7 groups based on their location in the structure. (Figure adapted from Grossman E, et al., *Annu Rev Biophys.,* 2012) [112].

1.3 Viruses and the NPC & its Transporters

Nucleoporins and nucleocytoplasmic transporters have been the target of a myriad of viruses for various reasons. Viruses that replicate in the nucleus usually target these proteins to enter and exit the nucleus for the life cycle and propagation of the virus.

1.3.1 Nuclear-Replicating Viruses

1.3.1.1 DNA Viruses

The *Herpesviridae* family is composed of several dsDNA viruses such as Herpes simplex virus type 1 (HSV-1), Varicella-Zoster virus (VZV), Epstein-Barr virus (EBV), and Human cytomegalovirus (HCMV), which are also known as Human herpesvirus 1 (HHV-1), HHV-3, HHV-4, and HHV-5, respectively. In the life cycle of these viruses, the capsid injects the viral genome into the nucleus, where replication and transcription occurs [178]. Multiple viral proteins then work in concert to take over cellular processes such as transcription for viral gene expression and nucleocytoplasmic transport of viral factors [179]. The HSV-1 proteins pUL25 and pUL36/pUL6, interact with the cytoplasmic FG-Nups NUP214 and NUPL2, respectively, for capsid import to the NPC, infection initiation, and viral DNA release into the nucleus [180]. ICP27 interacts with multiple export factors such as ALY/REF, NXF1 and XPO1 for efficient viral RNA export through the NXF1- and XPO1-mediated pathways [181-185]. ICP27 also interacts with NUP62 to block KPNB1- and TNPO1-dependent import to favour the export of viral mRNAs [186]. VZV interacts with ALY/REF and NXF1 via its IE4 protein for viral mRNA export through the NXF1-mediated RNA export pathway [187]. VZV can also interact with KPNB1 and XPO1 via its ORF9 protein for nucleocytoplasmic shuttling [188]. EBV can interact with NUP62 and NUP153 via its BGLF4 kinase, which phosphorylates these Nups to increase nuclear import of non-NLS-containing viral proteins and block the import of host proteins [189]. EBV protein SM is exported by XPO1 to the cytoplasm for its activity of increasing the expression of intronless genes, such as certain EBV genes involved in lytic replication [190]. The viral protein UL84 of HCMV can interact with KPNA1, KPNA2, KPNA3 and KPNA4, in complex with KPNB1 and RAN, for nuclear

import [191], while the viral protein UL79 interacts with TNPO1 for its import to the nucleus [192].

The *Papillomaviridae* family are also composed of dsDNA viruses of multiple types such as Human papillomavirus type 8 (HPV8), type 11 (HPV11) and type 16 (HPV16). HPV is internalized into cells via the L1 and L2 capsid proteins. The L2 minor capsid protein is responsible for the delivery of HPV viral DNA into the nucleus, while L1 remains at the endosome for degradation. The E2 protein binds to viral DNA and recruits the E1 helicase for viral DNA replication, while the E6 and E7 proteins are thought to promote cell proliferation [193, 194]. The L2 minor capsid protein uses IPO5 and TNPO1, as well as KPNB1 complexed with KPNA2, for viral DNA import in HPV11 and HPV16 [195, 196]. The E2 viral protein can also interact with KPNA1 and KPNA4 for nuclear import in HPV11 and HPV16 [197]. In HPV16, the E6 protein can enter the nucleus by interacting with KPNA2, in complex with KPNB1, and TNPO1 [198]. The E7 protein can mediate its nuclear transport by interacting with NUP62 in HPV8, HPV11 and HPV16, and NUP153 in HPV8 [199-201].

Hepatitis B virus (HBV) from the *Hepadnaviridae* family is a dsDNA virus, utilizing the reverse transcriptase enzyme for the synthesis of DNA from the viral mRNA [202]. The HBV core protein is exported by NXF1 for viral DNA synthesis, while the X protein is exported by and sequesters XPO1 as part of its role to induce liver carcinogenesis in chronically-infected hepatocytes [203, 204]. The HBV capsid interacts with NUP153 to regulate viral release into the nucleus [205].

1.3.1.2 RNA Viruses

Influenza A virus (IAV) is one of the few negative-sense RNA viruses to replicate in the nucleus. The polymerase basic protein 1 (PB1), part of the viral RNA polymerase complex, is imported to the nucleus by IPO5 for the accumulation of viral RNA required for efficient viral growth [206, 207]. PB1 also interacts with NUP54 for viral polymerase transcription and viral replication [208]. The viral protein PB2 can interact with KPNA1 and KPNA2 for nuclear import [209, 210], while the nucleoprotein (NP) interacts with KPNA2 for nuclear import and with KPNA4 for the regulation of viral replication, independent of its import function [210, 211]. The viral protein NS1 complexes with NXF1 and its co-factors,

NXT1 and RAE1, to block mRNA export [212]. The NP and NS2 viral proteins of IAV interact with XPO1 for the export of viral ribonucleoprotein complexes (vRNPs) to the cytoplasm, disfavouring the export of other XPO1 substrates [213-215]. The viral protein NP can also be exported directly to the cytoplasm by interacting with XPO1 for viral replication [216]. NXF1 is thought to play a role in the viral RNA export of most late proteins [217]. The phosphorylation of RANBP3, a XPO1 co-factor [70], is required at early and late stages of viral infection for vRNP export [218].

Human immunodeficiency virus type 1 (HIV-1) is retrovirus, which requires the use of the reverse transcriptase enzyme to convert its RNA genome into DNA for integration into the host genome. HIV-1 is part of a subgroup of retroviruses known as lentiviruses, as it can enter the nucleus through the NPC and infect non-dividing cells [219]. The pre-integration complex (PIC) of HIV-1 is able to enter the nucleus by using the viral protein integrase to interact with KPNA2, KPNA4 and TNPO3 [52, 53, 220, 221], as well as directly with the cytoplasmic FG-Nup RANBP2 [222]. Vpr also helps with PIC docking at the NPC by interacting with NUP54 and NUPL2 [223, 224]. HIV-1 also recruits other Nups and transporters such as NUP98 and IPO7 to facilitate with the nuclear import of its viral cDNA [56, 225]. The HIV-1 rev protein interacts with XPO1, NUP98 and NUP214 for the export of Rev and viral mRNA through the XPO1-dependent export pathway [226, 227], while suppressing the export of mRNAs by the NXF1 pathway [228].

1.3.2 Cytoplasmic-Replicating Viruses

Viruses that replicate in the cytoplasm do not require entry into the nucleus for its replication, but they can interact with nucleoporins and transporters to disrupt transport through the NPC to give the virus a growth advantage in the cell.

1.3.2.1 DNA Viruses

The *Poxviridae* family is the only viral family with a dsDNA genome to replicate in the cytoplasm. RNAi screens have elucidated multiple proteins from multiple functional groups which are important for cytoplasmic replication of Vaccinia virus (VACV), making the

requirement for NPC genes for replication to be unexpected. Out of the NPC and transporters elucidated to have an effect on VACV replication, NUP62 was shown to block viral morphogenesis when silenced [229].

1.3.2.2 RNA Viruses

The *Picornaviridae* family is composed of positive, single-stranded RNA viruses such as those from the Cardiovirus and the Enterovirus genus. The relationship between this viral family and the NPC, specifically, is that of nucleocytoplasmic transport disruption. Cardioviruses encode the Leader (L) protein, which has been shown to hyperphosphorylate multiple NPC proteins such as NUP62, NUP153 and NUP214 to inhibit protein import and export in Encephalomyocarditis virus (EMCV) [230], and NUP62 in Mengovirus, an EMCV subtype, to permeabilize the nuclear envelope and alter nucleocytoplasmic transport [231]. Enteroviruses encode the 2(A) protease, which can cleave NUP62, NUP98 and NUP153 in Poliovirus, and only NUP62 in Human rhinovirus, to disrupt nucleocytoplasmic trafficking like protein import and mRNA export [232-234].

The relationship between the *Flaviviridae* family and the NPC and its transporters, as seen with HCV in a previous section, is not well-understood. Other members such as Dengue virus have shown to interact with KPNB1 and XPO1 via its NS5 protein, suggesting that this nucleocytoplasmic shuttling is important for viral replication [235, 236]. Japanese encephalitis virus, another member, was shown to have increased replication when RANBP2 is silenced [237], which could suggest disrupting nucleocytoplasmic transport, such as protein import by KPNB1 [118], may provide a replication advantage in host cells.

Negative-sense RNA viruses, such as Human respiratory syncytial virus (RSV) from the Paramyxoviridae family and Vesicular stomatitis virus (VSV) from the Rhabdoviridae family, can interact with the NPC and its transporters via its Matrix (M) protein. In the case of RSV, the M protein interacts with KPNB1 for nuclear import and XPO1 for nuclear export later in the infection to localize at regions of virus assembly for viral production [238, 239]. On the other hand, the M protein of VSV can interact with NUP98 and RAE1 to block mRNA export to inhibit host protein transcription [240-242], and can interact with RAN to block the nucleocytoplasmic transport of certain proteins and RNAs [243].

1.4 Innate Antiviral Immune Response

1.4.1 Early Phase: Virus Recognition by PRRs

The innate immunity involves the recognition of pathogen-associated molecular patterns (PAMPs) by pattern-recognition receptors (PRRs). In humans, there currently exist five different PRR pathways: Toll-like receptors (TLRs), RIG-I-like receptors (RLRs), NOD-like receptors (NLRs), C-type lectin receptors (CLRs) and cGAS/STING. However, only the TLR, RLR and cGAS/STING pathway contain receptors recognizing viral genomes, while the NLR and CLR pathways have receptors recognize other macromolecules such as bacterial peptidoglycans and carbohydrates on the surface of pathogens, respectively [244-246].

The TLR pathway consists of extracellular receptors ranging from TLR1 to TLR11. TLR3, TLR7, and TLR9 recognize viral dsRNA, ssRNA and CpG-DNA, respectively in endosomal compartments. Once the receptor recognizes the virus, TLR3 signals through the TRIF adaptor protein, while TLR7 and TLR9 signal through MYD88 for the innate antiviral response [244-246].

The RLR pathway is composed of two cytoplasmic sensors RIG-I, which recognizes short dsRNA and 5' triphosphate dsRNA, and MDA5, which recognizes long dsRNA. RIG-I recognizes a multitude of viral RNA such as HCV and influenza virus. Sendai virus (SeV) is often used to specifically activate the RLR pathway via RIG-I sensing. When RIG-I and MDA5 sense viral RNA, their CARD domain becomes exposed and interacts with the CARD domain of MAVS, which causes MAVS to translocate to the mitochondria where it mediates its downstream signaling of the immune response [244-247].

In the cGAS/STING pathway, intracellular viral DNA is recognized by cyclic-GMP-AMP (cGAMP) synthase (cGAS), which will then synthesize cGAMP. The newly-synthesized cGAMP binds to STING localized at the ER, where it then signals downstream for the innate antiviral immunity [248].

1.4.2 Signaling Cascade

The TLR pathway leads to two signaling cascades: one mediated by TLR3 via TRIF, and the other mediated by TLR7 and TLR9 (and all other TLRs) via the MYD88 adaptor protein. TRIF interacts with TRAF3, which signals TBK1 and IKKε to phosphorylate IRF3, which induces IRF3 nuclear translocation for the activation of type I interferons (IFNs). TRIF also interacts with TRAF6 for the activation and nuclear translocation of NF-κB by phosphorylation, and hence degradation, of the NF-κB inhibitor IκB by the IKK-α/β/γ complex. MYD88 also interacts with TRAF6 for NF-κB activation and nuclear translocation for the activation of cytokines. However, MYD88 interaction with TRAF3 leads to the activation of IRF7, via phosphorylation by the IKK-α/IRAK1 complex, for the production of IFNs, similar to IRF3 [244].

In the RLR pathway, MAVS at the mitochondria signals through both TBK1 and IKKε, as well as the IKK-α/β/γ complex for the nuclear translocation of both IRF3/7 and NF-κB, respectively, for the production of IFNs and cytokines [244-247, 249].

The cGAS/STING pathway involves the binding of cGAMP to STING at the ER, where it recruits TBK1 and IKK, similar to MAVS in the RLR pathway, for the activation and nuclear translocation of IRF3 and NF-κB for the production of IFNs [248].

1.4.2.1 IRFs

There are currently nine members of the Interferon-regulatory factors (IRFs) family of transcription factors [250], which play a variety of roles such as the induction of IFNs and ISGs, such as in the case of IRF3 and IRF9, respectively [251]. They are characterized as having a N-terminal DNA-binding domain, which recognizes and binds to ISRE DNA sequences [252].

IRF1 was the first transcription factor found to bind to the PRDI domain on the IFNβ promoter [253, 254]. Upon IFN-α/β binding to their appropriate receptors, IRF1 expression is induced by the binding of the IFN-α-activated factor (AAF) complex, composed of STAT1 homodimers, to the IFN-γ-activated sequence (GAS) promoter [251]. IRF1 binds to IFN-stimulated regulatory element (ISRE) promoters for the expression of ISGs [251] such as PKR

and OAS [255, 256]. IRF1 can also activate IFNA4 expression, which is repressed by IRF3 [257]. IRF2 shares many sequence similarities and binding capacities with IRF1, and thus acts as a negative regulator of IRF1 function, such as binding to ISRE promoters to block induction of ISGs by IRF1 [258, 259].

IRF3 is activated through phosphorylation by multiple PRR pathways upon viral infection, where it translocates to the nucleus for the expression of type I interferons [244-249]. IRF3 is part of the DRAF1 complex, along with CREB-binding protein and p300, which binds to the ISRE [260]. IRF3 can induce the expression of ISGs, such as ISG15 and IP-10, without the ISGF3 complex of the JAK/STAT pathway [251].

IRF4 is only expressed in the B-cells and T-cells of lymphoid tissues, and has a similar DNA-binding domain to IRF1 and IRF2 as it can bind to the ISRE [261, 262]. It is able to repress IFN-dependent and IRF1-dependent activity, but differs from that of IRF2 [263].

IRF5 is activated via the TLR pathway through the MYD88 adaptor, where the translocation of IRF5 to the nucleus induces cytokine expression [264]. IRF6 sequence has the closest homology to IRF5 out of all the family members [265], and its only function to date is the positive regulation of nitric oxide synthase 2 (NOS2) transcription [266].

Upon IFN stimulation, IRF7 expression is induced by the ISGF3 complex binding to the ISRE promoter, where newly synthesized IRF7 is phosphorylated, similar to IRF3, for positive-feedback regulation on the expression of the IFN-α/β promoters with phosphorylated IRF-3 in the nucleus [251].

IRF8 expression is inducible by IFN-γ and is found in lymphoid tissues [267], where its activation is linked with T-cell activation [268]. IRF8 is able to bind to the ISRE only when complexed with IRF1 and IRF2, and acts as a negative regulator by blocking the binding of ISGF3 to this element [269].

IRF9 is well-known as being part of the ISGF3 complex, with STAT1 and STAT2, which induces the expression via the ISRE promoter of other IRFs like IRF7 and ISGs such as OAS and PKR [251].

1.4.2.2 NF-κB

There are currently five NF-κB transcription factors: p50/p105 (also known as NF-κB1), p52/p100 (also known as NF-κB2), p65 (also known as RelA), c-Rel, and RelB. Out of the five transcription factors, p50 and p52 have to be processed into their active form from the p105 and p100 precursors, respectively, while the other three factors are already synthesized into their transcriptionally active form. As part of the Rel family of proteins, they all contain a Rel homology domain, which is responsible for their dimerization in the form of homo- or heterodimers, as well as their translocation to the nucleus and ability to bind to DNA [270].

However, there are inhibitory NF-κB (IκB) proteins, which bind and cover the NLS of these family members to sequester them in the cytoplasm. Upon a viral infection, injury or stress, the NF-κB pathway is activated by the phosphorylation of IkB proteins, inducing their degradation, and releasing the NF-κB proteins, such as the p50/p65 and p50/c-Rel heterodimers, which can now translocate to the nucleus to promote the transcription of various factors involved in the innate antiviral response, inflammation and apoptosis [270, 271].

1.4.3 Late Phase: Interferon Activation of the JAK/STAT Pathway

Once type I interferons, such as IFNα and IFNβ, are produced, they are secreted and bind to IFNα receptors (IFNAR) in an autocrine and paracrine fashion. This activates the JAK/STAT pathway where STAT1 and STAT2 are phosphorylated on a tyrosine by JAK1 and TYK2. These STATs dimerize and associate with IRF9 to form the ISGF3 complex, which translocates to the nucleus and binds to the IFN-stimulated regulatory element (ISRE) promoter which drives the expression of other IRFs like IRF7 and interferon-stimulated genes (ISGs) such as OAS and PKR to induce an antiviral state in the infected cell and neighbouring cells [251, 272-274]. Transcription factors such as IRF3 can induce the expression of certain ISGs directly, such as ISG15 and IP-10, without having to signal through the JAK/STAT pathway [251]. Depending on the state of the cell, expressed ISGs such as TRAIL and XAF1 may induce apoptosis if the cell is unable to adequately combat the viral infection [275].

1.4.3.1 Transcriptional Control by Type I Interferons

Type I interferons have regulatory effects on the expression of factors associated with adaptive immunity such as increasing the expression of major histocompatibility antigens Class I and II via mRNA stabilization, which leads to the activation of macrophages, natural killer cells and cytotoxic T-cells and increase in antigen presentation [277]. These IFNs can also bind to specific receptors on CD8 T-cells to induce clonal expansion, differentiation and memory formation as a consequence of viral infections [278-280].

These IFNs, such as IFNβ, can also regulate the inflammation pathway by increasing the mRNA stability of negative factors such as IL-1ra, and destabilize the TNF-α and IL-1β mRNA to create a negative feedback loop [281].

1.4.3.2 Regulation of IFNβ Expression

IFNβ is a type I interferon and its expression is induced by the binding of both IRF3 and NF-kB p65 to the PRDIII domain and the PRDII domain, respectively, on the IFNB1 gene promoter [257, 282]. IRF1 can bind to the PRDI domain [253, 254], while ATF-2/c-Jun can bind to the PRDIV domain of this promoter [283, 284]. Once IFNβ binds to IFNAR to activate the production of ISGs via the JAK/STAT pathway, high levels of IRF7 is expressed, amplifying IFNβ expression during the late phase of the antiviral response [285].

IFNβ expression is negatively regulated throughout the innate antiviral response to prevent prolonged activation. At the level of effector proteins in the signaling cascade of the antiviral response, TBK1 activity can be negatively regulated by CYLD deubiquitination, which removes lysine 63-linked ubiquitin chains [286, 287], and proteasomal degradation by the E3 ubiquitin ligase TRIP, which adds lysine 48-linked ubiquitin chains [288]. At the level of transcription factors, IRF3 activity is negatively regulated via degradation by the proteasome [289]. On the other hand, NF-kB induces the transcription of its inhibitor IkBα as a negative feedback mechanism to prevent prolonged NF-kB activity [290-292]. NF-kB and IkBα form a complex and are then exported to the cytoplasm by XPO1 via the NES of IkBα to completely abolish NF-kB activity until further stimulation [293, 294]. In the JAK/STAT pathway, SOCS expression inhibits STAT phosphorylation by JAK, preventing ISG induction by ISGF3 and the amplification of IFNβ expression by IRF7 [276].

1.4.3.3 Type III Interferons

Another type of interferon that is activated in response to a viral infection is the type III interferons, which is composed of IFNλ1 (IL-29), IFNλ2 (IL-28A), and IFNλ3 (IL-28B) [295]. These interferons bind to the IFNλ receptor, which signals through the JAK/STAT pathway via phosphorylation of JAK1 and most importantly JAK2, in comparison to JAK1-only signaling in type I interferons [296]. The production of the type III interferons is induced by the RLR pathway, specifically in the localization of MAVS to peroxisomes [296], which differs from the localization of MAVS to the mitochondria for the signaling to produce type I interferons [297]. IRF3/7, and NF-κB are required for the induction of both types of interferons [298, 299], while AP-1 is only essential for type I interferons and dispensable for type III interferons [296]. The similarity between the players required for the induction of these two types of interferons, and the subsequent JAK/STAT signaling they induce, is reflected in the fact that there are no ISGs that are specifically associated to type III interferons [300, 301]. However, type I interferons, such as IFNα and IFNβ, are able to induce ISGs in greater magnitude with a bell curve effect over time, while type III interferons gradually induce ISG activation from a lower magnitude over a longer period of time [302].

1.5 NPC and Transporters: Targets for Viral Immune Evasion

As discussed in section 1.3, all different kinds of viruses, regardless if their genome is DNA- or RNA-based, interact with Nups and nucleocytoplasmic transporters for a variety of cellular processes such as viral entry into the nucleus for nuclear-replicating viruses or to disrupt normal nucleocytoplasmic transport to benefit viral replication of cytoplasmic-replicating viruses. In section 1.4, the innate antiviral immunity was described and how important transcription factors such as IRF3, NF-κB, and STAT1 translocate to the nucleus for the induction of IFNs and ISGs, respectively upon a viral infection. Various viruses have developed ways to evade the innate immune response by disrupting the Nups and transporters required for the proper localization of proteins to induce an antiviral state in the cell.

1.5.1 Positive ssRNA Viruses

Positive single-stranded RNA viruses like those from the Nidovirales order can disrupt the transport of important innate antiviral factors to the nucleus to inhibit the production of ISGs. In the case of Porcine reproductive and respiratory syndrome virus (PRRSV), the viral protein Nsp1β degrades KPNA1, thus inhibiting ISGF3 nuclear import [303]. Another example is the SARS coronavirus (SARS-CoV), where the viral protein ORF6 tethers KPNB1 to ER and Golgi membranes, hence blocking STAT1 nuclear import [304]. In the *Flaviviridae* family, the NS3/4A protease of HCV was suggested to interact with KPNB1 to prevent its interaction and nuclear translocation of STAT1 [19]. The NS5 protein of Dengue virus, another member of this family, can interact with a KPNA adaptor protein in complex with the KPNB1 carrier, for localization to the nucleus to reduce IL-8 in order to protect virus production [305]. In the *Picornaviridae* family, the 3C (protease) of the Foot-and-mouth disease virus induces KPNA1 degradation, blocking STAT1/2 nuclear import to inhibit the IFN response [306]. On the other hand, the Encephalomyocarditis virus can use its Leader protein to bind to RAN and completely disrupt nucleocytoplasmic transport causing the inhibition of IFN activity in the cell, as well as the efflux of nuclear proteins which can be used by the virus for replication [307].

1.5.2 Negative ssRNA Viruses

Negative single-stranded RNA viruses such as those from the Mononegavirales order can interact with import adaptors to disrupt the innate antiviral response such as in the case of the W protein of Nipah virus interacting with KPNA3 and KPNA4 for its nuclear localization to inhibit the activation of the IRF3-responsive promoter [308], while the VP24 protein of Ebola virus can interact with KPNA1, KPNA5 and KPNA6 to disrupt their interaction with tyrosine-phosphorylated STAT1, thus blocking STAT1 nuclear import and inhibiting ISG production [309, 310]. The Y1 protein of Sendai virus is localized to the nucleus by a RAN-dependent pathway, where it can inhibit ISG expression induced by IFN-α [311].

1.5.3 Induced Nucleoporin Expression during an Innate Antiviral Response

Although cytoplasmic-replication RNA viruses have developed ways to block the induction of an antiviral state primarily by inhibiting the nuclear localization of STAT1, the innate antiviral immune response can induce the expression of certain Nups to alleviate certain effects caused by the viral infection. During an infection by Vesicular stomatitis virus, the M protein targets NUP98 and RAE1 to block mRNA export. However, IFNs can induce the expression of the NUP98 gene, which encodes for both NUP96 and NUP98, and RAE1 to alleviate this mRNA export block [242, 312, 313]. NUP96 is thought to be important for the innate and adaptive immunity as mice with low expression of NUP96 were impaired in the induction of proteins following IFNα or IFNγ stimulation, resulting in mice which are more susceptible to viral infections [314].

1.6 Hypothesis & Objectives

Hypothesis:

The premise of my Master's project is based on the fact that viruses need to interact with host factors in order to promote their life cycle in the cell, while avoiding cellular responses that would interfere with that goal. In the case of HCV, a large number of virus-host interactions were elucidated with the majority not having an effect on viral replication (Germain et al., Mol. Cell. Proteomics 2014). This led us to postulate that these interactions may be beneficial to the virus by affecting other response and processes in the cell such as the innate antiviral immune response, metabolism and apoptosis.

Objective:

The objective of my project is to characterize HCV-host interactors that greatly modulate the innate antiviral immune response. The goal is to comprehend these viral-host interactions in order to uncover novel viral evasion mechanisms and apply it to other viral infections in the hopes of finding novel targets for panviral therapies.

Aims:

- To identify one or more proteins or a family/complex of proteins which greatly modulate the innate antiviral response when silenced from a selected list of HCV-host interactors
- To determine the effect that this/these protein(s) have on the innate antiviral response during a SeV infection biochemically
- To propose mechanisms that would explain the targeting of this/these proteins by viruses in the context of viral immune evasion

Chapter 2: A Microscopy-based RNAi Screen Identifies Key Nucleocytoplasmic Transporters that Control IRF3 and NF-κB Nuclear Translocation and Innate Antiviral Responses Following Viral Infection.

This chapter features the article, currently under preparation, titled "**A Microscopy-based RNAi Screen Identifies Key Nucleocytoplasmic Transporters that Control IRF3 and NF-κB Nuclear Translocation and Innate Antiviral Responses Following Viral Infection."** by Bridget Gagné, Martin Baril Ph.D., and Daniel Lamarre Ph.D.

The first author (Bridget Gagné) performed all experiments, as well as the analysis of results and the making of all figures for this article. The designing of experiments and the writing of the article were primarily done by the first author, with valuable input, insight and revisions by Martin Baril and Daniel Lamarre. Data from the LC-MS/MS analysis was used from the article "Elucidating novel hepatitis C virus-host interactions using combined mass spectrometry and functional genomics approaches." by Germain et al. (Molecular and Cellular Proteomics, 2014).

A Microscopy-based RNAi Screen Identifies Key Nucleocytoplasmic Transporters that Control IRF3 and NF-κB Nuclear Translocation and Innate Antiviral Responses Following Viral Infection.

Bridget Gagné[1,2], Martin Baril[1] and Daniel Lamarre[1,3].

[1]Centre de Recherche du CHUM (CRCHUM), Montréal, Québec, Canada. [2]Département de Biologie Moléculaire et [3]Faculté de Médecine, Université de Montréal, Montréal, Canada.

Correspondence should be addressed to D.L.

Running title: Nucleocytoplasmic transporters in innate antiviral immunity

SUMMARY

The nuclear pore complex is the gate between the nucleus and the cytoplasm, and where nucleocytoplasmic transport of macromolecules occurs via Karyopherin-β carriers such as CSE1L, KPNB1, RAN, TNPO1, and XPO1. In this study, a first RNAi screen, assessing the role of HCV-host interactors in virus-mediated production of IFNB1, identified the NPC and protein import as the most enriched GO terms. In order to obtain a comprehensive understanding of the proteins that are affecting the nuclear translocation of the key transcription factors IRF3 and p65 regulating IFNB1 production, we performed a microscopy-based RNAi screen targeting 60 nucleocytoplasmic transporters following SeV infection. Our kinetic screen allowed the classification of nucleoporins and nucleocytoplasmic transporters into three functional groups: reduced (25), delayed (4) or increased (2) nuclear translocation. Finally, knockdown of KPNB1, the hub protein highly targeted by viruses, led to a dramatic increase in SeV replication and earlier induction of apoptosis. Altogether, we identified key nucleocytoplasmic transporters as potential therapeutic targets for broad-spectrum antiviral therapies.

KEYWORDS: Innate antiviral immunity; nuclear pore complex; NPC; nucleocytoplasmic transport; RNAi screen; microscopy screen; virus-host interaction; nuclear translocation; IRF3; p65; NF-κB; KPNB1.

INTRODUCTION

The proteomic approach and functional RNAi screening of genes are used to elucidate virus-host interactions, such as cellular factors that are required for viruses to survive and replicate in host cells. The nuclear pore complex (NPC), composed of 30 proteins known as nucleoporins (Nups), and nucleocytoplasmic transporters have been found to significantly affect viral replication in many RNA viruses studied using these extensive screens [1-5]. Necessary interactions between viral proteins and NPC components and their transporters were seen in hepatitis C virus (HCV) [1, 6, 7], picornavirus [8], and HIV-1 [9, 10] to name a few. Influenza A virus, one of the few negative-sense RNA viruses to replicate in the nucleus, uses IPO5 to targets its polymerase complex to the nucleus, complexes with NXF1 and its co-factors to block mRNA export, and then uses XPO1 for the export of vRNPs to the cytoplasm [11-13]. In the case of HCV, the viral proteins core, NS2, NS3 and NS5A contain nuclear localization signals (NLS), and core is the only one to encode a XPO1-dependent nuclear export signal (NES) [14, 15], which suggests that the shuttling of core to the nucleus and back to the cytoplasm early in the HCV life cycle is important for viral replication [15]. Most recently, nuclear signals within core and NS2 were found to be important for early stages of viral replication, while NS3 and NS5A NLSs were important for later stages of viral replication such as assembly and egress [7]. There is also evidence that Nups accumulate in specific regions of the cytoplasm where HCV replication occurs, leading to the hypothesis that these Nups may be gating these viral compartments to favor viral replication and to prevent cytosolic RLR sensing following a viral infection [6, 7]. This hypothesis is supported by the

result that KPNB1, RAN and TNPO1, all involved with nucleocytoplasmic transport and elucidated to interact with NS3/4A, decrease HCV replication when silenced [1].

Viruses are also able to persist with their infections by interacting with NPC and its nucleocytoplasmic transporters to evade the innate immune antiviral response, furthering viral growth advantage. HCV NS3/4A was showed to bind KPNB1 and prevent the interaction with STAT1, the translocation of the ISGF3 complex to the nucleus and the production of ISGs [1]. Poliovirus and human rhinovirus encode a 2(A) protease, which is able to cleave NUP62, NUP98 and NUP153, disrupting nucleocytoplasmic trafficking such as protein import and mRNA export [16-19]. Nidovirales members can disrupt the transport of important innate antiviral factors to the nucleus to inhibit the production of ISGs such as in the case of Porcine reproductive and respiratory syndrome virus (PRRSV) degrading KPNA1, blocking ISGF3 nuclear import, while SARS coronavirus (SARS-CoV) tethers KPNB1 to ER and Golgi membranes, blocking STAT1 nuclear import [20, 21]. Mononegavirales members can interact with import adaptors to disrupt the innate antiviral response such as in the case of Nipah virus interacting with KPNA3 and KPNA4 for its viral protein nuclear localization to inhibit the activation of the IRF3-responsive promoter [22], while Ebolavirus interacts with KPNA1, KPNA5 and KPNA6 to disrupt their interaction with tyrosine-phosphorylated STAT1 for nuclear import, inhibiting ISG production [23, 24].

The NPC is the only structure where nucleocytoplasmic transport of macromolecules occurs [25]. The nucleocytoplasmic transport of proteins consists of 5 major players: KPNB1 and TNPO1 for import, XPO1 and CSE1L for export, and RAN for the energy gradient of this

active process [26]. For protein import from the cytoplasm into the nucleus, proteins with a NLS are bound by a Karyopherin-α (Kapα) adaptor protein and then both the NLS-containing protein and the adaptor are bound by a Karyopherin-β (Kapβ) carrier protein, which mediates the nuclear import of this complex [26, 27]. The main Kapβ carrier proteins for import are KPNB1 and TNPO1, which recognize a classical and a PY-NLS motif, respectively [26, 28]. For protein export from the nucleus into the cytoplasm, a Kapβ carrier protein, bound to Ran-GTP, binds directly to a protein containing a NES and transports this export complex to the cytoplasm. The main Kapβ carrier protein for export is XPO1, which binds to leucine-rich NES [26]. CSE1L is a Kapβ carrier protein involved in export, but for the recycling of Kapα adaptor proteins back to the cytoplasm for the formation of import complexes [26]. RAN, bound to either GDP or GTP, is important for establishing the energy gradient, giving directionality to the import and export pathways. The binding of Ran-GTP to the Kapβ of import complexes once they have entered the nucleus dissociates these complexes, while Ran-GAP hydrolyzation of Ran-GTP to Ran-GDP, bound to the Kapβ of export complexes, causes the complex to dissociate. Ran-GDP is recycled back to the nucleus via NUTF2, where its GDP is exchanged for a GTP by RCC1 for the formation of export complexes [26].

In this study, HCV-host interactors identified by LC-MS/MS analysis were investigated on virus-mediated innate antiviral response of knockdown cells expressing an inducible *IFNB1* promoter-driven reporter. Those with the greatest modulatory effects on IFNB1 production were enriched in GO Terms associated with the NPC and protein transport. Interestingly, these proteins were all elucidated to be NS3/4A interactors. The knockdown of KPNB1, the main Kapβ import carrier, showed the most significant decrease of ISG56 levels, which correlated

with a rapid and dramatic increase in viral protein levels. As the NPC and its transporters are found to interact with proteins from many viruses, the comprehensive effect of knocking down Nups and nucleocytoplasmic transporters on the innate antiviral immunity was further investigated by studying their effect on the nuclear translocation of transcription factors IRF3 and p65 required for IFNB1 production. Using a microscopy-based RNAi screen, we identified a major set of proteins that reduced the number of nuclei containing IRF3 and p65 over the time course of 10 hours post infection, and decreased IFNB1 production upon knockdown. Key nucleocytoplasmic transporters decreasing nuclear translocation included the major players KPNB1 and TNPO1 for import, CSE1L for export and RAN for the energy gradient. Interestingly, we observed a second set of proteins that delayed, increased or had differential effect on IRF3 and p65 nuclear translocation, but reduced IFNB1 production upon knockdown suggesting a role in the transport of other factors during the innate antiviral response. Finally, abrogation of the innate antiviral response and dramatic increase of viral proteins in KPNB1 knockdown cells led to an earlier and significant induction of apoptosis, highlighting the link between the innate antiviral response and viral replication.

RESULTS

Effect of viral-host interactor knockdown on the innate antiviral immunity

As previously described by our group, HCV-host interactors were identified using an IP-based approach of six 3xFLAG-tagged HCV proteins (core, NS2, NS3/4A, NS4B, NS5A and NS5B) [1]. Host proteins interacting with these viral proteins were analyzed by LC-MS/MS with 426 proteins being reproducibly detected with 2 or more peptides. Figure S1 shows the relative quantity of peptides found for 132 of these 426 proteins that were significantly enriched in one of the FLAG-IPs. However, only 13 of these 132 HCV interactors were described as modulators of the HCV replication and infection by Germain et al. (2014) [1], suggesting that these virus-host interactions may benefit the virus through the alteration of the innate antiviral immune response.

To test this possibility, we used ~5 independent shRNA-expressing lentiviral particles to knockdown each gene encoding the 132 proteins shown in Figure S1. As described in *Baril et al.*, the effect of these knockdowns on the innate antiviral immunity was measured using HEK 293T and A549 cells stably expressing an inducible *IFNB1* promoter driving the firefly luciferase reporter [29]. Infection of these cells with SeV activates the RLR pathway, ultimately leading to the nuclear translocation of the transcription factors AP-1, NF-κB and IRF3. These transcription factors will bind to the *IFNB1* promoter and induce the transcription of firefly luciferase, which is monitored by luminescence to quantify the innate antiviral response. In parallel, HEK 293T cells stably expressing the firefly luciferase from a nonimmune-related endogenous elongation factor 1 alpha (*EF1α*, also known as *EEF1A1*)

promoter are used as a control to measure cellular fitness and assess potential non-specific effects of shRNAs. RNAi screening in HEK 293T cells identified 15 virus-host interactors acting as positive regulators (PR) and 20 acting as negative regulators (NR) of the innate antiviral immunity (Figure 1A). The second RNAi screening in A549 cells identified 12 PR and 17 NR of the innate antiviral immunity (Figure 1B). In total, 53 virus-host interactors, with 11 being common in both cell lines, specifically affected reporter expression from the *IFNB1* promoter with at least two independent shRNAs, without affecting the constitutive expression of the *EF1α* promoter (see supplemental Table 2 for complete results of the 132 genes). The effect of silencing these 53 genes in HCV replication and the innate antiviral immunity is summarized in Figure S2, where only 12 greatly affected both viral replication and the immune response. The other 41 genes affected solely the innate antiviral immunity, suggesting that HCV proteins may be interacting with these host factors to subvert the response.

Gene Ontology enrichment

To elucidate whether these 53 virus-host interactors, which affect the innate antiviral immunity, are associated with one another through a particular complex or process in the cell, Gene Ontology (GO) enrichment was performed. Table I lists 10 statistically significant enriched terms ($p < 0.05$) in descending order of the most enriched GO Terms with the list of genes associated with each term. The two most enriched terms are Protein Import into the Nucleus, docking (enriched 72 fold with four proteins: CSE1L, KPNB1, TNPO1, XPO1) and Nuclear Pore (enriched 23 fold with six proteins: CSE1L, KPNB1, LBR, RAN, TNPO1, XPO1). While it could seem peculiar that a cytoplasmic virus like HCV would interact with

proteins involved with the NPC, it was previously shown that some HCV proteins like NS3 contained a NLS [7] and that the NPC could contribute to the compartmentalization of viral replication in the membranous web [6]. In addition, NS3/4A was shown to interact with KPNB1 to prevent STAT1 translocation to the nucleus following stimulation of the JAK-STAT signaling pathway by Type I IFNs [1]. With the exception of LBR, all proteins associated with the NPC and nucleocytoplasmic transport were elucidated to interact with NS3/4A, which is the main player in the evasion of the innate antiviral immune response through the cleavage of important signaling adaptors such as MAVS in the RLR pathway [30, 31] and TRIF in the TLR pathway [32].

Effect of silencing nucleocytoplasmic transporters on viral replication

Viruses interact with host proteins to promote viral growth by either hijacking cellular machineries to facilitate their replication or by disrupting the innate immune responses. Since knockdown of the five nucleocytoplasmic transporters, elucidated from the LC-MS/MS analysis as HCV NS3/4A interactors, all negatively affected IFNB1 production, we wanted to assess their potential effect on viral replication. Knockdown of XPO1, CSE1L, RAN, KPNB1 and TNPO1 in A549 (Figure 2) and HEK 293T (Figure S3) cells infected with SeV for 8 and 24 hours showed that KPNB1 knockdown led to a drastic increase in SeV replication in both cell lines in comparison to NT. This increase in SeV replication by KPNB1 knockdown was accompanied by an almost complete inhibition of the antiviral response at 8 hours as measured by ISG56 protein induction in A549 (Figure 2) and 24 hours in HEK 293T cells (Figure S3). These results suggest that KPNB1 could be targeted by the virus to disrupt the innate antiviral immunity and to promote viral replication, a mechanism employed by HCV's NS3/4A in

which it prevents the nuclear translocation of STAT1 to the nucleus via its interaction with KPNB1 [1].

RNAi screen targeting the NPC and its transport proteins

The interaction of the NPC and its transporters with HCV proteins combined with their effects on the innate antiviral immune response make this complex of proteins a study of interest to explore more fully [1, 6]. Due to their physiological role, we hypothesized that the observed effect of transporter proteins on the innate antiviral immunity was mediated by the regulation of the nuclear translocation of important transcription factors for the response. Although the nuclear translocation of IRF3 and p65 both occur after a phosphorylation event [27, 33], it is still not clear what kinds of interactions mediate this transport. IRF3 and p65 have both been shown to bind to more than one Kapα adaptor [34-37], but it has not been shown which Kapβ carrier or Nups are involved in this nuclear transport.

To test our hypothesis, a microscopy-based RNAi screen was performed on 60 proteins associated with the NPC and nucleocytoplasmic transport, focusing on the nuclear translocation of IRF3 and p65, important transcription factors for the Type I interferon response. Figure 3A explains in detail how the RNAi microscopy-screen was done. In brief, A549 cells were plated in transparent 96-well plates and every well was infected with a single lentivirus-encoding shRNA (~5 independent shRNAs per gene for 60 genes) at a MOI of 10 for four days to allow efficient knockdown of the targeted proteins. A control shRNA NT was included in each 96-well plate. Prior to fixation and permeabilization, cells were infected with SeV for 1, 3, 5, 8 or 10 hours, before nuclear labeling with Hoechst and antibody staining for

IRF3 or p65. Images of cells were captured in nine pre-determined fields for each well using an Operetta High Content Screening (HCS) Microscope. Images were then processed using Harmony software to delimitate the nuclear region and measure the fluorescence intensity of IRF3 or p65 within the nucleus. For each 96-well plate, a fluorescence cut-off was set to allow automated discrimination of cells with (green) or without (red) IRF3 or p65 nuclear staining (Figure 3A). This information allowed us to calculate the percentage of cells with IRF3 or p65 nuclear staining and to evaluate the effect of each shRNA on the nuclear translocation of these two transcription factors following SeV infection.

A representative time course experiment performed with the control shRNA NT showing the nuclear translocation of IRF3 or p65 over a 10-hour SeV infection is presented in Figure 3B. Graphic representation of these results can be plotted using the percentage of positive nuclear staining for IRF3 or p65 (Figure 3C). Over the course of a 10-hour SeV infection, we observed an increase in both IRF3 and p65 nuclear staining culminating to approximately 75% of positive cells at five hours post-infection, followed by a decrease to approximately 30% of positive cells at 10 hours. This microscopy kinetic was confirmed biochemically using cell fractionation and Western blot analysis (Figure 3D). Following SeV infection, we observed IRF3 phosphorylation on Ser386 starting at 1 hour, culminating at 5 hours and decreasing at 10 hours post-infection, similar to the amount of total IRF3 observed in the nucleus at these time points. Phosphorylated forms of IRF3 can also be observed using the total IRF3 antibody in both cytoplasmic and nuclear fractions. Phosphorylation of the NF-κB negative regulator NFKBIA on Ser32, leading to its ubiquitination and degradation, increases gradually from 1 to 10 hours post-infection. This degradation of NFKBIA allows p65 nuclear translocation, which

starts at 1 hour, culminates at 5 hours and decreases at 10 hours post-infection. This nuclear translocation of both IRF3 and p65 lead to the induction of antiviral response genes including ISG56 protein which is detectable starting at 3 hours post-infection. The cytoplasmic and nuclear fraction purity was confirmed by the strict histone 1 (H1) staining in the nucleus and constant p65 levels in the cytoplasm (coupled with the absence of p65 in the nucleus in the absence of SeV infection). Altogether, these biochemical observations correlated with the HCS imaging analysis, validating our approach to identify NPC components and their transporters in regulating the nuclear import of IRF3 and p65 transcription factors.

Effects of NPC and transporter proteins knockdown on nuclear translocation of IRF3 and p65

Using this methodology, we were able to directly measure the effect of every RNAi targeting 60 Nups and transporter proteins on the nuclear translocation of IRF3 and p65. As an example, three independent shRNA targeting KPNB1, which is the main Kapβ carrier for import, significantly affected nuclear translocation of both IRF3 and p65 when compared to the shRNA NT (Figure 4A). To facilitate their visualization and analysis, results obtained with the control shRNA NT were normalized to zero for every time point, allowing shRNA KPNB1 to be represented as relative percentage in the nucleus (Figure 4B). Using this representation, we showed that KPNB1 knockdown with three independent shRNAs leads to a strong decrease of IRF3 translocation to the nucleus at three and five hours post-infection, before coming back to normal level at eight and ten hours post-infection. A similar pattern is observed on p65 nuclear translocation, although with a less drastic decrease at three and five hours post-infection and culminating with increased p65 nuclear staining at eight and ten hours post-infection

compared to the shRNA NT. In addition, we used caspase-mediated poly [ADP-ribose] polymerase 1 (PARP1) cleavage, creating 89 kDa and 24 kDa fragments, to assess virus-mediated apoptosis. We observed that the increased SeV replication observed in KPNB1 knockdown A549 cells is accompanied with an earlier induction of apoptosis starting at 1 hour post-infection instead of 3 hours post-infection in the shRNA NT treated cells (Figure 4C). Altogether, these results demonstrate that KPNB1 knockdown blocks IRF3 and p65 translocation to the nucleus, impairing the antiviral response, which in turns likely leads to increased viral replication and cellular apoptosis.

Our RNAi screen allowed us to identified 33 Nups and transporter proteins for which knockdown with at least two independent shRNAs significantly affected nuclear translocation of IRF3 or p65 following SeV infection. Knockdown led to a decrease in translocation for 25 genes, a delay in translocation for 4 genes (KPNA3, NUP43, NUPL2 and TNPO2), an increase in translocation for 2 genes (KPNA4 and XPO1) and differential effect on IRF3 and p65 for 2 genes (KPNA5 and RANBP3). We further divided these 33 nucleocytoplasmic transporters and Nups into subgroups according to their function and localization, respectively. In Figure 5, we observed that knockdown of KPNA1-6 led to a distinct phenotype for 5 out the 6 adaptors with a major decrease of p65 nuclear translocation at 3 hours of SeV infection, with the exception of KPNA4. The effect of these adaptors on IRF3 is more variable as KPNA5 and KPNA4 delayed and increased translocation, respectively. The knockdown of KPNA5 shows a differential effect with a delay in translocation for IRF3 and a decrease in translocation for p65. In Figure 6, the functionally-grouped nucleocytoplasmic transporters mostly decrease the translocation of these transcriptions factors, which is expected

of the Kapβ carriers involved in import (IPO for importins and TNPO for transportins). However, TNPO2 knockdown demonstrated a delay in translocation for both factors, differing from TNPO1's knockdown phenotype (Figures 5B and S5). This suggests that TNPO2 is not a redundant transporter of TNPO1, in contrast to previous reports concerning the transport of HNRNPA1 and HUR [38]. The knockdown of the main Kapβ carrier for export XPO1 increased nuclear translocation of these factors, but with a transient increase for IRF3 and a sustained increase for p65 (Figures 5C and S6). Similar to KPNA5, RANBP3 knockdown caused a delay in IRF3 translocation and a transient decrease in p65, suggesting that RANBP3 may be using KPNA5 as an adaptor due to the similar phenotype for both IRF3 and p65 translocation (Figures 5C and S6). In Figure 6, the Nups are categorized by their localization in the NPC with the majority decreasing both IRF3 and p65 nuclear translocation, with the exception of NUPL2 (Figures 6A and S9) and NUP43 (Figures 6B and S10). NUPL2 knockdown increases IRF3 translocation at very early stages of infection, and it correlates with XPO1 knockdown effect on IRF3 as NUPL2 promotes XPO1 function [39]. NUP43 knockdown shows similar nuclear translocation phenotypes for both factors as seen in KPNA5 and RANBP3 knockdown, suggesting that NUP43 may be involved in the import of this RANBP3-KPNA5 import complex through the NPC.

Effects of NPC and transporter proteins knockdown on pIFNB1 induction following SeV infection

In parallel to the microscopy screen, we performed an A549 pIFNB1-LUC screen to characterize the effect of every shRNA on the *IFNB1* promoter induction following SeV infection. Our results showed that the majority of shRNAs significantly affecting the nuclear

translocation of IRF3 or p65 also decreased *IFNB1* promoter induction 6 hours post-SeV infection (including XPO1 and KPNA4 that increased IRF3 and p65 nuclear levels). *IFNB1* promoter results are presented in histograms next to each nuclear translocation curves in Figures 4A, 5B and S4-S12 (complete results can be found in supplementary Table S4). These histograms also included the effect of every shRNA on the cellular proliferation and survival, which is the ratio of the total number of nuclei for every shRNA in our microscopy screen divided by the total number of nuclei for the control shRNA NT included in the same 96-well plate. This allows us to discriminate between general effects of these shRNAs on cellular fitness versus their actual role in the innate antiviral immunity.

DISCUSSION

The goal of the study was to elucidate novel proteins, families or processes which affected the innate antiviral immunity from a subset of proteins previously elucidated to be interacting with one of six HCV proteins [1]. The main hypothesis was that viral-host interactors not affecting HCV replication when knocked down would instead affect the innate antiviral immunity, giving a plausible explanation to the virus-host interaction as the virus could be hijacking these host factors and interfering with their role in the immune response, thus allowing the virus a growth advantage in the cell [1]. From the viral-host interactors which greatly affected the innate antiviral response when knocked down, there was enrichment in the NPC term, more specifically in proteins involved in nucleocytoplasmic transport (Table I). This group of proteins leads to two distinct observations: the first being that, with the exception of LBR, these proteins were all elucidated to interact with NS3/4A (Figure S1); the second is that when knocked down during a viral infection, they all dramatically decreased the production of IFNB1 (Figure 1). As the viral life cycle of HCV takes place exclusively in the cytoplasm, it could seem surprising that HCV proteins interact with nucleocytoplasmic transporters [40]. However, many of the HCV proteins contain a NLS (core, NS2, NS3 and NS5A) and the core protein also contains a XPO1-dependent NES [14, 15], suggesting that shuttling of core in and out of the nucleus early in the HCV life cycle is important for viral replication [15]. There is also evidence which showed that Nups accumulate in specific regions of the cytoplasm where HCV replication occurs, leading to the hypothesis that these Nups may be gating these viral compartments to favor viral replication [7] and to prevent cytosolic RLR sensing following a viral infection [6]. This hypothesis is supported by the result that KPNB1, RAN and TNPO1,

all involved with nucleocytoplasmic transport and elucidated to interact with NS3/4A, were previously shown to decrease HCV replication [1]. For example, TNPO1 is well-known for mediating the nuclear import of HNRNPA1 through its M9 NLS [38, 41]. In the context of HCV, HNRNPA1 binds to the 5' and 3' UTR of HCV RNA [42], NS3/4A [43] and NS5B [42] and its silencing reduced viral replication [42, 44]. NS3/4A may be hijacking TNPO1 to cause cytoplasmic accumulation of HNRNPA1 leading to an increase in viral RNA translation from the HCV IRES [45], a mechanism that is also seen in HIV-1 [46]. It has also been shown that core and NS5A interact with KPNA1 [6], suggesting that CSE1L, which exports Kapα adaptor proteins back to the cytoplasm [26], could be required for the formation of viral protein import complexes in the cytoplasm. CSE1L was also shown to have an import function for the HIV-1 Vpr protein bound to KPNA1, where it imports and dissociates this complex in the nucleus [47]. In this study, we have elucidated XPO1 as a NS3/4A interactor (Figure S1) and XPO1 was previously shown to export both the core protein early in HCV infection [15] and DDX3X [48], which is targeted by core to lipid droplets [49, 50]. This suggests that XPO1 may be targeted by multiple HCV proteins over the course of HCV's replication cycle.

From the innate antiviral response stand point, we showed that, upon viral infection, reducing the expression of the main Kapβ nuclear import carrier KPNB1 reduces the nuclear translocation of IRF3 and p65, thus downregulating IFNB1 and ISG56 production. Importantly, KPNB1 knockdown led to a dramatic increase of SeV replication (Figures 2 and S3), supporting the hypothesis that affecting the innate antiviral response can directly impact viral replication. Interestingly, we observed an increase in KPNB1 protein level following SeV infection (Figure 4C) and previous report have shown that KPNB1 and other proteins involved

in nucleocytoplasmic transport such as RCC1, the Guanine Exchange Factor for RAN [51], were found to be overexpressed in hepatocellular carcinomas after liver transplantation due to chronic HCV infection [52]. Similarly to KPNB1, knockdown of CSE1L, which is involved in both import and export, as it exports Kapα adaptors for the formation of import complexes [26], also reduces the innate antiviral response. On the other hand, XPO1 is associated with protein export and has been shown to associate with DDX3X for nuclear export in the presence of HIV-1 rev protein [48]. Here we show that XPO1 knockdown leads to an accumulation of IRF3 and p65 in the nucleus (Figures 6C and S6), an observation in line with previously observed nuclear accumulation of p65 upon treatment with leptomycin B, a XPO1 inhibitor [53]. Despite this nuclear accumulation of transcription factors, XPO1 knockdown led to a decrease IFNB1 and ISG56 induction following SeV infection. This might result from the depletion of DDX3X from the cytoplasm, where it associates with TBK1 and IKBKE to enhance the induction of the IFN promoter [54, 55]. In addition, XPO1 knockdown could reduce the type I IFN JAK-STAT amplification loop by blocking the nuclear export of IFN-α1 mRNA [56, 57]. While TNPO1 is not known to bind to any effectors of the innate antiviral response, p65 was predicted to contain a hydrophobic PY-NLS that is recognized by TNPO1 [28]. This could explain the decreased IFNB1 production upon TNPO1 knockdown, as well as the decrease in p65 nuclear translocation (Figure S5).

In terms of adaptors, only KPNA3 and KPNA4 were determined to interact with the NLS of IRF3 *in vitro* [34], increasing the importance of determining how IRF3 enters the nucleus during a viral infection. Our results show that knocking down of the 6 Kapα adaptors individually led to distinct effects on IRF3 nuclear translocation. It seems that KPNA2, 3 and

5 are all involved with IRF3 nuclear import at the beginning of a viral infection, while KPNA1 and KPNA4 seems to affect its export. Near the end of the time course, KPNA1 affects nuclear import, while KPNA4 and KPNA5 affect its export. KPNA2 and KPNA3 do not have major effects on the translocation at late time points, while KPNA6 barely affects the translocation at all (Figure 5). It may seem strange to say that adaptors which are only used in import could have an effect on the export of a protein; however, trafficking of proteins is more complicated than import to the nucleus and export to the cytoplasm. It is possible that adaptors affecting export are actually just not releasing the protein from the import complex in the nucleus, which would explain why we could see IRF3 in the nucleus, but if it is still bound to an adaptor protein, then it is not carrying out its function.

KPNA1 (Importin α5), KPNA2 (Importin α1), KPNA3 (Importin α4), KPNA4 (Importin α3), KPNA5 (Importin α6) and KPNA6 (Importin α7) were all shown to be important for p65 nuclear translocation following SeV infection or TNF-α stimulation [35-37]. Our results demonstrated that the knockdown of these 6 Kapα adaptor proteins did indeed all effect p65 nuclear translocation, validating previous studies, with all except one showing the phenotype where p65 nuclear translocation dramatically decreased 3 hours of post-SeV infection (Figure 5). An interesting observation from this data is that KPNA4 knockdown increased p65 nuclear translocation, however it is the adaptor that is most targeted whether by host proteins, viral infections and even a fungal metabolite in order to disrupt p65 nuclear import by either reducing the expression of KPNA4 [58] or preventing the interaction by binding to KPNA4 [59] or to p65 [60], respectively. It is possible that KPNA4 is the main controller of p65 import, as the knockdown of the other adaptors causes a decrease at one time point (3 hours),

but is quickly brought back to normal levels at the next time point (5 hours). When KPNA4 is silenced, the rest of the adaptors may be over-compensating, causing this increase of p65 during the entire SeV infection time course.

There is virtually no literature which suggests a carrier for IRF3 nuclear translocation during a viral infection. Our results show that the importins had a major effect on IRF3 import upon knockdown with IPO4 having a major effect towards the end of the time course, while IPO7 and IPO8 had a general effect throughout the time course (Figures 6 and S4). TNPO1 and TNPO3 knockdown reduce IRF3 nuclear translocation throughout the time course, however TNPO2 knockdown increases nuclear translocation after the 5 hour time point, which suggests that carriers involved in the nucleocytoplasmic transport of IRF3 is not necessarily the same throughout the entire SeV infection (Figures 6 and S5).

In terms of import carriers for p65, one study found KPNB1 to be the main import carrier via the p65 NLS [37], which is supported by our findings (Figure 4). Another identified carrier for p65 import was IPO8, which apparently transports this factor in a NLS-independent fashion [37], where in our results we see a decrease in nuclear translocation during the entire time course (Figures 6 and S4). IPO7 and TNPO1 also seem to be potential import carriers as their knockdown reduces p65 nuclear translocation (Figure 6), which supports the finding of a predicted NLS that is recognized by TNPO1 [28]. IPO4 and TNPO3 knockdown only seem to affect import at 3 hours of SeV infection, and IPO4 knockdown increases p65 translocation at the first hour of infection (Figure 6). TNPO2 knockdown, like in the case of IRF3 nuclear translocation, increases p65 nuclear import after the 5 hour time point (Figure 6).

As the main carrier for export, XPO1 was shown to bind to IRF3 NES and the use of leptomycin B, a XPO1 inhibitor, demonstrated an accumulation of IRF3 in the nucleus [34]. Our results supported this with XPO1 knockdown causing nuclear accumulation of IRF3 during the early phase of the infection (Figures 6 and S6). RANBP3, a XPO1 cofactor for protein export [61, 62], increases nuclear translocation of IRF3 only at 8 hours of SeV infection. This is not the case of p65 nuclear translocation as RANBP3 knockdown affects only the nuclear import at 3 hours of SeV infection. It is not surprising that CSE1L knockdown would cause a dramatic decrease of nuclear IRF3 and p65 during the entirety of the SeV infection time course (Figures 6 and S6) as it is responsible for the export of Kapα back to the cytoplasm, and we have shown that the Kapα do play a role in the nuclear translocation of both factors (Figure 5).

The knockdown of proteins, which are known to export mRNA, such as NXF1 (also known as TAP), seems to have an effect on the import of IRF3 and p65 into the nucleus (Figures 6 and S7). However, it is not clear whether this decrease in IRF3 and p65 is due to the fact that the export of their mRNAs are reduced, diminishing the amount of proteins translated, thus decreasing the amount that is able to enter the nucleus.

The silencing of RAN affected both IRF3 and p65 nuclear translocation with a most drastic effect on IRF3 during 3 to 5 hours of SeV infection (Figure 6). This drastic effect may be due to two reasons: first, RAN in its GTP form is required to bind to import complexes to liberate NLS-containing proteins into the nucleus; second, CSE1L requires RanGTP to drive the export of Kapα back to the cytoplasm for the formation of import complexes [26]. NUTF2 and

RCC1 affect IRF3 nuclear import, but only at the beginning of the infection, as the knockdown of these two affect little during the last 2 hours of the time course (Figure 6). It seems that p65 nuclear import is most dependent on the availability of RanGTP in the nucleus as the knockdown of NUTF2, responsible for transporting RanGDP back to the nucleus, and RCC1, responsible for exchanging RanGDP for RanGTP, decrease p65 nuclear translocation just as much as RAN knockdown.

Multiple nucleoporins had similar phenotypes when knocked down on the nuclear translocation of IRF3 and p65, where the majority had a major effect at 1, 3, and 5 hours of SeV infection and went back to normal levels at 8 and 10 hours of infection (Figure 7). NUP88 was previously shown to regulate NF-κB activity via its nucleocytoplasmic transport [63], which is supported by our findings with a significant decrease of p65 nuclear translocation at 3 hours of SeV infection (Figures 7C and S11). Interestingly, hepatocellular carcinomas have increased levels of NUP88 [64], which can cause constitutive activation of NF-κB in both the nucleus and cytoplasm [63].

The only Nup with a distinct phenotype is NUPL2, which is known to promote protein export via XPO1 [39], and shows an increase at 1 and 10 hours of infection for IRF3 nuclear translocation, and 8 hours for p65 nuclear translocation (Figures 7 and S9). NUPL2 was found to interact with HIV-1 Vpr for docking at the nuclear envelope, suggesting that Vpr disrupts NUPL2 function to allow for the import of viral DNA into the nucleus [65].

Viruses, including HIV-1, have been shown to interact with NPC proteins such as NUP153 and nucleocytoplasmic transporter TNPO3 to evade the innate immune response [66]. RANBP2 was shown to reduce HIV-1 replication when silenced, and was important for HIV-1 nuclear import [67]. However, RANBP2 silencing caused an increase in viral replication for Japanese encephalitis virus [68, 69]. NUP214 was determined to be a host factor for enterovirus 71 replication as the overexpression of this Nup increased viral replication [70]. In this context, our work does not only allow insight into this complex nucleocytoplasmic transport machinery by elucidating components involved in the nuclear translocation of IRF3 and p65 transcription factors, but also identifies key host proteins targeted by viral evasion mechanisms as new potential therapeutic targets to treat a broad range of viral infections.

EXPERIMENTAL PROCEDURES

Cell culture

HEK 293T (Human Embryonic Kidney) cell lines were cultured in Dulbecco's Modified Eagle's Medium (DMEM, Wisent). A549 (human lung adenocarcinoma epithelial) cell lines were cultured in Ham's F-12 medium (Invitrogen). Both media were supplemented with 10% fetal bovine serum, 100 units/ml penicillin, 100 µg/ml streptomycin and 2 mM glutamine (all from Wisent) and 1% nonessential amino acids (Invitrogen) at 37 °C in an atmosphere of 5% CO_2. Cell populations of HEK 293T and A549 stably harbouring the pIFNB1-LUC and of HEK 293T stably harbouring the pEF1α-LUC used in the screens were produced after selection with 200µg/ml of hygromycin B (Wisent) and were previously described [29]. Transfections were performed with linear 25 kDa polyethylenimine (PEI) (Polysciences, Inc) at 3 µg PEI to 1 µg DNA ratio.

Expression vectors

RAN cDNA was purchased from GE Dharmacon/Open Biosystems. Following PCR-amplification, PCR product was cloned using Pfl23II/NotI enzymes into pcDNA3.1_FLAG-MCS(MB) expression vector [31]. 3xFLAG-NS3/4A, FLAG-XPO1 and MYC-NS3/4A have been described before [1]. All constructs were verified by Sanger sequencing and subsequent Western Blot analysis.

Lentiviral shRNA library production

From MISSION TRC lentiviral library (Sigma-Aldrich), 132 MS hits were selected and shRNA were produced as follows: five different shRNA-expressing lentiviruses per gene were produced individually in HEK 293T cells ($2x10^4$) that are plated one day prior to transfection. Transfections were performed using a Biomek FX (Beckman Coulter) enclosed in a class II

cabinet according to MISSION® Lentiviral Packaging Mix protocol (SHP001). Viruses were collected at 24 and 48 hours post transfection and were pooled prior to freezing. A non-target sequence (NT) shRNA-expressing control lentivirus and 4% of random samples of each plate were used to measure lentiviral titers for quality control purposes. Titers were determined by limiting dilution assays using HeLa cells. Briefly, samples were diluted in complete DMEM (1:400 or 1:10,000) and added to HeLa cells. Media was changed at day 3 and 5 with complete DMEM containing 1 μg/ml puromycin (Wisent). After four days of selection, cells were stained with 1.25% crystal violet and plaque-forming units (PFU) were counted to determine viral titer.

Large-scale shRNA production

293T cells were transfected with pRSV-REV, pMDLg/pRRE, pMD2-VSVg [71] and various shRNA-expressing pLKO.1-puro constructs (Sigma-Aldrich) using linear 25 kDa PEI (Polysciences, Inc) at 3 μg PEI to 1 μg DNA ratio. 48 hours after transfection, cell media was collected, filtered (0.45 μm filter), and aliquoted. Multiplicity of infection (MOI) was determined using limiting dilution assays as described in previous section.

Firefly luminescence assay

For screening, cells were seeded in white 96-well plates at a density of 5,000 HEK 293T pIFNB1_LUC, 5,000 A549 pIFNB1_LUC and 1,250 HEK 293T pEF1α-LUC in 100 μl of complete phenol-red free DMEM containing 4 μg/ml polybrene. Infection with lentivirus encoding shRNA were carried out immediately after cell seeding at a MOI of 10 and incubated for three days at 37 °C in an atmosphere of 5% CO_2. Cells were infected with 100 HAU/ml of SeV (Cantell Strain, Charles River Labs) for 6 hours for A549 and 16 hours for HEK 293T cells before cell lysis and firefly luminescence reading in a 100 mM Tris acetate,

20 mM Mg acetate, 2 mM EGTA, 3.6 mM ATP, 1% Brij 58, 0.7% β-mercaptoethanol and 45 μg/ml luciferine pH 7.9 buffer. All infections were performed in an enclosed class II cabinet.

Operetta microscopy

A549 cells were plated on clear 96-well plates at a density of 1000 cells in 100 μl complete Ham's F-12 medium containing 4 μg/ml polybrene. Infection with lentivirus encoding shRNA (five individual shRNAs per gene) were carried out immediately after cell seeding at a multiplicity of infection (MOI) of 10 and incubated for four days at 37 °C in an atmosphere of 5% CO_2. As control the MISSION® shRNA NT clone (Sigma SHC002) was included in each 96-well plate. Cells were infected with 100 HAU/ml of SeV (Cantell Strain, Charles River Labs) for 0, 1, 3, 5, 8 or 10 hours before being fixed with 4% paraformaldehyde-containing PBS for 20 minutes at room temperature and then permeabilized in 0.2% Triton X-100/PBS for 15 minutes. Blocking was made in PBS with 10% normal goat serum, 5% bovine serum albumin (BSA) and 0.02% sodium azide for 45 minutes at room temperature. Following three rapid washes, cells were labelled with mouse anti-IRF3 (SL-12; Santa Cruz Biotechnology) or rabbit anti-p65 (C-20; Santa Cruz Biotechnology) primary antibodies diluted in 5% BSA/0.02% sodium azide/PBS for 2 hours. Wells were washed three times in PBS and then labelled with anti-mouse AlexaFluor 488 or anti-rabbit AlexaFluor 488 secondary antibodies (Invitrogen) diluted in 5% BSA/0.02% sodium azide/PBS for 1 hour. Cells were extensively washed and incubated with Hoechst dye (Invitrogen) at a final concentration of 1μg/mL in PBS. Images of cells were captured in nine predetermined fields for each well (Operetta High Content Screening Microscope; Perkin Elmer) and images were processed using Harmony (Perkin Elmer). Cut-off for nuclear staining for IRF3 and p65 were between 230 to 300 and 515 to 735, respectively. Percentage of cells with IRF3 or p65 nuclear staining was calculated

by dividing the number of nuclei where nuclear fluorescence was higher than the cut-off for IRF3 or p65 staining by the total number of nuclei stained by Hoechst for the nine fields. The effect of a shRNA on cell proliferation and survival was evaluated by dividing the total number of nuclei in the nine fields of the five time points and dividing it by the total number of nuclei in the nine fields of the six time points of the shRNA NT control well included in every 96-well plate.

Western Blot analysis

Cells were washed twice with ice-cold phosphate-buffered saline (PBS; Wisent), harvested and lysed in 10mM Tris-HCl, 100mM NaCl, 0.5% Triton X-100, pH7.6 with EDTA-free Protease Inhibitor Cocktail (Roche). Cell lysates were clarified by centrifugation at 13,000 g for 15 min at 4 °C and subjected to sodium dodecyl sulfate-polyacrylamide gel (SDS-PAGE). Western Blot analysis was performed using the following antibodies: ACTIN was purchased from Chemicon International (Billerica, MA MAB1501R); FLAG was purchased from Sigma (St-Louis, MO, USA, F3165); CSE1L, IRF3 P-386, KPNB1 and TNPO1 were purchased from Abcam (Toronto, Ontario, Canada, ab96755, ab76493, ab2811, and ab10303); H1, p65, RAN and XPO1 were purchased from Santa Cruz Biotechnology (Dallas, TX, sc-8030, sc-8008, sc-58467, and sc-74454); IRF3 was purchased from Phoenix Airmid Biomedical (Oakville, ON, 18781); ISG56 was purchased from Novus Biologicals (Oakville, ON, NBP1-32329); NFKBIA P-32 was purchased from Cell Signaling Technology, Inc, (Danvers, MA, 2859). The antibody for PARP1 and Sendai Virus was a kind gift from MJ. Hébert and M. Servant, respectively. HRP-conjugated secondary antibodies were from Bio-Rad. The chemiluminescence reaction was performed using the Western Lighting Chemiluminescence Reagent Plus (PerkinElmer).

Co-immunoprecipitation

For co-immunoprecipitation, FLAG-tagged protein expressing cells were harvested and lysed as described above. Resulting cell extracts were adjusted to 1 mg/ml and subjected to IP as follows: pre-clearing of the lysates was done by incubating lysates with 40 µl of 50:50 slurry of immunoglobulin G-Sepharose (GE Healthcare) prepared in the lysis buffer with IgG beads for 1 hour. Pre-cleared lysate were immunoprecipitated by adding 20 µl of M2 anti-FLAG affinity gel (Sigma-Aldrich) prepared in TBS buffer (50 mM Tris-HCl, 150 mM NaCl, pH 7.4) overnight as described by the manufacturer. Immunoprecipitates were washed five times in lysis buffer. Elution was performed using 250 ng/µl purified FLAG peptide for 45 min at 4 °C (Sigma-Aldrich). Eluates were analyzed by Western Blotting.

Nuclear and Cytoplasmic Extraction

Nuclear and cytoplasmic extraction was performed on 4,000,000 A549 cells that were previously plated on 100 mm plates, infected with lentivirus encoding shRNA NT or KPNB1 (TRCN0000123189) at a MOI of 10 for three days and infected with SeV for 0, 1, 3, 5, 8 and 10 hours prior to harvesting. Nuclear and cytoplasmic fractions were prepared with NE-PER™ Nuclear and Cytoplasmic Extraction Reagents (Thermo Scientific) according to the manufacturer protocol.

Functional enrichment analysis

DAVID database was used for functional annotation [72, 73]. DAVID functional annotation chart tool was used to perform Gene Ontology biological process and InterPro protein domain analysis. Terms with a p-value smaller than $5x10^{-2}$ were considered as significantly overrepresented.

AUTHORS CONTRIBUTIONS

B.G., M.B. and D.L. designed all experiments. B.G. performed all experiments. B.G., M.B. and D.L. wrote the paper.

ACKNOWLEDGEMENTS

We thank K. Audette and J. Duchaine of the IRIC's screening facility. This work was supported by grants from the Canadian Institutes for Health Research (CIHR-MOP-115010 and CIHR-CI6-103135) and by the Novartis/Canadian Liver Foundation Hepatology Research Chair to D.L.

REFERENCES

1. Germain MA, Chatel-Chaix L, Gagne B, Bonneil E, Thibault P, Pradezynski F, et al. Elucidating novel hepatitis C virus-host interactions using combined mass spectrometry and functional genomics approaches. Molecular & cellular proteomics : MCP. 2014;13(1):184-203. doi: 10.1074/mcp.M113.030155. PubMed PMID: 24169621; PubMed Central PMCID: PMC3879614.
2. Karlas A, Machuy N, Shin Y, Pleissner KP, Artarini A, Heuer D, et al. Genome-wide RNAi screen identifies human host factors crucial for influenza virus replication. Nature. 2010;463(7282):818-22. doi: 10.1038/nature08760. PubMed PMID: 20081832.
3. Mehle A, Doudna JA. A host of factors regulating influenza virus replication. Viruses. 2010;2(2):566-73. doi: 10.3390/v2020566. PubMed PMID: 21994648; PubMed Central PMCID: PMC3185602.
4. Brass AL, Dykxhoorn DM, Benita Y, Yan N, Engelman A, Xavier RJ, et al. Identification of host proteins required for HIV infection through a functional genomic screen. Science. 2008;319(5865):921-6. doi: 10.1126/science.1152725. PubMed PMID: 18187620.
5. Konig R, Zhou Y, Elleder D, Diamond TL, Bonamy GM, Irelan JT, et al. Global analysis of host-pathogen interactions that regulate early-stage HIV-1 replication. Cell. 2008;135(1):49-60. doi: 10.1016/j.cell.2008.07.032. PubMed PMID: 18854154; PubMed Central PMCID: PMC2628946.
6. Neufeldt CJ, Joyce MA, Levin A, Steenbergen RH, Pang D, Shields J, et al. Hepatitis C virus-induced cytoplasmic organelles use the nuclear transport machinery to establish an environment conducive to virus replication. PLoS pathogens. 2013;9(10):e1003744. doi: 10.1371/journal.ppat.1003744. PubMed PMID: 24204278; PubMed Central PMCID: PMC3814334.
7. Levin A, Neufeldt CJ, Pang D, Wilson K, Loewen-Dobler D, Joyce MA, et al. Functional characterization of nuclear localization and export signals in hepatitis C virus proteins and their role in the membranous web. PloS one. 2014;9(12):e114629. doi: 10.1371/journal.pone.0114629. PubMed PMID: 25485706; PubMed Central PMCID: PMC4259358.
8. Porter FW, Bochkov YA, Albee AJ, Wiese C, Palmenberg AC. A picornavirus protein interacts with Ran-GTPase and disrupts nucleocytoplasmic transport. Proceedings of the National Academy of Sciences of the United States of America. 2006;103(33):12417-22. doi: 10.1073/pnas.0605375103. PubMed PMID: 16888036; PubMed Central PMCID: PMC1567894.
9. Levin A, Hayouka Z, Friedler A, Loyter A. Transportin 3 and importin alpha are required for effective nuclear import of HIV-1 integrase in virus-infected cells. Nucleus. 2010;1(5):422-31. doi: 10.4161/nucl.1.5.12903. PubMed PMID: 21326825; PubMed Central PMCID: PMC3037538.
10. Di Nunzio F, Danckaert A, Fricke T, Perez P, Fernandez J, Perret E, et al. Human nucleoporins promote HIV-1 docking at the nuclear pore, nuclear import and integration. PloS one. 2012;7(9):e46037. doi: 10.1371/journal.pone.0046037. PubMed PMID: 23049930; PubMed Central PMCID: PMC3457934.
11. Deng T, Engelhardt OG, Thomas B, Akoulitchev AV, Brownlee GG, Fodor E. Role of ran binding protein 5 in nuclear import and assembly of the influenza virus RNA polymerase

complex. Journal of virology. 2006;80(24):11911-9. doi: 10.1128/JVI.01565-06. PubMed PMID: 17005651; PubMed Central PMCID: PMC1676300.
12. Satterly N, Tsai PL, van Deursen J, Nussenzveig DR, Wang Y, Faria PA, et al. Influenza virus targets the mRNA export machinery and the nuclear pore complex. Proceedings of the National Academy of Sciences of the United States of America. 2007;104(6):1853-8. doi: 10.1073/pnas.0610977104. PubMed PMID: 17267598; PubMed Central PMCID: PMC1794296.
13. Neumann G, Hughes MT, Kawaoka Y. Influenza A virus NS2 protein mediates vRNP nuclear export through NES-independent interaction with hCRM1. The EMBO journal. 2000;19(24):6751-8. doi: 10.1093/emboj/19.24.6751. PubMed PMID: 11118210; PubMed Central PMCID: PMC305902.
14. Suzuki R, Sakamoto S, Tsutsumi T, Rikimaru A, Tanaka K, Shimoike T, et al. Molecular determinants for subcellular localization of hepatitis C virus core protein. Journal of virology. 2005;79(2):1271-81. doi: 10.1128/JVI.79.2.1271-1281.2005. PubMed PMID: 15613354; PubMed Central PMCID: PMC538550.
15. Cerutti A, Maillard P, Minisini R, Vidalain PO, Roohvand F, Pecheur EI, et al. Identification of a functional, CRM-1-dependent nuclear export signal in hepatitis C virus core protein. PloS one. 2011;6(10):e25854. doi: 10.1371/journal.pone.0025854. PubMed PMID: 22039426; PubMed Central PMCID: PMC3200325.
16. Yarbrough ML, Mata MA, Sakthivel R, Fontoura BM. Viral subversion of nucleocytoplasmic trafficking. Traffic. 2014;15(2):127-40. doi: 10.1111/tra.12137. PubMed PMID: 24289861; PubMed Central PMCID: PMC3910510.
17. Park N, Skern T, Gustin KE. Specific cleavage of the nuclear pore complex protein Nup62 by a viral protease. The Journal of biological chemistry. 2010;285(37):28796-805. doi: 10.1074/jbc.M110.143404. PubMed PMID: 20622012; PubMed Central PMCID: PMC2937907.
18. Park N, Katikaneni P, Skern T, Gustin KE. Differential targeting of nuclear pore complex proteins in poliovirus-infected cells. Journal of virology. 2008;82(4):1647-55. doi: 10.1128/JVI.01670-07. PubMed PMID: 18045934; PubMed Central PMCID: PMC2258732.
19. Castello A, Izquierdo JM, Welnowska E, Carrasco L. RNA nuclear export is blocked by poliovirus 2A protease and is concomitant with nucleoporin cleavage. Journal of cell science. 2009;122(Pt 20):3799-809. doi: 10.1242/jcs.055988. PubMed PMID: 19789179.
20. Wang R, Nan Y, Yu Y, Zhang YJ. Porcine reproductive and respiratory syndrome virus Nsp1beta inhibits interferon-activated JAK/STAT signal transduction by inducing karyopherin-alpha1 degradation. Journal of virology. 2013;87(9):5219-28. doi: 10.1128/JVI.02643-12. PubMed PMID: 23449802; PubMed Central PMCID: PMC3624296.
21. Frieman M, Yount B, Heise M, Kopecky-Bromberg SA, Palese P, Baric RS. Severe acute respiratory syndrome coronavirus ORF6 antagonizes STAT1 function by sequestering nuclear import factors on the rough endoplasmic reticulum/Golgi membrane. Journal of virology. 2007;81(18):9812-24. doi: 10.1128/JVI.01012-07. PubMed PMID: 17596301; PubMed Central PMCID: PMC2045396.
22. Shaw ML, Cardenas WB, Zamarin D, Palese P, Basler CF. Nuclear localization of the Nipah virus W protein allows for inhibition of both virus- and toll-like receptor 3-triggered signaling pathways. Journal of virology. 2005;79(10):6078-88. doi: 10.1128/JVI.79.10.6078-6088.2005. PubMed PMID: 15857993; PubMed Central PMCID: PMC1091709.

23. Reid SP, Valmas C, Martinez O, Sanchez FM, Basler CF. Ebola virus VP24 proteins inhibit the interaction of NPI-1 subfamily karyopherin alpha proteins with activated STAT1. Journal of virology. 2007;81(24):13469-77. doi: 10.1128/JVI.01097-07. PubMed PMID: 17928350; PubMed Central PMCID: PMC2168840.
24. Xu W, Edwards MR, Borek DM, Feagins AR, Mittal A, Alinger JB, et al. Ebola virus VP24 targets a unique NLS binding site on karyopherin alpha 5 to selectively compete with nuclear import of phosphorylated STAT1. Cell host & microbe. 2014;16(2):187-200. doi: 10.1016/j.chom.2014.07.008. PubMed PMID: 25121748; PubMed Central PMCID: PMC4188415.
25. Hoelz A, Debler EW, Blobel G. The structure of the nuclear pore complex. Annu Rev Biochem. 2011;80:613-43. doi: 10.1146/annurev-biochem-060109-151030. PubMed PMID: 21495847.
26. Cook A, Bono F, Jinek M, Conti E. Structural biology of nucleocytoplasmic transport. Annu Rev Biochem. 2007;76:647-71. doi: 10.1146/annurev.biochem.76.052705.161529. PubMed PMID: 17506639.
27. Terry LJ, Shows EB, Wente SR. Crossing the nuclear envelope: hierarchical regulation of nucleocytoplasmic transport. Science. 2007;318(5855):1412-6. doi: 10.1126/science.1142204. PubMed PMID: 18048681.
28. Lee BJ, Cansizoglu AE, Suel KE, Louis TH, Zhang Z, Chook YM. Rules for nuclear localization sequence recognition by karyopherin beta 2. Cell. 2006;126(3):543-58. doi: 10.1016/j.cell.2006.05.049. PubMed PMID: 16901787; PubMed Central PMCID: PMC3442361.
29. Baril M, Es-Saad S, Chatel-Chaix L, Fink K, Pham T, Raymond VA, et al. Genome-wide RNAi screen reveals a new role of a WNT/CTNNB1 signaling pathway as negative regulator of virus-induced innate immune responses. PLoS pathogens. 2013;9(6):e1003416. doi: 10.1371/journal.ppat.1003416. PubMed PMID: 23785285; PubMed Central PMCID: PMC3681753.
30. Meylan E, Curran J, Hofmann K, Moradpour D, Binder M, Bartenschlager R, et al. Cardif is an adaptor protein in the RIG-I antiviral pathway and is targeted by hepatitis C virus. Nature. 2005;437(7062):1167-72. Epub 2005/09/24. doi: 10.1038/nature04193. PubMed PMID: 16177806.
31. Baril M, Racine ME, Penin F, Lamarre D. MAVS dimer is a crucial signaling component of innate immunity and the target of hepatitis C virus NS3/4A protease. Journal of virology. 2009;83(3):1299-311. Epub 2008/11/28. doi: 10.1128/JVI.01659-08. PubMed PMID: 19036819; PubMed Central PMCID: PMC2620913.
32. Li K, Foy E, Ferreon JC, Nakamura M, Ferreon AC, Ikeda M, et al. Immune evasion by hepatitis C virus NS3/4A protease-mediated cleavage of the Toll-like receptor 3 adaptor protein TRIF. Proceedings of the National Academy of Sciences of the United States of America. 2005;102(8):2992-7. doi: 10.1073/pnas.0408824102. PubMed PMID: 15710891; PubMed Central PMCID: PMC548795.
33. Lin R, Heylbroeck C, Pitha PM, Hiscott J. Virus-dependent phosphorylation of the IRF-3 transcription factor regulates nuclear translocation, transactivation potential, and proteasome-mediated degradation. Molecular and cellular biology. 1998;18(5):2986-96. PubMed PMID: 9566918; PubMed Central PMCID: PMC110678.
34. Kumar KP, McBride KM, Weaver BK, Dingwall C, Reich NC. Regulated nuclear-cytoplasmic localization of interferon regulatory factor 3, a subunit of double-stranded RNA-

activated factor 1. Molecular and cellular biology. 2000;20(11):4159-68. PubMed PMID: 10805757; PubMed Central PMCID: PMC85785.
35. Fagerlund R, Kinnunen L, Kohler M, Julkunen I, Melen K. NF-{kappa}B is transported into the nucleus by importin {alpha}3 and importin {alpha}4. The Journal of biological chemistry. 2005;280(16):15942-51. doi: 10.1074/jbc.M500814200. PubMed PMID: 15677444.
36. Fagerlund R, Melen K, Cao X, Julkunen I. NF-kappaB p52, RelB and c-Rel are transported into the nucleus via a subset of importin alpha molecules. Cellular signalling. 2008;20(8):1442-51. doi: 10.1016/j.cellsig.2008.03.012. PubMed PMID: 18462924.
37. Liang P, Zhang H, Wang G, Li S, Cong S, Luo Y, et al. KPNB1, XPO7 and IPO8 mediate the translocation ofNF-kappaB/p65 into the nucleus. Traffic. 2013;14(11):1132-43. doi: 10.1111/tra.12097. PubMed PMID: 23906023.
38. Rebane A, Aab A, Steitz JA. Transportins 1 and 2 are redundant nuclear import factors for hnRNP A1 and HuR. Rna. 2004;10(4):590-9. PubMed PMID: 15037768; PubMed Central PMCID: PMC1370549.
39. Waldmann I, Spillner C, Kehlenbach RH. The nucleoporin-like protein NLP1 (hCG1) promotes CRM1-dependent nuclear protein export. Journal of cell science. 2012;125(Pt 1):144-54. doi: 10.1242/jcs.090316. PubMed PMID: 22250199.
40. Kim CW, Chang KM. Hepatitis C virus: virology and life cycle. Clinical and molecular hepatology. 2013;19(1):17-25. doi: 10.3350/cmh.2013.19.1.17. PubMed PMID: 23593605; PubMed Central PMCID: PMC3622851.
41. Pollard VW, Michael WM, Nakielny S, Siomi MC, Wang F, Dreyfuss G. A novel receptor-mediated nuclear protein import pathway. Cell. 1996;86(6):985-94. PubMed PMID: 8808633.
42. Kim CS, Seol SK, Song OK, Park JH, Jang SK. An RNA-binding protein, hnRNP A1, and a scaffold protein, septin 6, facilitate hepatitis C virus replication. Journal of virology. 2007;81(8):3852-65. doi: 10.1128/JVI.01311-06. PubMed PMID: 17229681; PubMed Central PMCID: PMC1866118.
43. Chatel-Chaix L, Melancon P, Racine ME, Baril M, Lamarre D. Y-box-binding protein 1 interacts with hepatitis C virus NS3/4A and influences the equilibrium between viral RNA replication and infectious particle production. Journal of virology. 2011;85(21):11022-37. doi: 10.1128/JVI.00719-11. PubMed PMID: 21849455; PubMed Central PMCID: PMC3194978.
44. Chatel-Chaix L, Germain MA, Motorina A, Bonneil E, Thibault P, Baril M, et al. A Host Yb-1 Ribonucleoprotein Complex Is Hijacked by Hepatitis C Virus for the Control of Ns3-Dependent Particle Production. J Virol. 2013. Epub 2013/08/30. doi: 10.1128/JVI.01474-13. PubMed PMID: 23986595.
45. Perard J, Leyrat C, Baudin F, Drouet E, Jamin M. Structure of the full-length HCV IRES in solution. Nat Commun. 2013;4:1612. doi: 10.1038/ncomms2611. PubMed PMID: 23511476.
46. Monette A, Ajamian L, Lopez-Lastra M, Mouland AJ. Human immunodeficiency virus type 1 (HIV-1) induces the cytoplasmic retention of heterogeneous nuclear ribonucleoprotein A1 by disrupting nuclear import: implications for HIV-1 gene expression. The Journal of biological chemistry. 2009;284(45):31350-62. doi: 10.1074/jbc.M109.048736. PubMed PMID: 19737937; PubMed Central PMCID: PMC2781532.
47. Takeda E, Murakami T, Matsuda G, Murakami H, Zako T, Maeda M, et al. Nuclear exportin receptor CAS regulates the NPI-1-mediated nuclear import of HIV-1 Vpr. PloS one.

2011;6(11):e27815. doi: 10.1371/journal.pone.0027815. PubMed PMID: 22110766; PubMed Central PMCID: PMC3218035.
48. Yedavalli VS, Neuveut C, Chi YH, Kleiman L, Jeang KT. Requirement of DDX3 DEAD box RNA helicase for HIV-1 Rev-RRE export function. Cell. 2004;119(3):381-92. doi: 10.1016/j.cell.2004.09.029. PubMed PMID: 15507209.
49. Oshiumi H, Ikeda M, Matsumoto M, Watanabe A, Takeuchi O, Akira S, et al. Hepatitis C virus core protein abrogates the DDX3 function that enhances IPS-1-mediated IFN-beta induction. PloS one. 2010;5(12):e14258. doi: 10.1371/journal.pone.0014258. PubMed PMID: 21170385; PubMed Central PMCID: PMC2999533.
50. Chatel-Chaix L, Germain MA, Motorina A, Bonneil E, Thibault P, Baril M, et al. A host YB-1 ribonucleoprotein complex is hijacked by hepatitis C virus for the control of NS3-dependent particle production. Journal of virology. 2013;87(21):11704-20. doi: 10.1128/JVI.01474-13. PubMed PMID: 23986595; PubMed Central PMCID: PMC3807372.
51. Bischoff FR, Ponstingl H. Catalysis of guanine nucleotide exchange on Ran by the mitotic regulator RCC1. Nature. 1991;354(6348):80-2. doi: 10.1038/354080a0. PubMed PMID: 1944575.
52. Das T, Diamond DL, Yeh M, Hassan S, Bryan JT, Reyes JD, et al. Molecular Signatures of Recurrent Hepatocellular Carcinoma Secondary to Hepatitis C Virus following Liver Transplantation. J Transplant. 2013;2013:878297. doi: 10.1155/2013/878297. PubMed PMID: 24377043; PubMed Central PMCID: PMC3860124.
53. Tam WF, Lee LH, Davis L, Sen R. Cytoplasmic sequestration of rel proteins by IkappaBalpha requires CRM1-dependent nuclear export. Molecular and cellular biology. 2000;20(6):2269-84. PubMed PMID: 10688673; PubMed Central PMCID: PMC110843.
54. Soulat D, Burckstummer T, Westermayer S, Goncalves A, Bauch A, Stefanovic A, et al. The DEAD-box helicase DDX3X is a critical component of the TANK-binding kinase 1-dependent innate immune response. The EMBO journal. 2008;27(15):2135-46. doi: 10.1038/emboj.2008.126. PubMed PMID: 18583960; PubMed Central PMCID: PMC2453059.
55. Schroder M, Baran M, Bowie AG. Viral targeting of DEAD box protein 3 reveals its role in TBK1/IKKepsilon-mediated IRF activation. The EMBO journal. 2008;27(15):2147-57. doi: 10.1038/emboj.2008.143. PubMed PMID: 18636090; PubMed Central PMCID: PMC2516890.
56. Kimura T, Hashimoto I, Nagase T, Fujisawa J. CRM1-dependent, but not ARE-mediated, nuclear export of IFN-alpha1 mRNA. Journal of cell science. 2004;117(Pt 11):2259-70. doi: 10.1242/jcs.01076. PubMed PMID: 15126627.
57. Kimura T, Hashimoto I, Nishizawa M, Ito S, Yamada H. Novel cis-active structures in the coding region mediate CRM1-dependent nuclear export of IFN-alpha 1 mRNA. Med Mol Morphol. 2010;43(3):145-57. doi: 10.1007/s00795-010-0492-5. PubMed PMID: 20857263.
58. Theiss AL, Jenkins AK, Okoro NI, Klapproth JM, Merlin D, Sitaraman SV. Prohibitin inhibits tumor necrosis factor alpha-induced nuclear factor-kappa B nuclear translocation via the novel mechanism of decreasing importin alpha3 expression. Molecular biology of the cell. 2009;20(20):4412-23. doi: 10.1091/mbc.E09-05-0361. PubMed PMID: 19710421; PubMed Central PMCID: PMC2762146.
59. Taylor SL, Frias-Staheli N, Garcia-Sastre A, Schmaljohn CS. Hantaan virus nucleocapsid protein binds to importin alpha proteins and inhibits tumor necrosis factor alpha-

induced activation of nuclear factor kappa B. Journal of virology. 2009;83(3):1271-9. doi: 10.1128/JVI.00986-08. PubMed PMID: 19019947; PubMed Central PMCID: PMC2620888.
60. Perez M, Soler-Torronteras R, Collado JA, Limones CG, Hellsten R, Johansson M, et al. The fungal metabolite galiellalactone interferes with the nuclear import of NF-kappaB and inhibits HIV-1 replication. Chem Biol Interact. 2014;214:69-76. doi: 10.1016/j.cbi.2014.02.012. PubMed PMID: 24631022.
61. Englmeier L, Fornerod M, Bischoff FR, Petosa C, Mattaj IW, Kutay U. RanBP3 influences interactions between CRM1 and its nuclear protein export substrates. EMBO reports. 2001;2(10):926-32. doi: 10.1093/embo-reports/kve200. PubMed PMID: 11571268; PubMed Central PMCID: PMC1084078.
62. Lindsay ME, Holaska JM, Welch K, Paschal BM, Macara IG. Ran-binding protein 3 is a cofactor for Crm1-mediated nuclear protein export. The Journal of cell biology. 2001;153(7):1391-402. PubMed PMID: 11425870; PubMed Central PMCID: PMC2150735.
63. Takahashi N, van Kilsdonk JW, Ostendorf B, Smeets R, Bruggeman SW, Alonso A, et al. Tumor marker nucleoporin 88 kDa regulates nucleocytoplasmic transport of NF-kappaB. Biochemical and biophysical research communications. 2008;374(3):424-30. doi: 10.1016/j.bbrc.2008.06.128. PubMed PMID: 18621024.
64. Knoess M, Kurz AK, Goreva O, Bektas N, Breuhahn K, Odenthal M, et al. Nucleoporin 88 expression in hepatitis B and C virus-related liver diseases. World journal of gastroenterology : WJG. 2006;12(36):5870-4. PubMed PMID: 17007055; PubMed Central PMCID: PMC4100670.
65. Le Rouzic E, Mousnier A, Rustum C, Stutz F, Hallberg E, Dargemont C, et al. Docking of HIV-1 Vpr to the nuclear envelope is mediated by the interaction with the nucleoporin hCG1. The Journal of biological chemistry. 2002;277(47):45091-8. doi: 10.1074/jbc.M207439200. PubMed PMID: 12228227.
66. Rasaiyaah J, Tan CP, Fletcher AJ, Price AJ, Blondeau C, Hilditch L, et al. HIV-1 evades innate immune recognition through specific cofactor recruitment. Nature. 2013;503(7476):402-5. Epub 2013/11/08. doi: 10.1038/nature12769. PubMed PMID: 24196705; PubMed Central PMCID: PMC3928559.
67. Meehan AM, Saenz DT, Guevera R, Morrison JH, Peretz M, Fadel HJ, et al. A cyclophilin homology domain-independent role for Nup358 in HIV-1 infection. PLoS pathogens. 2014;10(2):e1003969. doi: 10.1371/journal.ppat.1003969. PubMed PMID: 24586169; PubMed Central PMCID: PMC3930637.
68. Zhang LK, Chai F, Li HY, Xiao G, Guo L. Identification of host proteins involved in Japanese encephalitis virus infection by quantitative proteomics analysis. Journal of proteome research. 2013;12(6):2666-78. doi: 10.1021/pr400011k. PubMed PMID: 23647205.
69. Zhang R, Mehla R, Chauhan A. Perturbation of host nuclear membrane component RanBP2 impairs the nuclear import of human immunodeficiency virus -1 preintegration complex (DNA). PloS one. 2010;5(12):e15620. doi: 10.1371/journal.pone.0015620. PubMed PMID: 21179483; PubMed Central PMCID: PMC3001881.
70. Wang B, Zhang X, Zhao Z. Validation-based insertional mutagenesis for identification of Nup214 as a host factor for EV71 replication in RD cells. Biochemical and biophysical research communications. 2013;437(3):452-6. doi: 10.1016/j.bbrc.2013.06.101. PubMed PMID: 23831628.

71. Dull T, Zufferey R, Kelly M, Mandel RJ, Nguyen M, Trono D, et al. A third-generation lentivirus vector with a conditional packaging system. Journal of virology. 1998;72(11):8463-71. PubMed PMID: 9765382.
72. Dennis G, Jr., Sherman BT, Hosack DA, Yang J, Gao W, Lane HC, et al. DAVID: Database for Annotation, Visualization, and Integrated Discovery. Genome biology. 2003;4(5):P3. Epub 2003/05/08. PubMed PMID: 12734009; PubMed Central PMCID: PMC3720094.
73. Huang da W, Sherman BT, Lempicki RA. Systematic and integrative analysis of large gene lists using DAVID bioinformatics resources. Nature protocols. 2009;4(1):44-57. Epub 2009/01/10. doi: 10.1038/nprot.2008.211. PubMed PMID: 19131956.

FIGURES

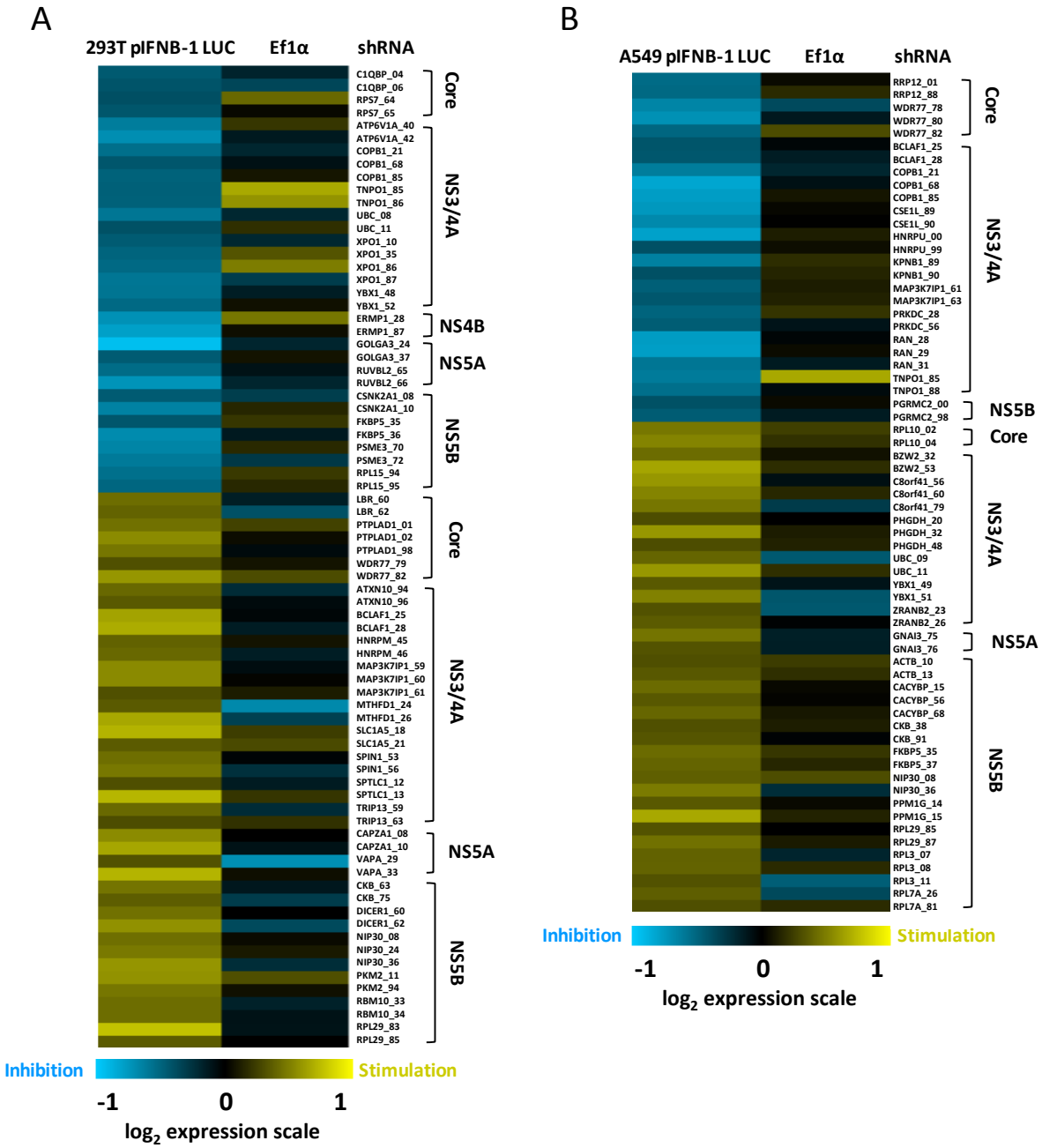
A
293T pIFNB-1 LUC
Ef1α
shRNA
C1QBP_04
C1QBP_06
RPS7_64
RPS7_65
ATP6V1A_40
ATP6V1A_42
COPB1_21
COPB1_68
COPB1_85
TNPO1_85
TNPO1_86
UBC_08
UBC_11
XPO1_10
XPO1_35
XPO1_86
XPO1_87
YBX1_48
YBX1_52
ERMP1_28
ERMP1_87
GOLGA3_24
GOLGA3_37
RUVBL2_65
RUVBL2_66
CSNK2A1_08
CSNK2A1_10
FKBP5_35
FKBP5_36
PSME3_70
PSME3_72
RPL15_94
RPL15_95
LBR_60
LBR_62
PTPLAD1_01
PTPLAD1_02
PTPLAD1_98
WDR77_79
WDR77_82
ATXN10_94
ATXN10_96
BCLAF1_25
BCLAF1_28
HNRPM_45
HNRPM_46
MAP3K7IP1_59
MAP3K7IP1_60
MAP3K7IP1_61
MTHFD1_24
MTHFD1_26
SLC1A5_18
SLC1A5_21
SPIN1_53
SPIN1_56
SPTLC1_12
SPTLC1_13
TRIP13_59
TRIP13_63
CAPZA1_08
CAPZA1_10
VAPA_29
VAPA_33
CKB_63
CKB_75
DICER1_60
DICER1_62
NIP30_08
NIP30_24
NIP30_36
PKM2_11
PKM2_94
RBM10_33
RBM10_34
RPL29_83
RPL29_85
Core
NS3/4A
NS4B
NS5A
NS5B
Core
NS3/4A
NS5A
NS5B
Inhibition
Stimulation
-1
0
1
log2 expression scale
B
A549 pIFNB-1 LUC
Ef1α
shRNA
RRP12_01
RRP12_88
WDR77_78
WDR77_80
WDR77_82
BCLAF1_25
BCLAF1_28
COPB1_21
COPB1_68
COPB1_85
CSE1L_89
CSE1L_90
HNRPU_00
HNRPU_99
KPNB1_89
KPNB1_90
MAP3K7IP1_61
MAP3K7IP1_63
PRKDC_28
PRKDC_56
RAN_28
RAN_29
RAN_31
TNPO1_85
TNPO1_88
PGRMC2_00
PGRMC2_98
RPL10_02
RPL10_04
BZW2_32
BZW2_53
C8orf41_56
C8orf41_60
C8orf41_79
PHGDH_20
PHGDH_32
PHGDH_48
UBC_09
UBC_11
YBX1_49
YBX1_51
ZRANB2_23
ZRANB2_26
GNAI3_75
GNAI3_76
ACTB_10
ACTB_13
CACYBP_15
CACYBP_56
CACYBP_68
CKB_38
CKB_91
FKBP5_35
FKBP5_37
NIP30_08
NIP30_36
PPM1G_14
PPM1G_15
RPL29_85
RPL29_87
RPL3_07
RPL3_08
RPL3_11
RPL7A_26
RPL7A_81
Core
NS3/4A
NS5B
Core
NS3/4A
NS5A
NS5B
Inhibition
Stimulation
-1
0
1
log2 expression scale

Figure 1. Knockdown of host proteins interacting with HCV modulates innate antiviral immunity

Heat map visualization of the *IFNB1* promoter activity following 53 gene hits whose silencing significantly inhibited SeV-mediated antiviral immunity (log_2 scale). shRNA screens were performed on HEK 293T (A) and A549 (B) cells stably expressing the firefly luciferase under the control of the *IFNB1* promoter. Results were normalized according to cells treated with shRNA NT (negative control set to 1 - black) based on an average of two independent experiments. The following criteria were applied to select hits: at least two shRNAs per gene with > 25 % effect on *IFNB1* promoter activity without affecting nonimmune-related endogenous promoter EF1α promoter activity. Hits are clustered by their corresponding viral binding-partners, and the last two digits of hits name correspond to the shRNA TRC number.

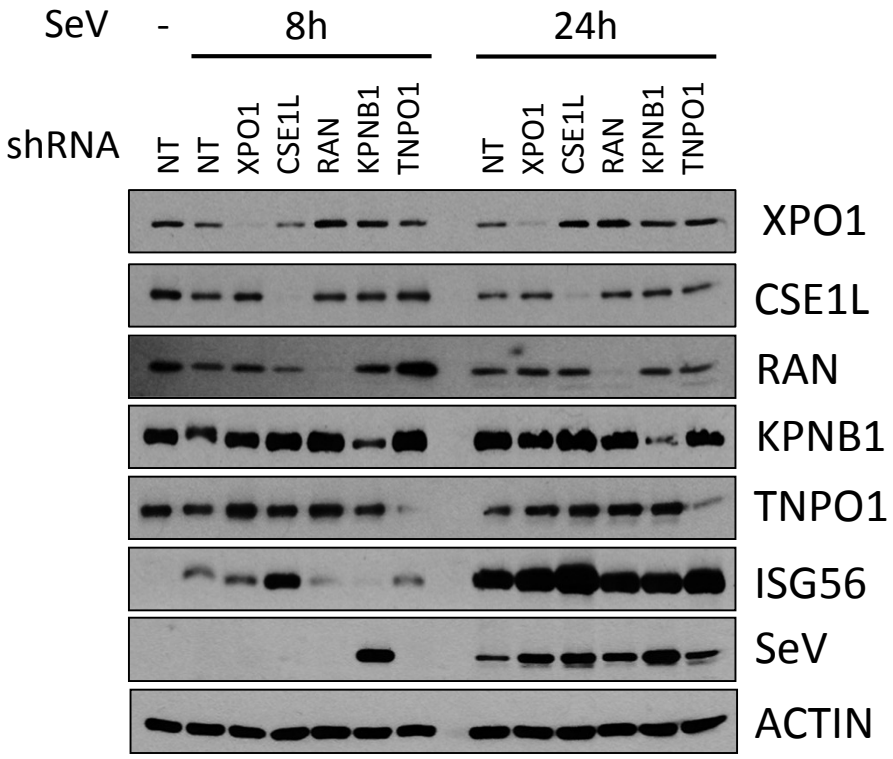

Figure 2. Effect of silencing nucleocytoplasmic transporters on ISG56 induction and SeV replication

Immunoblot analysis of A549 cells infected with SeV for 8 or 24 hours following knockdown of XPO1, CSE1L, RAN, KPNB1 and TNPO1 for three days. shRNA NT is used as a control.

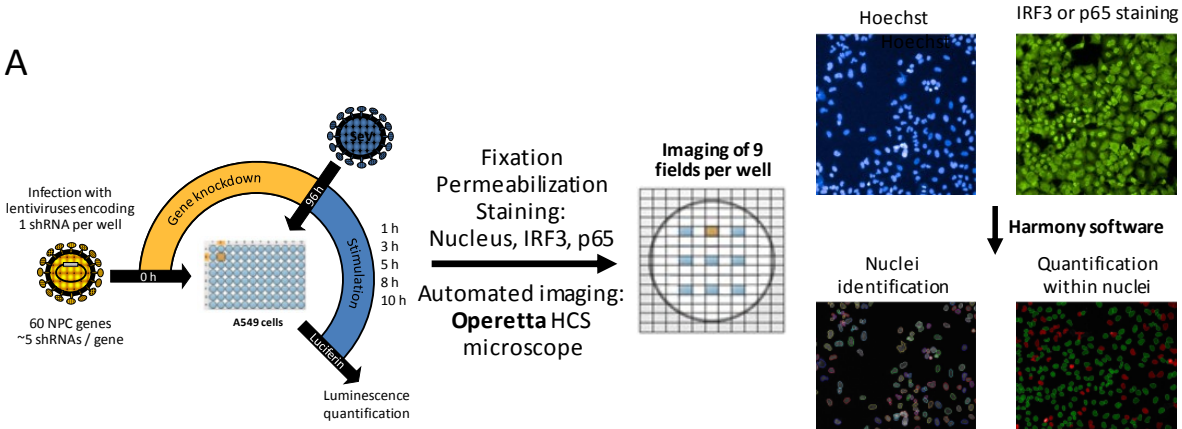
A
Infection with lentiviruses encoding 1 shRNA per well
60 NPC genes ~5 shRNAs / gene
0 h
Gene knockdown
96h
A549 cells
+SeV
Stimulation
1 h
3 h
5 h
8 h
10 h
Luciferin
Luminescence quantification
Fixation
Permeabilization
Staining:
Nucleus, IRF3, p65
Automated imaging:
Operetta HCS microscope
Imaging of 9 fields per well
Hoechst
IRF3 or p65 staining
Harmony software
Nuclei identification
Quantification within nuclei

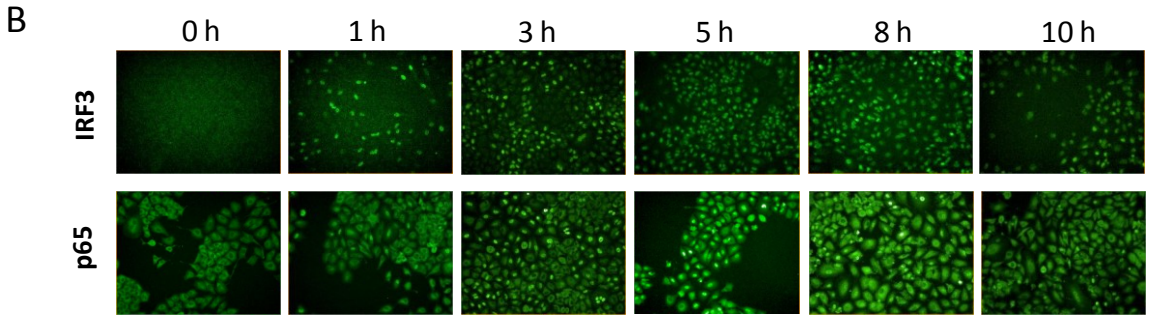
B
0 h
1 h
3 h
5 h
8 h
10 h
IRF3
p65

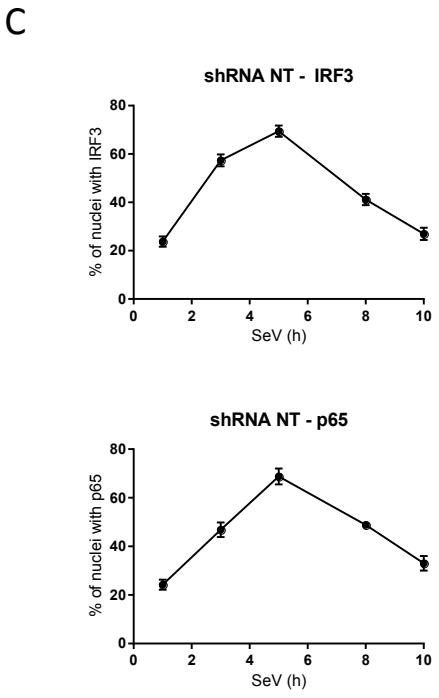
C
shRNA NT - IRF3
% of nuclei with IRF3
SeV (h)
shRNA NT - p65
% of nuclei with p65
SeV (h)

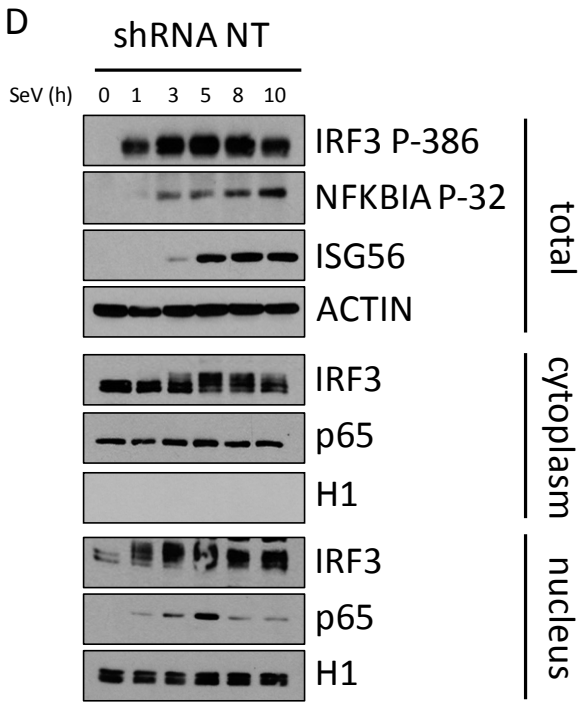
D
shRNA NT
SeV (h) 0 1 3 5 8 10
IRF3 P-386
NFKBIA P-32
ISG56
ACTIN
total
IRF3
p65
H1
cytoplasm
IRF3
p65
H1
nucleus

Figure 3. Microscopy-based shRNA screen to observe IRF3 and p65 nuclear translocation.

(A) Overview of the shRNA microscopy-screen. A549 cells were plated in 96-well plates and infected with a single lentivirus-encoding shRNA (~5 independent shRNAs per gene for 60 nucleocytoplasmic transporters) at a MOI of 10 for four days. A control shRNA NT was included in each 96-well plate. Cells were infected with SeV for 1, 3, 5, 8 or 10 hours before fixation, permeabilization, Hoechst nuclear labeling and antibody staining of IRF3 or p65 with Alexa Fluor 488 (green). Images of cells were captured in nine pre-determined fields for each well using an Operetta High Content Screening Microscope. Images were processed using Harmony software to delimitate the nuclear region and measure the fluorescence intensity of IRF3 or p65 within the nucleus. For each 96-well plate, a fluorescence cut-off was set to allow automated discrimination of cells with (green) or without (red) IRF3 or p65 nuclear staining and to calculate the percentage of cells with IRF3 or p65 nuclear staining for each shRNA. (B) Representative time course imaging performed with the control shRNA NT showing the nuclear translocation of IRF3 or p65 over a 10-hour SeV infection (one representative out of nine field images). (C) Graphic representation of the microscopy image-based analysis showing the percentage of cells with positive nuclear staining for IRF3 or p65. Over the course of a 10-hour SeV infection, we observe an increase in both IRF3 and p65 nuclear staining culminating with approximately 75% of positive cells at five hours post infection, followed by a decrease to approximately 30% of positive cells at 10 hours. (D) Immunoblot analysis of total cell lysate, cytoplasmic extract and nuclear extract of A549 cells infected with lentivirus encoding shRNA NT at a MOI of 10 for three days and infected with SeV for 0, 1, 3, 5, 8 and 10 hours prior to harvesting.

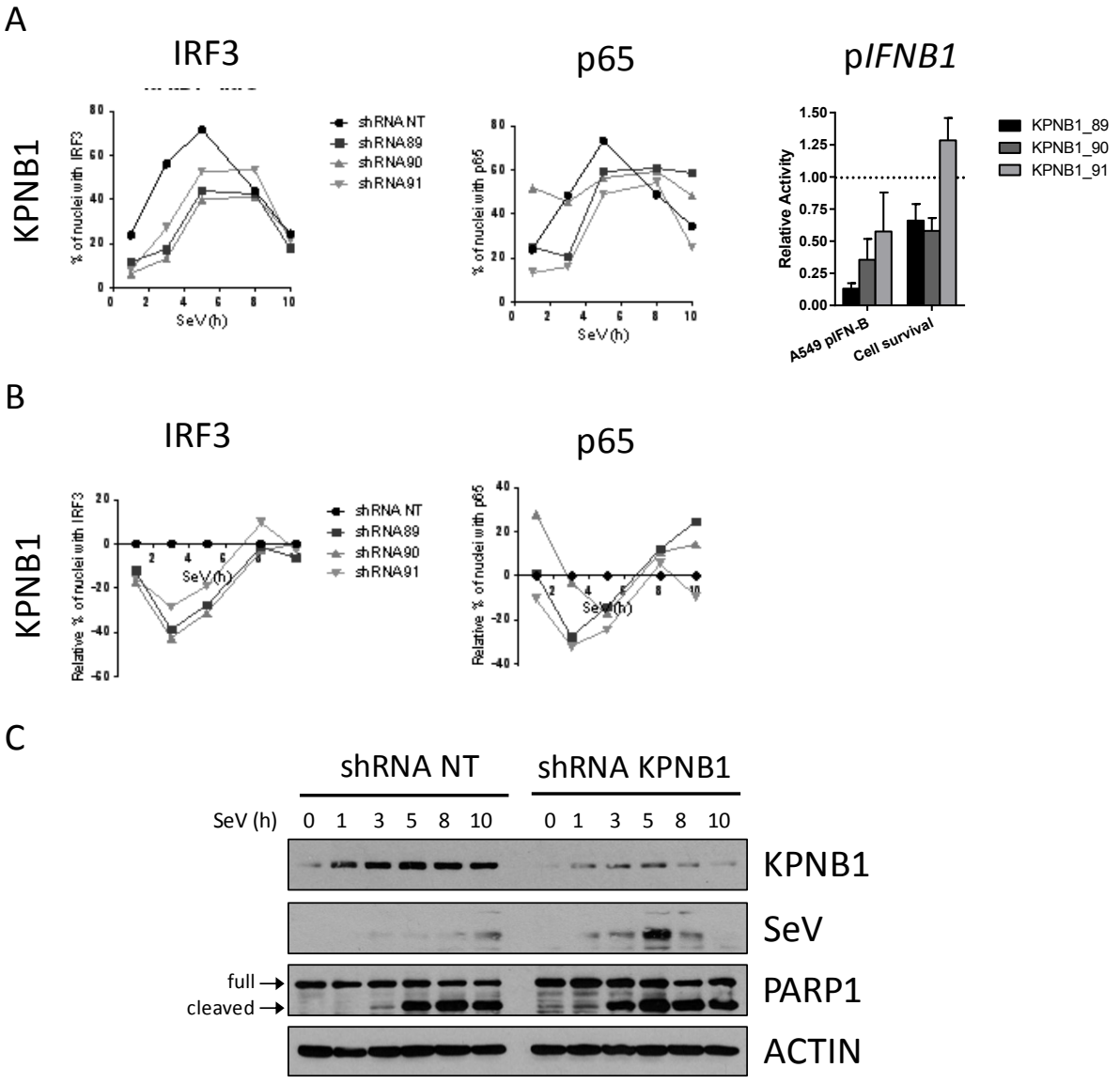

Figure 4. KPNB1 knockdown impairs IRF3 and p65 nuclear translocation and p*IFNB1* induction, while increasing SeV viral replication and apoptosis.

(A) Three independent shRNA targeting KPNB1 significantly affected nuclear translocation of both IRF3 (left panel) and p65 (middle panel) when compared to the shRNA NT. The effect of these shRNA-mediated knockdowns on SeV induced *IFNB1* promoter activity was measured in A549 cells stably expressing the firefly luciferase under the control of the *IFNB1* promoter

(right panel). In addition, the effect of a shRNA on cell proliferation and survival was evaluated using images from the microscopy screen (see Fig. 3) by dividing the total number of nuclei for a given shRNA and dividing it by the total number of nuclei for the shRNA NT control (right panel). (B) Alternative representation of results presented in (A) using relative percentage in the nucleus obtained after normalization of the control shRNA NT to zero for all time points. (C) Immunoblot analysis of A549 cells infected with SeV for 1, 3, 5, 8 or 10 hours following transduction with shRNA NT (control) or shRNA targeting KPNB1 for three days. PARP1 cleavage (arrows) is used as apoptosis readout.

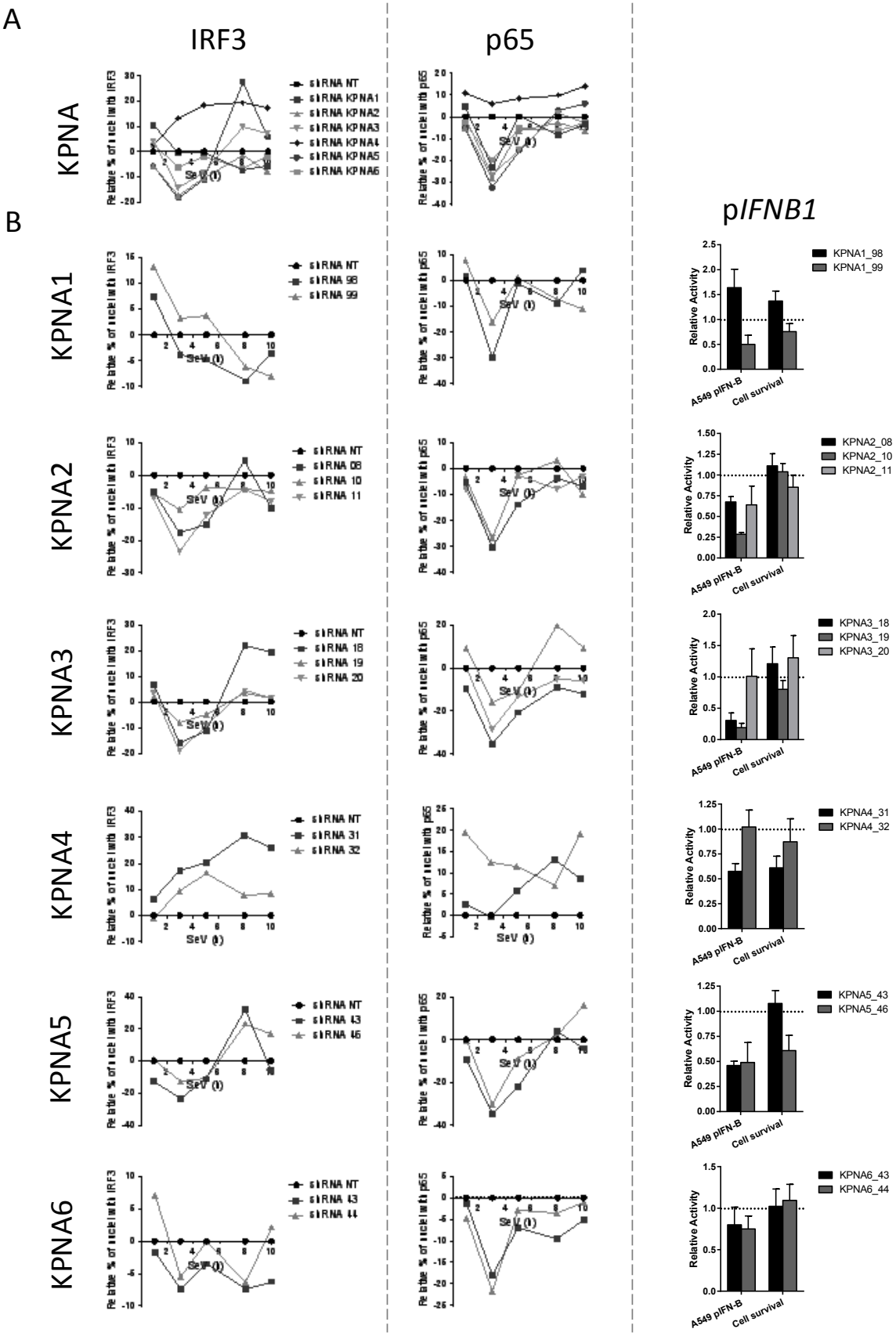
A
IRF3
p65
KPNA
siRNA NT
siRNA KPNA1
siRNA KPNA2
siRNA KPNA3
siRNA KPNA4
siRNA KPNA5
siRNA KPNA6
B
pIFNB1
KPNA1
KPNA2
KPNA3
KPNA4
KPNA5
KPNA6
siRNA 98
siRNA 99
siRNA 08
siRNA 10
siRNA 11
siRNA 18
siRNA 19
siRNA 20
siRNA 31
siRNA 32
siRNA 43
siRNA 46
siRNA 44
KPNA1_98
KPNA1_99
KPNA2_08
KPNA2_10
KPNA2_11
KPNA3_18
KPNA3_19
KPNA3_20
KPNA4_31
KPNA4_32
KPNA5_43
KPNA5_46
KPNA6_43
KPNA6_44
Relative Activity
A549 pIFN-B
Cell survival
SeV (h)

Figure 5. Effect of silencing KPNA adaptors on IRF3 and p65 nuclear translocation.

Relative percentage of cells containing IRF3 and p65 in the nucleus after normalization of the control shRNA NT to zero for all time points, as described in Figure 4. Results are presented as average of all shRNAs for each KPNA gene (A) and as individual shRNA for KPNA1-6 (B). The effect of shRNA-mediated knockdown on SeV induced *IFNB1* promoter activity and on cell proliferation and survival were calculated as described in Figure 4A (right panel).

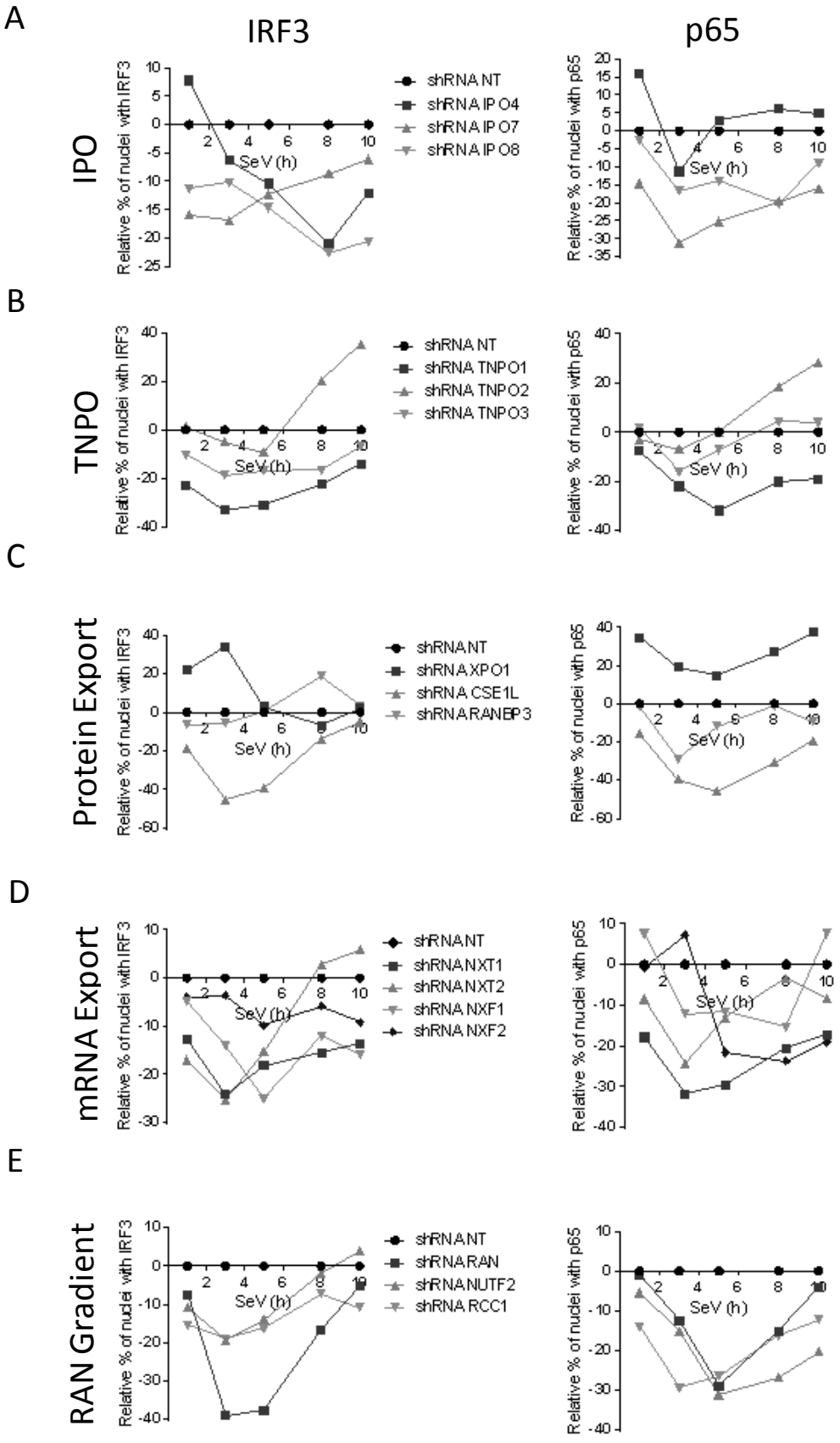
A
IRF3
p65
IPO
shRNA NT
shRNA IPO4
shRNA IPO7
shRNA IPO8
Relative % of nuclei with IRF3
Relative % of nuclei with p65
SeV (h)
B
TNPO
shRNA NT
shRNA TNPO1
shRNA TNPO2
shRNA TNPO3
C
Protein Export
shRNA NT
shRNA XPO1
shRNA CSE1L
shRNA RANBP3
D
mRNA Export
shRNA NT
shRNA NXT1
shRNA NXT2
shRNA NXF1
shRNA NXF2
E
RAN Gradient
shRNA NT
shRNA RAN
shRNA NUTF2
shRNA RCC1

Figure 6. Effect of silencing different transporter groups on IRF3 and p65 nuclear translocation.

Importins (IPO4, IPO7, IPO8), transportins (TNPO1, TNPO2, TNPO3), as well as proteins involved in protein export (XPO1, CSE1L, RANBP3), mRNA export (NXT1, NXT2, NXF1, NXF2) and the RAN gradient (RAN, NUTF2, RCC1) were knocked down. Results are presented as the average of all shRNAs in relative percentage of cells containing IRF3 and p65 in the nucleus after normalization of the control shRNA NT to zero for all time points, as described in Figure 5A. Individual shRNA results on IRF3 and p65 nuclear translocation, *IFNB1* promoter activity and cell proliferation and survival are described in Figures S4-S8.

A

IRF3

p65

Cytoplasmic FG-Nups + Filaments

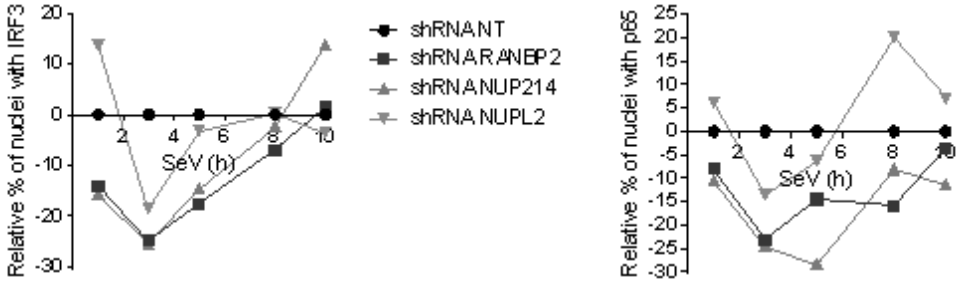

B

Outer-ring Nups

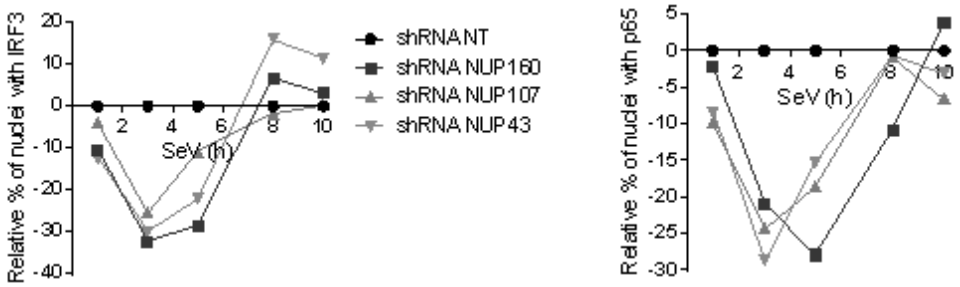

C

Linker Nups

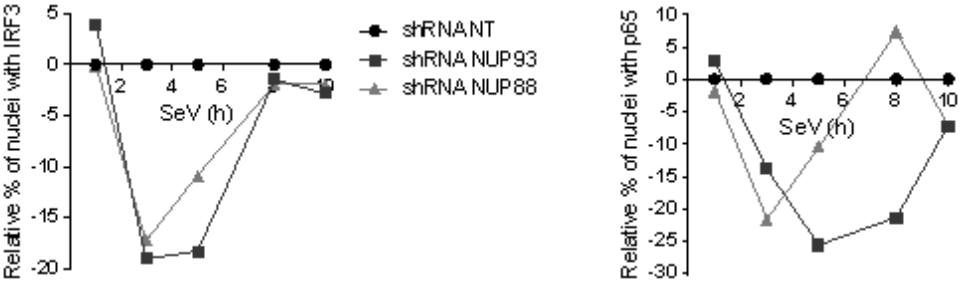

D

Central FG-Nups

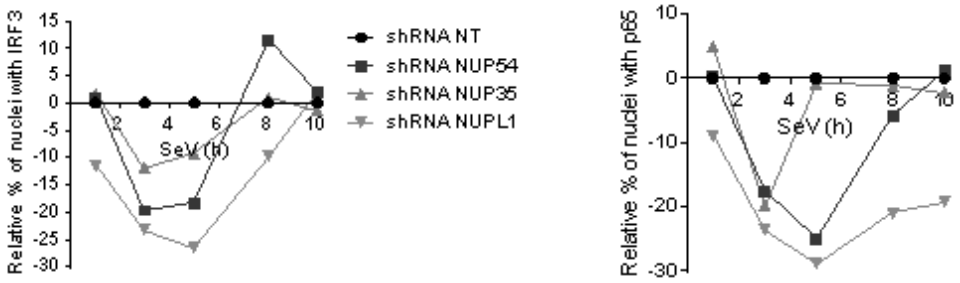

Figure 7. Effect of silencing Nups on IRF3 and p65 nuclear translocation.

Cytoplasmic FG-Nups and filaments (RANBP2, NUP214, NUPL2), outer-ring Nups (NUP43, NUP107, NUP160), linker Nups (NUP93, NUP88) and central FG-Nups (NUP54, NUP35, NUPL1) were knocked down. Results are presented as the average of all shRNAs in relative percentage of cells containing IRF3 and p65 in the nucleus after normalization of the control shRNA NT to zero for all time points, as described in Figure 5A. Individual shRNA results on IRF3 and p65 nuclear translocation, *IFNB1* promoter activity and cell proliferation and survival are described in Figures S9-S12.

GO TERM	Gene Count	Genes	Fold Enrichment	*p* value
Protein Import into Nucleus, Docking (BP)	4	CSE1L, KPNB1, TNPO1, XPO1	72	0.00002
Nuclear Pore (CC)	6	CSE1L, KPNB1, LBR, RAN, TNPO1, XPO1	23	0.000005
Translation Elongation (BP)	7	RPL10, RPL15, RPL29, RPL3, RPL7A, RPS7, UBC	21	0.00000073
Protein Import into Nucleus (BP)	5	CSE1L, KPNB1, RAN, TNPO1, XPO1	18	0.00016
Ribonucleoprotein Complex (CC)	11	ACTB, DICER1, RPL10, RPL15, RPL29, RPL3, RPL7A, RPS7, UBC, XPO1, YBX1	6.5	0.0000038
RNA Processing (BP)	6	DICER, RBM10, RPS7, WDR77, YBX1, ZRANB2	3.4	0.029
Nucleoplasm (CC)	8	ACTB, CSNK2A1, KPNB1, PRKDC, RAN, RUVBL2, UBC, XPO1	2.8	0.021
Cell Cycle (BP)	7	PHGDH, PPM1G, PSME3, RAN, SPIN1, TRIP13, UBC	2.8	0.035
Membrane-enclosed Lumen (CC)	13	ACTB, C1QBP, CACYBP, CSNK2A1, KPNB1, PRKDC, RAN, RPL3, RPS7, RRP12, RUVBL2, UBC, XPO1	2.1	0.011
Nucleotide Binding (MF)	14	ACTB, ATP6V1A, CSNK2A1, CKB, DICER1, GNAI3, MTHFD1, PHGDH, PKM2, PRKDC, RAN, RBM10, RUBVL2, TRIP13	1.9	0.018

Table 1. Gene ontology (GO) terms enrichment of HCV-host interactors affecting the innate antiviral immunity

GO biological process (BP), molecular functions (MF) and cellular compartment (CC) terms significantly enriched ($p < 0.05$) are indicated with their respective list of genes and fold enrichment. The GO terms incorrectly list XPO1 as being involved in protein import, when it is the main carrier for protein export.

SUPPLEMENTAL FIGURES

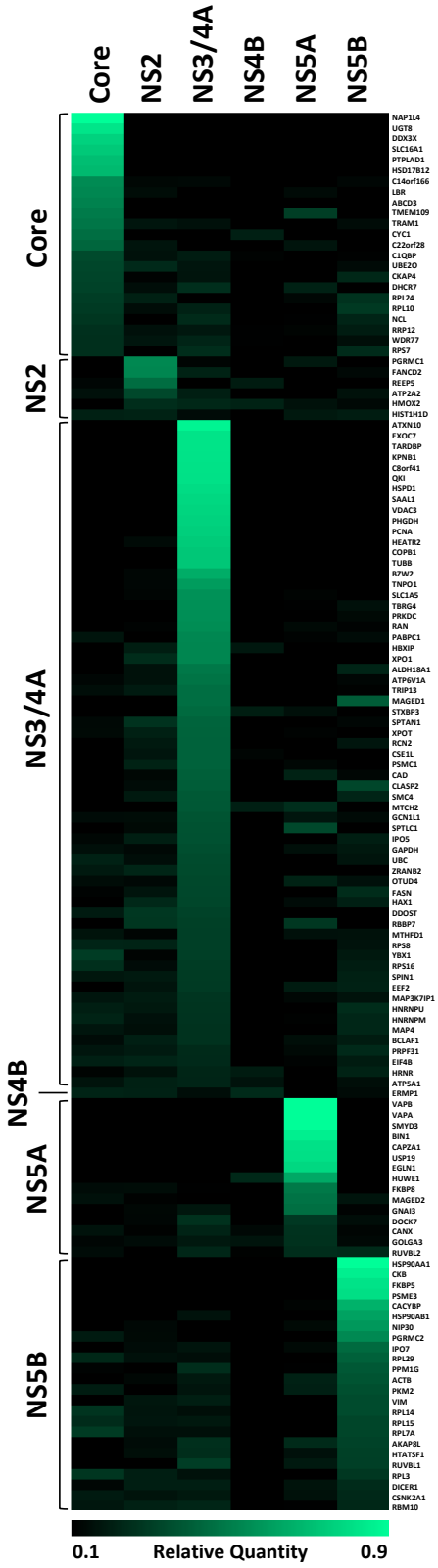

Figure S1. Host proteins specifically associated with HCV proteins

Heat map visualization of the 132 host protein quantities significantly enriched in one of the six experimental IPs of HCV proteins (3xFLAG-Core, -NS2, -NS3/4A, -NS4B, -NS5A and –NS5B), modified from Germain et al. (2014) [1]. Proportions of presence for each of the six experimental conditions are represented for host proteins hits (Σ six conditions = 1 for each host protein). The proteins are ordered from greatest to lowest proportion in their respective viral protein enrichment groups as determined by LC-MS/MS. The darker color correlates with the absence of the host protein in the condition, and brighter green indicates a high prevalence of the host protein in the condition ($\log_2$ scale).

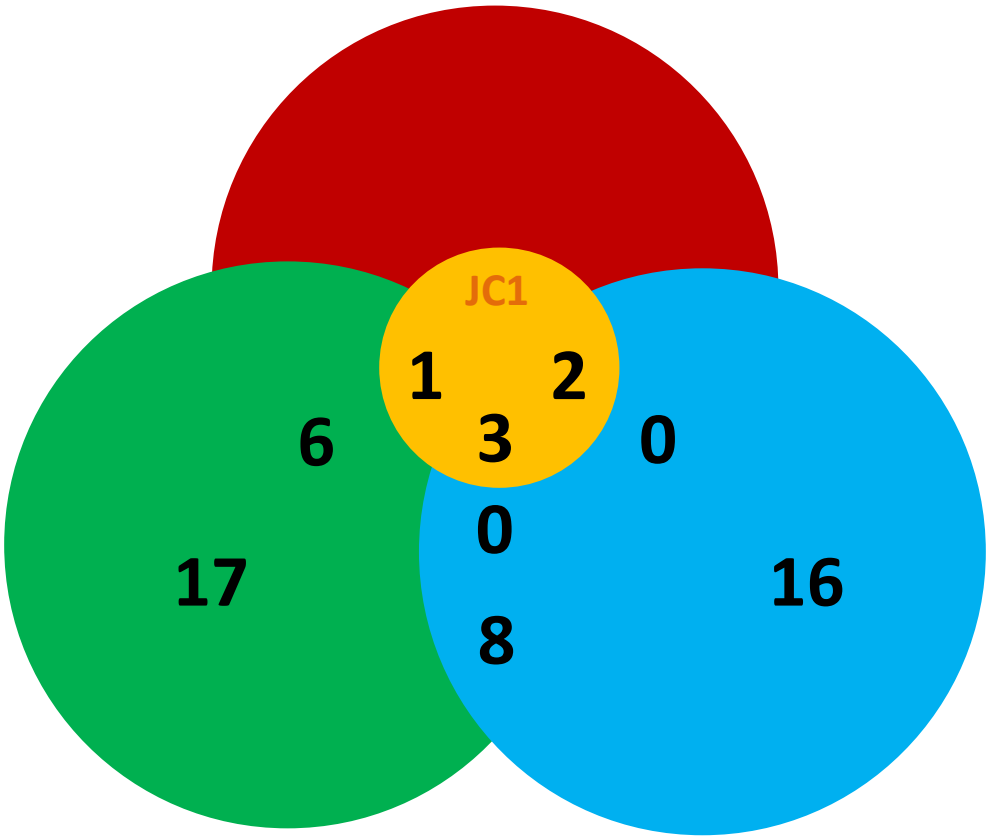

Figure S2. Venn Diagram of Virus-Host Interactors Greatly Modulating HCV Replication and the Innate Antiviral Immune Response

A Venn diagram representation of the effect of gene silencing on the 53 virus-host interactors greatly affecting the innate antiviral immune response in comparison to their effect on HCV replication. Only 12 out of the 53 interactors met the stringent criteria of Germain et al. (2014) [1] for having a major effect on viral replication, while the rest affected the immune response.

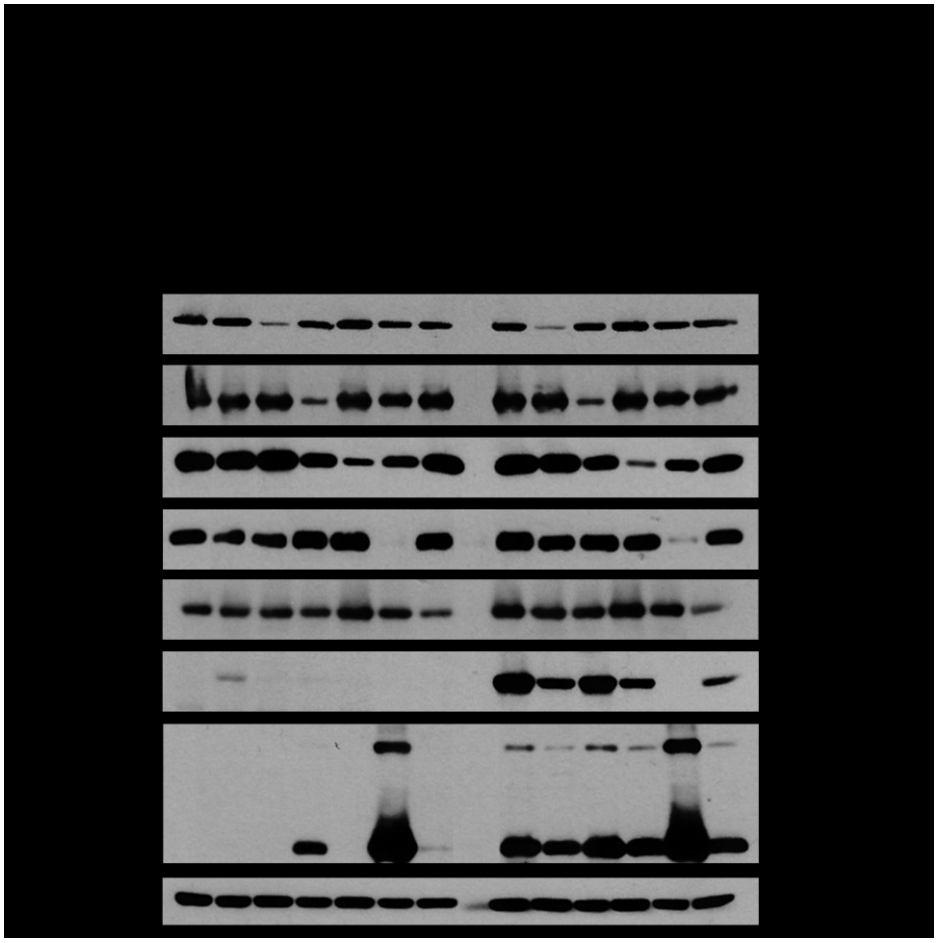

Figure S3. Effect of nucleocytoplasmic transporters knockdown on SeV replication.

Immunoblot analysis of HEK 293T cells infected with SeV for 8 or 24 hours following knockdown of XPO1, CSE1L, RAN, KPNB1 and TNPO1 for three days. shRNA NT is used as a control.

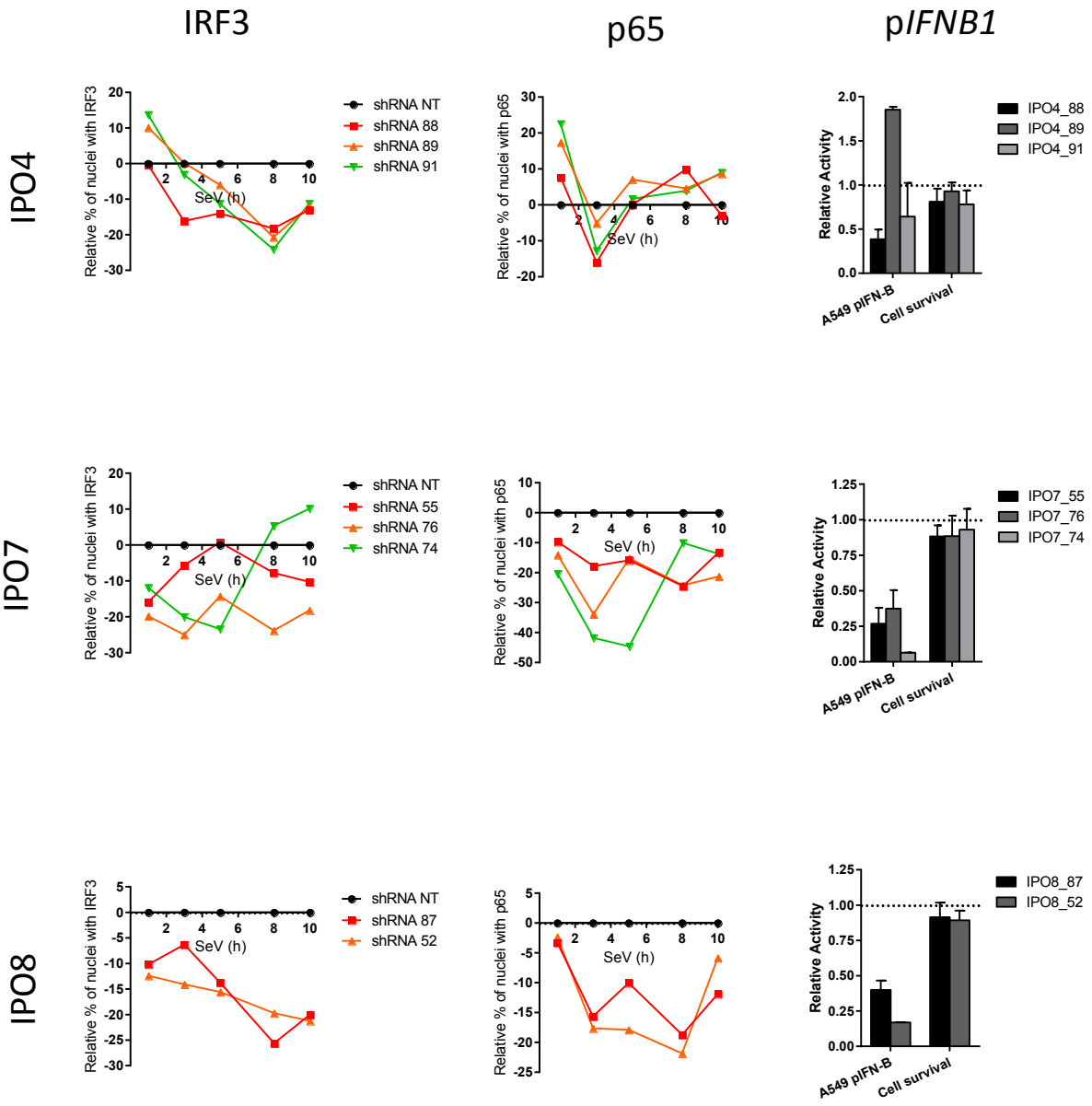

Figure S4. Effect of silencing importins on IRF3 and p65 nuclear translocation, p*IFNB1* induction and cellular fitness.

Effect of IPO4, IPO7 and IPO8 knockdown on the relative percentage of nuclei with IRF3 and p65 staining after normalization of the control shRNA NT to zero for all time points. The effect of these knockdowns on SeV induced *IFNB1* promoter activity was measured in A549

cells stably expressing the firefly luciferase under the control of the *IFNB1* promoter (right panel). In addition, the effect of a shRNA on cell proliferation and survival was evaluated using images from the microscopy screen.

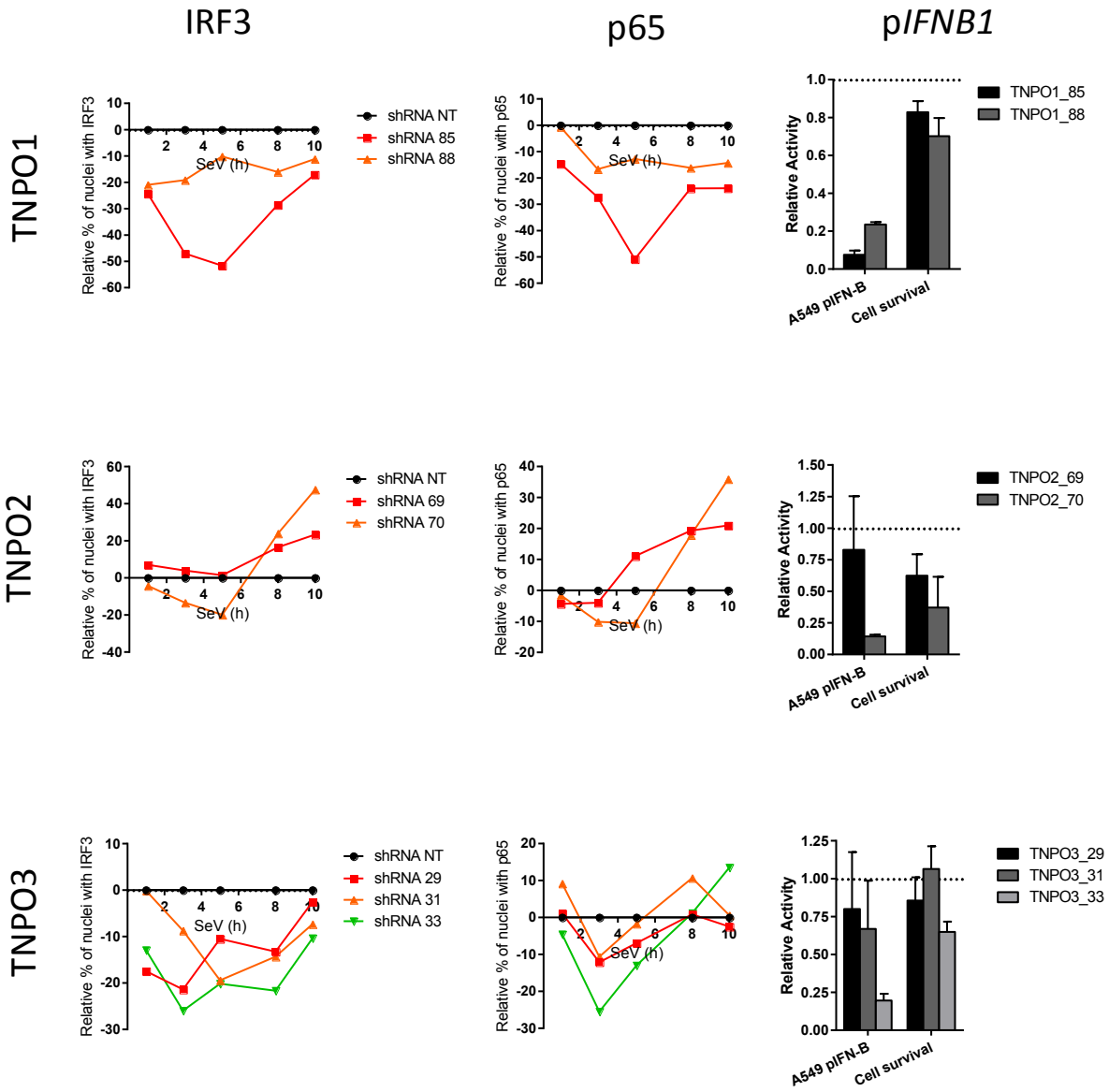

Figure S5. Effect of silencing transportins on IRF3 and p65 nuclear translocation, p*IFNB1* induction and cellular fitness.

Effect of TNPO1, TNPO2 and TNPO3 knockdown on the relative percentage of nuclei with IRF3 and p65 staining, *IFNB1* promoter activity and cellular fitness, as described in Figure S4.

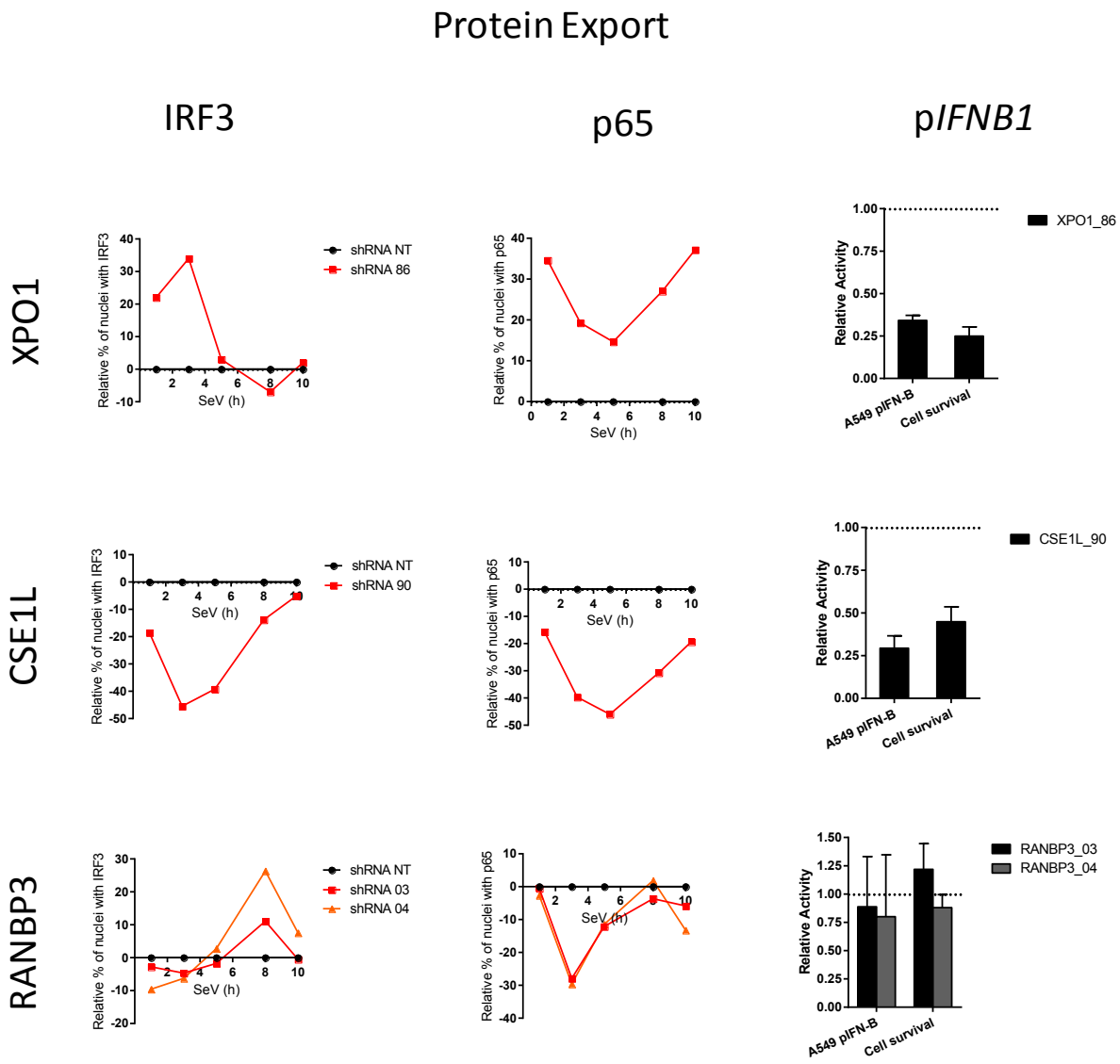

Figure S6. Effect of silencing proteins involved in protein export on IRF3 and p65 nuclear translocation, p*IFNB1* induction and cellular fitness.

Effect of XPO1, CSE1L and RANBP3 knockdown on the relative percentage of nuclei with IRF3 and p65 staining, *IFNB1* promoter activity and cellular fitness, as described in Figure S4.

mRNA Export

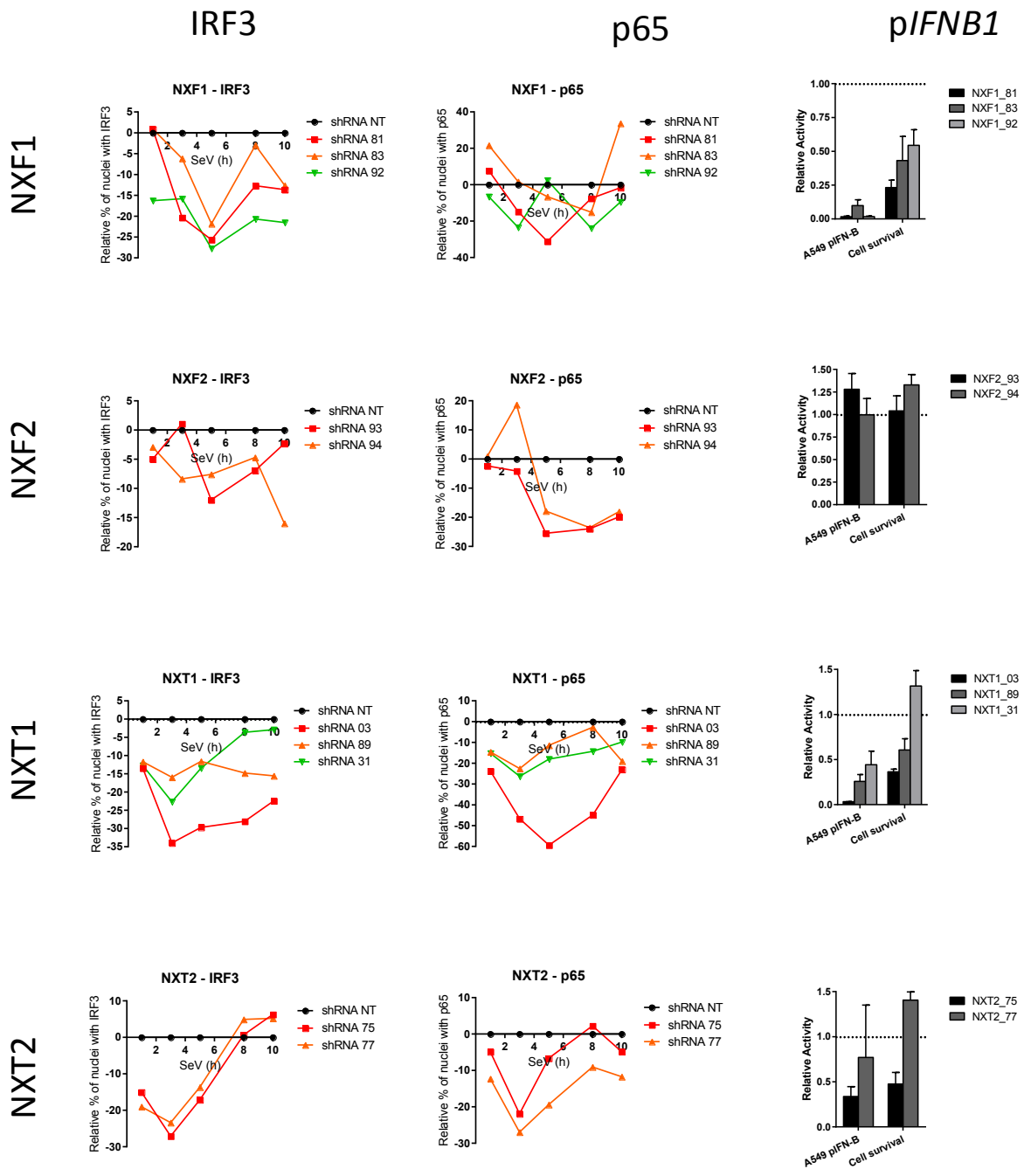
IRF3
p65
pIFNB1
NXF1
NXF2
NXT1
NXT2
NXF1 - IRF3
NXF1 - p65
NXF2 - IRF3
NXF2 - p65
NXT1 - IRF3
NXT1 - p65
NXT2 - IRF3
NXT2 - p65
Relative % of nuclei with IRF3
Relative % of nuclei with p65
SeV (h)
shRNA NT
shRNA 81
shRNA 83
shRNA 92
shRNA 93
shRNA 94
shRNA 03
shRNA 89
shRNA 31
shRNA 75
shRNA 77
Relative Activity
A549 pIFN-B
Cell survival
NXF1_81
NXF1_83
NXF1_92
NXF2_93
NXF2_94
NXT1_03
NXT1_89
NXT1_31
NXT2_75
NXT2_77

Figure S7. Effect of silencing proteins involved in mRNA export on IRF3 and p65 nuclear translocation, p*IFNB1* induction and cellular fitness.

Effect of NXT1, NXT2, NXF1 and NXF2 knockdown on the relative percentage of nuclei with IRF3 and p65 staining, *IFNB1* promoter activity and cellular fitness, as described in Figure S4.

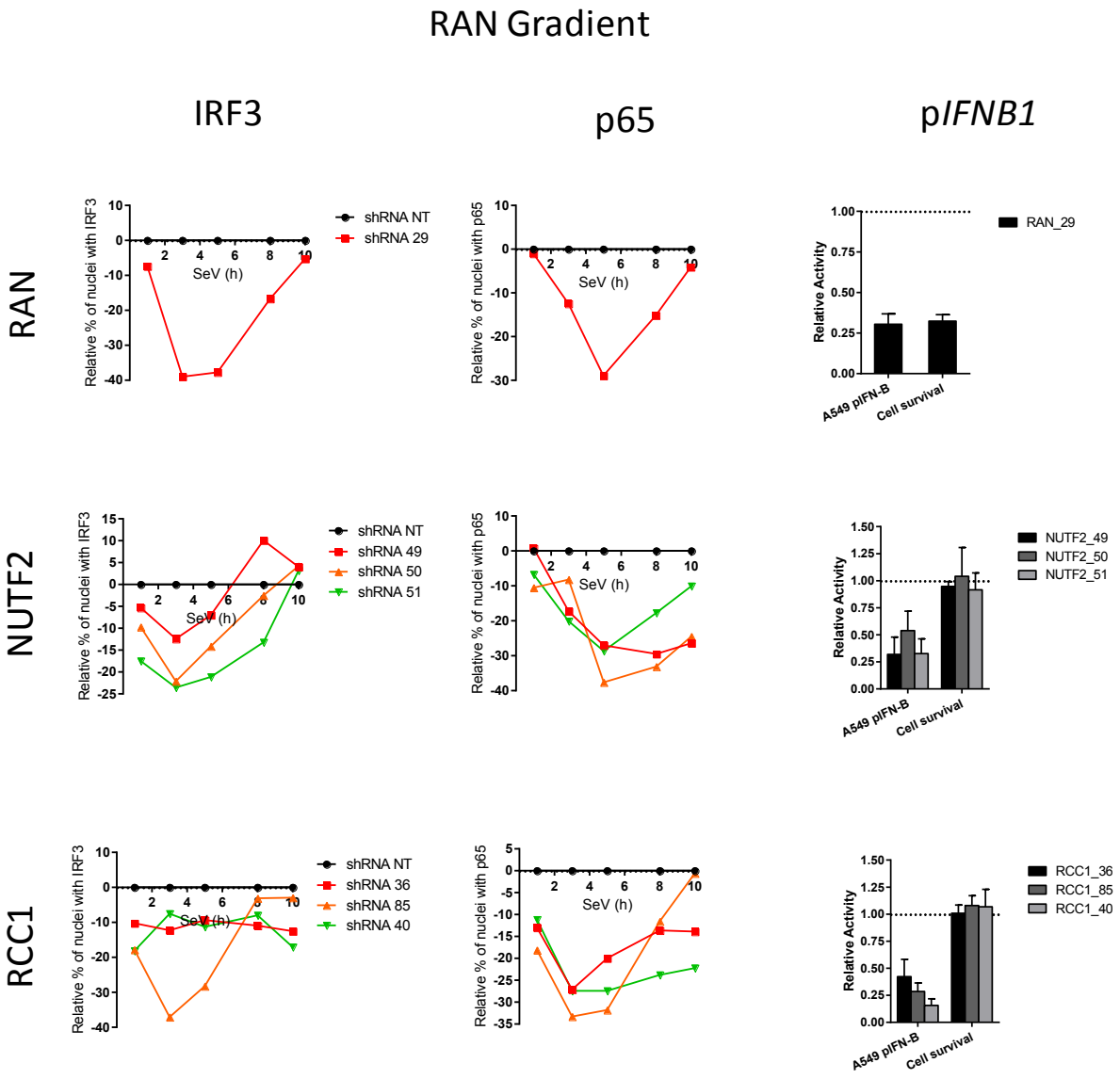

Figure S8. Effect of silencing proteins involved in the RAN gradient on IRF3 and p65 nuclear translocation, p*IFNB1* induction and cellular fitness.

Effect of RAN, NUTF2 and RCC1 knockdown on the relative percentage of nuclei with IRF3 and p65 staining, *IFNB1* promoter activity and cellular fitness, as described in Figure S4.

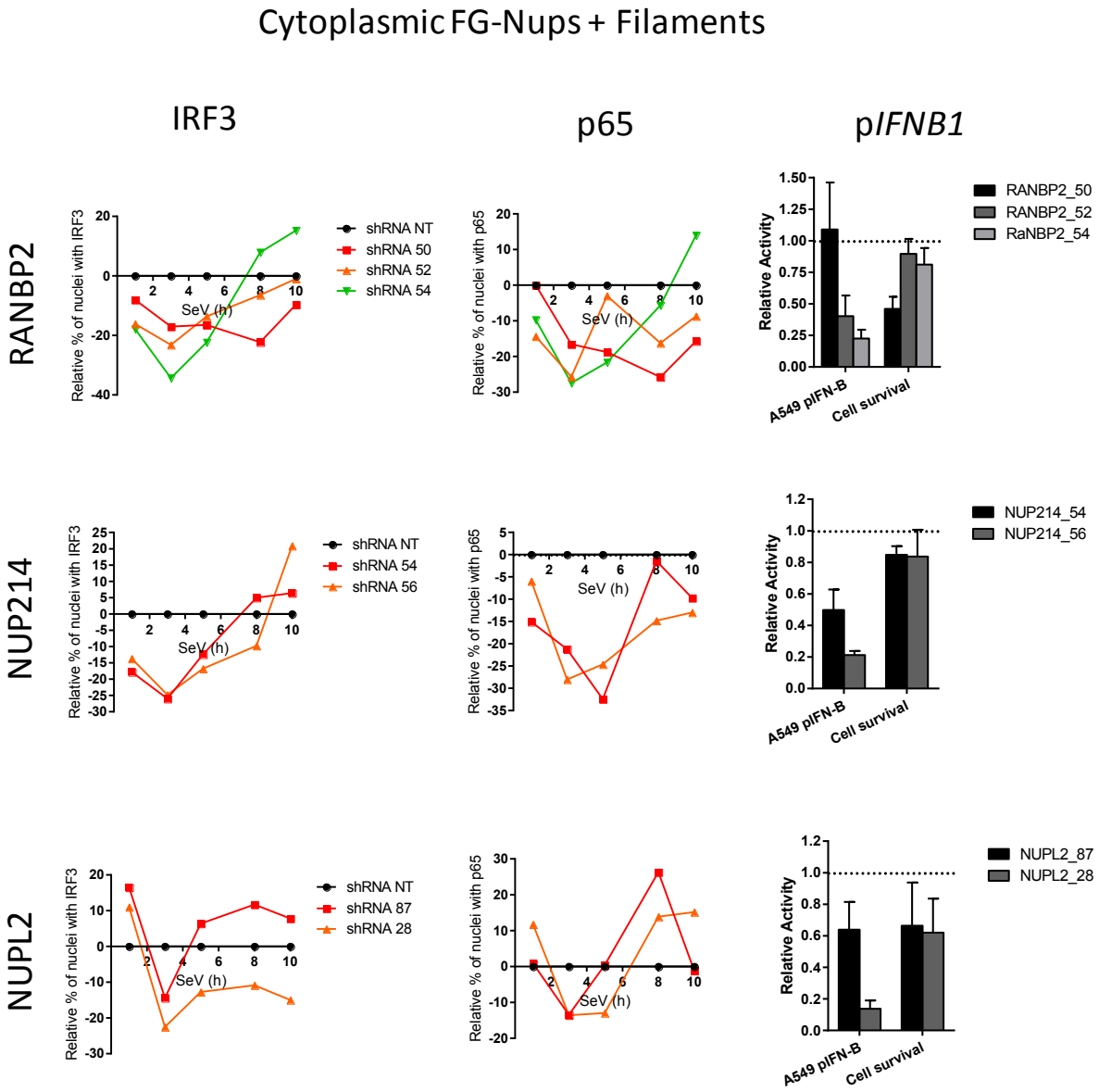

Figure S9. Effect of silencing cytoplasmic FG-Nups and filaments on IRF3 and p65 nuclear translocation, p*IFNB1* induction and cellular fitness.

Effect of RANBP2, NUP214 and NUPL2 knockdown on the relative percentage of nuclei with IRF3 and p65 staining, *IFNB1* promoter activity and cellular fitness, as described in Figure S4.

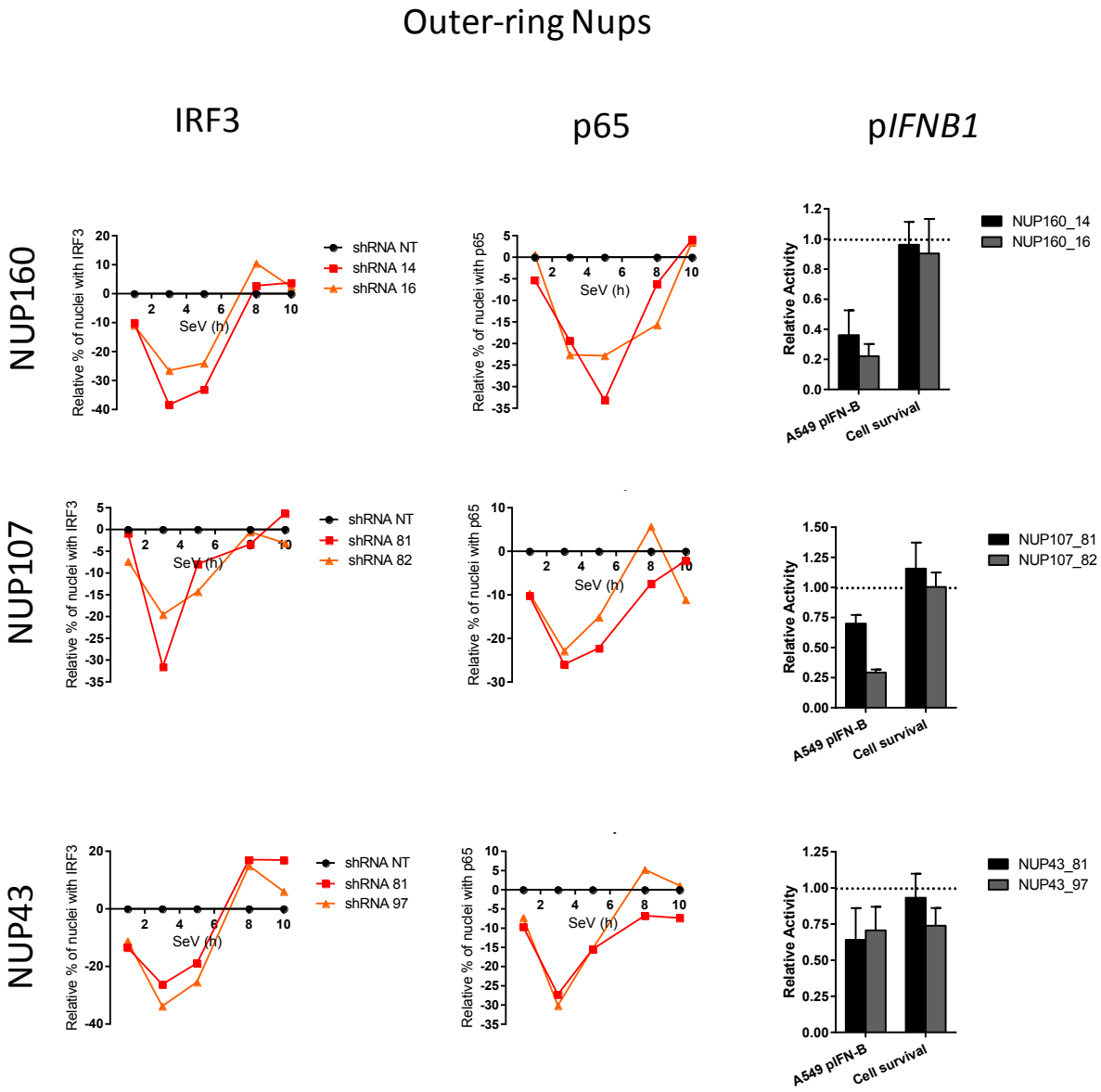

Figure S10. Effect of silencing outer-ring Nups on IRF3 and p65 nuclear translocation, p*IFNB1* induction and cellular fitness.

Effect of NUP43, NUP107 and NUP160 knockdown on the relative percentage of nuclei with IRF3 and p65 staining, *IFNB1* promoter activity and cellular fitness, as described in Figure S4.

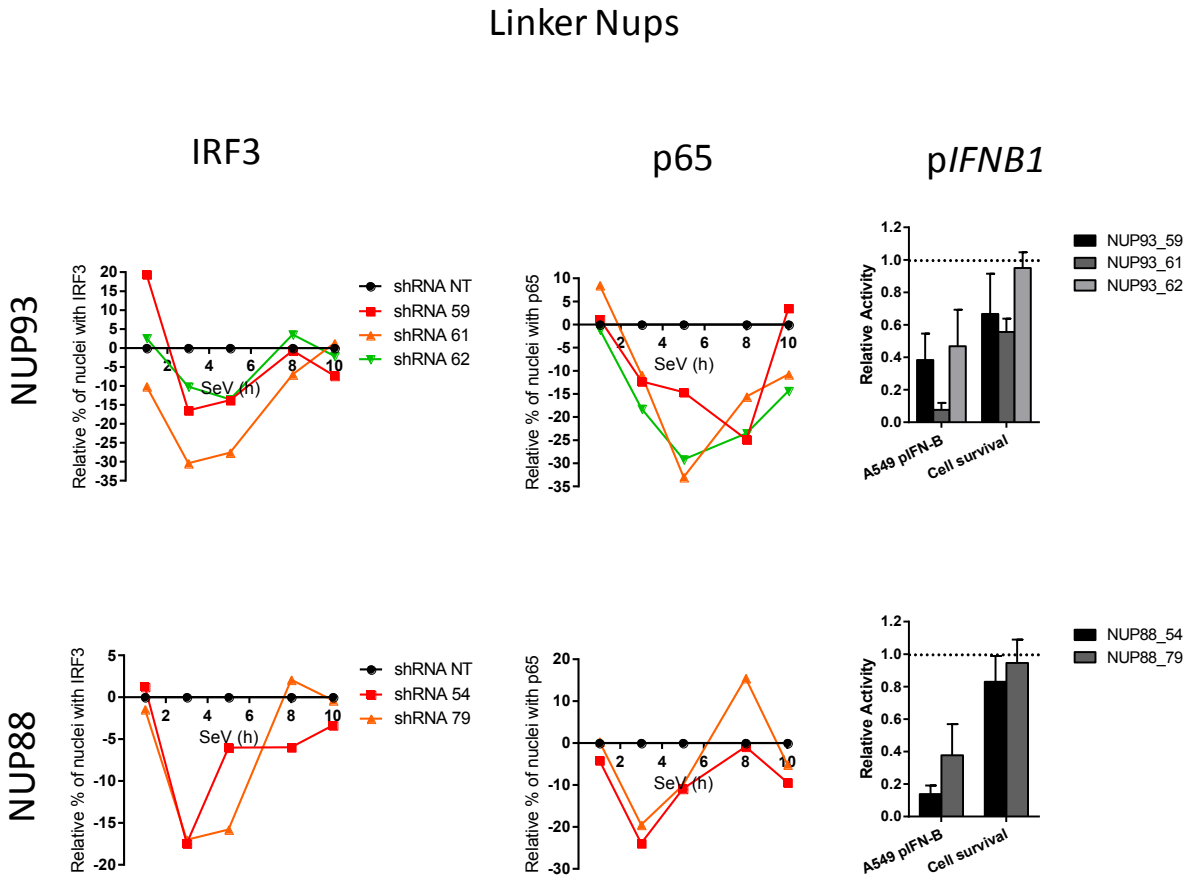

Figure S11. Effect of silencing linker Nups on IRF3 and p65 nuclear translocation, p*IFNB1* induction and cellular fitness.

Effect of NUP93 and NUP88 knockdown on the relative percentage of nuclei with IRF3 and p65 staining, *IFNB1* promoter activity and cellular fitness, as described in Figure S4.

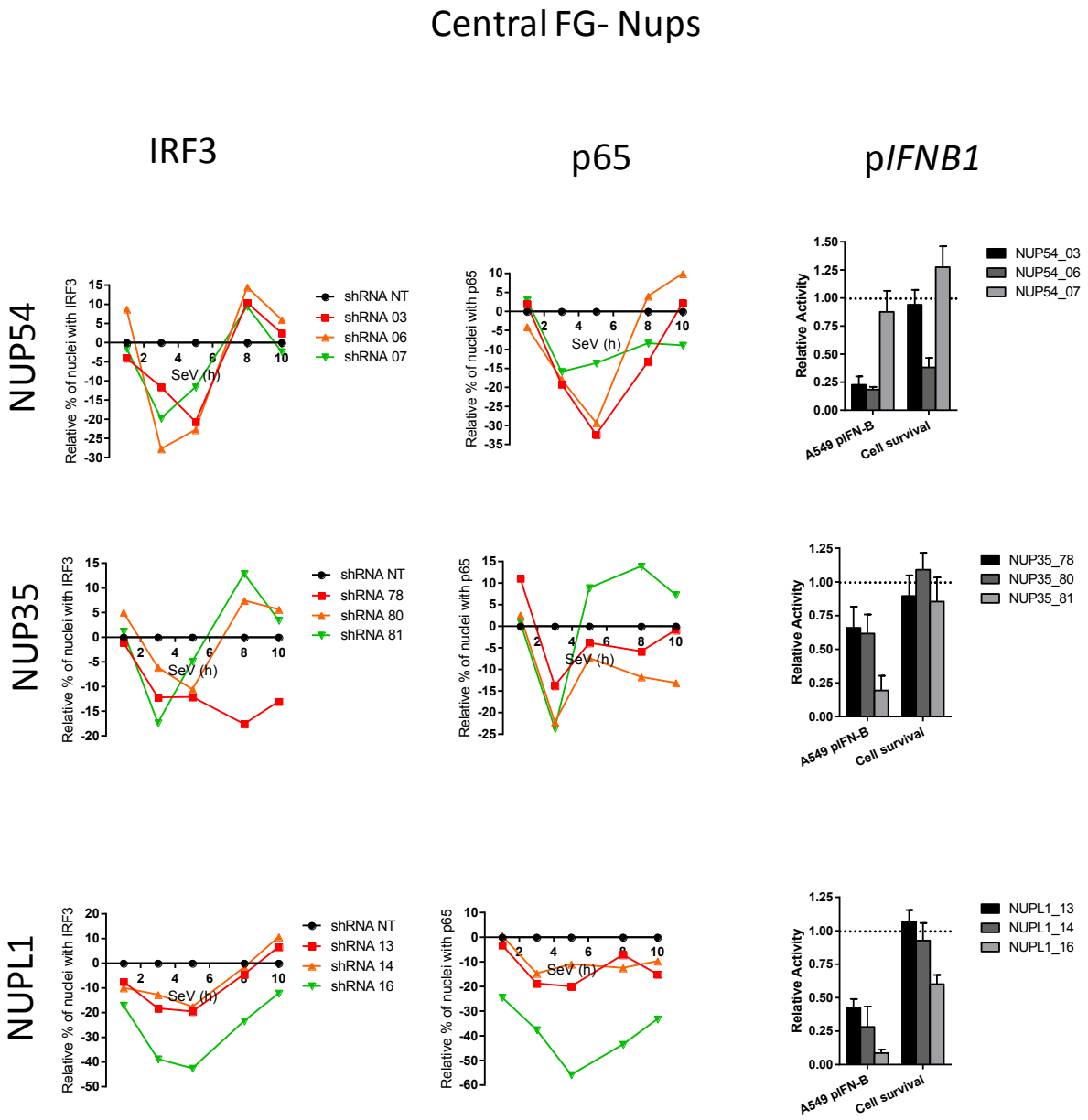

Figure S12. Effect of silencing central FG-Nups on IRF3 and p65 nuclear translocation, p*IFNB1* induction and cellular fitness.

Effect of NUP54, NUP35 and NUPL1 knockdown on the relative percentage of nuclei with IRF3 and p65 staining, *IFNB1* promoter activity and cellular fitness, as described in Figure S4.

UniProt ID	Protein	# of peptides	Sequence Coverage (%)	FC Core	FC NS2	FC NS3/4A	FC NS4B	FC NS5A	FC NS5B	Total	RQ Core	RQ NS2	RQ NS3/4A	RQ NS4B	RQ NS5A	RQ NS5B
IPI00002372	ABCD3	5	8.9	4.3	1.1	1.0	0.3	1.0	0.8	8.4	0.512	0.125	0.119	0.033	0.123	0.089
IPI00894365	ACTB	13	6.0	0.4	0.8	1.1	0.3	1.2	2.2	6.0	0.066	0.127	0.179	0.051	0.209	0.369
IPI00297455	AKAP8L	4	6.0	0.2	0.9	1.7	0.2	1.6	2.1	6.9	0.029	0.138	0.251	0.033	0.236	0.313
IPI00218547	ALDH18A1	6	10.0	0.5	1.2	3.5	0.3	0.3	1.6	7.4	0.069	0.157	0.480	0.034	0.041	0.219
IPI00219078	ATP2A2	8	8.0	1.0	2.2	1.3	0.4	0.6	1.1	6.7	0.154	0.331	0.198	0.065	0.094	0.159
IPI00440493	ATP5A1	7	5.0	1.2	1.5	1.6	1.2	0.8	1.1	7.4	0.164	0.204	0.219	0.160	0.105	0.148
IPI00007682	ATP6V1A	6	12.0	0.9	1.2	3.6	0.4	0.5	1.0	7.7	0.124	0.159	0.470	0.053	0.070	0.125
IPI00001636	ATXN10	4	1.0	0.5	0.9	14.2	0.1	0.3	0.3	16.3	0.028	0.056	0.870	0.008	0.018	0.020
IPI00413672	BCLAF1	10	2.0	0.7	1.0	1.2	0.3	0.7	0.9	4.7	0.140	0.203	0.261	0.056	0.149	0.190
IPI00220996	BIN1	21	2.8	0.4	1.1	0.4	0.1	14.3	0.4	16.8	0.023	0.066	0.024	0.008	0.853	0.025
IPI00894416	BZW2	3	6.0	0.6	1.2	6.2	0.4	0.4	0.7	9.5	0.060	0.125	0.648	0.043	0.046	0.077
IPI00792100	C14orf166	6	19.7	4.1	1.0	1.0	0.2	0.3	0.9	7.5	0.541	0.128	0.129	0.033	0.047	0.123
IPI00014230	C1QBP	7	31.0	2.1	1.0	1.2	0.7	0.5	0.7	6.2	0.338	0.158	0.191	0.113	0.088	0.112
IPI00550689	C22orf28	6	11.3	3.3	1.3	0.8	0.3	1.3	0.8	7.8	0.425	0.169	0.098	0.041	0.169	0.097
IPI00306207	C8orf41	3	6.1	0.4	0.4	9.2	0.4	0.4	0.4	11.3	0.037	0.037	0.814	0.037	0.037	0.037
IPI00395627	CACYBP	4	31.6	0.4	1.1	0.5	0.2	1.2	6.8	10.2	0.041	0.106	0.051	0.023	0.116	0.664
IPI00893035	CAD	6	3.0	0.8	1.0	3.0	0.3	1.6	0.9	7.5	0.101	0.127	0.404	0.034	0.210	0.124
IPI00020984	CANX	17	4.0	0.7	0.5	0.9	0.5	1.1	0.5	4.1	0.161	0.112	0.216	0.131	0.261	0.120
IPI00873484	CAPZA1	3	4.0	0.2	0.3	0.4	1.1	9.4	0.2	11.6	0.017	0.025	0.037	0.095	0.811	0.015
IPI00604713	CKAP4	6	10.0	2.1	0.7	1.1	0.6	0.5	1.5	6.5	0.319	0.114	0.166	0.095	0.078	0.227
IPI00022977	CKB	3	15.7	0.3	0.8	0.3	0.3	0.3	12.4	14.6	0.024	0.052	0.024	0.024	0.024	0.853
IPI00871686	CLASP2	2	1.0	0.7	1.0	2.7	0.1	0.1	2.2	6.9	0.099	0.140	0.395	0.021	0.021	0.324
IPI00295851	COPB1	2	2.6	0.5	1.1	8.0	0.5	0.5	0.5	11.0	0.042	0.103	0.730	0.042	0.042	0.042
IPI00022744	CSE1L	16	1.0	0.6	1.0	2.5	0.7	0.6	0.6	6.2	0.104	0.170	0.411	0.119	0.102	0.094
IPI00784195	CSNK2A1	3	4.0	1.1	1.0	1.1	0.5	1.0	1.4	6.1	0.187	0.165	0.179	0.082	0.158	0.229
IPI00029264	CYC1	3	9.8	3.2	0.7	0.6	1.4	0.4	0.7	7.0	0.451	0.102	0.092	0.203	0.052	0.101
IPI00297084	DDOST	3	4.0	1.3	1.9	2.2	0.4	0.7	0.5	6.9	0.185	0.277	0.312	0.053	0.095	0.079
IPI00215637	DDX3X	23	22.8	8.7	1.1	0.7	0.2	0.3	0.6	11.4	0.762	0.093	0.058	0.015	0.024	0.048
IPI00294501	DHCR7	4	8.0	1.9	0.9	1.6	0.1	1.3	0.4	6.2	0.312	0.144	0.250	0.019	0.208	0.067
IPI00219036	DICER1	12	8.0	0.9	1.5	1.5	0.6	1.2	1.8	7.3	0.123	0.198	0.198	0.077	0.163	0.240
IPI00815886	DOCK7	3	3.0	0.6	0.8	1.7	0.6	1.8	0.9	6.5	0.095	0.123	0.258	0.096	0.281	0.147
IPI00186290	EEF2	10	11.0	0.6	1.2	2.0	0.4	1.3	1.4	6.9	0.086	0.167	0.287	0.062	0.189	0.209
IPI00004928	EGLN1	10	27.7	0.4	0.9	0.5	0.2	10.3	0.8	13.1	0.031	0.070	0.042	0.013	0.783	0.061
IPI00012079	EIF4B	36	52.0	1.2	1.3	1.4	0.2	0.7	1.1	5.9	0.203	0.218	0.233	0.042	0.115	0.190
IPI00257903	ERMP1	2	4.0	1.3	1.3	0.9	1.5	0.4	0.9	6.3	0.214	0.207	0.146	0.238	0.060	0.135
IPI00172532	EXOC7	3	5.0	0.5	0.6	10.2	0.1	0.2	0.8	12.4	0.043	0.049	0.820	0.012	0.015	0.061
IPI00604399	FANCD2	3	0.0	0.5	4.4	1.8	0.2	0.4	1.1	8.3	0.064	0.524	0.211	0.027	0.044	0.131
IPI00026781	FASN	5	3.0	0.8	1.2	2.4	0.5	0.5	1.7	7.2	0.114	0.168	0.328	0.074	0.074	0.242
IPI00218775	FKBP5	12	31.0	0.3	1.1	0.5	0.2	0.7	12.5	15.3	0.019	0.074	0.035	0.010	0.043	0.818
IPI00640341	FKBP8	3	12.0	1.1	1.2	0.9	0.3	4.0	0.7	8.2	0.138	0.142	0.108	0.042	0.484	0.086
IPI00219018	GAPDH	7	21.0	1.0	0.9	2.4	0.3	1.0	1.2	6.8	0.151	0.129	0.350	0.038	0.151	0.180
IPI00001159	GCN1L1	30	4.0	0.9	1.0	2.5	0.3	1.2	0.9	6.8	0.139	0.141	0.368	0.045	0.171	0.136
IPI00220578	GNAI3	3	8.0	0.8	1.0	1.4	0.3	3.6	0.9	7.9	0.096	0.128	0.173	0.036	0.452	0.114
IPI00333419	GOLGA3	3	2.0	0.8	0.9	1.1	1.1	1.6	0.8	6.4	0.124	0.140	0.180	0.168	0.258	0.129
IPI00604587	HAX1	7	2.0	0.3	1.7	2.4	0.5	1.0	1.5	7.4	0.036	0.231	0.324	0.069	0.139	0.201
IPI00012831	HBXIP	2	36.0	0.1	0.7	1.8	0.6	0.1	0.1	3.4	0.035	0.195	0.525	0.176	0.035	0.035
IPI00242630	HEATR2	4	4.0	0.6	1.5	8.0	0.4	0.2	0.2	10.8	0.057	0.135	0.742	0.034	0.016	0.016
IPI00217466	HIST1H1D	2	5.0	1.4	1.5	1.0	0.5	1.3	1.4	7.0	0.206	0.212	0.139	0.073	0.179	0.192
IPI00026824	HMOX2	4	16.0	0.2	1.6	1.5	1.4	1.0	0.9	6.7	0.033	0.245	0.226	0.210	0.157	0.130
IPI00171903	HNRNPM	26	31.0	1.5	1.1	1.8	0.2	0.8	1.5	6.8	0.215	0.154	0.264	0.032	0.111	0.223
IPI00644079	HNRNPU	23	20.0	1.3	1.2	1.8	0.3	0.4	1.6	6.7	0.198	0.180	0.269	0.048	0.062	0.244
IPI00398625	HRNR	9	6.0	0.6	0.9	1.2	1.0	0.6	1.1	5.5	0.117	0.158	0.222	0.190	0.103	0.210
IPI00007676	HSD17B12	9	22.8	7.2	1.0	0.6	0.1	0.8	0.7	10.4	0.689	0.097	0.059	0.013	0.076	0.066
IPI00382470	HSP90AA1	19	6.0	0.2	0.3	0.4	0.2	0.5	15.2	16.7	0.012	0.017	0.022	0.009	0.030	0.910
IPI00414676	HSP90AB1	36	11.0	0.3	0.9	1.4	0.3	0.5	5.3	8.7	0.030	0.100	0.160	0.039	0.057	0.614
IPI00784154	HSPD1	25	45.0	0.3	0.6	9.2	0.4	0.7	0.3	11.5	0.027	0.051	0.795	0.035	0.063	0.030
IPI00644220	HTATSF1	4	8.0	0.7	1.0	1.7	0.3	1.1	2.1	6.8	0.100	0.149	0.245	0.044	0.156	0.307
IPI00445401	HUWE1	3	1.0	0.4	0.7	0.1	2.1	5.7	0.1	9.0	0.047	0.075	0.006	0.230	0.633	0.009
IPI00793443	IPO5	9	6.0	0.9	1.4	2.5	0.4	0.5	1.4	7.0	0.128	0.198	0.358	0.051	0.066	0.199
IPI00007402	IPO7	5	0.0	0.5	1.0	1.2	0.4	1.0	3.2	7.3	0.064	0.138	0.169	0.058	0.134	0.437
IPI00001639	KPNB1	18	24.0	0.3	1.2	11.1	0.3	0.4	0.4	13.6	0.021	0.091	0.816	0.019	0.027	0.027
IPI00292135	LBR	6	5.5	4.6	1.2	0.8	0.4	1.2	0.5	8.6	0.529	0.141	0.092	0.042	0.137	0.059
IPI00398845	MAGED1	6	1.0	0.2	0.6	3.9	0.3	0.3	3.4	8.6	0.023	0.070	0.449	0.031	0.036	0.392
IPI00337823	MAGED2	10	12.0	1.2	0.9	0.7	0.1	3.6	1.3	7.7	0.155	0.110	0.086	0.017	0.465	0.166
IPI00019459	MAP3K7IP1	15	18.0	1.0	1.1	1.5	0.4	0.7	0.9	5.7	0.172	0.189	0.272	0.078	0.127	0.161
IPI00888475	MAP4	6	6.0	1.1	1.0	1.8	0.6	0.7	1.5	6.7	0.171	0.149	0.261	0.088	0.106	0.224

UniProt ID	Protein	# of peptides	Sequence Coverage (%)	FC Core	FC NS2	FC NS3/4A	FC NS4B	FC NS5A	FC NS5B	Total	RQ Core	RQ NS2	RQ NS3/4A	RQ NS4B	RQ NS5A	RQ NS5B
IPI00003833	MTCH2	4	9.9	0.3	0.5	2.5	1.3	1.6	0.2	6.5	0.053	0.083	0.381	0.201	0.250	0.032
IPI00218342	MTHFD1	3	3.0	0.9	0.7	1.7	0.6	0.9	0.9	5.5	0.164	0.119	0.303	0.101	0.155	0.157
IPI00017763	NAP1L4	27	42.0	28.3	0.8	0.1	0.1	0.4	0.1	29.9	0.947	0.028	0.004	0.003	0.014	0.004
IPI00604620	NCL	42	32.0	1.6	0.6	1.4	0.3	0.6	1.3	6.0	0.275	0.106	0.236	0.058	0.108	0.217
IPI00178750	NIP30	4	16.0	0.2	1.3	0.5	0.8	1.3	5.8	10.0	0.024	0.131	0.050	0.081	0.132	0.581
IPI00399254	OTUD4	3	1.0	1.1	1.0	2.5	0.2	1.6	1.2	7.5	0.142	0.131	0.330	0.032	0.210	0.154
IPI00008524	PABPC1	19	14.0	0.9	0.0	2.9	0.3	0.6	0.8	5.6	0.166	0.005	0.527	0.049	0.114	0.138
IPI00021700	PCNA	5	21.0	0.6	1.1	8.3	0.2	0.5	0.3	11.0	0.054	0.097	0.753	0.021	0.046	0.029
IPI00220739	PGRMC1	5	24.0	0.6	4.1	0.9	0.4	1.4	0.4	7.7	0.073	0.531	0.121	0.048	0.181	0.047
IPI00005202	PGRMC2	3	14.0	1.2	0.9	0.3	0.2	0.4	3.4	6.4	0.185	0.134	0.046	0.038	0.065	0.533
IPI00011200	PHGDH	20	1.0	0.3	0.7	6.2	0.3	0.4	0.2	8.2	0.033	0.091	0.762	0.040	0.049	0.025
IPI00479186	PKM2	9	17.0	1.2	0.3	1.0	0.2	1.2	2.2	6.1	0.194	0.049	0.168	0.033	0.203	0.353
IPI00006167	PPM1G	12	34.0	0.7	0.6	1.5	0.3	0.7	2.3	6.0	0.113	0.105	0.246	0.044	0.109	0.382
IPI00296337	PRKDC	33	1.0	0.6	0.8	4.3	0.4	0.7	1.0	7.7	0.074	0.100	0.553	0.048	0.094	0.132
IPI00292000	PRPF31	9	18.0	1.0	1.1	1.4	0.2	0.8	1.4	5.9	0.171	0.186	0.238	0.037	0.133	0.234
IPI00011126	PSMC1	6	16.1	0.4	1.5	3.0	0.7	0.9	0.8	7.3	0.060	0.210	0.411	0.090	0.126	0.104
IPI00030243	PSME3	12	17.0	0.7	0.9	0.4	0.4	0.2	10.8	13.4	0.052	0.065	0.031	0.033	0.015	0.804
IPI00008998	PTPLAD1	3	7.8	8.2	1.2	0.3	0.5	0.4	1.2	11.8	0.700	0.098	0.025	0.038	0.032	0.106
IPI00736672	QKI	4	17.0	0.6	0.8	9.4	0.2	0.2	0.4	11.6	0.051	0.072	0.812	0.014	0.021	0.031
IPI00792352	RAN	4	20.0	0.4	0.9	4.1	0.3	1.0	0.9	7.6	0.053	0.113	0.548	0.039	0.134	0.114
IPI00395865	RBBP7	9	21.4	0.4	2.0	2.2	0.1	2.0	0.5	7.2	0.056	0.274	0.307	0.020	0.278	0.064
IPI00375731	RBM10	42	25.0	0.9	1.0	1.1	0.3	0.5	1.1	4.9	0.173	0.206	0.220	0.066	0.108	0.227
IPI00029628	RCN2	12	41.0	0.6	1.3	2.9	0.5	0.5	1.2	7.0	0.080	0.182	0.413	0.076	0.078	0.170
IPI00744902	REEP5	2	11.0	0.9	3.1	0.7	1.3	0.4	0.6	6.8	0.125	0.446	0.101	0.190	0.052	0.087
IPI00853161	RPL10	11	36.0	1.8	0.9	1.3	0.2	0.3	1.8	6.3	0.287	0.142	0.208	0.037	0.043	0.283
IPI00555744	RPL14	11	46.0	1.9	1.2	1.1	0.2	0.4	2.4	7.1	0.267	0.166	0.149	0.024	0.054	0.339
IPI00470528	RPL15	12	44.0	1.6	1.2	1.2	0.2	0.4	2.2	6.7	0.241	0.171	0.181	0.032	0.053	0.322
IPI00306332	RPL24	6	32.0	2.3	1.6	0.7	0.2	1.0	2.0	7.9	0.295	0.204	0.095	0.020	0.127	0.260
IPI00796934	RPL29	7	19.0	1.7	1.2	1.1	0.1	0.4	3.1	7.5	0.226	0.155	0.145	0.014	0.051	0.410
IPI00550021	RPL3	22	38.0	2.0	1.5	1.2	0.3	0.4	2.0	7.3	0.273	0.200	0.159	0.035	0.056	0.276
IPI00299573	RPL7A	17	47.0	2.0	1.0	1.0	0.2	0.4	2.2	6.9	0.291	0.152	0.151	0.032	0.052	0.322
IPI00221092	RPS16	10	53.0	1.6	0.9	1.9	0.2	0.5	1.2	6.3	0.251	0.140	0.294	0.038	0.084	0.193
IPI00013415	RPS7	10	46.0	1.4	0.6	1.4	0.4	0.6	1.4	5.8	0.251	0.103	0.245	0.062	0.100	0.240
IPI00872430	RPS8	11	37.0	1.4	1.4	2.0	0.3	0.4	1.0	6.4	0.217	0.214	0.303	0.040	0.067	0.160
IPI00101186	RRP12	2	2.0	1.7	1.0	1.2	0.7	0.8	1.3	6.7	0.254	0.154	0.176	0.108	0.116	0.192
IPI00021187	RUVBL1	6	2.9	0.3	0.7	2.1	0.5	1.3	2.1	7.1	0.044	0.105	0.295	0.070	0.184	0.301
IPI00009104	RUVBL2	2	6.0	0.7	0.2	1.2	0.6	1.3	1.2	5.2	0.138	0.046	0.224	0.110	0.245	0.238
IPI00304935	SAAL1	2	5.5	0.4	0.9	9.4	0.4	0.4	0.4	12.0	0.035	0.078	0.783	0.035	0.035	0.035
IPI00024650	SLC16A1	4	4.0	8.4	1.0	0.7	0.1	0.8	0.5	11.4	0.735	0.084	0.063	0.010	0.066	0.041
IPI00019472	SLC1A5	5	9.6	0.5	0.6	2.8	0.2	0.6	0.3	5.0	0.101	0.119	0.559	0.042	0.116	0.063
IPI00411559	SMC4	4	4.0	0.6	1.3	2.8	0.2	0.8	1.6	7.3	0.084	0.182	0.385	0.026	0.105	0.219
IPI00165073	SMYD3	5	12.4	0.2	1.3	0.2	0.1	23.0	0.2	25.0	0.007	0.051	0.009	0.005	0.920	0.009
IPI00550655	SPIN1	11	11.0	0.9	1.0	1.5	0.3	0.5	1.1	5.3	0.174	0.183	0.289	0.063	0.086	0.206
IPI00844215	SPTAN1	3	3.0	0.8	1.7	2.7	0.2	0.2	0.8	6.3	0.129	0.263	0.419	0.032	0.032	0.124
IPI00005745	SPTLC1	6	6.1	0.5	0.9	2.6	0.3	2.4	0.5	7.1	0.064	0.132	0.363	0.035	0.332	0.074
IPI00297626	STXBP3	4	7.8	0.3	0.6	3.1	1.4	1.1	0.6	7.1	0.046	0.079	0.438	0.196	0.152	0.088
IPI00025815	TARDBP	7	22.8	0.3	1.3	11.9	0.2	0.5	0.3	14.6	0.022	0.089	0.820	0.016	0.033	0.020
IPI00329625	TBRG4	4	5.0	0.4	0.7	4.3	0.2	0.8	1.2	7.7	0.056	0.095	0.557	0.032	0.107	0.154
IPI00031697	TMEM109	2	9.1	4.0	0.8	0.4	0.2	2.4	0.3	8.2	0.492	0.100	0.043	0.024	0.298	0.042
IPI00024364	TNPO1	4	5.0	0.5	0.9	4.3	0.2	0.7	0.7	7.2	0.067	0.123	0.593	0.024	0.099	0.094
IPI00219111	TRAM1	3	7.2	3.3	1.2	1.1	0.3	0.1	1.0	6.9	0.476	0.171	0.155	0.041	0.018	0.139
IPI00003505	TRIP13	4	7.0	1.1	1.4	3.3	0.2	0.6	0.8	7.4	0.145	0.186	0.451	0.023	0.084	0.111
IPI00011654	TUBB	42	38.0	0.3	0.9	7.4	0.5	0.5	0.7	10.2	0.027	0.084	0.728	0.048	0.046	0.066
IPI00179330	UBC	5	20.0	1.4	1.0	2.3	0.4	0.5	1.1	6.7	0.208	0.145	0.341	0.065	0.074	0.167
IPI00783378	UBE2O	9	15.0	2.6	1.9	1.4	0.6	0.5	1.1	8.1	0.323	0.234	0.172	0.070	0.064	0.137
IPI00294455	UGT8	8	10.0	11.8	1.2	0.6	0.2	0.3	0.3	14.3	0.822	0.083	0.039	0.014	0.022	0.021
IPI00789672	USP19	21	17.0	0.4	1.0	0.6	0.4	11.1	0.3	13.8	0.026	0.072	0.042	0.032	0.806	0.022
IPI00640416	VAPA	12	48.0	0.1	1.5	0.2	0.2	28.1	0.2	30.4	0.005	0.050	0.008	0.006	0.924	0.008
IPI00006211	VAPB	14	40.3	0.1	1.0	0.1	0.1	41.6	0.2	43.1	0.003	0.024	0.003	0.003	0.963	0.004
IPI00031804	VDAC3	6	23.0	0.1	1.3	10.4	1.0	0.5	0.1	13.4	0.007	0.098	0.773	0.074	0.038	0.009
IPI00418471	VIM	23	63.0	0.7	1.3	1.5	0.8	0.8	2.6	7.6	0.088	0.174	0.198	0.101	0.099	0.340
IPI00012202	WDR77	21	43.0	1.3	0.9	1.1	0.6	0.5	0.8	5.1	0.253	0.171	0.218	0.109	0.098	0.150
IPI00298961	XPO1	15	20.0	0.5	2.0	4.3	0.4	0.5	0.5	8.1	0.062	0.244	0.525	0.051	0.062	0.057
IPI00306290	XPOT	7	14.0	1.1	1.7	3.4	0.3	0.9	0.8	8.2	0.132	0.206	0.414	0.042	0.113	0.092
IPI00031812	YBX1	13	34.0	1.9	0.8	2.0	0.2	0.5	1.2	6.6	0.292	0.117	0.303	0.033	0.075	0.180
IPI00845348	ZRANB2	9	13.0	1.1	1.4	2.1	0.3	0.6	0.6	6.2	0.182	0.222	0.336	0.054	0.104	0.102

Table S1. Absolute and Relative Quantities of Host Proteins in the 6 HCV Protein Conditions

This table contains the results of the LC-MS/MS analysis with the absolute quantities, as well as the relative quantities of host proteins in the 6 viral protein conditions which are visually represented in Figure S1. This data is modified from Germain et al. (2014) [1].

Gene Name	IPI no	Gene ID	shRNA	Bait	Statistically enriched	293T pIFN-B		A549 pIFN-B		293T pEF1a
						mean	stdev	mean	stdev	mean
ABCD3	IPI00002372	NM_002858	TRCN0000059848	Core	yes	0.882	0.343	1.010	0.099	0.810
ABCD3	IPI00002372	NM_002858	TRCN0000059849	Core	yes	0.902	0.251	1.113	0.259	0.879
ABCD3	IPI00002372	NM_002858	TRCN0000059850	Core	yes	0.723	0.150	1.280	0.136	0.723
ABCD3	IPI00002372	NM_002858	TRCN0000059851	Core	yes	1.027	0.166	1.121	0.271	0.871
ABCD3	IPI00002372	NM_002858	TRCN0000059852	Core	yes	0.996	0.069	0.934	0.183	0.910
ACTB	IPI00894365	NM_001101	TRCN0000029409	NS5B	no	1.216	0.223	0.848	0.247	1.127
ACTB	IPI00894365	NM_001101	TRCN0000029410	NS5B	no	1.262	0.163	1.243	0.046	1.183
ACTB	IPI00894365	NM_001101	TRCN0000029412	NS5B	no	1.031	0.322	0.759	0.121	1.400
ACTB	IPI00894365	NM_001101	TRCN0000029413	NS5B	no	0.955	0.127	1.280	0.182	1.140
AKAP8L	IPI00297455	NM_014371	TRCN0000037999	NS5B	no	1.242	0.828	1.227	0.268	0.739
AKAP8L	IPI00297455	NM_014371	TRCN0000038000	NS5B	no	0.966	0.083	1.012	0.186	0.716
AKAP8L	IPI00297455	NM_014371	TRCN0000038001	NS5B	no	1.474	0.227	1.258	0.210	1.056
AKAP8L	IPI00297455	NM_014371	TRCN0000038002	NS5B	no	1.136	0.122	0.832	0.024	1.241
AKAP8L	IPI00297455	NM_014371	TRCN0000038003	NS5B	no	0.976	0.118	0.758	0.344	0.697
ALDH18A1	IPI00218547	NM_002860	TRCN0000064848	NS3/4A	no	1.089	0.763	0.732	0.001	1.051
ALDH18A1	IPI00218547	NM_002860	TRCN0000064849	NS3/4A	no	0.984	0.412	0.851	0.171	0.743
ALDH18A1	IPI00218547	NM_002860	TRCN0000064850	NS3/4A	no	0.950	0.053	0.807	0.228	0.867
ALDH18A1	IPI00218547	NM_002860	TRCN0000064851	NS3/4A	no	0.834	0.573	0.883	0.210	0.924
ALDH18A1	IPI00218547	NM_002860	TRCN0000064852	NS3/4A	no	0.711	0.401	1.298	0.494	1.190
ATP2A2	IPI00219078	NM_001681	TRCN0000038529	NS2	no	0.570	0.580	1.072	0.178	0.922
ATP2A2	IPI00219078	NM_001681	TRCN0000038530	NS2	no	1.034	0.689	0.712	0.091	1.332
ATP2A2	IPI00219078	NM_001681	TRCN0000038531	NS2	no	0.801	0.685	0.839	0.132	1.024
ATP2A2	IPI00219078	NM_001681	TRCN0000038532	NS2	no	0.852	0.559	0.794	0.192	1.005
ATP2A2	IPI00219078	NM_001681	TRCN0000038533	NS2	no	0.914	0.636	1.153	0.240	1.222
ATP5A1	IPI00440493	NM_004046	TRCN0000043423	NS3/4A	no	1.124	0.787	0.797	0.293	1.082
ATP5A1	IPI00440493	NM_004046	TRCN0000043424	NS3/4A	no	1.127	0.013	0.794	0.175	0.665
ATP5A1	IPI00440493	NM_004046	TRCN0000043425	NS3/4A	no	0.806	0.052	0.805	0.004	1.205
ATP5A1	IPI00440493	NM_004046	TRCN0000043426	NS3/4A	no	0.769	0.058	0.619	0.430	0.821
ATP5A1	IPI00440493	NM_004046	TRCN0000043427	NS3/4A	no	1.109	0.245	0.936	0.082	1.014
ATP6V1A	IPI00007682	NM_001690	TRCN0000029539	NS3/4A	no	0.789	0.177	0.977	0.222	1.017
ATP6V1A	IPI00007682	NM_001690	TRCN0000029540	NS3/4A	no	0.654	0.007	1.136	0.124	1.162
ATP6V1A	IPI00007682	NM_001690	TRCN0000029541	NS3/4A	no	0.876	0.209	1.049	0.011	0.879
ATP6V1A	IPI00007682	NM_001690	TRCN0000029542	NS3/4A	no	0.616	0.209	1.091	0.104	0.917
ATP6V1A	IPI00007682	NM_001690	TRCN0000029543	NS3/4A	no	0.806	0.129	0.813	0.018	0.725
ATXN10	IPI00001636	NM_013236	TRCN0000084093	NS3/4A	yes	1.230	0.210	0.919	0.030	0.685
ATXN10	IPI00001636	NM_013236	TRCN0000084094	NS3/4A	yes	1.331	0.162	1.011	0.001	0.862
ATXN10	IPI00001636	NM_013236	TRCN0000084095	NS3/4A	yes	1.160	0.656	1.092	0.014	0.782
ATXN10	IPI00001636	NM_013236	TRCN0000084096	NS3/4A	yes	1.280	0.147	0.910	0.040	0.966
ATXN10	IPI00001636	NM_013236	TRCN0000084097	NS3/4A	yes	0.966	0.044	0.940	0.063	0.957
BCLAF1	IPI00413672	XM_376537	TRCN0000020624	NS3/4A	no	0.915	0.627	0.958	0.021	0.999
BCLAF1	IPI00413672	XM_376537	TRCN0000020625	NS3/4A	no	1.568	0.436	0.749	0.289	0.979
BCLAF1	IPI00413672	XM_376537	TRCN0000020626	NS3/4A	no	1.103	0.101	0.876	0.129	0.978
BCLAF1	IPI00413672	XM_376537	TRCN0000020627	NS3/4A	no	1.106	0.761	0.890	0.140	1.169
BCLAF1	IPI00413672	XM_376537	TRCN0000020628	NS3/4A	no	1.606	0.645	0.742	0.117	0.907
BIN1	IPI00220996	NM_004305	TRCN0000118037	NS5A	yes	1.167	0.198	0.926	0.175	1.073
BIN1	IPI00220996	NM_004305	TRCN0000118038	NS5A	yes	0.955	0.076	1.241	0.470	1.071
BIN1	IPI00220996	NM_004305	TRCN0000118039	NS5A	yes	0.941	0.649	0.831	0.049	1.487
BIN1	IPI00220996	NM_004305	TRCN0000118040	NS5A	yes	1.203	0.025	0.984	0.059	0.994
BIN1	IPI00220996	NM_004305	TRCN0000118041	NS5A	yes	1.116	0.049	0.798	0.082	1.286
BZW2	IPI00894416	NM_014038	TRCN0000139465	NS3/4A	yes	0.932	0.135	1.208	0.364	1.234
BZW2	IPI00894416	NM_014038	TRCN0000140053	NS3/4A	yes	1.432	0.358	1.576	0.677	1.134
BZW2	IPI00894416	NM_014038	TRCN0000140132	NS3/4A	yes	1.159	0.230	1.350	0.205	1.050
BZW2	IPI00894416	NM_014038	TRCN0000141844	NS3/4A	yes	1.061	0.253	1.065	0.282	1.031
BZW2	IPI00894416	NM_014038	TRCN0000144193	NS3/4A	yes	0.835	0.009	1.164	0.128	1.093
C14orf166	IPI00792100	NM_016039	TRCN0000075123	Core	yes	0.957	0.061	1.084	0.068	1.335
C14orf166	IPI00792100	NM_016039	TRCN0000075124	Core	yes	1.046	0.011	1.101	0.212	1.675
C14orf166	IPI00792100	NM_016039	TRCN0000075125	Core	yes	0.896	0.105	1.170	0.127	0.642
C14orf166	IPI00792100	NM_016039	TRCN0000075126	Core	yes	0.817	0.022	0.928	0.187	0.718
C14orf166	IPI00792100	NM_016039	TRCN0000075127	Core	yes	1.209	0.237	1.162	0.057	0.702
C1QBP	IPI00014230	NM_001212	TRCN0000057103	Core	yes	0.786	0.013	1.238	0.099	1.224
C1QBP	IPI00014230	NM_001212	TRCN0000057104	Core	yes	0.737	0.122	0.930	0.212	0.885
C1QBP	IPI00014230	NM_001212	TRCN0000057106	Core	yes	0.751	0.075	1.094	0.024	0.786
C1QBP	IPI00014230	NM_001212	TRCN0000057107	Core	yes	0.949	0.124	1.105	0.126	1.345

Gene Name	IPI no	Gene ID	shRNA	Bait	Statistically enriched	293T pIFN-B		A549 pIFN-B		293T pEF1a
						mean	stdev	mean	stdev	mean
C22orf28	IPI00550689	NM_014306	TRCN0000075138	Core	yes	1.234	0.859	1.388	0.651	1.114
C22orf28	IPI00550689	NM_014306	TRCN0000075139	Core	yes	1.539	0.491	1.024	0.051	0.914
C22orf28	IPI00550689	NM_014306	TRCN0000075140	Core	yes	0.960	0.065	0.641	0.349	0.922
C22orf28	IPI00550689	NM_014306	TRCN0000075141	Core	yes	1.058	0.017	1.010	0.056	0.989
C22orf28	IPI00550689	NM_014306	TRCN0000075142	Core	yes	1.141	0.217	1.025	0.137	0.824
C8orf41	IPI00306207	NM_025115	TRCN0000121556	NS3/4A	yes	0.866	0.110	1.518	0.156	0.951
C8orf41	IPI00306207	NM_025115	TRCN0000138979	NS3/4A	yes	1.110	0.084	1.389	0.096	0.817
C8orf41	IPI00306207	NM_025115	TRCN0000139910	NS3/4A	yes	1.075	0.067	1.230	0.125	1.097
C8orf41	IPI00306207	NM_025115	TRCN0000143321	NS3/4A	yes	0.863	0.361	1.083	0.018	0.993
C8orf41	IPI00306207	NM_025115	TRCN0000144860	NS3/4A	yes	0.831	0.044	1.440	0.182	1.117
CACYBP	IPI00395627	NM_014412	TRCN0000127886	NS5B	yes	0.895	0.128	1.096	0.111	2.417
CACYBP	IPI00395627	NM_014412	TRCN0000130068	NS5B	yes	1.121	0.116	1.329	0.225	1.069
CACYBP	IPI00395627	NM_014412	TRCN0000131203	NS5B	yes	0.845	0.093	1.140	0.375	1.236
CACYBP	IPI00395627	NM_014412	TRCN0000146815	NS5B	yes	1.167	0.394	1.348	0.262	1.025
CACYBP	IPI00395627	NM_014412	TRCN0000148456	NS5B	yes	1.462	0.168	1.280	0.106	1.015
CAD	IPI00893035	NM_004341	TRCN0000045908	NS3/4A	no	1.116	0.083	0.740	0.524	0.928
CAD	IPI00893035	NM_004341	TRCN0000045909	NS3/4A	no	1.554	1.079	1.181	0.003	1.129
CAD	IPI00893035	NM_004341	TRCN0000045910	NS3/4A	no	1.071	0.141	1.132	0.001	1.045
CAD	IPI00893035	NM_004341	TRCN0000045911	NS3/4A	no	0.784	0.547	0.886	0.014	1.531
CAD	IPI00893035	NM_004341	TRCN0000045912	NS3/4A	no	0.995	0.026	0.954	0.124	0.906
CANX	IPI00020984	NM_001746	TRCN0000029354	NS5A	yes	0.947	0.656	0.942	0.151	0.891
CANX	IPI00020984	NM_001746	TRCN0000029355	NS5A	yes	1.318	0.013	0.987	0.133	0.678
CANX	IPI00020984	NM_001746	TRCN0000029356	NS5A	yes	1.075	0.109	0.888	0.022	0.907
CANX	IPI00020984	NM_001746	TRCN0000029357	NS5A	yes	1.140	0.224	0.785	0.211	0.935
CANX	IPI00020984	NM_001746	TRCN0000029358	NS5A	yes	1.243	0.135	0.887	0.373	1.030
CAPZA1	IPI00873484	NM_006135	TRCN0000116907	NS5A	yes	1.053	0.044	0.918	0.152	0.959
CAPZA1	IPI00873484	NM_006135	TRCN0000116908	NS5A	yes	1.467	0.359	1.219	0.335	1.003
CAPZA1	IPI00873484	NM_006135	TRCN0000116909	NS5A	yes	1.109	0.194	1.460	0.425	1.967
CAPZA1	IPI00873484	NM_006135	TRCN0000116910	NS5A	yes	1.582	0.463	0.750	0.246	0.941
CAPZA1	IPI00873484	NM_006135	TRCN0000116911	NS5A	yes	1.101	0.247	1.019	0.255	1.035
CKAP4	IPI00604713	NM_006825	TRCN0000123294	Core	no	0.902	0.041	0.899	0.050	0.689
CKAP4	IPI00604713	NM_006825	TRCN0000123295	Core	no	0.812	0.015	0.833	0.213	0.973
CKAP4	IPI00604713	NM_006825	TRCN0000123296	Core	no	0.956	0.020	0.998	0.002	0.835
CKAP4	IPI00604713	NM_006825	TRCN0000123297	Core	no	1.168	0.811	0.786	0.071	0.945
CKAP4	IPI00604713	NM_006825	TRCN0000123298	Core	no	1.202	0.228	1.032	0.072	0.844
CKB	IPI00022977	NM_001823	TRCN0000006051	NS5B	yes	1.052	0.232	1.210	0.048	0.910
CKB	IPI00022977	NM_001823	TRCN0000006052	NS5B	yes	1.028	0.717	1.176	0.012	1.132
CKB	IPI00022977	NM_001823	TRCN0000006053	NS5B	yes	1.245	0.870	1.110	0.204	1.220
CKB	IPI00022977	NM_001823	TRCN0000006054	NS5B	yes	1.132	0.778	1.254	0.205	1.147
CKB	IPI00022977	NM_001823	TRCN0000010991	NS5B	yes	1.075	0.009	1.269	0.015	0.987
CKB	IPI00022977	NM_001823	TRCN0000194869	NS5B	yes	1.144	0.797	0.826	0.270	1.271
CKB	IPI00022977	NM_001823	TRCN0000199179	NS5B	yes	1.042	0.053	0.764	0.184	1.022
CKB	IPI00022977	NM_001823	TRCN0000199363	NS5B	yes	1.378	0.523	0.984	0.021	0.923
CKB	IPI00022977	NM_001823	TRCN0000199638	NS5B	yes	0.976	0.025	1.248	0.281	1.086
CKB	IPI00022977	NM_001823	TRCN0000199875	NS5B	yes	1.291	0.041	0.991	0.061	0.814
CLASP2	IPI00871686	NM_015097	TRCN0000108255	NS3/4A	no	1.192	0.126	0.869	0.000	0.787
CLASP2	IPI00871686	NM_015097	TRCN0000108256	NS3/4A	no	1.227	0.113	1.042	0.184	0.800
CLASP2	IPI00871686	NM_015097	TRCN0000108257	NS3/4A	no	1.118	0.244	1.097	0.169	0.879
CLASP2	IPI00871686	NM_015097	TRCN0000108258	NS3/4A	no	0.967	0.012	0.979	0.010	1.035
CLASP2	IPI00871686	NM_015097	TRCN0000108259	NS3/4A	no	1.144	0.136	1.111	0.084	0.697
COPB1	IPI00295851	NM_016451	TRCN0000150921	NS3/4A	yes	0.684	0.386	0.654	0.136	0.880
COPB1	IPI00295851	NM_016451	TRCN0000151067	NS3/4A	yes	0.816	0.487	0.903	0.006	0.984
COPB1	IPI00295851	NM_016451	TRCN0000151483	NS3/4A	yes	1.188	0.072	0.862	0.120	0.951
COPB1	IPI00295851	NM_016451	TRCN0000155585	NS3/4A	yes	0.717	0.398	0.585	0.302	1.064
COPB1	IPI00295851	NM_016451	TRCN0000155168	NS3/4A	yes	0.744	0.313	0.567	0.282	0.945
CSE1L	IPI00022744	NM_001316	TRCN0000061788	NS3/4A	no	0.990	0.053	0.931	0.035	1.091
CSE1L	IPI00022744	NM_001316	TRCN0000061789	NS3/4A	no	1.080	0.169	0.596	0.218	1.024
CSE1L	IPI00022744	NM_001316	TRCN0000061790	NS3/4A	no	0.886	0.009	0.625	0.219	1.007
CSE1L	IPI00022744	NM_001316	TRCN0000061791	NS3/4A	no	1.111	0.218	1.024	0.067	1.182
CSE1L	IPI00022744	NM_001316	TRCN0000061792	NS3/4A	no	1.279	0.403	0.973	0.030	0.843
CSNK2A1	IPI00016613	NM_001895	TRCN0000000606	NS5B	no	0.973	0.052	1.033	0.152	1.017
CSNK2A1	IPI00016613	NM_001895	TRCN0000000607	NS5B	no	0.798	0.113	0.994	0.110	0.823
CSNK2A1	IPI00016613	NM_001895	TRCN0000000608	NS5B	no	0.732	0.159	1.081	0.011	0.811
CSNK2A1	IPI00016613	NM_001895	TRCN0000000609	NS5B	no	1.221	0.462	1.080	0.097	0.663
CSNK2A1	IPI00016613	NM_001895	TRCN0000000610	NS5B	no	0.642	0.417	1.008	0.016	1.112

Gene Name	IPI no	Gene ID	shRNA	Bait	Statistically enriched	293T pIFN-B		A549 pIFN-B		293T pEF1a
						mean	stdev	mean	stdev	mean
CYC1	IPI00029264	NM_001916	TRCN0000064603	Core	yes	0.722	0.154	0.960	0.029	0.675
CYC1	IPI00029264	NM_001916	TRCN0000064604	Core	yes	0.866	0.186	0.951	0.130	0.808
CYC1	IPI00029264	NM_001916	TRCN0000064605	Core	yes	0.823	0.188	0.811	0.091	0.674
CYC1	IPI00029264	NM_001916	TRCN0000064606	Core	yes	0.841	0.136	0.769	0.076	0.946
CYC1	IPI00029264	NM_001916	TRCN0000064607	Core	yes	0.785	0.148	0.842	0.227	0.754
DDOST	IPI00297084	NM_005216	TRCN0000035384	NS3/4A	no	0.885	0.002	1.107	0.025	0.676
DDOST	IPI00297084	NM_005216	TRCN0000035385	NS3/4A	no	0.783	0.353	1.127	0.345	0.896
DDOST	IPI00297084	NM_005216	TRCN0000035386	NS3/4A	no	1.052	0.011	1.128	0.163	1.038
DDOST	IPI00297084	NM_005216	TRCN0000035387	NS3/4A	no	0.841	0.379	0.904	0.477	0.989
DDOST	IPI00297084	NM_005216	TRCN0000035388	NS3/4A	no	1.309	0.169	0.861	0.088	1.071
DDX3X	IPI00215637	NM_001356	TRCN0000000001	Core	yes	1.022	0.035	0.945	0.276	1.173
DDX3X	IPI00215637	NM_001356	TRCN0000000002	Core	yes	1.159	0.336	0.861	0.307	1.490
DDX3X	IPI00215637	NM_001356	TRCN0000000003	Core	yes	1.169	0.095	1.123	0.022	1.379
DDX3X	IPI00215637	NM_001356	TRCN0000000004	Core	yes	0.942	0.198	1.175	0.164	1.314
DDX3X	IPI00215637	NM_001356	TRCN0000000005	Core	yes	0.823	0.290	0.751	0.250	1.242
DHCR7	IPI00294501	NM_001360	TRCN0000046598	Core	no	0.954	0.631	0.887	0.028	1.476
DHCR7	IPI00294501	NM_001360	TRCN0000046599	Core	no	0.602	0.244	0.996	0.021	1.074
DHCR7	IPI00294501	NM_001360	TRCN0000046600	Core	no	0.923	0.286	0.954	0.260	1.252
DHCR7	IPI00294501	NM_001360	TRCN0000046601	Core	no	1.162	0.143	0.872	0.111	1.146
DHCR7	IPI00294501	NM_001360	TRCN0000046602	Core	no	0.807	0.054	0.589	0.271	1.025
DICER1	IPI00219036	NM_030621	TRCN0000051258	NS5B	no	1.097	0.463	0.948	0.228	0.819
DICER1	IPI00219036	NM_030621	TRCN0000051259	NS5B	no	0.945	0.027	1.122	0.025	1.038
DICER1	IPI00219036	NM_030621	TRCN0000051260	NS5B	no	1.364	0.399	0.796	0.009	0.998
DICER1	IPI00219036	NM_030621	TRCN0000051261	NS5B	no	1.153	0.021	1.043	0.060	1.002
DICER1	IPI00219036	NM_030621	TRCN0000051262	NS5B	no	1.491	0.389	0.952	0.064	0.778
DOCK7	IPI00815886	NM_033407	TRCN0000127927	NS5A	no	1.210	0.512	1.137	0.338	0.884
DOCK7	IPI00815886	NM_033407	TRCN0000129042	NS5A	no	1.063	0.345	0.638	0.344	0.966
DOCK7	IPI00815886	NM_033407	TRCN0000130182	NS5A	no	1.050	0.102	1.026	0.172	0.935
DOCK7	IPI00815886	NM_033407	TRCN0000130338	NS5A	no	1.364	0.474	1.148	0.202	0.879
DOCK7	IPI00815886	NM_033407	TRCN0000131082	NS5A	no	1.057	0.277	1.229	0.286	1.050
EEF2	IPI00186290	NM_001961	TRCN0000047908	NS3/4A	no	1.371	0.525	1.074	0.208	1.073
EEF2	IPI00186290	NM_001961	TRCN0000047909	NS3/4A	no	0.922	0.131	0.719	0.222	1.008
EEF2	IPI00186290	NM_001961	TRCN0000047910	NS3/4A	no	1.122	0.373	0.979	0.076	0.998
EEF2	IPI00186290	NM_001961	TRCN0000047911	NS3/4A	no	1.085	0.228	0.976	0.124	1.031
EEF2	IPI00186290	NM_001961	TRCN0000047912	NS3/4A	no	0.889	0.130	0.826	0.205	1.111
EGLN1	IPI00004928	NM_022051	TRCN0000001042	NS5A	yes	1.022	0.032	0.813	0.061	1.466
EGLN1	IPI00004928	NM_022051	TRCN0000001043	NS5A	yes	0.987	0.067	0.784	0.048	0.939
EGLN1	IPI00004928	NM_022051	TRCN0000001044	NS5A	yes	0.615	0.115	0.759	0.116	1.054
EGLN1	IPI00004928	NM_022051	TRCN0000001045	NS5A	yes	1.087	0.127	1.387	0.684	0.807
EGLN1	IPI00004928	NM_022051	TRCN0000010578	NS5A	yes	0.949	0.145	1.161	0.194	1.112
EIF4B	IPI00012079	NM_001417	TRCN0000062598	NS3/4A	no	0.691	0.209	0.837	0.042	1.000
EIF4B	IPI00012079	NM_001417	TRCN0000062599	NS3/4A	no	1.264	0.298	0.946	0.056	1.083
EIF4B	IPI00012079	NM_001417	TRCN0000062600	NS3/4A	no	0.931	0.027	1.052	0.090	0.865
EIF4B	IPI00012079	NM_001417	TRCN0000062601	NS3/4A	no	1.049	0.152	1.159	0.138	1.168
EIF4B	IPI00012079	NM_001417	TRCN0000062602	NS3/4A	no	1.109	0.041	0.869	0.167	1.175
ERMP1	IPI00257903	NM_024896	TRCN0000133828	NS4B	no	0.609	0.382	0.829	0.118	1.383
ERMP1	IPI00257903	NM_024896	TRCN0000134194	NS4B	no	1.371	0.261	0.772	0.048	0.871
ERMP1	IPI00257903	NM_024896	TRCN0000136087	NS4B	no	0.580	0.354	1.159	0.078	1.043
ERMP1	IPI00257903	NM_024896	TRCN0000136345	NS4B	no	1.107	0.192	0.959	0.203	1.155
ERMP1	IPI00257903	NM_024896	TRCN0000138072	NS4B	no	0.863	0.135	0.816	0.209	1.017
EXOC7	IPI00172532	NM_015219	TRCN0000134799	NS3/4A	yes	1.230	0.315	0.802	0.013	0.964
EXOC7	IPI00172532	NM_015219	TRCN0000135057	NS3/4A	yes	1.157	0.233	1.144	0.225	0.802
EXOC7	IPI00172532	NM_015219	TRCN0000136114	NS3/4A	yes	1.102	0.222	1.055	0.009	0.874
EXOC7	IPI00172532	NM_015219	TRCN0000137267	NS3/4A	yes	1.032	0.214	0.777	0.303	0.910
EXOC7	IPI00172532	NM_015219	TRCN0000137284	NS3/4A	yes	1.197	0.184	0.963	0.027	0.989
FANCD2	IPI00604399	NM_033084	TRCN0000082838	NS2	no	0.978	0.065	0.933	0.059	1.256
FANCD2	IPI00604399	NM_033084	TRCN0000082839	NS2	no	1.138	0.059	1.017	0.242	1.199
FANCD2	IPI00604399	NM_033084	TRCN0000082840	NS2	no	0.986	0.154	1.058	0.057	0.798
FANCD2	IPI00604399	NM_033084	TRCN0000082841	NS2	no	1.099	0.118	1.011	0.015	1.011
FANCD2	IPI00604399	NM_033084	TRCN0000082842	NS2	no	0.979	0.231	1.088	0.067	1.195
FASN	IPI00026781	NM_004104	TRCN0000003125	NS3/4A	no	1.152	0.471	0.777	0.038	1.221
FASN	IPI00026781	NM_004104	TRCN0000003126	NS3/4A	no	1.025	0.194	1.099	0.384	1.039
FASN	IPI00026781	NM_004104	TRCN0000003127	NS3/4A	no	1.136	0.340	1.075	0.159	0.931
FASN	IPI00026781	NM_004104	TRCN0000003128	NS3/4A	no	0.767	0.078	0.871	0.225	1.166
FASN	IPI00026781	NM_004104	TRCN0000003129	NS3/4A	no	1.000	0.694	0.847	0.133	0.817

Gene Name	IPI no	Gene ID	shRNA	Bait	Statistically enriched	293T pIFN-B		A549 pIFN-B		293T pEF1a
						mean	stdev	mean	stdev	mean
FKBP5	IPI00218775	NM_004117	TRCN0000000234	NS5B	yes	0.870	0.084	1.034	0.256	1.080
FKBP5	IPI00218775	NM_004117	TRCN0000000235	NS5B	yes	0.744	0.055	1.347	0.374	1.164
FKBP5	IPI00218775	NM_004117	TRCN0000000236	NS5B	yes	0.623	0.138	0.767	0.039	0.919
FKBP5	IPI00218775	NM_004117	TRCN0000000237	NS5B	yes	0.835	0.059	1.319	0.297	1.114
FKBP5	IPI00218775	NM_004117	TRCN0000000238	NS5B	yes	0.856	0.086	1.099	0.168	0.689
FKBP8	IPI00640341	NM_012181	TRCN0000001100	NS5A	yes	1.175	0.031	1.063	0.098	0.898
FKBP8	IPI00640341	NM_012181	TRCN0000001101	NS5A	yes	1.291	0.019	1.124	0.153	1.085
FKBP8	IPI00640341	NM_012181	TRCN0000001102	NS5A	yes	0.980	0.010	1.073	0.183	1.281
FKBP8	IPI00640341	NM_012181	TRCN0000001103	NS5A	yes	1.138	0.250	0.830	0.196	1.243
FKBP8	IPI00640341	NM_012181	TRCN0000010595	NS5A	yes	0.700	0.174	1.145	0.217	0.926
GAPDH	IPI00219018	NM_002046	TRCN0000025828	NS3/4A	no	0.875	0.122	0.731	0.107	1.195
GAPDH	IPI00219018	NM_002046	TRCN0000025830	NS3/4A	no	1.052	0.728	0.947	0.149	0.911
GAPDH	IPI00219018	NM_002046	TRCN0000025836	NS3/4A	no	1.109	0.021	0.740	0.169	1.124
GAPDH	IPI00219018	NM_002046	TRCN0000025862	NS3/4A	no	1.498	0.467	0.947	0.126	1.192
GAPDH	IPI00219018	NM_002046	TRCN0000025867	NS3/4A	no	0.740	0.234	0.907	0.067	0.888
GCN1L1	IPI00001159	NM_006836	TRCN0000154822	NS3/4A	no	1.213	0.112	1.100	0.052	1.029
GCN1L1	IPI00001159	NM_006836	TRCN0000154964	NS3/4A	no	1.050	0.067	1.138	0.362	0.889
GCN1L1	IPI00001159	NM_006836	TRCN0000155124	NS3/4A	no	0.934	0.000	0.969	0.031	0.852
GCN1L1	IPI00001159	NM_006836	TRCN0000155566	NS3/4A	no	1.090	0.167	0.897	0.003	1.023
GCN1L1	IPI00001159	NM_006836	TRCN0000155944	NS3/4A	no	0.998	0.169	1.151	0.137	0.769
GNAI3	IPI00220578	NM_006496	TRCN0000036474	NS5A	yes	1.435	0.348	0.969	0.144	1.001
GNAI3	IPI00220578	NM_006496	TRCN0000036475	NS5A	yes	1.242	0.196	1.381	0.397	0.901
GNAI3	IPI00220578	NM_006496	TRCN0000036476	NS5A	yes	0.942	0.000	1.259	0.393	0.903
GNAI3	IPI00220578	NM_006496	TRCN0000036477	NS5A	yes	0.995	0.164	1.019	0.188	0.763
GNAI3	IPI00220578	NM_006496	TRCN0000036478	NS5A	yes	0.970	0.118	0.957	0.004	0.938
GOLGA3	IPI00333419	NM_005895	TRCN0000140436	NS5A	no	0.861	0.107	0.943	0.115	0.923
GOLGA3	IPI00333419	NM_005895	TRCN0000140437	NS5A	no	0.733	0.127	1.124	0.253	1.057
GOLGA3	IPI00333419	NM_005895	TRCN0000140981	NS5A	no	1.074	0.105	1.274	0.194	0.873
GOLGA3	IPI00333419	NM_005895	TRCN0000142624	NS5A	no	0.522	0.270	0.850	0.130	0.881
GOLGA3	IPI00333419	NM_005895	TRCN0000143671	NS5A	no	0.765	0.289	1.033	0.213	0.856
HAX1	IPI00604587	NM_006118	TRCN0000061773	NS3/4A	no	0.974	0.036	0.979	0.073	0.972
HAX1	IPI00604587	NM_006118	TRCN0000061774	NS3/4A	no	1.075	0.186	1.020	0.291	1.040
HAX1	IPI00604587	NM_006118	TRCN0000061775	NS3/4A	no	1.056	0.079	1.061	0.073	1.068
HAX1	IPI00604587	NM_006118	TRCN0000061776	NS3/4A	no	0.895	0.114	1.050	0.043	1.058
HAX1	IPI00604587	NM_006118	TRCN0000061777	NS3/4A	no	1.222	0.338	1.005	0.157	0.799
HBXIP	IPI00012831	NM_006402	TRCN0000151965	NS3/4A	yes	1.378	0.484	1.271	0.152	0.916
HBXIP	IPI00012831	NM_006402	TRCN0000152793	NS3/4A	yes	1.233	0.118	1.042	0.106	1.000
HBXIP	IPI00012831	NM_006402	TRCN0000152794	NS3/4A	yes	0.953	0.341	0.812	0.191	1.162
HBXIP	IPI00012831	NM_006402	TRCN0000153069	NS3/4A	yes	0.944	0.191	0.971	0.107	1.024
HBXIP	IPI00012831	NM_006402	TRCN0000153443	NS3/4A	yes	1.241	0.285	1.116	0.081	1.071
HEATR2	IPI00242630	NM_017802	TRCN0000129000	NS3/4A	yes	1.071	0.039	1.100	0.041	1.168
HEATR2	IPI00242630	NM_017802	TRCN0000130727	NS3/4A	yes	0.971	0.026	1.015	0.197	1.113
HEATR2	IPI00242630	NM_017802	TRCN0000146272	NS3/4A	yes	0.981	0.047	0.948	0.131	0.870
HEATR2	IPI00242630	NM_017802	TRCN0000149052	NS3/4A	yes	0.907	0.129	1.108	0.153	0.925
HIST1H1D	IPI00217466	NM_005320	TRCN0000106800	NS2	no	1.359	0.551	1.066	0.105	1.063
HIST1H1D	IPI00217466	NM_005320	TRCN0000106801	NS2	no	1.042	0.214	1.116	0.198	1.062
HIST1H1D	IPI00217466	NM_005320	TRCN0000106802	NS2	no	0.996	0.369	1.203	0.080	0.965
HIST1H1D	IPI00217466	NM_005320	TRCN0000106803	NS2	no	0.892	0.102	0.949	0.269	0.882
HIST1H1D	IPI00217466	NM_005320	TRCN0000106804	NS2	no	0.875	0.327	0.760	0.096	1.075
HMOX2	IPI00026824	NM_002134	TRCN0000045253	NS2	no	0.603	0.427	0.903	0.360	0.727
HMOX2	IPI00026824	NM_002134	TRCN0000045254	NS2	no	1.108	0.235	1.041	0.351	0.730
HMOX2	IPI00026824	NM_002134	TRCN0000045255	NS2	no	0.855	0.092	1.004	0.095	0.932
HMOX2	IPI00026824	NM_002134	TRCN0000045256	NS2	no	0.788	0.345	0.852	0.202	1.014
HMOX2	IPI00026824	NM_002134	TRCN0000045257	NS2	no	0.889	0.162	0.930	0.023	0.858
HNRPM	IPI00171903	NM_005968	TRCN0000001243	NS3/4A	no	1.228	0.011	0.922	0.034	1.007
HNRPM	IPI00171903	NM_005968	TRCN0000001244	NS3/4A	no	1.151	0.102	0.984	0.080	1.047
HNRPM	IPI00171903	NM_005968	TRCN0000001245	NS3/4A	no	1.312	0.026	0.580	0.383	1.056
HNRPM	IPI00171903	NM_005968	TRCN0000001246	NS3/4A	no	1.330	0.105	1.063	0.178	0.906
HNRPM	IPI00171903	NM_005968	TRCN0000001247	NS3/4A	no	1.200	0.223	0.976	0.156	0.726
HNRPU	IPI00644079	NM_031844	TRCN0000001297	NS3/4A	no	1.153	0.117	1.053	0.093	1.111
HNRPU	IPI00644079	NM_031844	TRCN0000001298	NS3/4A	no	0.898	0.106	0.812	0.098	1.125
HNRPU	IPI00644079	NM_031844	TRCN0000001299	NS3/4A	no	1.188	0.229	0.761	0.021	1.040
HNRPU	IPI00644079	NM_031844	TRCN0000001300	NS3/4A	no	1.575	0.417	0.577	0.380	1.087

Gene Name	IPI no	Gene ID	shRNA	Bait	Statistically enriched	293T pIFN-B		A549 pIFN-B		293T pEF1a
						mean	stdev	mean	stdev	mean
HRNR	IPI00398625	NM_001009931	TRCN0000159239	NS3/4A	no	1.118	0.166	0.823	0.080	0.930
HRNR	IPI00398625	NM_001009931	TRCN0000159268	NS3/4A	no	1.213	0.018	1.078	0.296	1.038
HRNR	IPI00398625	NM_001009931	TRCN0000159629	NS3/4A	no	1.186	0.255	0.832	0.087	0.976
HRNR	IPI00398625	NM_001009931	TRCN0000159662	NS3/4A	no	0.908	0.087	0.967	0.088	0.945
HSD17B12	IPI00007676	NM_016142	TRCN0000027140	Core	yes	0.920	0.114	1.133	0.078	0.982
HSD17B12	IPI00007676	NM_016142	TRCN0000027145	Core	yes	1.151	0.159	1.001	0.036	0.917
HSD17B12	IPI00007676	NM_016142	TRCN0000027189	Core	yes	1.055	0.197	1.060	0.061	0.998
HSD17B12	IPI00007676	NM_016142	TRCN0000027192	Core	yes	1.123	0.010	0.859	0.262	1.020
HSD17B12	IPI00007676	NM_016142	TRCN0000027218	Core	yes	0.678	0.058	1.123	0.102	1.001
HSP90AA1	IPI00382470	NM_005348	TRCN0000001025	NS5B	yes	1.585	0.253	0.854	0.164	0.922
HSP90AA1	IPI00382470	NM_005348	TRCN0000001026	NS5B	yes	0.969	0.142	1.148	0.208	0.999
HSP90AA1	IPI00382470	NM_005348	TRCN0000001027	NS5B	yes	1.055	0.155	0.984	0.039	0.901
HSP90AA1	IPI00382470	NM_005348	TRCN0000001028	NS5B	yes	1.013	0.132	1.280	0.072	0.923
HSP90AA1	IPI00382470	NM_005348	TRCN0000010575	NS5B	yes	1.137	0.171	1.090	0.115	0.993
HSP90AB1	IPI00414676	NM_007355	TRCN0000008747	NS5B	yes	1.005	0.161	1.000	0.178	0.938
HSP90AB1	IPI00414676	NM_007355	TRCN0000008748	NS5B	yes	0.890	0.615	0.934	0.069	1.041
HSP90AB1	IPI00414676	NM_007355	TRCN0000008749	NS5B	yes	0.787	0.167	0.790	0.030	1.077
HSP90AB1	IPI00414676	NM_007355	TRCN0000008750	NS5B	yes	1.046	0.710	1.232	0.574	1.080
HSP90AB1	IPI00414676	NM_007355	TRCN0000008751	NS5B	yes	1.234	0.125	0.881	0.042	1.011
HSPD1	IPI00784154	NM_002156	TRCN0000029444	NS3/4A	yes	0.760	0.058	1.188	0.198	0.814
HSPD1	IPI00784154	NM_002156	TRCN0000029445	NS3/4A	yes	1.063	0.001	1.307	0.073	0.931
HSPD1	IPI00784154	NM_002156	TRCN0000029446	NS3/4A	yes	1.043	0.036	1.208	0.270	0.807
HSPD1	IPI00784154	NM_002156	TRCN0000029447	NS3/4A	yes	0.933	0.371	1.048	0.135	0.727
HSPD1	IPI00784154	NM_002156	TRCN0000029448	NS3/4A	yes	1.251	0.175	1.154	0.094	0.900
HTATSF1	IPI00644220	NM_014500	TRCN0000006587	NS5B	no	0.836	0.198	1.180	0.260	0.950
HTATSF1	IPI00644220	NM_014500	TRCN0000006588	NS5B	no	0.972	0.555	1.054	0.038	0.929
HTATSF1	IPI00644220	NM_014500	TRCN0000006589	NS5B	no	0.966	0.157	1.184	0.065	0.878
HTATSF1	IPI00644220	NM_014500	TRCN0000006590	NS5B	no	0.768	0.226	0.994	0.053	0.913
HTATSF1	IPI00644220	NM_014500	TRCN0000006591	NS5B	no	0.762	0.136	1.162	0.006	1.008
HUWE1	IPI00445401	NM_031407	TRCN0000073303	NS5A	yes	0.597	0.427	0.837	0.134	1.117
HUWE1	IPI00445401	NM_031407	TRCN0000073304	NS5A	yes	0.957	0.089	1.135	0.175	1.093
HUWE1	IPI00445401	NM_031407	TRCN0000073305	NS5A	yes	0.789	0.153	0.725	0.429	1.126
HUWE1	IPI00445401	NM_031407	TRCN0000073306	NS5A	yes	1.033	0.177	1.315	0.035	0.862
HUWE1	IPI00445401	NM_031407	TRCN0000073307	NS5A	yes	0.842	0.204	0.937	0.208	1.078
IPO5	IPI00793443	NM_002271	TRCN0000150535	NS3/4A	no	1.189	0.093	0.853	0.053	1.091
IPO5	IPI00793443	NM_002271	TRCN0000151824	NS3/4A	no	1.076	0.725	0.746	0.269	1.293
IPO5	IPI00793443	NM_002271	TRCN0000152127	NS3/4A	no	1.063	0.258	0.973	0.150	1.038
IPO5	IPI00793443	NM_002271	TRCN0000152684	NS3/4A	no	1.447	1.006	0.839	0.310	0.887
IPO5	IPI00793443	NM_002271	TRCN0000153065	NS3/4A	no	1.020	0.143	0.583	0.361	0.851
IPO7	IPI00007402	NM_006391	TRCN0000150676	NS5B	yes	0.723	0.086	0.822	0.202	0.981
IPO7	IPI00007402	NM_006391	TRCN0000151374	NS5B	yes	0.841	0.053	0.631	0.466	0.818
IPO7	IPI00007402	NM_006391	TRCN0000155501	NS5B	yes	0.908	0.035	0.930	0.074	0.960
IPO7	IPI00007402	NM_006391	TRCN0000156655	NS5B	yes	1.037	0.151	0.949	0.181	0.900
IPO7	IPI00007402	NM_006391	TRCN0000156994	NS5B	yes	0.776	0.231	0.940	0.492	1.085
KPNB1	IPI00001639	NM_002265	TRCN0000123189	NS3/4A	yes	1.115	0.215	0.645	0.302	1.134
KPNB1	IPI00001639	NM_002265	TRCN0000123190	NS3/4A	yes	0.818	0.151	0.760	0.334	1.109
KPNB1	IPI00001639	NM_002265	TRCN0000123191	NS3/4A	yes	0.956	0.041	0.903	0.094	0.898
KPNB1	IPI00001639	NM_002265	TRCN0000123192	NS3/4A	yes	0.442	0.272	1.027	0.678	0.974
KPNB1	IPI00001639	NM_002265	TRCN0000123193	NS3/4A	yes	0.938	0.026	1.093	0.280	1.249
LBR	IPI00292135	NM_002296	TRCN0000060458	Core	yes	1.137	0.095	0.976	0.051	1.272
LBR	IPI00292135	NM_002296	TRCN0000060459	Core	yes	1.062	0.168	0.719	0.111	1.355
LBR	IPI00292135	NM_002296	TRCN0000060460	Core	yes	1.351	0.260	0.780	0.116	0.903
LBR	IPI00292135	NM_002296	TRCN0000060461	Core	yes	1.187	0.202	1.059	0.126	0.807
LBR	IPI00292135	NM_002296	TRCN0000060462	Core	yes	1.314	0.293	1.066	0.054	0.759
MAGED1	IPI00398845	NM_006986	TRCN0000004235	NS3/4A	yes	1.021	0.063	1.220	0.132	1.143
MAGED1	IPI00398845	NM_006986	TRCN0000004236	NS3/4A	yes	0.941	0.148	1.160	0.163	0.926
MAGED1	IPI00398845	NM_006986	TRCN0000004237	NS3/4A	yes	0.822	0.246	1.283	0.223	1.106
MAGED1	IPI00398845	NM_006986	TRCN0000004238	NS3/4A	yes	0.932	0.165	1.302	0.295	1.030
MAGED1	IPI00398845	NM_006986	TRCN0000004239	NS3/4A	yes	1.163	0.034	1.383	0.148	1.520
MAGED2	IPI00337823	NM_201222	TRCN0000115787	NS5A	yes	1.044	0.118	0.914	0.201	1.236
MAGED2	IPI00337823	NM_201222	TRCN0000115789	NS5A	yes	1.345	0.506	0.827	0.041	0.881
MAGED2	IPI00337823	NM_201222	TRCN0000115791	NS5A	yes	0.848	0.578	1.047	0.028	1.100

Gene Name	IPI no	Gene ID	shRNA	Bait	Statistically enriched	293T pIFN-B		A549 pIFN-B		293T pEF1a
						mean	stdev	mean	stdev	mean
MAP3K7IP1	IPI00019459	NM_006116	TRCN0000001859	NS3/4A	no	1.466	0.129	1.121	0.083	0.960
MAP3K7IP1	IPI00019459	NM_006116	TRCN0000001860	NS3/4A	no	1.465	0.349	1.002	0.017	1.014
MAP3K7IP1	IPI00019459	NM_006116	TRCN0000001861	NS3/4A	no	1.249	0.331	0.723	0.081	1.084
MAP3K7IP1	IPI00019459	NM_006116	TRCN0000001862	NS3/4A	no	0.964	0.086	0.795	0.111	0.807
MAP3K7IP1	IPI00019459	NM_006116	TRCN0000001863	NS3/4A	no	0.935	0.645	0.742	0.322	1.099
MAP4	IPI00888475	NM_002375	TRCN0000117162	NS3/4A	no	0.983	0.001	0.890	0.044	0.832
MAP4	IPI00888475	NM_002375	TRCN0000117163	NS3/4A	no	0.963	0.049	0.996	0.290	0.868
MAP4	IPI00888475	NM_002375	TRCN0000117164	NS3/4A	no	0.829	0.066	0.733	0.358	0.841
MAP4	IPI00888475	NM_002375	TRCN0000117165	NS3/4A	no	1.084	0.033	0.834	0.120	0.828
MAP4	IPI00888475	NM_002375	TRCN0000117166	NS3/4A	no	1.055	0.172	0.898	0.144	1.133
MTCH2	IPI00003833	NM_014342	TRCN0000059393	NS3/4A	no	0.978	0.049	0.910	0.236	1.129
MTCH2	IPI00003833	NM_014342	TRCN0000059394	NS3/4A	no	1.051	0.029	0.972	0.100	1.038
MTCH2	IPI00003833	NM_014342	TRCN0000059395	NS3/4A	no	1.246	0.555	1.013	0.225	0.874
MTCH2	IPI00003833	NM_014342	TRCN0000059396	NS3/4A	no	1.477	0.580	1.157	0.100	1.257
MTCH2	IPI00003833	NM_014342	TRCN0000059397	NS3/4A	no	0.897	0.102	0.877	0.201	0.965
MTHFD1	IPI00218342	NM_005956	TRCN0000036524	NS3/4A	no	1.280	0.411	0.744	0.063	0.627
MTHFD1	IPI00218342	NM_005956	TRCN0000036525	NS3/4A	no	1.135	0.347	0.901	0.003	0.932
MTHFD1	IPI00218342	NM_005956	TRCN0000036526	NS3/4A	no	1.587	0.832	1.006	0.339	0.801
MTHFD1	IPI00218342	NM_005956	TRCN0000036527	NS3/4A	no	1.131	0.051	0.878	0.087	1.065
MTHFD1	IPI00218342	NM_005956	TRCN0000036528	NS3/4A	no	0.946	0.647	0.713	0.200	1.022
NAP1L4	IPI00017763	NM_005969	TRCN0000151026	Core	yes	0.823	0.078	1.111	0.068	0.922
NAP1L4	IPI00017763	NM_005969	TRCN0000151475	Core	yes	0.977	0.036	0.907	0.195	0.909
NAP1L4	IPI00017763	NM_005969	TRCN0000154499	Core	yes	0.709	0.337	1.023	0.169	1.141
NAP1L4	IPI00017763	NM_005969	TRCN0000155016	Core	yes	0.834	0.072	1.148	0.243	0.749
NAP1L4	IPI00017763	NM_005969	TRCN0000156041	Core	yes	0.866	0.478	1.356	0.397	1.016
NCL	IPI00604620	NM_005381	TRCN0000062283	Core	no	1.233	0.106	1.233	0.400	1.254
NCL	IPI00604620	NM_005381	TRCN0000062284	Core	no	0.879	0.212	0.897	0.252	0.852
NCL	IPI00604620	NM_005381	TRCN0000062285	Core	no	1.050	0.164	1.114	0.198	0.972
NCL	IPI00604620	NM_005381	TRCN0000062286	Core	no	1.161	0.233	1.310	0.435	1.173
NCL	IPI00604620	NM_005381	TRCN0000062287	Core	no	0.753	0.220	0.774	0.472	1.304
NIP30	IPI00178750	NM_024946	TRCN0000121524	NS5B	yes	1.395	0.448	1.170	0.207	1.076
NIP30	IPI00178750	NM_024946	TRCN0000121524	NS5B	yes	0.826	0.131	1.260	0.394	1.276
NIP30	IPI00178750	NM_024946	TRCN0000121525	NS5B	yes	1.100	0.184	0.819	0.204	0.894
NIP30	IPI00178750	NM_024946	TRCN0000121525	NS5B	yes	0.566	0.139	0.844	0.071	1.307
NIP30	IPI00178750	NM_024946	TRCN0000121736	NS5B	yes	1.511	0.138	1.408	0.412	0.859
NIP30	IPI00178750	NM_024946	TRCN0000121736	NS5B	yes	1.211	0.201	1.532	0.294	1.304
NIP30	IPI00178750	NM_024946	TRCN0000122208	NS5B	yes	1.358	0.227	1.117	0.265	1.033
NIP30	IPI00178750	NM_024946	TRCN0000122208	NS5B	yes	0.811	0.003	1.303	0.429	1.236
NIP30	IPI00178750	NM_024946	TRCN0000122520	NS5B	yes	1.177	0.133	1.029	0.020	0.859
NIP30	IPI00178750	NM_024946	TRCN0000122520	NS5B	yes	0.848	0.175	1.038	0.059	1.040
OTUD4	IPI00399254	NM_014928	TRCN0000133659	NS3/4A	no	1.246	0.298	0.904	0.119	1.104
OTUD4	IPI00399254	NM_014928	TRCN0000134411	NS3/4A	no	1.048	0.065	0.946	0.089	0.930
OTUD4	IPI00399254	NM_014928	TRCN0000134658	NS3/4A	no	1.178	0.348	1.090	0.387	1.074
OTUD4	IPI00399254	NM_014928	TRCN0000135253	NS3/4A	no	0.773	0.193	0.872	0.151	0.863
OTUD4	IPI00399254	NM_014928	TRCN0000138670	NS3/4A	no	1.188	0.211	1.212	0.036	1.195
PABPC1	IPI00794246	NM_002568	TRCN0000074638	NS3/4A	no	1.106	0.100	1.258	0.408	1.554
PABPC1	IPI00008524	NM_002568	TRCN0000074639	NS3/4A	no	1.068	0.385	0.967	0.296	1.259
PABPC1	IPI00008524	NM_002568	TRCN0000074640	NS3/4A	no	0.830	0.131	0.740	0.121	0.935
PABPC1	IPI00794246	NM_002568	TRCN0000074641	NS3/4A	no	1.214	0.035	1.011	0.004	1.013
PABPC1	IPI00794246	NM_002568	TRCN0000074642	NS3/4A	no	1.221	0.462	1.068	0.177	1.109
PCNA	IPI00021700	NM_002592	TRCN0000003861	NS3/4A	yes	1.103	0.192	1.135	0.208	0.944
PCNA	IPI00021700	NM_002592	TRCN0000003862	NS3/4A	yes	1.203	0.127	1.083	0.163	0.767
PCNA	IPI00021700	NM_002592	TRCN0000003863	NS3/4A	yes	1.234	0.330	1.309	0.184	0.930
PCNA	IPI00021700	NM_002592	TRCN0000003864	NS3/4A	yes	1.345	0.245	1.085	0.134	1.178
PCNA	IPI00021700	NM_002592	TRCN0000010826	NS3/4A	yes	1.146	0.187	1.212	0.325	0.876
PGRMC1	IPI00220739	NM_006667	TRCN0000062903	NS2	yes	1.416	0.619	1.011	0.021	0.911
PGRMC2	IPI00005202	NM_006320	TRCN0000061298	NS5B	yes	1.161	0.172	0.731	0.035	0.913
PGRMC2	IPI00005202	NM_006320	TRCN0000061299	NS5B	yes	0.991	0.683	0.793	0.167	1.014
PGRMC2	IPI00005202	NM_006320	TRCN0000061300	NS5B	yes	1.020	0.097	0.759	0.081	1.032
PGRMC2	IPI00005202	NM_006320	TRCN0000061301	NS5B	yes	1.140	0.779	0.972	0.020	1.000
PGRMC2	IPI00005202	NM_006320	TRCN0000061302	NS5B	yes	0.877	0.039	0.822	0.232	1.171

Gene Name	IPI no	Gene ID	shRNA	Bait	Statistically enriched	293T pIFN-B		A549 pIFN-B		293T pEF1a
						mean	stdev	mean	stdev	mean
PHGDH	IPI00011200	NM_006623	TRCN0000028501	NS3/4A	yes	0.714	0.100	1.271	0.235	1.114
PHGDH	IPI00011200	NM_006623	TRCN0000028520	NS3/4A	yes	1.016	0.191	1.239	0.372	1.000
PHGDH	IPI00011200	NM_006623	TRCN0000028532	NS3/4A	yes	1.331	0.131	1.516	0.468	1.084
PHGDH	IPI00011200	NM_006623	TRCN0000028545	NS3/4A	yes	1.008	0.456	1.181	0.227	1.084
PHGDH	IPI00011200	NM_006623	TRCN0000028548	NS3/4A	yes	1.088	0.091	1.238	0.098	1.097
PKM2	IPI00479186	NM_182471	TRCN0000037611	NS5B	no	1.497	0.499	0.673	0.247	1.244
PKM2	IPI00479186	NM_182471	TRCN0000195352	NS5B	no	0.899	0.242	1.019	0.019	1.518
PKM2	IPI00479186	NM_182471	TRCN0000195405	NS5B	no	1.079	0.747	0.812	0.085	0.967
PKM2	IPI00479186	NM_182471	TRCN0000196588	NS5B	no	1.076	0.148	1.055	0.085	0.997
PKM2	IPI00479186	NM_182471	TRCN0000199494	NS5B	no	1.383	0.017	1.086	0.039	1.049
PPM1G	IPI00006167	NM_002707	TRCN0000001213	NS5B	no	0.904	0.167	0.910	0.109	0.873
PPM1G	IPI00006167	NM_002707	TRCN0000001214	NS5B	no	0.816	0.086	1.283	0.330	1.028
PPM1G	IPI00006167	NM_002707	TRCN0000001215	NS5B	no	0.800	0.082	1.590	0.794	1.101
PPM1G	IPI00006167	NM_002707	TRCN0000001216	NS5B	no	1.085	0.129	1.035	0.045	0.973
PPM1G	IPI00006167	NM_002707	TRCN0000001217	NS5B	no	0.853	0.069	1.179	0.118	1.287
PRKDC	IPI00296337	NM_006904	TRCN0000006255	NS3/4A	yes	0.909	0.153	0.790	0.200	0.662
PRKDC	IPI00296337	NM_006904	TRCN0000006256	NS3/4A	yes	1.095	0.025	0.728	0.380	0.934
PRKDC	IPI00296337	NM_006904	TRCN0000006257	NS3/4A	yes	1.013	0.160	0.984	0.153	0.901
PRKDC	IPI00296337	NM_006904	TRCN0000006258	NS3/4A	yes	0.933	0.121	1.026	0.161	0.991
PRKDC	IPI00296337	NM_006904	TRCN0000006259	NS3/4A	yes	1.154	0.073	1.148	0.261	1.034
PRKDC	IPI00296337	NM_006904	TRCN0000194719	NS3/4A	yes	0.919	0.156	0.893	0.144	0.984
PRKDC	IPI00296337	NM_006904	TRCN0000194985	NS3/4A	yes	1.092	0.064	1.181	0.061	1.039
PRKDC	IPI00296337	NM_006904	TRCN0000195491	NS3/4A	yes	0.822	0.168	1.054	0.263	0.940
PRKDC	IPI00296337	NM_006904	TRCN0000196328	NS3/4A	yes	0.603	0.182	0.711	0.457	1.157
PRKDC	IPI00296337	NM_006904	TRCN0000197152	NS3/4A	yes	1.064	0.035	1.182	0.026	0.993
PRPF31	IPI00292000	NM_015629	TRCN0000001180	NS3/4A	no	1.143	0.021	0.947	0.003	0.854
PRPF31	IPI00292000	NM_015629	TRCN0000001181	NS3/4A	no	1.383	0.019	0.919	0.112	0.887
PRPF31	IPI00292000	NM_015629	TRCN0000001182	NS3/4A	no	0.985	0.173	1.003	0.069	1.027
PRPF31	IPI00292000	NM_015629	TRCN0000001183	NS3/4A	no	0.877	0.117	0.938	0.229	1.029
PRPF31	IPI00292000	NM_015629	TRCN0000001184	NS3/4A	no	0.740	0.306	0.946	0.080	1.001
PSMC1	IPI00011126	NM_002802	TRCN0000050503	NS3/4A	no	0.913	0.054	1.247	0.122	1.190
PSMC1	IPI00011126	NM_002802	TRCN0000050504	NS3/4A	no	0.885	0.060	1.113	0.040	0.893
PSMC1	IPI00011126	NM_002802	TRCN0000050505	NS3/4A	no	1.063	0.094	0.885	0.025	1.011
PSMC1	IPI00011126	NM_002802	TRCN0000050506	NS3/4A	no	0.738	0.135	1.014	0.010	1.057
PSMC1	IPI00011126	NM_002802	TRCN0000050507	NS3/4A	no	1.310	0.159	0.936	0.147	0.955
PSME3	IPI00030243	NM_005789	TRCN0000058068	NS5B	yes	0.793	0.000	0.846	0.511	0.982
PSME3	IPI00030243	NM_005789	TRCN0000058069	NS5B	yes	0.801	0.075	0.960	0.159	1.274
PSME3	IPI00030243	NM_005789	TRCN0000058070	NS5B	yes	0.636	0.010	0.831	0.482	1.123
PSME3	IPI00030243	NM_005789	TRCN0000058071	NS5B	yes	0.520	0.070	1.061	0.383	0.747
PSME3	IPI00030243	NM_005789	TRCN0000058072	NS5B	yes	0.659	0.079	0.944	0.012	0.825
PTPLAD1	IPI00008998	NM_016395	TRCN0000072998	Core	yes	1.386	0.168	0.863	0.144	0.967
PTPLAD1	IPI00008998	NM_016395	TRCN0000073000	Core	yes	0.844	0.143	1.035	0.226	1.016
PTPLAD1	IPI00008998	NM_016395	TRCN0000073001	Core	yes	1.365	0.395	0.955	0.194	1.200
PTPLAD1	IPI00008998	NM_016395	TRCN0000073002	Core	yes	1.468	0.610	1.003	0.081	1.037
QKI	IPI00736672	NM_006775	TRCN0000015183	NS3/4A	yes	0.985	0.158	0.980	0.211	1.146
QKI	IPI00736672	NM_006775	TRCN0000015184	NS3/4A	yes	0.837	0.103	0.849	0.074	1.037
QKI	IPI00736672	NM_006775	TRCN0000015185	NS3/4A	yes	1.342	0.450	1.047	0.266	1.155
QKI	IPI00736672	NM_006775	TRCN0000015186	NS3/4A	yes	1.069	0.063	1.018	0.153	0.941
QKI	IPI00736672	NM_006775	TRCN0000015187	NS3/4A	yes	1.002	0.022	1.151	0.304	0.973
RAN	IPI00792352	NM_006325	TRCN0000047928	NS3/4A	yes	0.821	0.567	0.588	0.414	0.984
RAN	IPI00792352	NM_006325	TRCN0000047929	NS3/4A	yes	0.695	0.094	0.583	0.393	1.034
RAN	IPI00792352	NM_006325	TRCN0000047930	NS3/4A	yes	1.130	0.056	0.766	0.007	1.025
RAN	IPI00792352	NM_006325	TRCN0000047931	NS3/4A	yes	0.761	0.165	0.667	0.378	0.914
RAN	IPI00792352	NM_006325	TRCN0000047932	NS3/4A	yes	1.013	0.334	1.054	0.013	0.839
RBBP7	IPI00395865	NM_002893	TRCN0000038884	NS3/4A	no	0.965	0.053	1.019	0.101	1.067
RBBP7	IPI00395865	NM_002893	TRCN0000038885	NS3/4A	no	0.825	0.096	0.828	0.138	1.210
RBBP7	IPI00395865	NM_002893	TRCN0000038886	NS3/4A	no	0.880	0.109	1.015	0.049	0.935
RBBP7	IPI00395865	NM_002893	TRCN0000038887	NS3/4A	no	1.252	0.382	1.033	0.527	1.171
RBBP7	IPI00395865	NM_002893	TRCN0000038888	NS3/4A	no	1.016	0.026	1.312	0.215	0.919

Gene Name	IPI no	Gene ID	shRNA	Bait	Statistically enriched	293T pIFN-B		A549 pIFN-B		293T pEF1a
						mean	stdev	mean	stdev	mean
RBM10	IPI00375731	NM_005676	TRCN0000074733	NS5B	no	1.351	0.414	1.035	0.046	0.894
RBM10	IPI00375731	NM_005676	TRCN0000074734	NS5B	no	1.350	0.199	1.495	0.344	0.941
RBM10	IPI00375731	NM_005676	TRCN0000074735	NS5B	no	1.019	0.126	1.002	0.078	1.252
RBM10	IPI00375731	NM_005676	TRCN0000074736	NS5B	no	0.794	0.175	0.742	0.186	1.480
RBM10	IPI00375731	NM_005676	TRCN0000074737	NS5B	no	1.157	0.800	1.335	0.219	1.472
RCN2	IPI00029628	NM_002902	TRCN0000029489	NS3/4A	no	0.808	0.046	0.884	0.273	1.017
RCN2	IPI00029628	NM_002902	TRCN0000029490	NS3/4A	no	0.690	0.048	1.184	0.353	0.940
RCN2	IPI00029628	NM_002902	TRCN0000029491	NS3/4A	no	0.853	0.210	0.964	0.050	1.031
RCN2	IPI00029628	NM_002902	TRCN0000029492	NS3/4A	no	0.972	0.166	0.975	0.054	1.051
RCN2	IPI00029628	NM_002902	TRCN0000029493	NS3/4A	no	0.792	0.236	0.979	0.057	1.173
REEP5	IPI00744902	NM_005669	TRCN0000117837	NS2	yes	0.863	0.090	0.739	0.298	1.264
REEP5	IPI00744902	NM_005669	TRCN0000117838	NS2	yes	0.904	0.044	0.788	0.031	1.063
REEP5	IPI00744902	NM_005669	TRCN0000117839	NS2	yes	1.032	0.142	1.147	0.005	1.006
REEP5	IPI00744902	NM_005669	TRCN0000117840	NS2	yes	1.149	0.354	0.932	0.097	0.998
REEP5	IPI00744902	NM_005669	TRCN0000117841	NS2	yes	1.010	0.043	1.014	0.099	1.206
RPL10	IPI00853161	NM_006013	TRCN0000117602	Core	no	0.719	0.195	1.392	0.081	1.192
RPL10	IPI00853161	NM_006013	TRCN0000117603	Core	no	0.876	0.161	1.176	0.255	1.212
RPL10	IPI00853161	NM_006013	TRCN0000117604	Core	no	0.990	0.018	1.440	0.044	1.148
RPL10	IPI00853161	NM_006013	TRCN0000117605	Core	no	0.966	0.426	1.201	0.218	1.177
RPL10	IPI00853161	NM_006013	TRCN0000117606	Core	no	1.014	0.180	0.808	0.233	1.124
RPL14	IPI00555744	NM_003973	TRCN0000117487	NS5B	no	0.981	0.163	1.063	0.117	1.202
RPL14	IPI00555744	NM_003973	TRCN0000117488	NS5B	no	0.857	0.104	1.092	0.076	1.184
RPL14	IPI00555744	NM_003973	TRCN0000117489	NS5B	no	0.927	0.110	1.468	0.386	1.036
RPL14	IPI00555744	NM_003973	TRCN0000117490	NS5B	no	1.374	0.272	0.924	0.415	0.976
RPL14	IPI00555744	NM_003973	TRCN0000117491	NS5B	no	0.850	0.061	1.257	0.230	0.899
RPL15	IPI00470528	NM_002948	TRCN0000117692	NS5B	no	0.790	0.332	0.839	0.174	1.170
RPL15	IPI00470528	NM_002948	TRCN0000117693	NS5B	no	1.017	0.433	0.794	0.177	0.949
RPL15	IPI00470528	NM_002948	TRCN0000117694	NS5B	no	0.682	0.273	0.783	0.341	1.172
RPL15	IPI00470528	NM_002948	TRCN0000117695	NS5B	no	0.706	0.173	0.799	0.258	1.119
RPL15	IPI00470528	NM_002948	TRCN0000117696	NS5B	no	0.878	0.008	0.890	0.040	1.293
RPL24	IPI00306332	NM_000986	TRCN0000117642	Core	no	0.899	0.473	1.185	0.010	1.250
RPL24	IPI00306332	NM_000986	TRCN0000117643	Core	no	0.826	0.150	0.979	0.073	1.002
RPL24	IPI00306332	NM_000986	TRCN0000117644	Core	no	0.859	0.287	1.025	0.025	1.280
RPL24	IPI00306332	NM_000986	TRCN0000117645	Core	no	1.107	0.012	1.001	0.062	1.246
RPL24	IPI00306332	NM_000986	TRCN0000117646	Core	no	1.115	0.200	1.046	0.199	1.151
RPL29	IPI00419919	NM_000992	TRCN0000072983	NS5B	no	1.705	0.744	1.021	0.078	0.938
RPL29	IPI00419919	NM_000992	TRCN0000072984	NS5B	no	1.070	0.025	0.923	0.155	0.856
RPL29	IPI00419919	NM_000992	TRCN0000072985	NS5B	no	1.284	0.353	1.260	0.520	0.999
RPL29	IPI00419919	NM_000992	TRCN0000072986	NS5B	no	0.926	0.371	1.026	0.095	0.938
RPL29	IPI00419919	NM_000992	TRCN0000072987	NS5B	no	1.213	0.089	1.367	0.096	1.078
RPL3	IPI00550021	NM_000967	TRCN0000117507	NS5B	no	0.698	0.100	1.313	0.120	0.884
RPL3	IPI00550021	NM_000967	TRCN0000117508	NS5B	no	0.857	0.201	1.317	0.205	1.125
RPL3	IPI00550021	NM_000967	TRCN0000117509	NS5B	no	1.037	0.002	0.878	0.163	1.042
RPL3	IPI00550021	NM_000967	TRCN0000117510	NS5B	no	0.904	0.158	1.066	0.129	1.070
RPL3	IPI00550021	NM_000967	TRCN0000117511	NS5B	no	1.156	0.062	1.255	0.122	0.725
RPL7A	IPI00299573	NM_000972	TRCN0000155029	NS5B	no	0.923	0.217	1.067	0.255	0.774
RPL7A	IPI00299573	NM_000972	TRCN0000155839	NS5B	no	0.771	0.283	1.352	0.366	0.745
RPL7A	IPI00299573	NM_000972	TRCN0000156926	NS5B	no	0.763	0.264	1.300	0.093	0.781
RPL7A	IPI00299573	NM_000972	TRCN0000157678	NS5B	no	0.525	0.197	1.208	0.161	0.882
RPL7A	IPI00299573	NM_000972	TRCN0000157881	NS5B	no	0.775	0.167	1.246	0.023	1.127
RPS16	IPI00221092	NM_001020	TRCN0000005471	NS3/4A	no	0.743	0.315	0.949	0.182	0.974
RPS16	IPI00221092	NM_001020	TRCN0000005472	NS3/4A	no	1.012	0.182	1.087	0.036	0.901
RPS16	IPI00221092	NM_001020	TRCN0000005473	NS3/4A	no	1.263	0.134	0.930	0.190	1.026
RPS16	IPI00221092	NM_001020	TRCN0000010941	NS3/4A	no	0.901	0.144	1.240	0.031	1.368
RPS7	IPI00013415	NM_001011	TRCN0000074763	Core	no	1.037	0.259	0.915	0.309	1.911
RPS7	IPI00013415	NM_001011	TRCN0000074764	Core	no	0.763	0.076	0.716	0.296	1.331
RPS7	IPI00013415	NM_001011	TRCN0000074765	Core	no	0.746	0.021	0.798	0.342	1.025
RPS7	IPI00013415	NM_001011	TRCN0000074766	Core	no	1.206	0.069	1.011	0.019	0.891
RPS7	IPI00013415	NM_001011	TRCN0000074767	Core	no	1.136	0.037	0.774	0.289	0.838

Gene Name	IPI no	Gene ID	shRNA	Bait	Statistically enriched	293T pIFN-B		A549 pIFN-B		293T pEF1a
						mean	stdev	mean	stdev	mean
RPS8	IPI00872430	NM_001012	TRCN0000074778	NS3/4A	no	0.876	0.138	0.753	0.153	0.815
RPS8	IPI00872430	NM_001012	TRCN0000074779	NS3/4A	no	1.134	0.005	1.125	0.136	1.055
RPS8	IPI00872430	NM_001012	TRCN0000074780	NS3/4A	no	1.023	0.031	0.885	0.129	0.663
RPS8	IPI00872430	NM_001012	TRCN0000074782	NS3/4A	no	1.274	0.206	1.268	0.352	0.867
RRP12	IPI00101186	NM_015179	TRCN0000154708	Core	no	0.735	0.220	1.032	0.066	0.792
RRP12	IPI00101186	NM_015179	TRCN0000155347	Core	no	0.865	0.078	0.866	0.196	1.038
RRP12	IPI00101186	NM_015179	TRCN0000156901	Core	no	0.950	0.427	0.695	0.103	1.031
RRP12	IPI00101186	NM_015179	TRCN0000157732	Core	no	0.981	0.061	1.005	0.408	0.794
RRP12	IPI00101186	NM_015179	TRCN0000157888	Core	no	0.653	0.328	0.699	0.314	1.124
RUVBL1	IPI00021187	NM_003707	TRCN0000018911	NS5B	no	1.084	0.300	0.965	0.208	1.009
RUVBL1	IPI00021187	NM_003707	TRCN0000018912	NS5B	no	0.998	0.096	0.777	0.197	0.898
RUVBL1	IPI00021187	NM_003707	TRCN0000018913	NS5B	no	1.008	0.205	1.054	0.125	0.691
RUVBL1	IPI00021187	NM_003707	TRCN0000018914	NS5B	no	1.240	0.219	1.064	0.186	0.968
RUVBL2	IPI00009104	NM_006666	TRCN0000051563	NS5A	no	0.842	0.204	1.372	0.402	1.220
RUVBL2	IPI00009104	NM_006666	TRCN0000051564	NS5A	no	0.909	0.011	0.831	0.150	0.979
RUVBL2	IPI00009104	NM_006666	TRCN0000051565	NS5A	no	0.692	0.017	1.047	0.099	0.942
RUVBL2	IPI00009104	NM_006666	TRCN0000051566	NS5A	no	0.604	0.017	0.789	0.150	0.880
RUVBL2	IPI00009104	NM_006666	TRCN0000051567	NS5A	no	0.809	0.202	1.003	0.007	1.012
SAAL1	IPI00304935	NM_138421	TRCN0000121563	NS3/4A	yes	0.775	0.259	1.088	0.056	1.245
SAAL1	IPI00304935	NM_138421	TRCN0000121596	NS3/4A	yes	1.284	0.108	1.117	0.255	1.119
SAAL1	IPI00304935	NM_138421	TRCN0000121738	NS3/4A	yes	0.967	0.121	0.962	0.014	0.859
SAAL1	IPI00304935	NM_138421	TRCN0000122312	NS3/4A	yes	1.037	0.070	0.948	0.119	1.075
SAAL1	IPI00304935	NM_138421	TRCN0000122424	NS3/4A	yes	1.036	0.019	0.991	0.297	0.974
SLC16A1	IPI00024650	NM_003051	TRCN0000038339	Core	yes	0.635	0.102	1.102	0.011	1.070
SLC16A1	IPI00024650	NM_003051	TRCN0000038340	Core	yes	1.014	0.002	1.031	0.154	0.787
SLC16A1	IPI00024650	NM_003051	TRCN0000038341	Core	yes	0.944	0.106	1.052	0.084	0.829
SLC16A1	IPI00024650	NM_003051	TRCN0000038342	Core	yes	1.193	0.126	0.844	0.313	0.723
SLC16A1	IPI00024650	NM_003051	TRCN0000038343	Core	yes	0.785	0.245	0.908	0.114	0.807
SLC1A5	IPI00019472	NM_005628	TRCN0000043118	NS3/4A	yes	1.640	0.452	1.224	0.177	1.185
SLC1A5	IPI00019472	NM_005628	TRCN0000043119	NS3/4A	yes	0.977	0.207	1.231	0.117	0.941
SLC1A5	IPI00019472	NM_005628	TRCN0000043120	NS3/4A	yes	1.141	0.171	1.186	0.237	1.249
SLC1A5	IPI00019472	NM_005628	TRCN0000043121	NS3/4A	yes	1.286	0.148	1.683	0.857	1.228
SLC1A5	IPI00019472	NM_005628	TRCN0000043122	NS3/4A	yes	1.259	0.154	1.319	0.557	1.252
SMC4	IPI00411559	NM_005496	TRCN0000150860	NS3/4A	no	0.656	0.172	1.147	0.111	1.664
SMC4	IPI00411559	NM_005496	TRCN0000154723	NS3/4A	no	1.052	0.252	1.053	0.290	2.127
SMC4	IPI00411559	NM_005496	TRCN0000154901	NS3/4A	no	1.169	0.019	1.245	0.231	0.872
SMC4	IPI00411559	NM_005496	TRCN0000155428	NS3/4A	no	0.968	0.178	1.204	0.013	1.703
SMC4	IPI00411559	NM_005496	TRCN0000155500	NS3/4A	no	0.961	0.080	0.877	0.011	0.957
SMYD3	IPI00165073	NM_022743	TRCN0000123289	NS5A	yes	1.121	0.216	0.753	0.446	0.790
SMYD3	IPI00165073	NM_022743	TRCN0000123290	NS5A	yes	1.040	0.043	0.815	0.173	1.036
SMYD3	IPI00165073	NM_022743	TRCN0000123291	NS5A	yes	1.097	0.227	0.946	0.076	0.847
SMYD3	IPI00165073	NM_022743	TRCN0000123292	NS5A	yes	1.101	0.761	0.872	0.056	0.795
SMYD3	IPI00165073	NM_022743	TRCN0000123293	NS5A	yes	1.338	0.117	0.893	0.121	1.015
SPIN1	IPI00550655	NM_032038	TRCN0000059953	NS3/4A	no	1.356	0.049	1.177	0.085	0.984
SPIN1	IPI00550655	NM_032038	TRCN0000059954	NS3/4A	no	0.839	0.177	0.860	0.155	0.676
SPIN1	IPI00550655	NM_032038	TRCN0000059955	NS3/4A	no	1.121	0.163	0.849	0.178	1.191
SPIN1	IPI00550655	NM_032038	TRCN0000059956	NS3/4A	no	1.392	0.291	0.984	0.020	0.848
SPIN1	IPI00550655	NM_032038	TRCN0000059957	NS3/4A	no	0.948	0.219	0.776	0.324	1.164
SPTAN1	IPI00844215	NM_003127	TRCN0000053668	NS3/4A	no	0.811	0.112	0.946	0.078	0.863
SPTAN1	IPI00844215	NM_003127	TRCN0000053669	NS3/4A	no	0.658	0.089	0.996	0.112	0.829
SPTAN1	IPI00844215	NM_003127	TRCN0000053670	NS3/4A	no	0.916	0.160	0.957	0.251	1.064
SPTAN1	IPI00844215	NM_003127	TRCN0000053671	NS3/4A	no	1.002	0.003	1.143	0.163	1.176
SPTAN1	IPI00844215	NM_003127	TRCN0000053672	NS3/4A	no	0.890	0.257	0.835	0.269	0.794
SPTLC1	IPI00005745	NM_006415	TRCN0000035009	NS3/4A	no	0.951	0.658	0.930	0.016	1.102
SPTLC1	IPI00005745	NM_006415	TRCN0000035011	NS3/4A	no	1.068	0.740	1.094	0.393	0.800
SPTLC1	IPI00005745	NM_006415	TRCN0000035012	NS3/4A	no	1.245	0.364	0.889	0.138	0.912
SPTLC1	IPI00005745	NM_006415	TRCN0000035013	NS3/4A	no	1.653	0.654	1.077	0.242	1.161

Gene Name	IPI no	Gene ID	shRNA	Bait	Statistically enriched	293T pIFN-B		A549 pIFN-B		293T pEF1a
						mean	stdev	mean	stdev	mean
STXBP3	IPI00297626	NM_007269	TRCN0000158420	NS3/4A	no	1.147	0.073	0.891	0.233	1.638
STXBP3	IPI00297626	NM_007269	TRCN0000159248	NS3/4A	no	1.122	0.272	0.915	0.191	0.878
STXBP3	IPI00297626	NM_007269	TRCN0000159454	NS3/4A	no	1.544	0.332	1.040	0.254	1.435
STXBP3	IPI00297626	NM_007269	TRCN0000160342	NS3/4A	no	1.081	0.251	1.259	0.168	0.865
TARDBP	IPI00025815	NM_007375	TRCN0000016038	NS3/4A	yes	1.119	0.045	0.831	0.040	0.913
TARDBP	IPI00025815	NM_007375	TRCN0000016039	NS3/4A	yes	1.032	0.222	1.278	0.605	1.160
TARDBP	IPI00025815	NM_007375	TRCN0000016040	NS3/4A	yes	1.227	0.201	1.025	0.217	0.957
TARDBP	IPI00025815	NM_007375	TRCN0000016041	NS3/4A	yes	1.093	0.291	0.965	0.231	0.803
TARDBP	IPI00025815	NM_007375	TRCN0000016042	NS3/4A	yes	1.020	0.047	1.160	0.184	0.948
TBRG4	IPI00329625	NM_004749	TRCN0000154962	NS3/4A	yes	0.971	0.005	0.885	0.393	0.878
TBRG4	IPI00329625	NM_004749	TRCN0000155887	NS3/4A	yes	0.717	0.172	0.757	0.156	1.205
TBRG4	IPI00329625	NM_004749	TRCN0000156248	NS3/4A	yes	1.210	0.249	0.885	0.152	0.960
TBRG4	IPI00329625	NM_004749	TRCN0000157725	NS3/4A	yes	0.954	0.002	0.975	0.220	0.986
TBRG4	IPI00329625	NM_004749	TRCN0000157762	NS3/4A	yes	1.006	0.010	0.904	0.263	1.196
TMEM109	IPI00031697	NM_024092	TRCN0000122488	Core	yes	0.888	0.600	1.124	0.005	1.429
TMEM109	IPI00031697	NM_024092	TRCN0000141032	Core	yes	0.989	0.097	0.744	0.278	0.799
TMEM109	IPI00031697	NM_024092	TRCN0000143379	Core	yes	1.310	0.427	0.920	0.154	0.954
TMEM109	IPI00031697	NM_024092	TRCN0000144064	Core	yes	0.958	0.068	1.127	0.091	0.716
TMEM109	IPI00031697	NM_024092	TRCN0000145161	Core	yes	0.989	0.235	1.335	0.365	1.599
TNPO1	IPI00024364	NM_002270	TRCN0000038284	NS3/4A	yes	1.201	0.509	1.038	0.109	1.340
TNPO1	IPI00024364	NM_002270	TRCN0000038285	NS3/4A	yes	0.720	0.254	0.658	0.312	1.592
TNPO1	IPI00024364	NM_002270	TRCN0000038286	NS3/4A	yes	0.720	0.039	0.881	0.076	1.502
TNPO1	IPI00024364	NM_002270	TRCN0000038287	NS3/4A	yes	0.950	0.295	0.865	0.070	0.644
TNPO1	IPI00024364	NM_002270	TRCN0000038288	NS3/4A	yes	1.284	0.425	0.684	0.182	0.967
TRAM1	IPI00219111	NM_014294	TRCN0000062938	Core	yes	1.194	0.002	1.071	0.207	1.189
TRAM1	IPI00219111	NM_014294	TRCN0000062939	Core	yes	1.103	0.135	1.097	0.214	1.072
TRAM1	IPI00219111	NM_014294	TRCN0000062940	Core	yes	1.344	0.249	0.819	0.106	1.084
TRAM1	IPI00219111	NM_014294	TRCN0000062941	Core	yes	1.088	0.238	0.867	0.301	1.490
TRAM1	IPI00219111	NM_014294	TRCN0000062942	Core	yes	0.926	0.174	0.949	0.151	1.204
TRIP13	IPI00003505	NM_004237	TRCN0000022059	NS3/4A	no	1.336	0.083	1.432	0.415	0.862
TRIP13	IPI00003505	NM_004237	TRCN0000022060	NS3/4A	no	1.153	0.016	1.214	0.039	1.171
TRIP13	IPI00003505	NM_004237	TRCN0000022061	NS3/4A	no	1.196	0.187	0.852	0.237	1.312
TRIP13	IPI00003505	NM_004237	TRCN0000022062	NS3/4A	no	1.208	0.347	0.878	0.011	0.906
TRIP13	IPI00003505	NM_004237	TRCN0000022063	NS3/4A	no	1.239	0.318	1.134	0.309	1.146
TUBB	IPI00011654	NM_178014	TRCN0000074358	NS3/4A	yes	0.891	0.167	1.101	0.323	1.114
TUBB	IPI00011654	NM_178014	TRCN0000074359	NS3/4A	yes	1.132	0.168	0.964	0.144	1.418
TUBB	IPI00011654	NM_178014	TRCN0000074360	NS3/4A	yes	1.060	0.219	1.028	0.333	1.051
TUBB	IPI00011654	NM_178014	TRCN0000074361	NS3/4A	yes	1.022	0.123	1.298	0.225	1.249
TUBB	IPI00011654	NM_178014	TRCN0000074362	NS3/4A	yes	1.111	0.150	1.409	0.321	1.158
UBC	IPI00784990	NM_021009	TRCN0000011107	NS3/4A	no	0.708	0.210	1.210	0.071	0.855
UBC	IPI00784990	NM_021009	TRCN0000011108	NS3/4A	no	0.668	0.172	1.085	0.185	0.876
UBC	IPI00784990	NM_021009	TRCN0000011109	NS3/4A	no	0.755	0.229	1.326	0.020	0.739
UBC	IPI00784990	NM_021009	TRCN0000011110	NS3/4A	no	0.806	0.377	0.920	0.445	0.719
UBC	IPI00784990	NM_021009	TRCN0000011111	NS3/4A	no	0.758	0.314	1.517	0.147	1.143
UBE2O	IPI00783378	NM_022066	TRCN0000004587	Core	no	0.878	0.121	0.629	0.317	1.038
UBE2O	IPI00783378	NM_022066	TRCN0000004588	Core	no	1.035	0.009	1.049	0.187	1.118
UBE2O	IPI00783378	NM_022066	TRCN0000004589	Core	no	0.946	0.020	0.914	0.119	0.661
UBE2O	IPI00783378	NM_022066	TRCN0000004590	Core	no	1.333	0.018	0.944	0.152	0.900
UBE2O	IPI00783378	NM_022066	TRCN0000010895	Core	no	1.207	0.164	1.064	0.024	0.848
UGT8	IPI00294455	NM_003360	TRCN0000035704	Core	yes	0.922	0.631	0.796	0.333	0.943
UGT8	IPI00294455	NM_003360	TRCN0000035705	Core	yes	1.170	0.102	0.844	0.315	0.746
UGT8	IPI00294455	NM_003360	TRCN0000035706	Core	yes	0.984	0.678	0.791	0.236	0.881
UGT8	IPI00294455	NM_003360	TRCN0000035707	Core	yes	1.167	0.803	0.647	0.210	0.877
UGT8	IPI00294455	NM_003360	TRCN0000035708	Core	yes	1.850	1.087	0.874	0.068	0.796

Gene Name	IPI no	Gene ID	shRNA	Bait	Statistically enriched	293T pIFN-B		A549 pIFN-B		293T pEF1a
						mean	stdev	mean	stdev	mean
USP19	IPI00016589	XM_496642	TRCN0000051713	NS5A	yes	0.979	0.008	1.066	0.183	0.799
USP19	IPI00016589	XM_496642	TRCN0000051714	NS5A	yes	0.981	0.152	1.103	0.002	0.789
USP19	IPI00016589	XM_496642	TRCN0000051715	NS5A	yes	1.068	0.034	1.134	0.036	1.125
USP19	IPI00016589	XM_496642	TRCN0000051716	NS5A	yes	1.149	0.294	1.120	0.113	1.019
USP19	IPI00016589	XM_496642	TRCN0000051717	NS5A	yes	1.371	0.117	1.020	0.013	0.970
VAPA	IPI00640416	NM_003574	TRCN0000029129	NS5A	yes	1.253	0.346	1.179	0.103	0.615
VAPA	IPI00640416	NM_003574	TRCN0000029130	NS5A	yes	1.074	0.099	1.057	0.070	1.085
VAPA	IPI00640416	NM_003574	TRCN0000029131	NS5A	yes	1.189	0.082	0.988	0.154	1.087
VAPA	IPI00640416	NM_003574	TRCN0000029132	NS5A	yes	1.081	0.025	1.093	0.330	1.044
VAPA	IPI00640416	NM_003574	TRCN0000029133	NS5A	yes	1.640	0.377	1.108	0.200	1.044
VAPB	IPI00006211	NM_004738	TRCN0000151599	NS5A	yes	1.092	0.061	1.019	0.175	1.113
VAPB	IPI00006211	NM_004738	TRCN0000152239	NS5A	yes	0.962	0.090	0.856	0.196	1.033
VAPB	IPI00006211	NM_004738	TRCN0000152888	NS5A	yes	0.830	0.037	1.004	0.035	1.242
VAPB	IPI00006211	NM_004738	TRCN0000153862	NS5A	yes	1.178	0.199	0.997	0.013	1.168
VAPB	IPI00006211	NM_004738	TRCN0000156377	NS5A	yes	0.934	0.055	0.976	0.027	1.199
VDAC3	IPI00031804	NM_005662	TRCN0000139639	NS3/4A	yes	0.931	0.178	1.096	0.083	1.307
VDAC3	IPI00031804	NM_005662	TRCN0000140435	NS3/4A	yes	0.896	0.049	0.841	0.180	1.016
VDAC3	IPI00031804	NM_005662	TRCN0000141213	NS3/4A	yes	1.244	0.066	1.025	0.003	1.071
VDAC3	IPI00031804	NM_005662	TRCN0000144497	NS3/4A	yes	1.044	0.055	0.940	0.085	1.104
VDAC3	IPI00031804	NM_005662	TRCN0000145346	NS3/4A	yes	1.067	0.198	1.043	0.065	1.201
VIM	IPI00418471	NM_003380	TRCN0000029119	NS5B	no	0.874	0.179	0.852	0.373	1.135
VIM	IPI00418471	NM_003380	TRCN0000029120	NS5B	no	1.134	0.230	1.233	0.052	1.146
VIM	IPI00418471	NM_003380	TRCN0000029121	NS5B	no	1.152	0.202	1.075	0.053	0.960
VIM	IPI00418471	NM_003380	TRCN0000029122	NS5B	no	1.260	0.316	1.100	0.105	0.984
VIM	IPI00418471	NM_003380	TRCN0000029123	NS5B	no	1.087	0.252	1.013	0.003	0.825
WDR77	IPI00012202	NM_024102	TRCN0000072778	Core	no	0.522	0.244	0.636	0.299	0.775
WDR77	IPI00012202	NM_024102	TRCN0000072779	Core	no	1.249	0.105	0.919	0.230	1.057
WDR77	IPI00012202	NM_024102	TRCN0000072780	Core	no	1.105	0.048	0.611	0.463	0.920
WDR77	IPI00012202	NM_024102	TRCN0000072781	Core	no	1.182	0.302	0.816	0.123	1.172
WDR77	IPI00012202	NM_024102	TRCN0000072782	Core	no	1.515	0.267	0.706	0.252	1.233
XPO1	IPI00298961	NM_003400	TRCN0000150975	NS3/4A	yes	0.967	0.058	1.072	0.191	0.738
XPO1	IPI00298961	NM_003400	TRCN0000150975	NS3/4A	yes	0.725	0.240	1.023	0.170	0.873
XPO1	IPI00298961	NM_003400	TRCN0000152210	NS3/4A	yes	0.801	0.068	0.998	0.103	0.742
XPO1	IPI00298961	NM_003400	TRCN0000152210	NS3/4A	yes	0.732	0.053	1.109	0.053	0.876
XPO1	IPI00298961	NM_003400	TRCN0000152787	NS3/4A	yes	0.669	0.067	0.809	0.344	0.812
XPO1	IPI00298961	NM_003400	TRCN0000152787	NS3/4A	yes	0.647	0.195	0.858	0.416	1.081
XPO1	IPI00298961	NM_003400	TRCN0000153235	NS3/4A	yes	0.719	0.100	1.000	0.126	1.002
XPO1	IPI00298961	NM_003400	TRCN0000153235	NS3/4A	yes	0.712	0.034	1.011	0.046	1.260
XPO1	IPI00298961	NM_003400	TRCN0000154386	NS3/4A	yes	0.759	0.135	0.875	0.118	1.373
XPO1	IPI00298961	NM_003400	TRCN0000154386	NS3/4A	yes	0.697	0.224	0.849	0.092	1.410
XPOT	IPI00306290	NM_007235	TRCN0000059898	NS3/4A	no	1.233	0.018	0.999	0.091	1.377
XPOT	IPI00306290	NM_007235	TRCN0000059899	NS3/4A	no	1.141	0.157	0.911	0.040	1.022
XPOT	IPI00306290	NM_007235	TRCN0000059900	NS3/4A	no	1.292	0.168	0.914	0.046	0.743
XPOT	IPI00306290	NM_007235	TRCN0000059901	NS3/4A	no	1.191	0.051	1.074	0.073	0.993
XPOT	IPI00306290	NM_007235	TRCN0000059902	NS3/4A	no	1.224	0.144	0.901	0.066	1.028
YBX1	IPI00031812	NM_004559	TRCN0000007948	NS3/4A	no	0.671	0.123	0.722	0.272	0.905
YBX1	IPI00031812	NM_004559	TRCN0000007949	NS3/4A	no	0.929	0.638	1.282	0.308	0.936
YBX1	IPI00031812	NM_004559	TRCN0000007950	NS3/4A	no	0.850	0.108	0.911	0.140	1.268
YBX1	IPI00031812	NM_004559	TRCN0000007951	NS3/4A	no	0.858	0.163	1.430	0.347	0.747
YBX1	IPI00031812	NM_004559	TRCN0000007952	NS3/4A	no	0.698	0.209	1.205	0.220	1.048
ZRANB2	IPI00845348	NM_005455	TRCN0000013423	NS3/4A	no	1.207	0.027	1.254	0.100	0.741
ZRANB2	IPI00845348	NM_005455	TRCN0000013424	NS3/4A	no	0.658	0.077	0.769	0.299	1.046
ZRANB2	IPI00845348	NM_005455	TRCN0000013425	NS3/4A	no	1.144	0.009	1.023	0.029	1.113
ZRANB2	IPI00845348	NM_005455	TRCN0000013426	NS3/4A	no	1.107	0.146	1.290	0.577	0.990
ZRANB2	IPI00845348	NM_005455	TRCN0000013427	NS3/4A	no	0.889	0.152	0.837	0.228	1.195

Table S2. Effect of the 132 Virus-Host Interactors on the Innate Antiviral Immunity

This table contains the results of the RNAi screen on the 132 virus-host interactors and the effects of their gene silencing on the innate antiviral immunity. The average of 2 separate experiments is shown for the HEK 293T and A549 cell lines. Ef1α is used as a measurement of cellular fitness to eliminate shRNAs with non-specific effects and prioritizing genes affecting only the *IFNB1* promoter.

IRF3 Nuclear Translocation							
Gene Name	Gene ID	shRNA	SeV 1h	SeV 3h	SeV 5h	SeV 8h	SeV 10h
NT			27%	54%	66%	40%	25%
NT			22%	59%	71%	42%	30%
NT			24%	56%	72%	44%	24%
NT			23%	59%	69%	38%	28%
CSE1L	NM_001316	TRCN0000061790	-16%	-44%	-34%	-8%	-6%
CSE1L	NM_001316	TRCN0000061790	-21%	-47%	-45%	-19%	-4%
DDX19A	NM_018332	TRCN0000050218	12%	-4%	1%	5%	-7%
DDX19A	NM_018332	TRCN0000050219	9%	-5%	-2%	13%	-7%
DDX19A	NM_018332	TRCN0000050220	-10%	-27%	-25%	-6%	-11%
DDX19A	NM_018332	TRCN0000050221	3%	17%	2%	11%	1%
DDX19A	NM_018332	TRCN0000050222	0%	2%	1%	7%	-9%
DDX19B	NM_007242	TRCN0000051128	-4%	-28%	-25%	-8%	-9%
DDX19B	NM_007242	TRCN0000051129	25%	4%	-8%	-18%	-18%
DDX19B	NM_007242	TRCN0000051130	1%	7%	-16%	-17%	-21%
DDX19B	NM_007242	TRCN0000051131	-1%	-8%	-12%	-15%	-18%
DDX19B	NM_007242	TRCN0000051132	8%	3%	9%	18%	19%
GLE1L	NM_001499	TRCN0000077938	24%	4%	-2%	2%	-12%
GLE1L	NM_001499	TRCN0000077939	-12%	6%	-11%	4%	-14%
GLE1L	NM_001499	TRCN0000077940	-14%	-27%	-24%	17%	22%
GLE1L	NM_001499	TRCN0000077941	-5%	-4%	-2%	0%	-8%
GLE1L	NM_001499	TRCN0000077942	11%	-11%	2%	-6%	-9%
HRB	NM_004504	TRCN0000060223	7%	13%	-4%	-6%	-7%
HRB	NM_004504	TRCN0000060224	1%	-10%	-14%	-10%	-19%
HRB	NM_004504	TRCN0000060225	-5%	-19%	-12%	4%	-10%
HRB	NM_004504	TRCN0000060226	26%	11%	3%	14%	2%
HRB	NM_004504	TRCN0000060227	19%	10%	3%	8%	-3%
HRBL	NM_006076	TRCN0000149837	12%	11%	-14%	-31%	-17%
HRBL	NM_006076	TRCN0000148766	6%	1%	0%	3%	-10%
HRBL	NM_006076	TRCN0000146397	3%	4%	-4%	5%	4%
HRBL	NM_006076	TRCN0000147372	-7%	-17%	2%	1%	7%
IPO11	NM_016338	TRCN0000159422	-2%	-1%	-11%	-8%	-14%
IPO11	NM_016338	TRCN0000160347	4%	3%	9%	3%	-2%
IPO11	NM_016338	TRCN0000158471	-12%	10%	-16%	-20%	-19%
IPO11	NM_016338	TRCN0000158885	-7%	7%	-7%	-10%	-14%
IPO4	NM_024658	TRCN0000072488	0%	-16%	-14%	-18%	-13%
IPO4	NM_024658	TRCN0000072489	10%	0%	-6%	-21%	-12%
IPO4	NM_024658	TRCN0000072491	14%	-3%	-11%	-24%	-11%
IPO4	NM_024658	TRCN0000072492	19%	-9%	2%	16%	15%
IPO7	NM_006391	TRCN0000156655	-16%	-6%	1%	-8%	-10%
IPO7	NM_006391	TRCN0000150676	-20%	-25%	-14%	-24%	-18%
IPO7	NM_006391	TRCN0000156994	-13%	-4%	7%	-17%	-6%
IPO7	NM_006391	TRCN0000151374	-12%	-20%	-23%	5%	10%
IPO7	NM_006391	TRCN0000155501	-5%	-6%	-2%	-3%	-2%
IPO8	NM_006390	TRCN0000156712	13%	-8%	5%	-15%	-15%
IPO8	NM_006390	TRCN0000151987	-10%	-6%	-14%	-26%	-20%
IPO8	NM_006390	TRCN0000156852	-12%	-14%	-16%	-20%	-21%
IPO8	NM_006390	TRCN0000156073	-8%	-2%	-9%	-6%	-11%
IPO8	NM_006390	TRCN0000150605	-9%	-8%	-5%	-10%	-13%
KPNA1	NM_002264	TRCN0000065298	7%	-4%	-5%	-9%	-4%
KPNA1	NM_002264	TRCN0000065299	13%	3%	4%	-6%	-8%
KPNA1	NM_002264	TRCN0000065300	4%	-14%	-14%	-10%	-9%
KPNA1	NM_002264	TRCN0000065301	-2%	-5%	-7%	-10%	-12%
KPNA1	NM_002264	TRCN0000065302	-13%	-21%	-18%	0%	4%

IRF3 Nuclear Translocation							
Gene Name	Gene ID	shRNA	SeV 1h	SeV 3h	SeV 5h	SeV 8h	SeV 10h
KPNA2	NM_002266	TRCN0000065308	-5%	-18%	-15%	4%	-10%
KPNA2	NM_002266	TRCN0000065310	-5%	-11%	-4%	-4%	-5%
KPNA2	NM_002266	TRCN0000065311	-7%	-24%	-12%	-4%	-8%
KPNA2	NM_002266	TRCN0000065312	9%	-14%	-21%	-23%	-17%
KPNA2	NM_002266	TRCN0000065309	-4%	2%	-8%	-13%	-15%
KPNA3	NM_002267	TRCN0000065318	7%	-16%	-11%	22%	19%
KPNA3	NM_002267	TRCN0000065319	1%	-8%	-5%	3%	1%
KPNA3	NM_002267	TRCN0000065320	3%	-19%	-9%	4%	2%
KPNA3	NM_002267	TRCN0000065321	1%	-14%	-6%	-13%	-12%
KPNA3	NM_002267	TRCN0000065322	-6%	-1%	-3%	8%	-6%
KPNA4	NM_002268	TRCN0000065328	21%	7%	-7%	-19%	-17%
KPNA4	NM_002268	TRCN0000065329	-8%	-12%	-10%	2%	-14%
KPNA4	NM_002268	TRCN0000065330	2%	2%	2%	3%	0%
KPNA4	NM_002268	TRCN0000065331	6%	17%	20%	31%	26%
KPNA4	NM_002268	TRCN0000065332	-1%	9%	16%	8%	9%
KPNA5	NM_002269	TRCN0000064943	-12%	-24%	-11%	32%	-6%
KPNA5	NM_002269	TRCN0000064944	5%	-14%	-5%	-9%	-6%
KPNA5	NM_002269	TRCN0000064945	28%	1%	-1%	-26%	-16%
KPNA5	NM_002269	TRCN0000064946	1%	-13%	-11%	23%	17%
KPNA5	NM_002269	TRCN0000064947	8%	-5%	-13%	-16%	-18%
KPNA6	NM_012316	TRCN0000065043	-2%	-7%	-4%	-7%	-6%
KPNA6	NM_012316	TRCN0000065044	7%	-5%	0%	-6%	2%
KPNA6	NM_012316	TRCN0000065045	-12%	-26%	-21%	5%	4%
KPNA6	NM_012316	TRCN0000065047	34%	3%	-13%	-18%	-17%
KPNA6	NM_012316	TRCN0000065046	-4%	-7%	4%	11%	4%
KPNB1	NM_002265	TRCN0000123189	-12%	-39%	-28%	-1%	-6%
KPNB1	NM_002265	TRCN0000123190	-17%	-43%	-32%	-3%	0%
KPNB1	NM_002265	TRCN0000123191	-16%	-29%	-19%	10%	-3%
KPNB1	NM_002265	TRCN0000123192	-12%	-35%	-40%	-22%	-9%
KPNB1	NM_002265	TRCN0000123193	4%	-19%	-6%	-8%	-12%
NUP107	NM_020401	TRCN0000072478	-1%	-16%	-8%	18%	20%
NUP107	NM_020401	TRCN0000072479	2%	-6%	-6%	-8%	-6%
NUP107	NM_020401	TRCN0000072480	3%	-1%	-10%	-5%	-5%
NUP107	NM_020401	TRCN0000072481	-1%	-32%	-8%	-3%	4%
NUP107	NM_020401	TRCN0000072482	-7%	-20%	-14%	-1%	-3%
NUP153	NM_005124	TRCN0000060243	11%	-3%	-4%	2%	-17%
NUP153	NM_005124	TRCN0000060244	-7%	-20%	-13%	15%	8%
NUP153	NM_005124	TRCN0000060245	14%	7%	1%	12%	-3%
NUP153	NM_005124	TRCN0000060246	19%	5%	-2%	-1%	-19%
NUP153	NM_005124	TRCN0000060247	9%	-3%	3%	12%	-2%
NUP155	NM_004298	TRCN0000059913	7%	-15%	-20%	3%	-16%
NUP155	NM_004298	TRCN0000059914	0%	-11%	7%	13%	-17%
NUP155	NM_004298	TRCN0000059915	3%	-19%	-7%	18%	-7%
NUP155	NM_004298	TRCN0000059916	-2%	-7%	-5%	0%	-10%
NUP155	NM_004298	TRCN0000059917	-7%	-5%	-3%	4%	-12%
NUP160	XM_113678	TRCN0000060113	-7%	-15%	-12%	4%	-8%
NUP160	XM_113678	TRCN0000060114	-10%	-38%	-33%	3%	4%
NUP160	XM_113678	TRCN0000060115	4%	-8%	-7%	-1%	-14%
NUP160	XM_113678	TRCN0000060116	-11%	-27%	-24%	11%	2%
NUP160	XM_113678	TRCN0000060117	-6%	-10%	-8%	-10%	-13%
NUP205	XM_371954	TRCN0000060023	-5%	-18%	-22%	4%	10%
NUP205	XM_371954	TRCN0000060024	-4%	-32%	-31%	4%	2%
NUP205	XM_371954	TRCN0000060025	7%	-13%	-8%	-5%	-5%
NUP205	XM_371954	TRCN0000060027	-12%	-9%	-9%	0%	-9%

IRF3 Nuclear Translocation							
Gene Name	Gene ID	shRNA	SeV 1h	SeV 3h	SeV 5h	SeV 8h	SeV 10h
NUP210	NM_024923	TRCN0000153158	-17%	-5%	-6%	-3%	-8%
NUP210	NM_024923	TRCN0000156619	-18%	-1%	-9%	-8%	-10%
NUP210	NM_024923	TRCN0000157497	-12%	-1%	-5%	3%	-1%
NUP210	NM_024923	TRCN0000152698	-16%	-36%	-24%	-10%	-6%
NUP210	NM_024923	TRCN0000157612	-7%	-8%	-16%	-23%	-18%
NUP214	NM_005085	TRCN0000005554	-18%	-26%	-12%	5%	6%
NUP214	NM_005085	TRCN0000005555	-3%	-1%	-5%	-9%	-5%
NUP214	NM_005085	TRCN0000005556	-14%	-25%	-17%	-10%	21%
NUP214	NM_005085	TRCN0000005557	-12%	-19%	-6%	-28%	-12%
NUP214	NM_005085	TRCN0000005558	4%	-11%	-8%	-7%	2%
NUP35	NM_138285	TRCN0000072378	-1%	-12%	-12%	-18%	-13%
NUP35	NM_138285	TRCN0000072379	-5%	-6%	-19%	-4%	-4%
NUP35	NM_138285	TRCN0000072380	5%	-6%	-11%	7%	6%
NUP35	NM_138285	TRCN0000072381	1%	-17%	-5%	13%	3%
NUP35	NM_138285	TRCN0000072382	32%	11%	1%	-10%	-14%
NUP37	NM_024057	TRCN0000152222	-14%	-17%	-5%	26%	31%
NUP37	NM_024057	TRCN0000153319	-9%	-5%	-1%	-10%	-13%
NUP37	NM_024057	TRCN0000151312	-10%	0%	9%	21%	30%
NUP37	NM_024057	TRCN0000151233	0%	-13%	-3%	6%	0%
NUP37	NM_024057	TRCN0000156008	0%	1%	2%	-5%	-7%
NUP43	NM_024647	TRCN0000134871	-5%	-11%	4%	1%	4%
NUP43	NM_024647	TRCN0000134068	-5%	-26%	-26%	-15%	-14%
NUP43	NM_024647	TRCN0000133881	-13%	-26%	-19%	17%	17%
NUP43	NM_024647	TRCN0000137797	-11%	-34%	-25%	15%	6%
NUP43	NM_024647	TRCN0000137417	7%	7%	-4%	15%	-7%
NUP50	NM_007172	TRCN0000158766	-11%	-7%	-10%	3%	-1%
NUP50	NM_007172	TRCN0000159335	0%	-12%	0%	6%	-3%
NUP50	NM_007172	TRCN0000158499	2%	-6%	-5%	-10%	-17%
NUP50	NM_007172	TRCN0000160160	-3%	3%	11%	1%	-8%
NUP54	NM_017426	TRCN0000059903	-4%	-12%	-21%	10%	3%
NUP54	NM_017426	TRCN0000059904	18%	11%	-11%	-5%	-12%
NUP54	NM_017426	TRCN0000059905	33%	21%	11%	-6%	1%
NUP54	NM_017426	TRCN0000059906	9%	-28%	-23%	14%	6%
NUP54	NM_017426	TRCN0000059907	-2%	-20%	-12%	9%	-2%
NUP62	NM_012346	TRCN0000059288	8%	8%	0%	6%	2%
NUP62	NM_012346	TRCN0000059289	3%	-2%	-7%	4%	-9%
NUP62	NM_012346	TRCN0000059290	8%	-1%	-17%	-18%	-21%
NUP62	NM_012346	TRCN0000059291	12%	5%	-13%	-10%	-18%
NUP62	NM_012346	TRCN0000059292	8%	-4%	-4%	5%	-12%
NUP88	NM_002532	TRCN0000141654	1%	-17%	-6%	-6%	-3%
NUP88	NM_002532	TRCN0000142510	3%	-3%	-3%	6%	3%
NUP88	NM_002532	TRCN0000139972	0%	-8%	-2%	9%	-7%
NUP88	NM_002532	TRCN0000145079	-1%	-17%	-16%	2%	0%
NUP88	NM_002532	TRCN0000145530	3%	-28%	-18%	19%	22%
NUP93	NM_014669	TRCN0000059958	10%	0%	-11%	3%	2%
NUP93	NM_014669	TRCN0000059959	19%	-16%	-14%	-1%	-7%
NUP93	NM_014669	TRCN0000059960	2%	-7%	-22%	-15%	-15%
NUP93	NM_014669	TRCN0000059961	-10%	-30%	-28%	-7%	1%
NUP93	NM_014669	TRCN0000059962	3%	-10%	-14%	4%	-2%
NUP98	NM_005387	TRCN0000046913	9%	-6%	-4%	0%	4%
NUP98	NM_005387	TRCN0000046914	22%	3%	-2%	7%	1%
NUP98	NM_005387	TRCN0000046915	9%	-4%	-4%	2%	0%
NUP98	NM_005387	TRCN0000046916	9%	1%	3%	6%	-2%
NUP98	NM_005387	TRCN0000046917	-5%	-10%	-7%	5%	-4%

IRF3 Nuclear Translocation							
Gene Name	Gene ID	shRNA	SeV 1h	SeV 3h	SeV 5h	SeV 8h	SeV 10h
NUPL1	NM_014089	TRCN0000013513	-7%	-18%	-19%	-4%	7%
NUPL1	NM_014089	TRCN0000013514	-10%	-13%	-18%	-2%	11%
NUPL1	NM_014089	TRCN0000013515	-4%	-5%	0%	-10%	-9%
NUPL1	NM_014089	TRCN0000013516	-17%	-39%	-43%	-23%	-12%
NUPL1	NM_014089	TRCN0000013517	-11%	-21%	-14%	2%	-5%
NUPL2	NM_007342	TRCN0000128180	7%	-6%	-10%	1%	1%
NUPL2	NM_007342	TRCN0000130187	17%	-14%	6%	12%	8%
NUPL2	NM_007342	TRCN0000129199	15%	0%	5%	-5%	-2%
NUPL2	NM_007342	TRCN0000130430	30%	0%	-10%	5%	-4%
NUPL2	NM_007342	TRCN0000129028	11%	-23%	-13%	-11%	-15%
NUTF2	NM_005796	TRCN0000038549	-5%	-12%	-7%	10%	4%
NUTF2	NM_005796	TRCN0000038550	-10%	-22%	-14%	-3%	4%
NUTF2	NM_005796	TRCN0000038551	-17%	-24%	-21%	-13%	3%
NUTF2	NM_005796	TRCN0000038552	12%	3%	-11%	-19%	-11%
NUTF2	NM_005796	TRCN0000038553	-13%	-8%	-2%	-10%	-3%
NXF1	NM_006362	TRCN0000007580	-2%	0%	-3%	-8%	-6%
NXF1	NM_006362	TRCN0000007581	1%	-20%	-26%	-13%	-14%
NXF1	NM_006362	TRCN0000007582	4%	-1%	-7%	-8%	-11%
NXF1	NM_006362	TRCN0000007583	1%	-6%	-22%	-3%	-13%
NXF1	NM_006362	TRCN0000011092	-16%	-16%	-28%	-21%	-22%
NXF2	NM_017809	TRCN0000059293	-5%	1%	-12%	-7%	-2%
NXF2	NM_017809	TRCN0000059294	-3%	-8%	-8%	-5%	-16%
NXF2	NM_017809	TRCN0000059296	-1%	-6%	-1%	3%	8%
NXF2	NM_017809	TRCN0000059297	-3%	4%	-10%	-11%	-14%
NXF3	NM_022052	TRCN0000060323	9%	-1%	3%	19%	1%
NXF3	NM_022052	TRCN0000060324	8%	2%	-2%	10%	0%
NXF3	NM_022052	TRCN0000060325	9%	22%	0%	13%	-1%
NXF3	NM_022052	TRCN0000060326	7%	-1%	-3%	-1%	-20%
NXF3	NM_022052	TRCN0000060327	11%	-9%	2%	12%	-7%
NXT1	NM_013248	TRCN0000148803	-13%	-34%	-30%	-28%	-22%
NXT1	NM_013248	TRCN0000148689	-12%	-16%	-12%	-15%	-16%
NXT1	NM_013248	TRCN0000147131	-13%	-23%	-13%	-4%	-3%
NXT1	NM_013248	TRCN0000146408	-6%	-13%	2%	30%	23%
NXT1	NM_013248	TRCN0000149160	-9%	-7%	-4%	-10%	-10%
NXT2	NM_018698	TRCN0000038574	-3%	-6%	2%	21%	14%
NXT2	NM_018698	TRCN0000038575	-15%	-27%	-17%	1%	6%
NXT2	NM_018698	TRCN0000038576	-17%	5%	-8%	-17%	-8%
NXT2	NM_018698	TRCN0000038577	-19%	-23%	-14%	5%	5%
NXT2	NM_018698	TRCN0000038578	-8%	-12%	-22%	-17%	-4%
POM121	NM_172020	TRCN0000060068	-14%	-18%	-14%	1%	-7%
POM121	NM_172020	TRCN0000060069	-10%	-20%	-18%	4%	-4%
POM121	NM_172020	TRCN0000060070	-5%	-12%	-3%	10%	-1%
POM121	NM_172020	TRCN0000060071	-10%	-20%	-3%	0%	-4%
RAN	NM_006325	TRCN000047929	4%	-39%	-44%	-12%	-8%
RAN	NM_006325	TRCN000047929	-18%	-39%	-31%	-21%	-2%
RANBP2	NM_006267	TRCN0000003450	-8%	-17%	-16%	-22%	-10%
RANBP2	NM_006267	TRCN0000003451	-14%	0%	-4%	-13%	-5%
RANBP2	NM_006267	TRCN0000003452	-16%	-23%	-14%	-6%	-1%
RANBP2	NM_006267	TRCN0000003453	-14%	-11%	-10%	-9%	0%
RANBP2	NM_006267	TRCN0000003454	-18%	-34%	-22%	8%	15%
RANBP3	NM_003624	TRCN0000073003	-3%	-5%	-2%	11%	0%
RANBP3	NM_003624	TRCN0000073004	-10%	-6%	3%	26%	8%
RANBP3	NM_003624	TRCN0000073005	-6%	-7%	-7%	-3%	-3%
RANBP3	NM_003624	TRCN0000073006	20%	-4%	-18%	-23%	-18%
RANBP3	NM_003624	TRCN0000073007	5%	3%	0%	19%	12%
RANBP5	NM_002271	TRCN0000150535	-9%	4%	-2%	-16%	-19%
RANBP5	NM_002271	TRCN0000153065	9%	7%	-4%	-14%	-15%
RANBP5	NM_002271	TRCN0000152684	6%	18%	11%	16%	19%
RANBP5	NM_002271	TRCN0000152127	-3%	-11%	3%	11%	2%
RANBP5	NM_002271	TRCN0000151824	1%	4%	-1%	-23%	-20%

IRF3 Nuclear Translocation							
Gene Name	Gene ID	shRNA	SeV 1h	SeV 3h	SeV 5h	SeV 8h	SeV 10h
RANBP6	NM_012416	TRCN0000148876	-9%	-8%	-12%	1%	-4%
RANBP6	NM_012416	TRCN0000146440	-15%	-41%	-34%	-15%	-3%
RANBP6	NM_012416	TRCN0000147280	0%	8%	8%	6%	4%
RANBP6	NM_012416	TRCN0000148942	-11%	-5%	-8%	-7%	-14%
RANBP6	NM_012416	TRCN0000149838	-15%	-9%	-14%	-11%	-17%
RANGAP1	NM_002883	TRCN0000047328	-9%	1%	-9%	-4%	9%
RANGAP1	NM_002883	TRCN0000047329	-2%	-6%	-7%	10%	6%
RANGAP1	NM_002883	TRCN0000047330	-3%	-12%	-8%	1%	-16%
RANGAP1	NM_002883	TRCN0000047331	-1%	-9%	-9%	6%	-5%
RANGAP1	NM_002883	TRCN0000047332	-19%	-23%	-8%	15%	2%
RCC1	NM_001269	TRCN0000157236	-10%	-12%	-9%	-11%	-13%
RCC1	NM_001269	TRCN0000151199	-10%	-9%	-2%	0%	-8%
RCC1	NM_001269	TRCN0000157685	-18%	-37%	-28%	-3%	-3%
RCC1	NM_001269	TRCN0000157981	-14%	-10%	-5%	-15%	-13%
RCC1	NM_001269	TRCN0000152440	-18%	-8%	-11%	-8%	-17%
RCC2	NM_018715	TRCN0000150578	-11%	15%	11%	-7%	2%
RCC2	NM_018715	TRCN0000154474	-1%	10%	5%	-17%	-15%
RCC2	NM_018715	TRCN0000154827	-14%	-3%	-6%	-6%	-13%
RCC2	NM_018715	TRCN0000153686	-12%	-8%	0%	-20%	-18%
RCC2	NM_018715	TRCN0000151164	-18%	-30%	-10%	6%	2%
RGPD4	NM_182588	TRCN0000017738	-7%	-3%	-15%	-19%	-7%
RGPD4	NM_182588	TRCN0000017739	9%	0%	-9%	-14%	0%
RGPD4	NM_182588	TRCN0000017740	24%	6%	-1%	-18%	-5%
RGPD4	NM_182588	TRCN0000017741	-4%	-19%	-16%	-17%	-9%
RGPD4	NM_182588	TRCN0000017742	28%	-10%	-11%	5%	20%
RNUT1	NM_005701	TRCN0000038569	-8%	-20%	-17%	-2%	2%
RNUT1	NM_005701	TRCN0000038570	-9%	-5%	-15%	-13%	-2%
RNUT1	NM_005701	TRCN0000038571	-5%	-3%	-1%	-6%	-3%
RNUT1	NM_005701	TRCN0000038572	-11%	-6%	-6%	-5%	-6%
RNUT1	NM_005701	TRCN0000038573	-13%	-5%	-2%	-14%	-11%
TNPO1	NM_002270	TRCN0000038284	-7%	-18%	-23%	-18%	-16%
TNPO1	NM_002270	TRCN0000038285	-24%	-47%	-52%	-29%	-17%
TNPO1	NM_002270	TRCN0000038286	-6%	-6%	-11%	-5%	2%
TNPO1	NM_002270	TRCN0000038287	-11%	-23%	-8%	-4%	-1%
TNPO1	NM_002270	TRCN0000038288	-21%	-19%	-10%	-16%	-11%
TNPO2	NM_013433	TRCN0000043468	-8%	-14%	-11%	0%	4%
TNPO2	NM_013433	TRCN0000043469	7%	4%	1%	17%	23%
TNPO2	NM_013433	TRCN0000043470	-4%	-13%	-20%	24%	48%
TNPO2	NM_013433	TRCN0000043471	10%	-16%	-13%	-4%	1%
TNPO2	NM_013433	TRCN0000043472	17%	9%	5%	2%	-9%
TNPO3	NM_012470	TRCN0000038329	-17%	-21%	-10%	-13%	-3%
TNPO3	NM_012470	TRCN0000038330	-5%	3%	-9%	-15%	-12%
TNPO3	NM_012470	TRCN0000038331	0%	-9%	-19%	-14%	-7%
TNPO3	NM_012470	TRCN0000038333	-13%	-26%	-20%	-22%	-10%
TNPO3	NM_012470	TRCN0000038332	-9%	4%	-4%	-28%	-20%
TPR	NM_003292	TRCN0000060063	-1%	9%	-7%	-17%	-12%
TPR	NM_003292	TRCN0000060064	-11%	-20%	-11%	-1%	-11%
TPR	NM_003292	TRCN0000060065	0%	11%	-2%	6%	-2%
TPR	NM_003292	TRCN0000060066	12%	8%	-9%	-6%	-13%
TPR	NM_003292	TRCN0000060067	-2%	3%	3%	7%	6%
XPO1	NM_003400	TRCN000154386	22%	34%	3%	-7%	2%
XPO4	NM_022459	TRCN0000159557	-5%	-1%	3%	-10%	-13%
XPO4	NM_022459	TRCN0000159095	-17%	-2%	-11%	-16%	-10%
XPO4	NM_022459	TRCN0000160271	-5%	7%	5%	-2%	-8%
XPO4	NM_022459	TRCN0000159918	-11%	-29%	-1%	20%	23%
XPO4	NM_022459	TRCN0000159748	-11%	-1%	-3%	-4%	-8%

p65 Nuclear Translocation							
Gene Name	Gene ID	shRNA	SeV 1h	SeV 3h	SeV 5h	SeV 8h	SeV 10h
NT			27%	43%	69%	50%	34%
NT			22%	46%	67%	48%	29%
NT			24%	48%	73%	49%	34%
NT			24%	50%	66%	48%	36%
CSE1L	NM_001316	TRCN0000061790	-16%	-40%	-48%	-29%	-22%
CSE1L	NM_001316	TRCN0000061790	-15%	-39%	-44%	-32%	-17%
DDX19A	NM_018332	TRCN0000050218	17%	19%	-8%	6%	20%
DDX19A	NM_018332	TRCN0000050219	1%	-14%	-18%	-19%	-11%
DDX19A	NM_018332	TRCN0000050220	8%	-13%	-19%	-1%	-9%
DDX19A	NM_018332	TRCN0000050221	22%	12%	5%	4%	7%
DDX19A	NM_018332	TRCN0000050222	3%	-15%	-1%	-1%	-2%
DDX19B	NM_007242	TRCN0000051128	-6%	-27%	-26%	-17%	2%
DDX19B	NM_007242	TRCN0000051129	7%	-6%	-20%	-1%	7%
DDX19B	NM_007242	TRCN0000051130	-3%	-6%	-23%	-18%	-7%
DDX19B	NM_007242	TRCN0000051131	5%	-3%	-24%	-24%	-12%
DDX19B	NM_007242	TRCN0000051132	44%	27%	7%	22%	16%
GLE1L	NM_001499	TRCN0000077938	4%	-13%	-5%	21%	3%
GLE1L	NM_001499	TRCN0000077939	1%	-11%	14%	3%	25%
GLE1L	NM_001499	TRCN0000077940	-10%	-30%	-19%	-2%	0%
GLE1L	NM_001499	TRCN0000077941	-17%	-34%	-25%	-22%	-18%
GLE1L	NM_001499	TRCN0000077942	3%	-19%	7%	11%	7%
HRB	NM_004504	TRCN0000060223	-8%	-18%	-32%	-20%	2%
HRB	NM_004504	TRCN0000060224	-3%	-6%	-25%	-22%	-6%
HRB	NM_004504	TRCN0000060225	-5%	-25%	-29%	-13%	-15%
HRB	NM_004504	TRCN0000060226	26%	17%	5%	24%	33%
HRB	NM_004504	TRCN0000060227	26%	27%	5%	11%	13%
HRBL	NM_006076	TRCN0000149837	-4%	17%	-7%	-30%	-1%
HRBL	NM_006076	TRCN0000148766	-4%	-3%	7%	-4%	-9%
HRBL	NM_006076	TRCN0000146397	12%	-18%	-2%	3%	8%
HRBL	NM_006076	TRCN0000147372	-5%	-21%	3%	-14%	-8%
IPO11	NM_016338	TRCN0000159422	-11%	-11%	-18%	-26%	-17%
IPO11	NM_016338	TRCN0000160347	-11%	-13%	-8%	-17%	-4%
IPO11	NM_016338	TRCN0000158471	1%	-4%	-2%	-8%	4%
IPO11	NM_016338	TRCN0000158885	14%	3%	12%	8%	19%
IPO4	NM_024658	TRCN0000072488	8%	-16%	0%	10%	-3%
IPO4	NM_024658	TRCN0000072489	17%	-5%	7%	5%	9%
IPO4	NM_024658	TRCN0000072491	23%	-13%	2%	4%	9%
IPO4	NM_024658	TRCN0000072492	8%	-11%	0%	7%	8%
IPO7	NM_006391	TRCN0000156655	-10%	-18%	-16%	-25%	-13%
IPO7	NM_006391	TRCN0000150676	-14%	-34%	-15%	-24%	-21%
IPO7	NM_006391	TRCN0000156994	38%	6%	15%	23%	29%
IPO7	NM_006391	TRCN0000151374	-20%	-42%	-45%	-10%	-14%
IPO7	NM_006391	TRCN0000155501	-6%	-10%	1%	-5%	-9%
IPO8	NM_006390	TRCN0000156712	37%	20%	13%	13%	24%
IPO8	NM_006390	TRCN0000151987	-3%	-16%	-10%	-19%	-12%
IPO8	NM_006390	TRCN0000156852	-2%	-18%	-18%	-22%	-6%
IPO8	NM_006390	TRCN0000156073	4%	-15%	-17%	-5%	-8%
IPO8	NM_006390	TRCN0000150605	-9%	-25%	-8%	-8%	-13%
KPNA1	NM_002264	TRCN0000065298	2%	-30%	-1%	-9%	4%
KPNA1	NM_002264	TRCN0000065299	8%	-16%	1%	-7%	-11%
KPNA1	NM_002264	TRCN0000065300	4%	-21%	-6%	25%	3%
KPNA1	NM_002264	TRCN0000065301	0%	-16%	-4%	-1%	-4%
KPNA1	NM_002264	TRCN0000065302	-7%	-14%	-23%	-12%	-8%

p65 Nuclear Translocation							
Gene Name	Gene ID	shRNA	SeV 1h	SeV 3h	SeV 5h	SeV 8h	SeV 10h
KPNA2	NM_002266	TRCN0000065308	-5%	-30%	-14%	-4%	-7%
KPNA2	NM_002266	TRCN0000065310	-3%	-27%	-3%	3%	-10%
KPNA2	NM_002266	TRCN0000065311	-8%	-26%	-2%	-8%	-3%
KPNA2	NM_002266	TRCN0000065312	4%	-20%	-3%	24%	27%
KPNA2	NM_002266	TRCN0000065309	8%	2%	7%	2%	11%
KPNA3	NM_002267	TRCN0000065318	-9%	-35%	-21%	-9%	-12%
KPNA3	NM_002267	TRCN0000065319	9%	-16%	-11%	20%	9%
KPNA3	NM_002267	TRCN0000065320	0%	-28%	-13%	-5%	-6%
KPNA3	NM_002267	TRCN0000065321	0%	-16%	-1%	7%	-9%
KPNA3	NM_002267	TRCN0000065322	1%	-16%	-9%	-6%	-9%
KPNA4	NM_002268	TRCN0000065328	13%	15%	0%	0%	-11%
KPNA4	NM_002268	TRCN0000065329	-17%	-36%	-35%	-11%	-18%
KPNA4	NM_002268	TRCN0000065330	5%	-12%	-1%	-6%	-8%
KPNA4	NM_002268	TRCN0000065331	3%	0%	6%	13%	9%
KPNA4	NM_002268	TRCN0000065332	20%	12%	11%	7%	19%
KPNA5	NM_002269	TRCN0000064943	-9%	-34%	-22%	4%	-4%
KPNA5	NM_002269	TRCN0000064944	-5%	-22%	1%	3%	0%
KPNA5	NM_002269	TRCN0000064945	16%	-4%	-10%	-15%	0%
KPNA5	NM_002269	TRCN0000064946	-1%	-30%	-9%	2%	16%
KPNA5	NM_002269	TRCN0000064947	-8%	-21%	-6%	3%	-3%
KPNA6	NM_012316	TRCN0000065043	-1%	-18%	-7%	-9%	-5%
KPNA6	NM_012316	TRCN0000065044	-5%	-22%	-3%	-3%	-1%
KPNA6	NM_012316	TRCN0000065045	-15%	-36%	-27%	-13%	-10%
KPNA6	NM_012316	TRCN0000065047	24%	0%	-4%	9%	14%
KPNA6	NM_012316	TRCN0000065046	-4%	-3%	4%	9%	13%
KPNB1	NM_002265	TRCN0000123189	1%	-28%	-14%	12%	25%
KPNB1	NM_002265	TRCN0000123190	28%	-3%	-17%	11%	14%
KPNB1	NM_002265	TRCN0000123191	-10%	-32%	-24%	6%	-10%
KPNB1	NM_002265	TRCN0000123192	16%	-11%	-28%	-16%	25%
KPNB1	NM_002265	TRCN0000123193	19%	-14%	2%	13%	3%
NUP107	NM_020401	TRCN0000072478	-9%	-34%	-18%	-1%	-8%
NUP107	NM_020401	TRCN0000072479	-4%	-16%	-8%	-2%	-10%
NUP107	NM_020401	TRCN0000072480	-7%	-25%	-4%	5%	-11%
NUP107	NM_020401	TRCN0000072481	-10%	-26%	-22%	-7%	-2%
NUP107	NM_020401	TRCN0000072482	-10%	-23%	-15%	6%	-11%
NUP153	NM_005124	TRCN0000060243	-1%	10%	17%	15%	32%
NUP153	NM_005124	TRCN0000060244	13%	-9%	-17%	8%	37%
NUP153	NM_005124	TRCN0000060245	9%	4%	0%	0%	5%
NUP153	NM_005124	TRCN0000060246	-4%	-6%	-5%	0%	0%
NUP153	NM_005124	TRCN0000060247	-3%	-3%	-12%	-1%	2%
NUP155	NM_004298	TRCN0000059913	-9%	-21%	-47%	-31%	-21%
NUP155	NM_004298	TRCN0000059914	1%	5%	-2%	-18%	1%
NUP155	NM_004298	TRCN0000059915	5%	-12%	-19%	-5%	-14%
NUP155	NM_004298	TRCN0000059916	0%	0%	-7%	-16%	-10%
NUP155	NM_004298	TRCN0000059917	19%	2%	-18%	-21%	1%
NUP160	XM_113678	TRCN0000060113	2%	-11%	-13%	-1%	1%
NUP160	XM_113678	TRCN0000060114	-5%	-19%	-33%	-6%	4%
NUP160	XM_113678	TRCN0000060115	3%	-4%	-16%	-13%	-8%
NUP160	XM_113678	TRCN0000060116	1%	-23%	-23%	-16%	3%
NUP160	XM_113678	TRCN0000060117	3%	-3%	-20%	10%	7%
NUP205	XM_371954	TRCN0000060023	1%	-23%	-34%	-11%	-9%
NUP205	XM_371954	TRCN0000060024	3%	-8%	-31%	-18%	-11%
NUP205	XM_371954	TRCN0000060025	5%	-7%	-17%	-4%	-4%
NUP205	XM_371954	TRCN0000060027	8%	-10%	-19%	-9%	0%

p65 Nuclear Translocation							
Gene Name	Gene ID	shRNA	SeV 1h	SeV 3h	SeV 5h	SeV 8h	SeV 10h
NUP210	NM_024923	TRCN0000153158	-13%	-22%	-13%	-19%	-13%
NUP210	NM_024923	TRCN0000156619	-11%	-22%	-8%	-6%	-11%
NUP210	NM_024923	TRCN0000157497	-10%	4%	-10%	-11%	-15%
NUP210	NM_024923	TRCN0000152698	-19%	-39%	-33%	-17%	-13%
NUP210	NM_024923	TRCN0000157612	-2%	-10%	12%	-11%	-8%
NUP214	NM_005085	TRCN0000005554	-15%	-21%	-32%	-1%	-10%
NUP214	NM_005085	TRCN0000005555	-1%	-12%	-8%	-17%	-8%
NUP214	NM_005085	TRCN0000005556	-6%	-28%	-25%	-15%	-13%
NUP214	NM_005085	TRCN0000005557	4%	-19%	9%	-9%	-5%
NUP214	NM_005085	TRCN0000005558	3%	-12%	-16%	-6%	-7%
NUP35	NM_138285	TRCN0000072378	11%	-14%	-4%	-6%	-1%
NUP35	NM_138285	TRCN0000072379	-4%	-13%	-16%	-11%	-11%
NUP35	NM_138285	TRCN0000072380	3%	-22%	-7%	-12%	-13%
NUP35	NM_138285	TRCN0000072381	1%	-24%	9%	14%	7%
NUP35	NM_138285	TRCN0000072382	9%	-18%	1%	3%	-2%
NUP37	NM_024057	TRCN0000152222	-16%	-20%	-16%	-3%	-2%
NUP37	NM_024057	TRCN0000153319	-14%	-13%	-9%	-8%	-11%
NUP37	NM_024057	TRCN0000151312	26%	13%	12%	28%	34%
NUP37	NM_024057	TRCN0000151233	-7%	-20%	-16%	-6%	-5%
NUP37	NM_024057	TRCN0000156008	-10%	-19%	-9%	-11%	-9%
NUP43	NM_024647	TRCN0000134871	-5%	-16%	-1%	4%	-4%
NUP43	NM_024647	TRCN0000134068	15%	-8%	-11%	2%	-5%
NUP43	NM_024647	TRCN0000133881	-10%	-27%	-15%	-7%	-7%
NUP43	NM_024647	TRCN0000137797	-7%	-30%	-15%	5%	1%
NUP43	NM_024647	TRCN0000137417	14%	-2%	0%	23%	12%
NUP50	NM_007172	TRCN0000158766	-8%	-17%	-10%	0%	-1%
NUP50	NM_007172	TRCN0000159335	-9%	-9%	-11%	-9%	-5%
NUP50	NM_007172	TRCN0000158499	-8%	-15%	0%	3%	1%
NUP50	NM_007172	TRCN0000160160	-5%	-8%	-7%	-3%	1%
NUP54	NM_017426	TRCN0000059903	2%	-19%	-32%	-13%	2%
NUP54	NM_017426	TRCN0000059904	15%	-1%	0%	-17%	-2%
NUP54	NM_017426	TRCN0000059905	37%	21%	7%	32%	33%
NUP54	NM_017426	TRCN0000059906	-4%	-18%	-29%	4%	10%
NUP54	NM_017426	TRCN0000059907	3%	-16%	-14%	-8%	-9%
NUP62	NM_012346	TRCN0000059288	15%	2%	1%	-12%	27%
NUP62	NM_012346	TRCN0000059289	2%	-4%	-22%	12%	-11%
NUP62	NM_012346	TRCN0000059290	1%	5%	-25%	-24%	-13%
NUP62	NM_012346	TRCN0000059291	18%	9%	-2%	7%	-4%
NUP62	NM_012346	TRCN0000059292	-6%	-13%	-43%	-25%	-18%
NUP88	NM_002532	TRCN0000141654	-4%	-24%	-11%	-1%	-9%
NUP88	NM_002532	TRCN0000142510	12%	-11%	4%	7%	-5%
NUP88	NM_002532	TRCN0000139972	-3%	-11%	-4%	1%	-11%
NUP88	NM_002532	TRCN0000145079	0%	-19%	-10%	16%	-5%
NUP88	NM_002532	TRCN0000145530	10%	-13%	-5%	5%	3%
NUP93	NM_014669	TRCN0000059958	16%	5%	-12%	-10%	-5%
NUP93	NM_014669	TRCN0000059959	1%	-12%	-15%	-25%	4%
NUP93	NM_014669	TRCN0000059960	-3%	-1%	-17%	0%	-11%
NUP93	NM_014669	TRCN0000059961	9%	-11%	-33%	-16%	-11%
NUP93	NM_014669	TRCN0000059962	-1%	-18%	-29%	-23%	-14%
NUP98	NM_005387	TRCN0000046913	-1%	-6%	-2%	-2%	2%
NUP98	NM_005387	TRCN0000046914	3%	-8%	-9%	9%	15%
NUP98	NM_005387	TRCN0000046915	-1%	-4%	-7%	7%	19%
NUP98	NM_005387	TRCN0000046916	27%	16%	22%	26%	28%
NUP98	NM_005387	TRCN0000046917	-8%	-10%	-14%	10%	-2%

p65 Nuclear Translocation							
Gene Name	Gene ID	shRNA	SeV 1h	SeV 3h	SeV 5h	SeV 8h	SeV 10h
NUPL1	NM_014089	TRCN0000013513	-3%	-19%	-20%	-7%	-15%
NUPL1	NM_014089	TRCN0000013514	1%	-15%	-11%	-12%	-10%
NUPL1	NM_014089	TRCN0000013515	-4%	-9%	-8%	-13%	-8%
NUPL1	NM_014089	TRCN0000013516	-24%	-38%	-56%	-44%	-33%
NUPL1	NM_014089	TRCN0000013517	2%	1%	-5%	8%	5%
NUPL2	NM_007342	TRCN0000128180	-5%	-12%	-12%	7%	-19%
NUPL2	NM_007342	TRCN0000130187	1%	-13%	0%	26%	-1%
NUPL2	NM_007342	TRCN0000129199	-3%	-3%	-9%	-5%	-11%
NUPL2	NM_007342	TRCN0000130430	15%	10%	-16%	-6%	27%
NUPL2	NM_007342	TRCN0000129028	12%	-14%	-13%	14%	15%
NUTF2	NM_005796	TRCN0000038549	1%	-17%	-27%	-30%	-26%
NUTF2	NM_005796	TRCN0000038550	-11%	-8%	-38%	-33%	-24%
NUTF2	NM_005796	TRCN0000038551	-7%	-20%	-29%	-18%	-10%
NUTF2	NM_005796	TRCN0000038552	2%	9%	-3%	-1%	-4%
NUTF2	NM_005796	TRCN0000038553	-2%	-16%	-10%	-11%	-9%
NXF1	NM_006362	TRCN0000007580	3%	5%	7%	-6%	5%
NXF1	NM_006362	TRCN0000007581	8%	-15%	-31%	-7%	-2%
NXF1	NM_006362	TRCN0000007582	6%	-3%	9%	17%	12%
NXF1	NM_006362	TRCN0000007583	22%	2%	-7%	-15%	34%
NXF1	NM_006362	TRCN0000011092	-7%	-23%	2%	-24%	-9%
NXF2	NM_017809	TRCN0000059293	-2%	-4%	-25%	-24%	-20%
NXF2	NM_017809	TRCN0000059294	1%	-1%	-18%	-24%	-18%
NXF2	NM_017809	TRCN0000059296	5%	2%	0%	3%	0%
NXF2	NM_017809	TRCN0000059297	18%	-1%	9%	8%	16%
NXF3	NM_022052	TRCN0000060323	5%	5%	1%	11%	16%
NXF3	NM_022052	TRCN0000060324	1%	-8%	-4%	6%	11%
NXF3	NM_022052	TRCN0000060325	14%	15%	-1%	-6%	2%
NXF3	NM_022052	TRCN0000060326	1%	2%	-14%	-13%	-16%
NXF3	NM_022052	TRCN0000060327	-6%	-7%	-12%	-21%	-18%
NXT1	NM_013248	TRCN0000148803	-24%	-47%	-59%	-45%	-23%
NXT1	NM_013248	TRCN0000148689	-15%	-23%	-11%	-3%	-19%
NXT1	NM_013248	TRCN0000147131	-15%	-26%	-18%	-14%	-10%
NXT1	NM_013248	TRCN0000146408	-6%	-19%	-1%	3%	-2%
NXT1	NM_013248	TRCN0000149160	-12%	-27%	-25%	-34%	-24%
NXT2	NM_018698	TRCN0000038574	2%	-18%	-12%	-3%	-2%
NXT2	NM_018698	TRCN0000038575	-5%	-22%	-7%	2%	-5%
NXT2	NM_018698	TRCN0000038576	-10%	-14%	-16%	-25%	-5%
NXT2	NM_018698	TRCN0000038577	-12%	-27%	-19%	-9%	-12%
NXT2	NM_018698	TRCN0000038578	6%	-3%	-10%	10%	13%
POM121	NM_172020	TRCN0000060068	-2%	-14%	-21%	-7%	-6%
POM121	NM_172020	TRCN0000060069	-3%	-8%	-24%	-11%	-1%
POM121	NM_172020	TRCN0000060070	-1%	1%	-11%	17%	9%
POM121	NM_172020	TRCN0000060071	-2%	-17%	-26%	-9%	-6%
RAN	NM_006325	TRCN000047929	0%	-23%	-34%	-19%	-10%
RAN	NM_006325	TRCN000047929	-2%	-2%	-24%	-11%	2%
RANBP2	NM_006267	TRCN0000003450	0%	-17%	-19%	-26%	-16%
RANBP2	NM_006267	TRCN0000003451	29%	-2%	11%	21%	35%
RANBP2	NM_006267	TRCN0000003452	-14%	-26%	-3%	-16%	-9%
RANBP2	NM_006267	TRCN0000003453	4%	1%	-5%	4%	0%
RANBP2	NM_006267	TRCN0000003454	-10%	-27%	-22%	-6%	14%
RANBP3	NM_003624	TRCN0000073003	-1%	-28%	-12%	-4%	-6%
RANBP3	NM_003624	TRCN0000073004	-3%	-30%	-11%	2%	-13%
RANBP3	NM_003624	TRCN0000073005	9%	-18%	-5%	-4%	-9%
RANBP3	NM_003624	TRCN0000073006	26%	0%	10%	31%	19%
RANBP3	NM_003624	TRCN0000073007	0%	-7%	-6%	4%	-4%
RANBP5	NM_002271	TRCN0000150535	-15%	-13%	-8%	-21%	-18%
RANBP5	NM_002271	TRCN0000153065	3%	16%	-7%	9%	-2%
RANBP5	NM_002271	TRCN0000152684	4%	-5%	21%	28%	24%
RANBP5	NM_002271	TRCN0000152127	-16%	-25%	-15%	-8%	-9%
RANBP5	NM_002271	TRCN0000151824	8%	-12%	4%	0%	9%

p65 Nuclear Translocation								
Gene Name	Gene ID	shRNA		SeV 1h	SeV 3h	SeV 5h	SeV 8h	SeV 10h
RANBP6	NM_012416	TRCN0000148876		-8%	-21%	-7%	-10%	-10%
RANBP6	NM_012416	TRCN0000146440		-20%	-44%	-54%	-26%	-25%
RANBP6	NM_012416	TRCN0000147280		-1%	0%	9%	3%	11%
RANBP6	NM_012416	TRCN0000148942		-13%	-21%	-10%	-10%	-19%
RANBP6	NM_012416	TRCN0000149838		-5%	-20%	-10%	-22%	-12%
RANGAP1	NM_002883	TRCN0000047328		-7%	-4%	-9%	8%	21%
RANGAP1	NM_002883	TRCN0000047329		3%	-3%	-16%	14%	1%
RANGAP1	NM_002883	TRCN0000047330		2%	1%	-16%	11%	-4%
RANGAP1	NM_002883	TRCN0000047331		-9%	-12%	-8%	14%	5%
RANGAP1	NM_002883	TRCN0000047332		-5%	-20%	-1%	1%	5%
RCC1	NM_001269	TRCN0000157236		-13%	-27%	-20%	-14%	-14%
RCC1	NM_001269	TRCN0000151199		-12%	-21%	-3%	-8%	-1%
RCC1	NM_001269	TRCN0000157685		-18%	-33%	-32%	-12%	-1%
RCC1	NM_001269	TRCN0000157981		-7%	-17%	-8%	-9%	4%
RCC1	NM_001269	TRCN0000152440		-11%	-27%	-27%	-24%	-22%
RCC2	NM_018715	TRCN0000150578		-4%	-3%	-5%	-19%	-1%
RCC2	NM_018715	TRCN0000154474		-9%	-3%	-12%	-19%	-11%
RCC2	NM_018715	TRCN0000154827		-11%	-18%	-9%	-25%	-15%
RCC2	NM_018715	TRCN0000153686		-2%	-8%	-15%	-2%	-1%
RCC2	NM_018715	TRCN0000151164		-14%	-28%	-25%	-6%	-11%
RGPD4	NM_182588	TRCN0000017738		7%	-10%	-14%	-26%	-19%
RGPD4	NM_182588	TRCN0000017739		9%	-2%	-6%	-8%	-9%
RGPD4	NM_182588	TRCN0000017740		48%	10%	15%	32%	28%
RGPD4	NM_182588	TRCN0000017741		-8%	-24%	-27%	-13%	-12%
RGPD4	NM_182588	TRCN0000017742		-3%	-25%	-29%	-21%	-19%
RNUT1	NM_005701	TRCN0000038569		-13%	-28%	-41%	-29%	-19%
RNUT1	NM_005701	TRCN0000038570		-1%	4%	-2%	-10%	-5%
RNUT1	NM_005701	TRCN0000038571		3%	7%	22%	27%	33%
RNUT1	NM_005701	TRCN0000038572		9%	-7%	-7%	-3%	1%
RNUT1	NM_005701	TRCN0000038573		1%	-10%	-9%	-8%	-5%
TNPO1	NM_002270	TRCN0000038284		9%	-12%	-7%	-4%	-6%
TNPO1	NM_002270	TRCN0000038285		-15%	-27%	-51%	-24%	-24%
TNPO1	NM_002270	TRCN0000038286		-4%	-18%	-4%	1%	-14%
TNPO1	NM_002270	TRCN0000038287		-8%	-16%	-18%	-4%	-14%
TNPO1	NM_002270	TRCN0000038288		-1%	-17%	-13%	-16%	-14%
TNPO2	NM_013433	TRCN0000043468		32%	13%	4%	20%	29%
TNPO2	NM_013433	TRCN0000043469		-4%	-4%	11%	19%	21%
TNPO2	NM_013433	TRCN0000043470		-2%	-10%	-11%	18%	36%
TNPO2	NM_013433	TRCN0000043471		-1%	-13%	-8%	11%	-1%
TNPO2	NM_013433	TRCN0000043472		-2%	12%	10%	6%	2%
TNPO3	NM_012470	TRCN0000038329		1%	-12%	-7%	1%	-2%
TNPO3	NM_012470	TRCN0000038330		8%	-4%	-4%	4%	-3%
TNPO3	NM_012470	TRCN0000038331		9%	-11%	-2%	11%	1%
TNPO3	NM_012470	TRCN0000038333		-5%	-25%	-13%	1%	14%
TNPO3	NM_012470	TRCN0000038332		2%	2%	15%	6%	1%
TPR	NM_003292	TRCN0000060063		14%	10%	1%	0%	18%
TPR	NM_003292	TRCN0000060064		-12%	-29%	-35%	-15%	-1%
TPR	NM_003292	TRCN0000060065		10%	11%	-1%	-15%	4%
TPR	NM_003292	TRCN0000060066		7%	5%	-7%	9%	12%
TPR	NM_003292	TRCN0000060067		27%	9%	-5%	3%	21%
XPO1	NM_003400	TRCN000154386		27%	18%	20%	35%	35%
XPO1	NM_003400	TRCN000154386		42%	20%	9%	19%	39%
XPO4	NM_022459	TRCN0000159557		-3%	-9%	-4%	-4%	-3%
XPO4	NM_022459	TRCN0000159095		-15%	-37%	-37%	-34%	-24%
XPO4	NM_022459	TRCN0000160271		4%	1%	-2%	9%	24%
XPO4	NM_022459	TRCN0000159918		-15%	-34%	-20%	7%	6%
XPO4	NM_022459	TRCN0000159748		-5%	-5%	5%	-1%	-8%

Table S3. Effect of Silencing Nucleoporins and Nucleocytoplasmic Transporters on IRF3 and p65 Nuclear Translocation

This table contains the results of the RNAi screen of the 60 Nucleoporins and nucleocytoplasmic transporters and their effect on the nuclear translocation of IRF3 and p65 during a 10-hour SeV infection time course. Non-target (NT) values are in absolute percentages, while all other values are presented in relative percentage.

p*IFNB1* Inhibition				
Gene Name	**Gene ID**	**shRNA**	**n=1**	**n=2**
CSE1L	NM_001316	TRCN0000061790	76%	35%
DDX19A	NM_018332	TRCN0000050218	12%	35%
DDX19A	NM_018332	TRCN0000050219	8%	38%
DDX19A	NM_018332	TRCN0000050220	93%	79%
DDX19A	NM_018332	TRCN0000050221	82%	66%
DDX19A	NM_018332	TRCN0000050222	63%	42%
DDX19B	NM_007242	TRCN0000051128	87%	67%
DDX19B	NM_007242	TRCN0000051129	83%	71%
DDX19B	NM_007242	TRCN0000051130	22%	-31%
DDX19B	NM_007242	TRCN0000051131	64%	31%
DDX19B	NM_007242	TRCN0000051132	64%	56%
GLE1L	NM_001499	TRCN0000077938	76%	54%
GLE1L	NM_001499	TRCN0000077939	57%	6%
GLE1L	NM_001499	TRCN0000077940	26%	-18%
GLE1L	NM_001499	TRCN0000077941	88%	81%
GLE1L	NM_001499	TRCN0000077942	77%	29%
HRB	NM_004504	TRCN0000060223	-190%	-174%
HRB	NM_004504	TRCN0000060224	75%	63%
HRB	NM_004504	TRCN0000060225	73%	49%
HRB	NM_004504	TRCN0000060226	87%	77%
HRB	NM_004504	TRCN0000060227	53%	22%
HRBL	NM_006076	TRCN0000146397	65%	55%
HRBL	NM_006076	TRCN0000147372	34%	3%
HRBL	NM_006076	TRCN0000148766	91%	74%
HRBL	NM_006076	TRCN0000149837	40%	-16%
IPO11	NM_016338	TRCN0000158471	30%	-17%
IPO11	NM_016338	TRCN0000158885	40%	-8%
IPO11	NM_016338	TRCN0000159422	65%	58%
IPO11	NM_016338	TRCN0000160347	-5%	-41%
IPO4	NM_024658	TRCN0000072488	69%	54%
IPO4	NM_024658	TRCN0000072489	-88%	-83%
IPO4	NM_024658	TRCN0000072491	63%	9%
IPO4	NM_024658	TRCN0000072492	44%	-26%
IPO7	NM_006391	TRCN0000150676	72%	53%
IPO7	NM_006391	TRCN0000151374	94%	94%
IPO7	NM_006391	TRCN0000155501	45%	25%
IPO7	NM_006391	TRCN0000156655	81%	65%
IPO7	NM_006391	TRCN0000156994	48%	20%

p*IFNB1* Inhibition					
Gene Name	**Gene ID**	**shRNA**		**n=1**	**n=2**
IPO8	NM_006390	TRCN0000150605		55%	32%
IPO8	NM_006390	TRCN0000151987		65%	55%
IPO8	NM_006390	TRCN0000156073		58%	40%
IPO8	NM_006390	TRCN0000156712		82%	75%
IPO8	NM_006390	TRCN0000156852		83%	83%
KPNA1	NM_002264	TRCN0000065298		-38%	-90%
KPNA1	NM_002264	TRCN0000065299		37%	63%
KPNA1	NM_002264	TRCN0000065300		79%	68%
KPNA1	NM_002264	TRCN0000065301		23%	18%
KPNA1	NM_002264	TRCN0000065302		58%	59%
KPNA2	NM_002266	TRCN0000065308		37%	28%
KPNA2	NM_002266	TRCN0000065309		70%	73%
KPNA2	NM_002266	TRCN0000065310		52%	20%
KPNA2	NM_002266	TRCN0000065311		41%	69%
KPNA2	NM_002266	TRCN0000065312		80%	55%
KPNA3	NM_002267	TRCN0000065318		78%	61%
KPNA3	NM_002267	TRCN0000065319		86%	76%
KPNA3	NM_002267	TRCN0000065320		30%	-32%
KPNA3	NM_002267	TRCN0000065321		36%	-25%
KPNA3	NM_002267	TRCN0000065322		55%	26%
KPNA4	NM_002268	TRCN0000065328		23%	-24%
KPNA4	NM_002268	TRCN0000065329		85%	74%
KPNA4	NM_002268	TRCN0000065330		43%	31%
KPNA4	NM_002268	TRCN0000065331		37%	48%
KPNA4	NM_002268	TRCN0000065332		10%	-14%
KPNA5	NM_002269	TRCN0000064943		51%	57%
KPNA5	NM_002269	TRCN0000064944		50%	34%
KPNA5	NM_002269	TRCN0000064945		69%	22%
KPNA5	NM_002269	TRCN0000064946		65%	37%
KPNA5	NM_002269	TRCN0000064947		76%	84%
KPNA6	NM_012316	TRCN0000065043		35%	5%
KPNA6	NM_012316	TRCN0000065044		36%	14%
KPNA6	NM_012316	TRCN0000065045		79%	78%
KPNA6	NM_012316	TRCN0000065046		54%	73%
KPNA6	NM_012316	TRCN0000065047		55%	23%
KPNB1	NM_002265	TRCN0000123189		84%	90%
KPNB1	NM_002265	TRCN0000123190		76%	53%
KPNB1	NM_002265	TRCN0000123191		64%	21%
KPNB1	NM_002265	TRCN0000123192		98%	97%
KPNB1	NM_002265	TRCN0000123193		26%	60%

p*IFNB1* Inhibition				
Gene Name	**Gene ID**	**shRNA**	**n=1**	**n=2**
NUP107	NM_020401	TRCN0000072478	66%	31%
NUP107	NM_020401	TRCN0000072479	-7%	-32%
NUP107	NM_020401	TRCN0000072480	63%	48%
NUP107	NM_020401	TRCN0000072481	35%	25%
NUP107	NM_020401	TRCN0000072482	73%	69%
NUP153	NM_005124	TRCN0000060243	48%	43%
NUP153	NM_005124	TRCN0000060244	76%	77%
NUP153	NM_005124	TRCN0000060245	9%	-26%
NUP153	NM_005124	TRCN0000060246	42%	27%
NUP153	NM_005124	TRCN0000060247	59%	44%
NUP155	NM_004298	TRCN0000059913	92%	78%
NUP155	NM_004298	TRCN0000059914	63%	42%
NUP155	NM_004298	TRCN0000059915	51%	73%
NUP155	NM_004298	TRCN0000059916	-3%	-54%
NUP155	NM_004298	TRCN0000059917	5%	-29%
NUP160	XM_113678	TRCN0000060113	68%	71%
NUP160	XM_113678	TRCN0000060114	76%	52%
NUP160	XM_113678	TRCN0000060115	76%	40%
NUP160	XM_113678	TRCN0000060116	84%	72%
NUP160	XM_113678	TRCN0000060117	43%	-21%
NUP205	XM_371954	TRCN0000060023	71%	66%
NUP205	XM_371954	TRCN0000060024	72%	71%
NUP205	XM_371954	TRCN0000060025	65%	52%
NUP205	XM_371954	TRCN0000060027	14%	-19%
NUP210	NM_024923	TRCN0000152698	83%	89%
NUP210	NM_024923	TRCN0000153158	-3%	-16%
NUP210	NM_024923	TRCN0000156619	79%	61%
NUP210	NM_024923	TRCN0000157497	52%	29%
NUP210	NM_024923	TRCN0000157612	87%	85%
NUP214	NM_005085	TRCN0000005554	59%	41%
NUP214	NM_005085	TRCN0000005555	52%	13%
NUP214	NM_005085	TRCN0000005556	81%	77%
NUP214	NM_005085	TRCN0000005557	57%	59%
NUP214	NM_005085	TRCN0000005558	46%	-8%
NUP35	NM_138285	TRCN0000072378	45%	23%
NUP35	NM_138285	TRCN0000072379	52%	16%
NUP35	NM_138285	TRCN0000072380	48%	28%
NUP35	NM_138285	TRCN0000072381	88%	73%
NUP35	NM_138285	TRCN0000072382	56%	12%

p*IFNB1* Inhibition					
Gene Name	**Gene ID**	**shRNA**		**n=1**	**n=2**
NUP37	NM_024057	TRCN0000151233		54%	38%
NUP37	NM_024057	TRCN0000151312		62%	71%
NUP37	NM_024057	TRCN0000152222		69%	62%
NUP37	NM_024057	TRCN0000153319		54%	46%
NUP37	NM_024057	TRCN0000156008		34%	44%
NUP43	NM_024647	TRCN0000133881		51%	20%
NUP43	NM_024647	TRCN0000134068		61%	67%
NUP43	NM_024647	TRCN0000134871		60%	28%
NUP43	NM_024647	TRCN0000137417		27%	70%
NUP43	NM_024647	TRCN0000137797		41%	18%
NUP50	NM_007172	TRCN0000158499		60%	27%
NUP50	NM_007172	TRCN0000158766		56%	5%
NUP50	NM_007172	TRCN0000159335		47%	22%
NUP50	NM_007172	TRCN0000160160		33%	12%
NUP54	NM_017426	TRCN0000059903		83%	72%
NUP54	NM_017426	TRCN0000059904		-23%	-62%
NUP54	NM_017426	TRCN0000059905		46%	-2%
NUP54	NM_017426	TRCN0000059906		80%	83%
NUP54	NM_017426	TRCN0000059907		26%	-1%
NUP62	NM_012346	TRCN0000059288		62%	58%
NUP62	NM_012346	TRCN0000059289		7%	-12%
NUP62	NM_012346	TRCN0000059290		42%	30%
NUP62	NM_012346	TRCN0000059291		63%	50%
NUP62	NM_012346	TRCN0000059292		61%	36%
NUP88	NM_002532	TRCN0000139972		61%	-37%
NUP88	NM_002532	TRCN0000141654		90%	82%
NUP88	NM_002532	TRCN0000142510		27%	-29%
NUP88	NM_002532	TRCN0000145079		76%	49%
NUP88	NM_002532	TRCN0000145530		60%	16%
NUP93	NM_014669	TRCN0000059958		44%	-24%
NUP93	NM_014669	TRCN0000059959		73%	50%
NUP93	NM_014669	TRCN0000059960		52%	26%
NUP93	NM_014669	TRCN0000059961		95%	89%
NUP93	NM_014669	TRCN0000059962		69%	37%
NUP98	NM_005387	TRCN0000046913		63%	55%
NUP98	NM_005387	TRCN0000046914		86%	78%
NUP98	NM_005387	TRCN0000046915		61%	78%
NUP98	NM_005387	TRCN0000046916		74%	50%
NUP98	NM_005387	TRCN0000046917		61%	53%

p*IFNB1* Inhibition					
Gene Name	**Gene ID**	**shRNA**		**n=1**	**n=2**
NUPL1	NM_014089	TRCN0000013513		62%	53%
NUPL1	NM_014089	TRCN0000013514		83%	61%
NUPL1	NM_014089	TRCN0000013515		68%	19%
NUPL1	NM_014089	TRCN0000013516		93%	90%
NUPL1	NM_014089	TRCN0000013517		85%	83%
NUPL2	NM_007342	TRCN0000128180		60%	35%
NUPL2	NM_007342	TRCN0000129028		90%	83%
NUPL2	NM_007342	TRCN0000129199		6%	-76%
NUPL2	NM_007342	TRCN0000130187		49%	24%
NUPL2	NM_007342	TRCN0000130430		98%	96%
NUTF2	NM_005796	TRCN0000038549		80%	57%
NUTF2	NM_005796	TRCN0000038550		59%	33%
NUTF2	NM_005796	TRCN0000038551		77%	58%
NUTF2	NM_005796	TRCN0000038552		46%	27%
NUTF2	NM_005796	TRCN0000038553		37%	5%
NXF1	NM_006362	TRCN0000007580		19%	-10%
NXF1	NM_006362	TRCN0000007581		99%	98%
NXF1	NM_006362	TRCN0000007582		88%	76%
NXF1	NM_006362	TRCN0000007583		93%	87%
NXF1	NM_006362	TRCN0000011092		99%	98%
NXF2	NM_017809	TRCN0000059293		-16%	-40%
NXF2	NM_017809	TRCN0000059294		13%	-12%
NXF2	NM_017809	TRCN0000059296		33%	16%
NXF2	NM_017809	TRCN0000059297		56%	57%
NXF3	NM_022052	TRCN0000060323		-3%	42%
NXF3	NM_022052	TRCN0000060324		33%	17%
NXF3	NM_022052	TRCN0000060325		34%	1%
NXF3	NM_022052	TRCN0000060326		60%	-1%
NXF3	NM_022052	TRCN0000060327		32%	17%
NXT1	NM_013248	TRCN0000146408		84%	71%
NXT1	NM_013248	TRCN0000147131		67%	45%
NXT1	NM_013248	TRCN0000148689		80%	69%
NXT1	NM_013248	TRCN0000148803		97%	97%
NXT1	NM_013248	TRCN0000149160		58%	26%
NXT2	NM_018698	TRCN0000038574		37%	15%
NXT2	NM_018698	TRCN0000038575		74%	59%
NXT2	NM_018698	TRCN0000038576		24%	-16%
NXT2	NM_018698	TRCN0000038577		64%	-18%
NXT2	NM_018698	TRCN0000038578		79%	89%

p*IFNB1* Inhibition					
Gene Name	**Gene ID**	**shRNA**		**n=1**	**n=2**
POM121	NM_172020	TRCN0000060068		62%	26%
POM121	NM_172020	TRCN0000060069		48%	-32%
POM121	NM_172020	TRCN0000060070		74%	61%
POM121	NM_172020	TRCN0000060071		91%	92%
RAN	NM_006325	TRCN000047929		64%	75%
RANBP2	NM_006267	TRCN0000003450		17%	-35%
RANBP2	NM_006267	TRCN0000003451		73%	80%
RANBP2	NM_006267	TRCN0000003452		48%	71%
RANBP2	NM_006267	TRCN0000003453		46%	23%
RANBP2	NM_006267	TRCN0000003454		73%	82%
RANBP3	NM_003624	TRCN0000073003		43%	-20%
RANBP3	NM_003624	TRCN0000073004		59%	-19%
RANBP3	NM_003624	TRCN0000073005		24%	-61%
RANBP3	NM_003624	TRCN0000073006		64%	70%
RANBP3	NM_003624	TRCN0000073007		81%	43%
RANBP5	NM_002271	TRCN0000150535		9%	39%
RANBP5	NM_002271	TRCN0000151824		71%	72%
RANBP5	NM_002271	TRCN0000152127		43%	38%
RANBP5	NM_002271	TRCN0000152684		64%	81%
RANBP5	NM_002271	TRCN0000153065		93%	92%
RANBP6	NM_012416	TRCN0000146440		92%	85%
RANBP6	NM_012416	TRCN0000147280		42%	40%
RANBP6	NM_012416	TRCN0000148876		42%	21%
RANBP6	NM_012416	TRCN0000148942		36%	-40%
RANBP6	NM_012416	TRCN0000149838		48%	43%
RANGAP1	NM_002883	TRCN0000047328		6%	11%
RANGAP1	NM_002883	TRCN0000047329		20%	47%
RANGAP1	NM_002883	TRCN0000047330		5%	37%
RANGAP1	NM_002883	TRCN0000047331		57%	41%
RANGAP1	NM_002883	TRCN0000047332		35%	11%
RCC1	NM_001269	TRCN0000151199		44%	31%
RCC1	NM_001269	TRCN0000152440		89%	80%
RCC1	NM_001269	TRCN0000157236		69%	46%
RCC1	NM_001269	TRCN0000157685		77%	66%
RCC1	NM_001269	TRCN0000157981		81%	46%
RCC2	NM_018715	TRCN0000150578		-47%	-90%
RCC2	NM_018715	TRCN0000151164		80%	68%
RCC2	NM_018715	TRCN0000153686		68%	59%
RCC2	NM_018715	TRCN0000154474		52%	40%
RCC2	NM_018715	TRCN0000154827		34%	18%

p*IFNB1* Inhibition					
Gene Name	**Gene ID**	**shRNA**		**n=1**	**n=2**
RGPD4	NM_182588	TRCN0000017738		59%	57%
RGPD4	NM_182588	TRCN0000017739		41%	12%
RGPD4	NM_182588	TRCN0000017740		68%	51%
RGPD4	NM_182588	TRCN0000017741		59%	35%
RGPD4	NM_182588	TRCN0000017742		85%	76%
RNUT1	NM_005701	TRCN0000038569		87%	85%
RNUT1	NM_005701	TRCN0000038570		49%	39%
RNUT1	NM_005701	TRCN0000038571		72%	64%
RNUT1	NM_005701	TRCN0000038572		37%	-6%
RNUT1	NM_005701	TRCN0000038573		36%	-1%
TNPO1	NM_002270	TRCN0000038284		82%	67%
TNPO1	NM_002270	TRCN0000038285		94%	91%
TNPO1	NM_002270	TRCN0000038286		82%	70%
TNPO1	NM_002270	TRCN0000038287		49%	9%
TNPO1	NM_002270	TRCN0000038288		76%	77%
TNPO2	NM_013433	TRCN0000043468		82%	57%
TNPO2	NM_013433	TRCN0000043469		47%	-13%
TNPO2	NM_013433	TRCN0000043470		85%	87%
TNPO2	NM_013433	TRCN0000043471		93%	85%
TNPO2	NM_013433	TRCN0000043472		8%	14%
TNPO3	NM_012470	TRCN0000038329		47%	-7%
TNPO3	NM_012470	TRCN0000038330		73%	63%
TNPO3	NM_012470	TRCN0000038331		56%	11%
TNPO3	NM_012470	TRCN0000038332		30%	-4%
TNPO3	NM_012470	TRCN0000038333		84%	77%
TPR	NM_003292	TRCN0000060063		61%	61%
TPR	NM_003292	TRCN0000060064		82%	52%
TPR	NM_003292	TRCN0000060065		71%	57%
TPR	NM_003292	TRCN0000060066		65%	57%
TPR	NM_003292	TRCN0000060067		58%	32%
XPO1	NM_003400	TRCN000154386		67%	65%
XPO4	NM_022459	TRCN0000159095		88%	75%
XPO4	NM_022459	TRCN0000159557		49%	28%
XPO4	NM_022459	TRCN0000159748		37%	3%
XPO4	NM_022459	TRCN0000159918		67%	46%
XPO4	NM_022459	TRCN0000160271		23%	7%

Cell Survival							
Gene Name	Gene ID	shRNA	SeV 1h	SeV 3h	SeV 5h	SeV 8h	SeV 10h
DDX19A	NM_018332	TRCN0000050218	78%	65%	61%	49%	45%
DDX19A	NM_018332	TRCN0000050219	111%	87%	110%	76%	97%
DDX19A	NM_018332	TRCN0000050220	81%	80%	86%	88%	86%
DDX19A	NM_018332	TRCN0000050221	62%	53%	31%	27%	37%
DDX19A	NM_018332	TRCN0000050222	83%	76%	97%	96%	112%
DDX19B	NM_007242	TRCN0000051128	44%	46%	59%	89%	74%
DDX19B	NM_007242	TRCN0000051129	66%	57%	57%	41%	50%
DDX19B	NM_007242	TRCN0000051130	107%	108%	116%	129%	140%
DDX19B	NM_007242	TRCN0000051131	146%	136%	137%	144%	158%
DDX19B	NM_007242	TRCN0000051132	40%	28%	34%	46%	40%
GLE1L	NM_001499	TRCN0000077938	69%	63%	69%	64%	44%
GLE1L	NM_001499	TRCN0000077939	94%	79%	84%	98%	62%
GLE1L	NM_001499	TRCN0000077940	90%	111%	145%	155%	107%
GLE1L	NM_001499	TRCN0000077941	83%	70%	73%	56%	39%
GLE1L	NM_001499	TRCN0000077942	103%	131%	170%	152%	113%
HRB	NM_004504	TRCN0000060223	98%	104%	112%	123%	146%
HRB	NM_004504	TRCN0000060224	104%	99%	92%	94%	78%
HRB	NM_004504	TRCN0000060225	80%	82%	80%	76%	86%
HRB	NM_004504	TRCN0000060226	46%	40%	24%	9%	13%
HRB	NM_004504	TRCN0000060227	93%	96%	72%	40%	45%
HRBL	NM_006076	TRCN0000149837	81%	59%	45%	31%	30%
HRBL	NM_006076	TRCN0000148766	82%	62%	40%	22%	17%
HRBL	NM_006076	TRCN0000146397	65%	50%	39%	17%	17%
HRBL	NM_006076	TRCN0000147372	104%	96%	87%	89%	74%
IPO11	NM_016338	TRCN0000159422	112%	102%	117%	136%	109%
IPO11	NM_016338	TRCN0000160347	144%	157%	181%	197%	161%
IPO11	NM_016338	TRCN0000158471	126%	128%	144%	161%	140%
IPO11	NM_016338	TRCN0000158885	71%	76%	53%	48%	38%
IPO4	NM_024658	TRCN0000072488	99%	74%	88%	84%	60%
IPO4	NM_024658	TRCN0000072489	78%	93%	96%	106%	91%
IPO4	NM_024658	TRCN0000072491	64%	77%	93%	95%	61%
IPO4	NM_024658	TRCN0000072492	86%	90%	103%	105%	81%
IPO7	NM_006391	TRCN0000156655	91%	86%	97%	91%	76%
IPO7	NM_006391	TRCN0000150676	75%	75%	85%	101%	106%
IPO7	NM_006391	TRCN0000156994	69%	72%	65%	87%	69%
IPO7	NM_006391	TRCN0000151374	87%	101%	92%	112%	73%
IPO7	NM_006391	TRCN0000155501	97%	118%	94%	102%	76%
IPO8	NM_006390	TRCN0000156712	63%	60%	68%	62%	58%
IPO8	NM_006390	TRCN0000151987	87%	95%	103%	96%	76%
IPO8	NM_006390	TRCN0000156852	97%	91%	93%	86%	79%
IPO8	NM_006390	TRCN0000156073	92%	89%	101%	99%	78%
IPO8	NM_006390	TRCN0000150605	84%	90%	86%	76%	51%
KPNA1	NM_002264	TRCN0000065298	115%	118%	150%	161%	141%
KPNA1	NM_002264	TRCN0000065299	53%	71%	83%	97%	74%
KPNA1	NM_002264	TRCN0000065300	58%	48%	57%	42%	37%
KPNA1	NM_002264	TRCN0000065301	97%	101%	138%	124%	104%
KPNA1	NM_002264	TRCN0000065302	93%	81%	97%	110%	66%
KPNA2	NM_002266	TRCN0000065308	103%	107%	135%	113%	97%
KPNA2	NM_002266	TRCN0000065310	111%	98%	113%	108%	89%
KPNA2	NM_002266	TRCN0000065311	80%	79%	106%	93%	68%
KPNA2	NM_002266	TRCN0000065312	28%	26%	41%	36%	23%
KPNA2	NM_002266	TRCN0000065309	94%	90%	78%	79%	72%

Cell Survival							
Gene Name	Gene ID	shRNA	SeV 1h	SeV 3h	SeV 5h	SeV 8h	SeV 10h
KPNA3	NM_002267	TRCN0000065318	93%	109%	148%	151%	104%
KPNA3	NM_002267	TRCN0000065319	73%	83%	101%	81%	63%
KPNA3	NM_002267	TRCN0000065320	94%	106%	161%	175%	116%
KPNA3	NM_002267	TRCN0000065321	96%	89%	123%	115%	72%
KPNA3	NM_002267	TRCN0000065322	107%	115%	175%	133%	111%
KPNA4	NM_002268	TRCN0000065328	78%	72%	95%	89%	66%
KPNA4	NM_002268	TRCN0000065329	66%	69%	77%	72%	40%
KPNA4	NM_002268	TRCN0000065330	113%	106%	131%	128%	116%
KPNA4	NM_002268	TRCN0000065331	68%	65%	70%	61%	41%
KPNA4	NM_002268	TRCN0000065332	105%	114%	84%	77%	56%
KPNA5	NM_002269	TRCN0000064943	89%	101%	120%	117%	112%
KPNA5	NM_002269	TRCN0000064944	88%	101%	126%	78%	64%
KPNA5	NM_002269	TRCN0000064945	65%	78%	92%	78%	64%
KPNA5	NM_002269	TRCN0000064946	63%	64%	82%	55%	40%
KPNA5	NM_002269	TRCN0000064947	32%	35%	51%	42%	36%
KPNA6	NM_012316	TRCN0000065043	92%	95%	137%	104%	83%
KPNA6	NM_012316	TRCN0000065044	114%	98%	139%	108%	88%
KPNA6	NM_012316	TRCN0000065045	108%	106%	137%	154%	102%
KPNA6	NM_012316	TRCN0000065047	60%	59%	66%	54%	42%
KPNA6	NM_012316	TRCN0000065046	91%	72%	80%	72%	54%
KPNB1	NM_002265	TRCN0000123189	56%	55%	75%	84%	60%
KPNB1	NM_002265	TRCN0000123190	49%	58%	72%	63%	48%
KPNB1	NM_002265	TRCN0000123191	114%	123%	155%	136%	114%
KPNB1	NM_002265	TRCN0000123192	6%	4%	6%	7%	6%
KPNB1	NM_002265	TRCN0000123193	53%	52%	76%	62%	53%
NUP107	NM_020401	TRCN0000072478	123%	100%	146%	127%	99%
NUP107	NM_020401	TRCN0000072479	120%	122%	162%	182%	141%
NUP107	NM_020401	TRCN0000072480	97%	77%	113%	116%	89%
NUP107	NM_020401	TRCN0000072481	104%	105%	151%	121%	97%
NUP107	NM_020401	TRCN0000072482	91%	90%	118%	107%	96%
NUP153	NM_005124	TRCN0000060243	101%	102%	81%	71%	74%
NUP153	NM_005124	TRCN0000060244	23%	16%	17%	28%	30%
NUP153	NM_005124	TRCN0000060245	109%	109%	121%	118%	111%
NUP153	NM_005124	TRCN0000060246	88%	86%	91%	75%	62%
NUP153	NM_005124	TRCN0000060247	117%	119%	107%	97%	102%
NUP155	NM_004298	TRCN0000059913	60%	64%	83%	89%	88%
NUP155	NM_004298	TRCN0000059914	61%	65%	57%	70%	79%
NUP155	NM_004298	TRCN0000059915	100%	97%	98%	82%	84%
NUP155	NM_004298	TRCN0000059916	131%	110%	147%	141%	137%
NUP155	NM_004298	TRCN0000059917	91%	77%	120%	124%	127%
NUP160	XM_113678	TRCN0000060113	76%	84%	71%	69%	62%
NUP160	XM_113678	TRCN0000060114	75%	86%	103%	109%	109%
NUP160	XM_113678	TRCN0000060115	104%	95%	103%	89%	89%
NUP160	XM_113678	TRCN0000060116	74%	76%	80%	129%	93%
NUP160	XM_113678	TRCN0000060117	110%	94%	120%	85%	112%
NUP205	XM_371954	TRCN0000060023	58%	66%	66%	83%	64%
NUP205	XM_371954	TRCN0000060024	48%	53%	70%	77%	56%
NUP205	XM_371954	TRCN0000060025	84%	96%	79%	87%	72%
NUP205	XM_371954	TRCN0000060027	120%	96%	141%	124%	129%
NUP210	NM_024923	TRCN0000153158	134%	153%	163%	169%	161%
NUP210	NM_024923	TRCN0000156619	103%	87%	90%	65%	51%
NUP210	NM_024923	TRCN0000157497	121%	116%	118%	139%	132%
NUP210	NM_024923	TRCN0000152698	76%	77%	73%	90%	65%
NUP210	NM_024923	TRCN0000157612	95%	97%	100%	97%	77%

Cell Survival							
Gene Name	Gene ID	shRNA	SeV 1h	SeV 3h	SeV 5h	SeV 8h	SeV 10h
NUP214	NM_005085	TRCN0000005554	88%	92%	80%	81%	83%
NUP214	NM_005085	TRCN0000005555	101%	79%	60%	69%	84%
NUP214	NM_005085	TRCN0000005556	94%	74%	61%	85%	105%
NUP214	NM_005085	TRCN0000005557	114%	94%	91%	96%	120%
NUP214	NM_005085	TRCN0000005558	69%	64%	39%	47%	57%
NUP35	NM_138285	TRCN0000072378	81%	92%	109%	97%	69%
NUP35	NM_138285	TRCN0000072379	71%	75%	87%	130%	98%
NUP35	NM_138285	TRCN0000072380	97%	108%	126%	117%	97%
NUP35	NM_138285	TRCN0000072381	80%	90%	99%	101%	57%
NUP35	NM_138285	TRCN0000072382	86%	91%	94%	86%	67%
NUP37	NM_024057	TRCN0000152222	106%	112%	98%	117%	127%
NUP37	NM_024057	TRCN0000153319	102%	113%	110%	103%	106%
NUP37	NM_024057	TRCN0000151312	70%	67%	65%	81%	67%
NUP37	NM_024057	TRCN0000151233	122%	140%	151%	143%	125%
NUP37	NM_024057	TRCN0000156008	115%	109%	110%	120%	89%
NUP43	NM_024647	TRCN0000134871	103%	105%	155%	135%	106%
NUP43	NM_024647	TRCN0000134068	101%	70%	108%	105%	90%
NUP43	NM_024647	TRCN0000133881	80%	94%	115%	103%	74%
NUP43	NM_024647	TRCN0000137797	75%	68%	85%	85%	56%
NUP43	NM_024647	TRCN0000137417	42%	51%	68%	68%	52%
NUP50	NM_007172	TRCN0000158766	146%	159%	158%	190%	167%
NUP50	NM_007172	TRCN0000159335	135%	140%	130%	132%	111%
NUP50	NM_007172	TRCN0000158499	102%	106%	99%	127%	95%
NUP50	NM_007172	TRCN0000160160	132%	141%	165%	160%	131%
NUP54	NM_017426	TRCN0000059903	100%	82%	111%	98%	79%
NUP54	NM_017426	TRCN0000059904	83%	72%	88%	115%	97%
NUP54	NM_017426	TRCN0000059905	36%	38%	28%	25%	26%
NUP54	NM_017426	TRCN0000059906	29%	37%	32%	43%	50%
NUP54	NM_017426	TRCN0000059907	120%	107%	129%	157%	124%
NUP62	NM_012346	TRCN0000059288	40%	39%	53%	97%	49%
NUP62	NM_012346	TRCN0000059289	122%	117%	143%	98%	162%
NUP62	NM_012346	TRCN0000059290	114%	119%	140%	147%	159%
NUP62	NM_012346	TRCN0000059291	96%	74%	79%	70%	64%
NUP62	NM_012346	TRCN0000059292	121%	114%	90%	101%	77%
NUP88	NM_002532	TRCN0000141654	79%	84%	104%	88%	60%
NUP88	NM_002532	TRCN0000142510	116%	122%	157%	147%	112%
NUP88	NM_002532	TRCN0000139972	128%	127%	153%	113%	94%
NUP88	NM_002532	TRCN0000145079	79%	101%	113%	99%	81%
NUP88	NM_002532	TRCN0000145530	74%	95%	120%	114%	88%
NUP93	NM_014669	TRCN0000059958	60%	63%	58%	74%	58%
NUP93	NM_014669	TRCN0000059959	54%	62%	51%	111%	56%
NUP93	NM_014669	TRCN0000059960	123%	137%	114%	83%	140%
NUP93	NM_014669	TRCN0000059961	57%	51%	55%	47%	69%
NUP93	NM_014669	TRCN0000059962	105%	83%	90%	104%	93%
NUP98	NM_005387	TRCN0000046913	48%	54%	46%	32%	87%
NUP98	NM_005387	TRCN0000046914	102%	90%	62%	26%	24%
NUP98	NM_005387	TRCN0000046915	85%	72%	68%	51%	99%
NUP98	NM_005387	TRCN0000046916	50%	60%	41%	49%	33%
NUP98	NM_005387	TRCN0000046917	81%	90%	77%	60%	45%
NUPL1	NM_014089	TRCN0000013513	114%	94%	101%	114%	111%
NUPL1	NM_014089	TRCN0000013514	98%	112%	80%	81%	92%
NUPL1	NM_014089	TRCN0000013515	114%	101%	82%	102%	88%
NUPL1	NM_014089	TRCN0000013516	67%	55%	51%	66%	61%
NUPL1	NM_014089	TRCN0000013517	70%	80%	67%	51%	41%

Cell Survival							
Gene Name	Gene ID	shRNA	SeV 1h	SeV 3h	SeV 5h	SeV 8h	SeV 10h
NUPL2	NM_007342	TRCN0000128180	83%	101%	118%	120%	105%
NUPL2	NM_007342	TRCN0000130187	70%	55%	105%	30%	72%
NUPL2	NM_007342	TRCN0000129199	115%	98%	121%	95%	94%
NUPL2	NM_007342	TRCN0000130430	15%	13%	7%	4%	4%
NUPL2	NM_007342	TRCN0000129028	88%	57%	81%	42%	42%
NUTF2	NM_005796	TRCN0000038549	96%	101%	91%	91%	94%
NUTF2	NM_005796	TRCN0000038550	75%	114%	76%	127%	128%
NUTF2	NM_005796	TRCN0000038551	95%	89%	67%	99%	109%
NUTF2	NM_005796	TRCN0000038552	77%	82%	72%	74%	77%
NUTF2	NM_005796	TRCN0000038553	90%	112%	90%	108%	113%
NXF1	NM_006362	TRCN0000007580	106%	102%	93%	100%	105%
NXF1	NM_006362	TRCN0000007581	29%	25%	25%	14%	23%
NXF1	NM_006362	TRCN0000007582	72%	67%	58%	38%	44%
NXF1	NM_006362	TRCN0000007583	42%	29%	37%	74%	34%
NXF1	NM_006362	TRCN0000011092	62%	69%	55%	44%	42%
NXF2	NM_017809	TRCN0000059293	95%	89%	103%	101%	132%
NXF2	NM_017809	TRCN0000059294	130%	124%	123%	136%	151%
NXF2	NM_017809	TRCN0000059296	91%	89%	91%	59%	58%
NXF2	NM_017809	TRCN0000059297	79%	76%	80%	80%	90%
NXF3	NM_022052	TRCN0000060323	110%	133%	136%	128%	132%
NXF3	NM_022052	TRCN0000060324	127%	116%	128%	112%	125%
NXF3	NM_022052	TRCN0000060325	105%	95%	100%	91%	92%
NXF3	NM_022052	TRCN0000060326	110%	110%	116%	111%	100%
NXF3	NM_022052	TRCN0000060327	122%	118%	117%	134%	127%
NXT1	NM_013248	TRCN0000148803	35%	37%	41%	36%	33%
NXT1	NM_013248	TRCN0000148689	70%	68%	71%	49%	45%
NXT1	NM_013248	TRCN0000147131	135%	106%	141%	151%	125%
NXT1	NM_013248	TRCN0000146408	122%	97%	84%	110%	95%
NXT1	NM_013248	TRCN0000149160	140%	146%	140%	115%	99%
NXT2	NM_018698	TRCN0000038574	143%	119%	134%	179%	183%
NXT2	NM_018698	TRCN0000038575	66%	50%	50%	34%	37%
NXT2	NM_018698	TRCN0000038576	104%	94%	101%	109%	136%
NXT2	NM_018698	TRCN0000038577	125%	143%	147%	148%	140%
NXT2	NM_018698	TRCN0000038578	40%	31%	30%	27%	26%
POM121	NM_172020	TRCN0000060068	102%	92%	117%	116%	98%
POM121	NM_172020	TRCN0000060069	82%	83%	71%	69%	74%
POM121	NM_172020	TRCN0000060070	104%	109%	113%	117%	111%
POM121	NM_172020	TRCN0000060071	99%	87%	81%	60%	54%
RANBP2	NM_006267	TRCN0000003450	41%	45%	33%	52%	58%
RANBP2	NM_006267	TRCN0000003451	56%	48%	32%	28%	35%
RANBP2	NM_006267	TRCN0000003452	87%	89%	72%	100%	101%
RANBP2	NM_006267	TRCN0000003453	102%	72%	72%	52%	58%
RANBP2	NM_006267	TRCN0000003454	96%	87%	65%	70%	89%
RANBP3	NM_003624	TRCN0000073003	97%	106%	138%	152%	116%
RANBP3	NM_003624	TRCN0000073004	86%	93%	101%	90%	70%
RANBP3	NM_003624	TRCN0000073005	104%	98%	139%	149%	142%
RANBP3	NM_003624	TRCN0000073006	40%	40%	55%	55%	42%
RANBP3	NM_003624	TRCN0000073007	103%	86%	127%	78%	58%
RANBP5	NM_002271	TRCN0000150535	128%	124%	115%	119%	111%
RANBP5	NM_002271	TRCN0000153065	32%	36%	35%	20%	26%
RANBP5	NM_002271	TRCN0000152684	56%	66%	50%	58%	42%
RANBP5	NM_002271	TRCN0000152127	141%	124%	165%	178%	159%
RANBP5	NM_002271	TRCN0000151824	76%	74%	84%	77%	61%

Cell Survival							
Gene Name	Gene ID	shRNA	SeV 1h	SeV 3h	SeV 5h	SeV 8h	SeV 10h
RANBP6	NM_012416	TRCN0000148876	111%	120%	103%	90%	80%
RANBP6	NM_012416	TRCN0000146440	102%	108%	104%	131%	91%
RANBP6	NM_012416	TRCN0000147280	69%	77%	82%	111%	96%
RANBP6	NM_012416	TRCN0000148942	125%	128%	125%	119%	101%
RANBP6	NM_012416	TRCN0000149838	115%	122%	106%	117%	95%
RANGAP1	NM_002883	TRCN0000047328	59%	44%	50%	35%	49%
RANGAP1	NM_002883	TRCN0000047329	88%	79%	81%	56%	70%
RANGAP1	NM_002883	TRCN0000047330	105%	87%	87%	98%	120%
RANGAP1	NM_002883	TRCN0000047331	66%	57%	50%	56%	44%
RANGAP1	NM_002883	TRCN0000047332	86%	98%	98%	116%	95%
RCC1	NM_001269	TRCN0000157236	95%	105%	103%	110%	91%
RCC1	NM_001269	TRCN0000151199	116%	122%	130%	134%	108%
RCC1	NM_001269	TRCN0000157685	103%	107%	116%	118%	96%
RCC1	NM_001269	TRCN0000157981	142%	141%	163%	145%	135%
RCC1	NM_001269	TRCN0000152440	105%	114%	122%	113%	80%
RCC2	NM_018715	TRCN0000150578	152%	146%	155%	160%	158%
RCC2	NM_018715	TRCN0000154474	131%	124%	135%	151%	133%
RCC2	NM_018715	TRCN0000154827	145%	137%	135%	137%	116%
RCC2	NM_018715	TRCN0000153686	81%	86%	78%	71%	74%
RCC2	NM_018715	TRCN0000151164	76%	88%	110%	117%	108%
RGPD4	NM_182588	TRCN0000017738	122%	97%	87%	77%	86%
RGPD4	NM_182588	TRCN0000017739	91%	90%	71%	71%	96%
RGPD4	NM_182588	TRCN0000017740	22%	20%	20%	24%	26%
RGPD4	NM_182588	TRCN0000017741	84%	89%	92%	75%	81%
RGPD4	NM_182588	TRCN0000017742	128%	108%	106%	99%	127%
RNUT1	NM_005701	TRCN0000038569	45%	57%	50%	50%	54%
RNUT1	NM_005701	TRCN0000038570	114%	107%	113%	137%	145%
RNUT1	NM_005701	TRCN0000038571	28%	23%	17%	12%	13%
RNUT1	NM_005701	TRCN0000038572	87%	92%	83%	74%	74%
RNUT1	NM_005701	TRCN0000038573	139%	131%	131%	141%	156%
CSE1L	NM_001316	TRCN0000061790	41%	38%	48%	45%	34%
CSE1L	NM_001316	TRCN0000061790	45%	33%	61%	54%	49%
RAN	NM_006325	TRCN000047929	31%	27%	32%	27%	35%
RAN	NM_006325	TRCN000047929	36%	33%	33%	30%	40%
XPO1	NM_003400	TRCN000154386	29%	29%	20%	16%	25%
XPO1	NM_003400	TRCN000154386	30%	33%	23%	21%	22%
TNPO1	NM_002270	TRCN0000038284	56%	68%	49%	41%	39%
TNPO1	NM_002270	TRCN0000038285	77%	79%	81%	91%	87%
TNPO1	NM_002270	TRCN0000038286	50%	43%	53%	47%	60%
TNPO1	NM_002270	TRCN0000038287	89%	115%	87%	73%	78%
TNPO1	NM_002270	TRCN0000038288	69%	74%	84%	62%	61%
TNPO2	NM_013433	TRCN0000043468	48%	47%	58%	59%	76%
TNPO2	NM_013433	TRCN0000043469	85%	67%	67%	52%	40%
TNPO2	NM_013433	TRCN0000043470	80%	20%	23%	28%	36%
TNPO2	NM_013433	TRCN0000043471	81%	91%	78%	76%	88%
TNPO2	NM_013433	TRCN0000043472	108%	74%	74%	86%	65%
TNPO3	NM_012470	TRCN0000038329	109%	92%	83%	74%	71%
TNPO3	NM_012470	TRCN0000038330	88%	77%	50%	44%	45%
TNPO3	NM_012470	TRCN0000038331	119%	91%	89%	118%	116%
TNPO3	NM_012470	TRCN0000038333	57%	67%	63%	62%	75%
TNPO3	NM_012470	TRCN0000038332	109%	103%	98%	98%	94%
TPR	NM_003292	TRCN0000060063	55%	53%	61%	56%	67%
TPR	NM_003292	TRCN0000060064	86%	71%	74%	92%	69%
TPR	NM_003292	TRCN0000060065	31%	20%	12%	93%	12%
TPR	NM_003292	TRCN0000060066	61%	64%	63%	30%	39%
TPR	NM_003292	TRCN0000060067	92%	81%	96%	80%	85%
XPO4	NM_022459	TRCN0000159557	101%	123%	156%	154%	122%
XPO4	NM_022459	TRCN0000159095	46%	61%	46%	47%	38%
XPO4	NM_022459	TRCN0000160271	63%	80%	68%	54%	38%
XPO4	NM_022459	TRCN0000159918	62%	76%	89%	88%	60%
XPO4	NM_022459	TRCN0000159748	108%	105%	129%	121%	93%

Table S4. Effect of Silencing Nucleoporins and Nucleocytoplasmic Transporters on p*IFNB1* promoter and Cellular Fitness

This table contains the results of the RNAi screen of the 60 nucleoporins and nucleocytoplasmic transporters and their effect on the p*IFNB1* promoter and cellular fitness. Results on the promoter are represented in percentage of promoter inhibition from 2 separate experiments. Cellular fitness is represented in percentage of cell survival for each time point of the SeV infection.

Chapter 3: Discussion

3.1 Investigation of HCV-Host Interactors in the Modulation of the Innate Antiviral Response

The current study endeavored to determine whether HCV-host interactors elucidated by Germain et al. (Mol. Cell. Proteomics 2014) had an effect on the innate antiviral response [19]. Many of the host proteins identified were previously known to interact with other viruses, suggesting that a restricted number of host proteins or families are hijacked to benefit their life cycle, either as cofactors to enhance replication or as restriction factors to evade the innate antiviral response.

Based on the hypothesis that viruses could interact with host factors for evasion mechanisms, 132 genes were silenced from 426 proteins identified by Germain et al. (2014) (Figure S1) to measure their effect on the innate immune response by measuring IFNB1 production. This assay used SeV infection to induce the response in two cell lines, HEK 293T and A549, which both contained a stably integrated IFNB1 promoter linked to a firefly luciferase gene. A stable cell line that expressed a firefly luciferase gene under a Ef1α promoter was also used as a control to measure cellular fitness and specificity for the effects of the silenced genes on the IFNB1 promoter. From this assay, 53 genes had a significant effect on the response with 12 previously identified for having an effect on HCV replication when silenced as shown in the study by Germain et al. (2014) (Figure S2). The other 41 genes affected the SeV-mediated IFNB1 production in one or both cell lines (HEK 293T and A549), supporting the hypothesis that virus-host interactions not having an effect on viral replication could be involved in the modulation of the innate antiviral response.

Of the 53 genes affecting the innate antiviral immunity, host factors elucidated to interact with a viral protein were almost evenly split into positive regulators (inhibit when silenced) and negative regulators (stimulate when silenced) of the immune response (Figure 1). The only exception are NS5B-host interactors as there are more of these proteins considered as negative regulators (12 in yellow) than positive regulators (5 in blue) of the innate immune response.

When comparing the innate immune modulators in HEK 293T and A549 cell lines (Figure 3.1), 11 common interactors were identified including NS3/4A interactors COPB1 and

TNPO1 (positive regulators), and NS5B interactors CKB, NIP30 and RPL29 (negative regulators). Other common interactors have different effects on the different cells lines (WDR77 as a core interactor, BCLAF1, MAP3K7IP1, UBC and YBX1 as NS3/4A interactors, and FKBP5 as a NS5B interactor) (see Figure 1).

Finally, in order to better understand which cellular processes may be targeted by the virus to reduce the innate immune response by an immune evasion mechanism, Gene Ontology (GO) enrichment was performed on the 53 interactors. This resulted in "protein import into the nucleus, docking" and the "nuclear pore" as the GO terms with the highest enrichment (Table I). Interestingly, the proteins associated with these terms were all, except one, elucidated to interact with NS3/4A (CSE1L, KPNB1, RAN, TNPO1 and XPO1), which is well-known for its role in evading the antiviral response by cleaving key adaptors MAVS and TRIF of the RLR and TLR pathways, respectively [315, 316]. Upon further inspection, these five genes were found to be positive regulators in the innate antiviral immunity RNAi screen (Figure 1), while KPNB1, RAN, and TNPO1 were all previously determined to play a role in HCV replication by Germain et al. (2014) [19]. These results strongly suggest that the proteins associated with nucleocytoplasmic transport and the nuclear pore complexes are targeted by multiple viruses to reduce the innate antiviral response through their modulation of IFNB1 production.

Figure 3.1: Silencing of Host Interactors in Modulation of SeV-mediated Innate Response of Different Human Cell Lines

The figure above presents the total number of HCV-host interactors, which modulate the innate antiviral response in two cell lines in a pie chart where 11 interactors were common in both cell lines to affect the response in a positive or negative manner.

3.2 Validation of the Interactors on the Innate Antiviral Response

The five interactors CSE1L, KPNB1, RAN, TNPO1 and XPO1 were further investigated by first demonstrating the reduced expression of proteins by efficient knockdown in A549 and HEK 293T cell lines. In the HEK 293T cell line, the silencing of the five genes confirmed the reduction of ISG56 expression at 8 hours, which continued at 24 hours of infection with KPNB1 silencing resulting in no ISG56 expression (Figure S3). In A549, ISG56 levels are also reduced in RAN and KPNB1 silencing, while unexpectedly CSE1L silencing increased expression at 8 hours post-infection. A different phenotype is observed at 24 hours post-infection, in which ISG56 expression was slightly increased in XPO1, CSE1L and TNPO1 silencing, while RAN and KPNB1 knockdown remained at levels similar to the control (Figure 2).

We then investigated the silencing of these genes on SeV infection. Interestingly, KPNB1 silencing was able to rapidly induce the expression of viral protein at 8 hours of infection in A549, while all silenced genes at 24 hours post-infection had an overall increase in viral protein expression (Figure 2). In HEK 293T cells, the rapid induction of viral protein expression was confirmed in KPNB1 silenced cells, in addition with CSE1L knockdown 8 hours post-infection. At 24 hours, the viral expression is slightly diminished in XPO1, RAN, and TNPO1 silenced cells, with an increase still prominent in KPNB1 knockdown cells (Figure S3).

The innate antiviral response differs between the two cells lines as the kinetics in A549 occur quicker than in HEK 293T cells with 8 hours post-infection in A549 is comparable to 24 hours-post infection in HEK 293T cells. At 24 hours, the first wave of the response is already over in A549 cells, which explains why the expression of ISG56 seems to be more or less normalized among the different gene silencing (Figure 2), while a distinct difference in ISG56 expression can still be seen in HEK 293T cells at 24 hours post-infection (Figure S3).

Overall, the data suggest that these proteins involved in nucleocytoplasmic transport do have an effect on the innate antiviral response as revealed by the reduced levels of ISG56 proteins at variable time in both cell lines, which explain the rapid expression of SeV proteins, especially in the case of KPNB1 silencing. However, further mechanistic studies were

required in order determine at which stage of the response, such as viral sensing, signaling cascade, and nuclear translocation of transcription factors, these proteins act upon to affect IFNB1 production and the ISG56 response.

3.3 Epistatic Studies of the Interactors on the Innate Antiviral Response

To determine at what level of the innate immune response these nucleocytoplasmic transporters could be affecting, an epistatic assay was performed in order to gain mechanistic insight at each step of the pathway and to rule out any indirect effects, such as the inhibition of early steps of SeV infection, to decrease the innate antiviral response. Preliminary studies were performed with the five interactors.

XPO1 silencing decreased IFNB1 production when infected with SeV in both HEK 293T and A549 cells. Stimulating downstream of the pathway by overexpressing MAVS, the key adaptor in the RLR pathway, still had reduced levels of IFNB1 when XPO1 was silenced in comparison to the NT control. These reduction effects are not due to cellular fitness as shown by the EF1α promoter (Figure 3.2). Despite the overexpression of IRF3(5D), a constitutively active form of IRF3 which translocates to the nucleus, XPO1 silencing still reduced IFNB1 production. However, silencing of XPO1 had no effect on ISG56 expression when stimulated with IFN-α, a type I interferon, and overexpression of IRF3(5D) (Figure 3.3). Since ISG56 is an IRF3-dependent ISG, this suggests that the reason overexpression of IRF3(5D) did not restore IFNB1 levels is due to NF-κB p65 being affected by XPO1 silencing, as both IRF3 and p65 are required for sufficient activation of the transcription of the IFNB promoter [257]. This may seem to contradict the results shown in Figure S6, where XPO1 knockdown increases p65 nuclear translocation (Figure S6) and should therefore increase IFNB1 expression. However, the nuclear localization of NF-κB p65 activates not only IFNB1 transcription, but also the transcription of IκB proteins as a negative feedback mechanism to regulate NF-kB p65 activity through binding and export to the cytoplasm [294]. In the context of XPO1 silencing, it has been shown using the XPO1 inhibitor Leptomycin B that IκB:NF-κB complexes accumulate in the nucleus, which lead to a reduction in NF-κB activity [292].

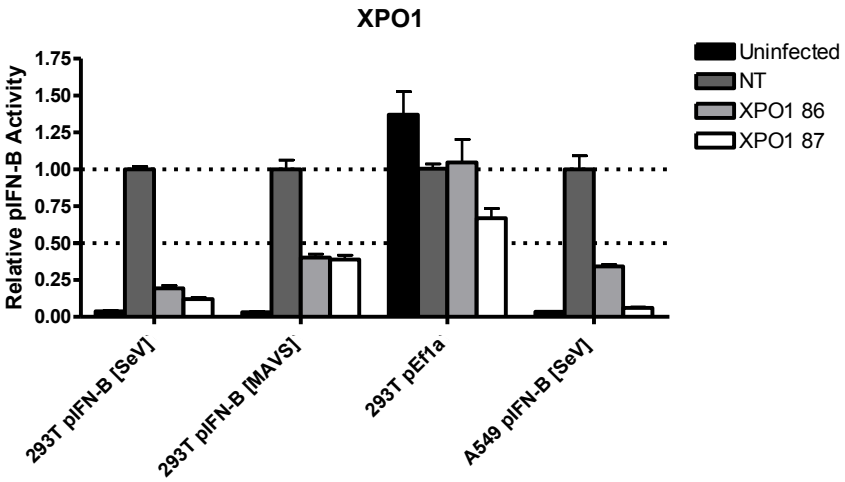

Figure 3.2: Epistatic study of XPO1 Silencing on the Innate Antiviral Response (1)

This figure shows the effect of XPO1 silencing on the innate antiviral response at the level of SeV infection and MAVS overexpression. XPO1 shRNA 86 is the same shRNA used in Figure 2. Data is the average of triplicate wells per condition with corresponding errors bars.

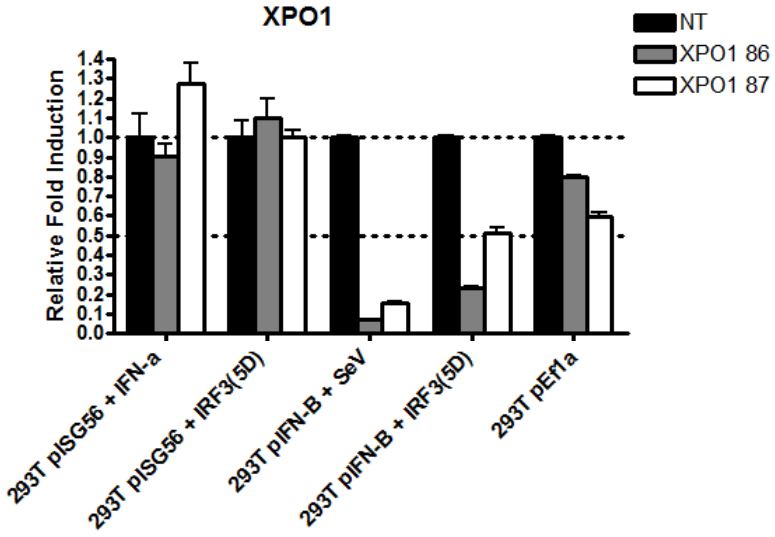

Figure 3.3.: Epistatic study of XPO1 Silencing on the Innate Antiviral Response (2)

This figure shows the effect of XPO1 silencing on the innate antiviral response at the level of SeV infection, IFN-α stimulation and IRF3(5D) overexpression in IFNB1 and ISG56

promoter readouts. XPO1 shRNA 86 is the same shRNA used in Figure 2. Data is the average of triplicate wells per condition with corresponding errors bars.

The silencing of CSE1L reduces IFNB1 production in HEK 293T cells and A549 cells upon SeV infection. In HEK 293T cells, stimulating downstream by overexpressing Poly I:C, a viral dsRNA mimetic recognized by RIG-I [317], still leads to reduced IFNB1 levels when CSE1L is silenced. However, CSE1L knockdown has no effect on the IFNB1 promoter when MAVS is overexpressed (Figure 3.4), and when IRF3(5D) is overexpressed (Figure 3.5) suggesting that CSE1L is acting between RIG-I sensing and signaling by MAVS. However, ISG56 expression was decreased when stimulated with IFN-α stimulation and IRF3(5D) overexpression when CSE1L is silenced, which is the complete opposite to the effect shown in XPO1 knockdown for this promoter (Figure 3.3). This suggests that CSE1L may be affecting ISG56 expression via the JAK/STAT pathway as the ISGF3 complex, composed of STAT1, STAT2 and IRF9, and can also induce the expression of ISG56 by binding to the ISRE during this second phase of the antiviral response [318]. Although IRF3 and p65 translocation to the nucleus is reduced upon CSE1L knockdown during a SeV infection in A549 cells, it cannot be said for sure that it is also the case in HEK 293T cells, and would have to be investigated further.

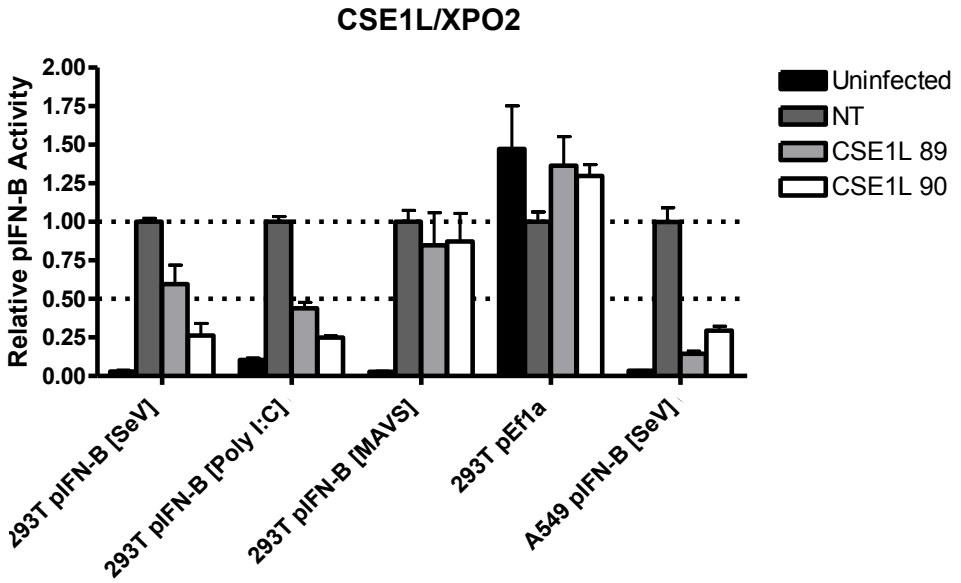

Figure 3.4: Epistatic study of CSE1L Silencing on the Innate Antiviral Response (1)

This figure shows the effect of CSE1L silencing on the innate antiviral response at the level of SeV infection, Poly I:C overexpression, and MAVS overexpression. CSE1L shRNA 90 is the same shRNA used in Figure 2. Data is the average of triplicate wells per condition with corresponding errors bars.

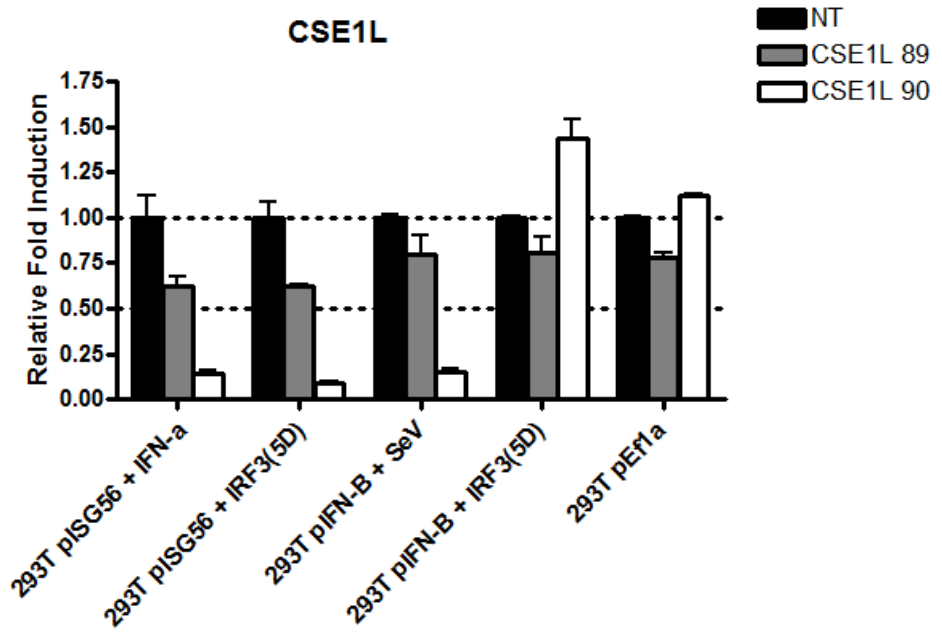

Figure 3.5: Epistatic study of CSE1L Silencing on the Innate Antiviral Response (2)

This figure shows the effect of CSE1L silencing on the innate antiviral response at the level of SeV infection, IFN-α stimulation and IRF3(5D) overexpression in IFNB1 and ISG56 promoter readouts. CSE1L shRNA 90 is the same shRNA used in Figure 2. Data is the average of triplicate wells per condition with corresponding errors bars.

In the case of RAN silencing, IFNB1 production and ISG56 expression is reduced no matter what the stimulation or overexpression of the different levels of the response (Figure 3.6 and 3.7). This may be due to RAN's role in both protein import and export, which could be affecting any number of proteins and may be the reason for this effect on the response.

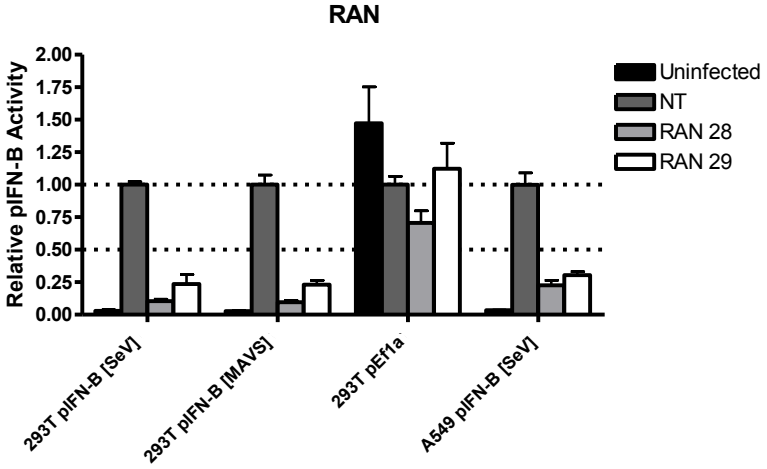

Figure 3.6: Epistatic study of RAN Silencing on the Innate Antiviral Response (1)

This figure shows the effect of RAN silencing on the innate antiviral response at the level of SeV infection and MAVS overexpression. RAN shRNA 29 is the same shRNA used in Figure 2. Data is the average of triplicate wells per condition with corresponding errors bars.

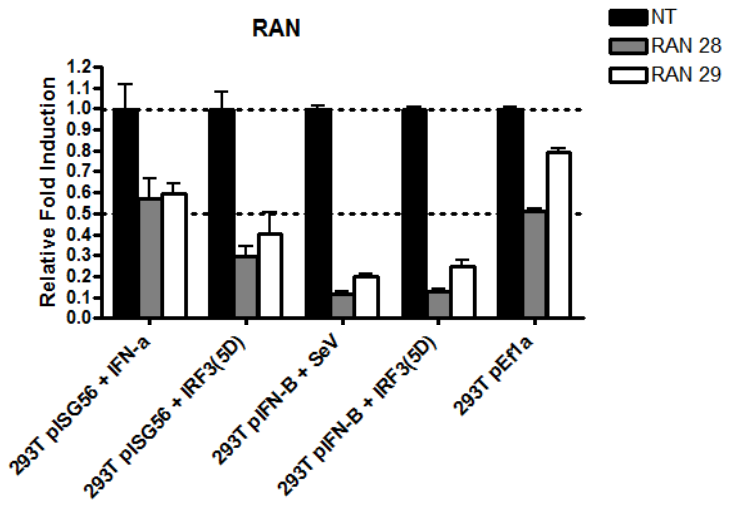

Figure 3.7: Epistatic study of RAN Silencing on the Innate Antiviral Response (2)

This figure shows the effect of RAN silencing on the innate antiviral response at the level of SeV infection, IFN-α stimulation and IRF3(5D) overexpression in IFNB1 and ISG56 promoter readouts. RAN shRNA 29 is the same shRNA used in Figure 2. Data is the average of triplicate wells per condition with corresponding errors bars.

KPNB1 silencing decreased IFNB1 expression at every level of the response until IRF3(5D) overexpression, but the effect remains inconclusive due to differential effect between the two shRNAs. Since the shRNA used in Figure 2 is shRNA 89, this would suggest that the reduction of IFNB1 by KPNB1 silencing can be rescued by the overexpression of IRF3(5D). Based on the shRNA 89, the effect on ISG56 expression is inconclusive due to the error bars, and would require further validation (Figure 3.8).

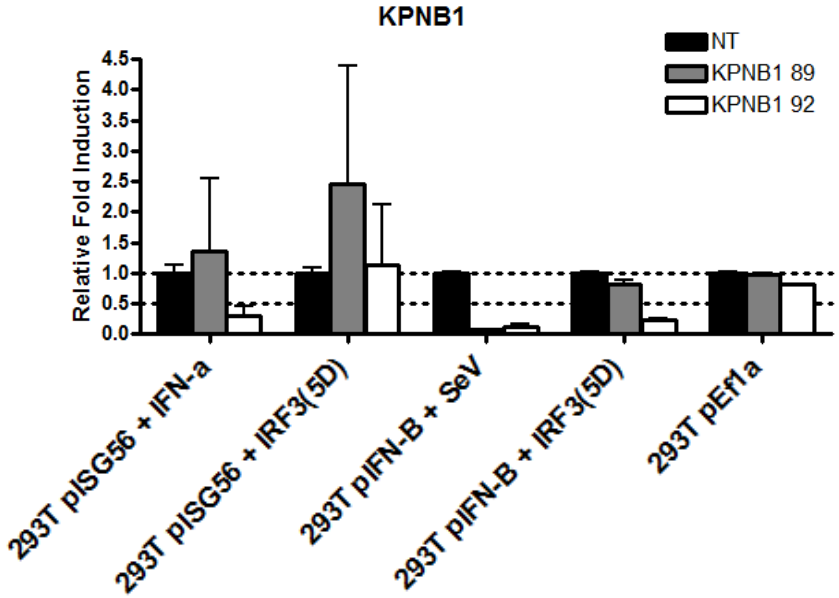

Figure 3.8: Epistatic study of KPNB1 Silencing on the Innate Antiviral Response

This figure shows the effect of KPNB1 silencing on the innate antiviral response at the level of SeV infection, IFN-α stimulation and IRF3(5D) overexpression in IFNB1 and ISG56 promoter readouts. KPNB1 shRNA 89 is the same shRNA used in Figure 2. Data is the average of triplicate wells per condition with corresponding errors bars.

For TNPO1 silencing, IFNB1 production is at every level of the response until IRF3(5D) overexpression level of the response. The ISG56 expression induced by IFN-α stimulation is also reduced when TNPO1 is silenced, but the effect on IRF3(5D) on ISG56 expression is inconclusive during TNPO1 knockdown (Figure 3.9). These preliminary results suggest that TNPO1 knockdown is affecting other transcription factors required for IFNB1 promoter activation, such as NF-κB p65, as IRF3(5D) overexpression does not rescue the phenotype, and has an inconclusive effect on the ISG56 promoter. This result is supported by the decrease in IRF3 and p65 nuclear translocation upon TNPO1 knockdown in A549 cells (Figure S5).

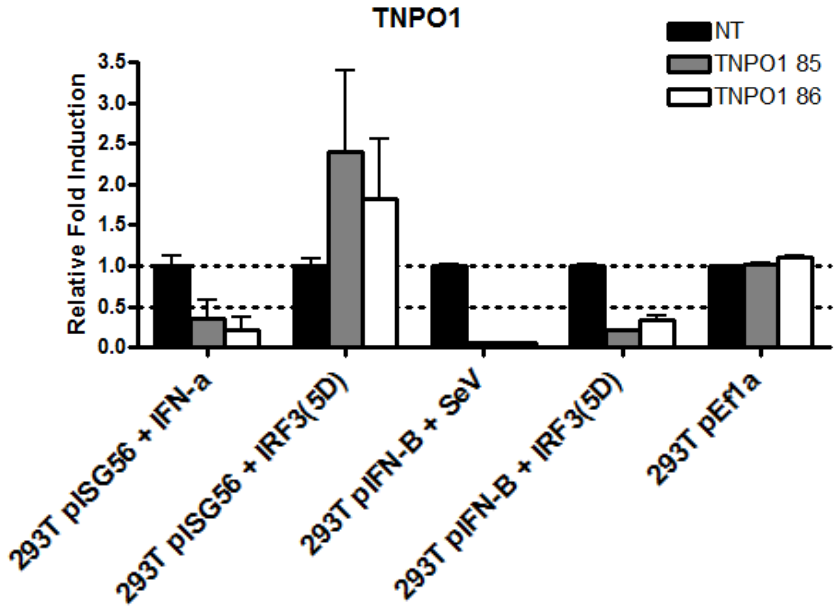

Figure 3.9: Epistatic study of TNPO1 Silencing on the Innate Antiviral Response

This figure shows the effect of TNPO1 silencing on the innate antiviral response at the level of SeV infection, IFN-α stimulation and IRF3(5D) overexpression in IFNB1 and ISG56 promoter readouts. TNPO1 shRNA 85 is the same shRNA used in Figure 2. Data is the average of triplicate wells per condition with corresponding errors bars.

Overall, preliminary data with the five interactors affecting the innate antiviral response are consistent with modulation at the level of nuclear translocation, which could involve IRF3, NF-κB p65 and/or ISGF3.

3.4 Development of a Screen to Measure IRF3 and p65 Nuclear Translocation during Viral Infection

Previous results show that the five proteins associated with nucleocytoplasmic transporters had an effect on IFNB1 production (Figure 1), ISG56 expression and SeV replication (Figure 2). Preliminary data suggested that this effect on the innate antiviral response may be at the level of nuclear translocation of transcription factors such as IRF3 and NF-κB p65, which are required for the production of IFNs such as IFNβ [244]. The goal was to develop an assay that allowed us to gain mechanistic insight on the modulation of these key transcription factors by directly evaluating their nuclear translocation during the innate antiviral response.

The result is the development of a microscopy-based assay, where the nuclear translocation of IRF3 and p65 can be measured over a 10-hour viral infection time course. Since nuclear translocation can involve multiple players such as a variety of transporters and nucleoporins for proper entry into the nucleus, the number of genes studied was expanded to cover approximately 60 genes to better understand the mechanism by which IRF3 and p65 enter and exit nucleus. The cell line of choice was A549 as four of the five nucleocytoplasmic transporters were found as positive regulators in the primary screen, and the knockdown of these genes were also validated in this cell line (Figure 2). In addition, the rapidity of the response upon infection and the large cytoplasm of these cells facilitate the quantitative and qualitative measurement of the nuclear translocation of these transcription factors over time.

The IRF3 and p65 nuclear translocation observed in the microscopy-based assay over a 10-hour SeV infection time course (Figure 3C) was validated biochemically using nuclear/cytoplasmic fractionation (Figure 3D), where the increase of IRF3 and p65 in the nucleus matched the results generated by the microscopy assay (Figure 3B). In addition, the phosphorylation of IRF3 and the NF-κB inhibitor NFKBIA were also a measure of the induction of the innate antiviral response and the nuclear translocation of IRF3 and p65, respectively (Figure 3D). The validity of the microscopy using a biochemical method increased the confidence of using this assay to a medium throughput level of RNAi screening.

This microscopy-based screen has several strengths: the first is being able to normalize the data from well to well. Since the number of nuclei may not be equal from well to well, the analysis uses the percentage of nuclei, instead of the total number of nuclei containing these transcription factors. This analysis makes the results in duplicate wells, as well as from plate to plate, consistent and reproducible.

Another strength is that the threshold level set can be visually confirmed using the software as nuclei that do not make the cut are marked in red, and nuclei that are above the threshold are marked in green. This allows for better fine tuning of the threshold, instead of setting the levels to completely remove background levels of uninfected cells. Overall, the main strength of this technique is that hundreds of genes can be studied at once using a low number of cells (in the thousands) in 96-well and even 384-well plates with the ability to look at hundreds of cells per field, and quantifying phenotypes using software. The standard immunofluorescence technique requires hundreds of thousands of cells, but only allows for twenty to fifty cells to be visualized at once depending on the magnification, and phenotypes cannot be quantified without being biased. Our study looked only at the nuclear translocation of IRF3 and p65 using Hoechst for nuclear staining. However, with the proper compartment staining, the study of any protein to any compartment, such as the mitochondria or lipid droplets, could be studied with proper optimization.

There were weaknesses to this assay as IRF3 and p65 nuclear translocation were looked at separately, as staining these two proteins at once would cause their signals to bleed into one another, making it difficult to accurately measure their signals separately. Another limitation is the staining: in the case of p65, which is stained in the cytoplasm of uninfected cells, some cells contain so much p65 staining in the cytoplasm that it bleeds into the boundary delineated by the Harmony software as the nucleus, where the staining ends up hitting the threshold and this nuclei is counted as containing p65 in the nucleus, when it is not the case upon visual inspection. This limitation is due to having only the staining of the nuclei by Hoechst and not having another staining, such as Phalloidin, for the cytoplasm [319]. This double compartment staining would allow for the measurement of the fluorescence intensity in each compartment for each cell [41], completely avoiding false positives measured due to single-compartment staining. If these weaknesses were to be overcome, more complex data

could be generated such as which nuclei contain both IRF3 and p65 and which contain only one or the other, as well as the fluorescence intensity in both the nuclei and cytoplasmic compartments for an overall picture of the nuclear translocation of these factors.

We performed a microscopy-based RNAi screen to study approximately sixty genes involved in the nuclear pore complex from the seven different sections of the pore: cytoplasmic FG-Nups and filaments, transmembrane-ring Nups, outer-ring Nups, linker Nups, inner-ring Nups, central FG-Nups, and the nuclear FG-Nups and the nuclear basket (Figure 7, S9 to S12). Genes involving nucleocytoplasmic transport were also studied such as those involved in protein import (adaptors, importins, transportins), protein export, mRNA export and the establishment of the RAN energy gradient (Figures 5, 6, S4 to S8). The screen allowed for the identification of several Nups and transporters involved in the import and export of IRF3 and p65 at different time points of the infection.

The novelty of this assay is the combination of microscopy (qualitative) and medium throughput RNAi screen results (quantitative) to measure the phenotype of IRF3 and p65 nuclear translocation over time, a valuable readout of the innate antiviral response. The 10-hour time course allows for the measurement of IRF3 and p65 nuclear translocation at the start, peak and end of the first wave of the innate antiviral response. The measurement of IRF3 and p65 in the nucleus is reproducible from well to well from plate to plate, allowing for all the genes studied to be compared together and not only within the plate the shRNA was placed in. The validation of the microscopy results using a biochemical method increases the significance and confidence of the results obtained by the analysis program.

3.5 Microscopy Results: IRF3 and p65 Translocation

In this microscopy RNAi screen, the 58 genes studied for their effect on the nuclear translocation of IRF3 and p65 were divided into their functional and structural groups of nucleocytoplasmic transporters and nucleoporins, respectively. The article identified 33 genes, in which 25 had an overall decrease, 4 had a delay, 2 had an increase and 2 others had differential effects when silenced on the nuclear translocation of IRF3 and p65.

The Kapα adaptor proteins had varying effects on IRF3 nuclear translocation. For p65 nuclear translocation, 5 out of 6 of these adaptors decreased this factor's translocation significantly at 3 hours post-infection by 2 or more shRNAs per gene (Figure 5). The only adaptor that did not have this phenotype is KPNA4, whose silencing increased IRF3 and p65 nuclear localization overall. Interestingly, KPNA4 has been targeted by a cellular protein [320], an active metabolite [321], a fungal metabolite [322], and a virus [323], in order to affect its interaction with p65 and prevent nuclear translocation, which suggests that KPNA4 may be an import adaptor for this transcription factor for a different mechanism. Based on the data shown in Figure 5, one possible explanation for the increase in both transcription factors when KPNA4 is silenced may be due to a compensatory mechanism by the other 5 adaptors to import p65 in the absence of KPNA4, as these other adaptors have been shown to bind to p65 [270, 324-326]. The reverse could be said for the significant decrease at 3 hours post-infection of p65 by the silencing of the 5 other adaptors, as it would suggest these 5 participate in the nuclear translocation of p65 early in the antiviral response, while KPNA4 handles the import during the latter half of the response. In terms of IFNB1 production at 6 hours post-infection, it was significantly decreased when KPNA2, KPNA3, and KPNA5 were silenced (Figure 5B), which could be attributed to these 3 genes decreasing both IRF3 and p65 nuclear translocation at 3 hours post-infection (Figure 5B). KPNA1 and KPNA4 had different effects between shRNAs, while KPNA6 had only a slight decrease on IFNB1 production when these genes were silenced. Further validation would be required on the shRNAs' efficacy to knockdown their target gene to eliminate shRNAs with off-target effects for these 3 genes, and then determine if there is causality between the effect of the shRNA on IRF3 and p65 nuclear translocation and IFNB1 production or if other factors that require these adaptors are at play.

The next group are the proteins involved in protein import. Silencing of KPNB1, the main import carrier, decreased nuclear translocation of IRF3 and p65 in the first five hours of SeV infection (Figure 4), which explains the negative effect on ISG56 expression with shRNA 89 at 8 hours post-infection (Figure 2) and IFNB1 production at 6 hours post-infection (Figure 4). The microscopy results show that IRF3 and p65 nuclear localization return to normal levels despite the silencing of KPNB1, suggesting that the effects on ISG56 expression and IFNB1 production is due to the negative effect on IRF3 and p65 nuclear translocation early in the innate antiviral response prior to these readouts at 8 and 6 hours post-infection, respectively. The KPNB1 knockdown induces an earlier induction of apoptosis as seen by the cleavage of PARP1 (Figure 4C), suggesting that the weakened innate response leads to a greater infectivity of SeV and thus activate other cellular processes in attempts to restrict the spread of the virus. This is further supported by the decrease in IFNB1 production upon knockdown of KPNB1 by shRNA 89 (also used in Figure 4C) and shRNA 90, where both shRNAs showed a decrease in cell survival (Figure 4A). It is plausible that shRNA 91 may not be as effective in knocking down KPNB1 as the previous two shRNAs, as there is a significant error bar when looking at the decrease in IFNB1 production, thus no negative effect on cell survival (Figure 4A). This would need to be confirmed by measuring the mRNA levels of KPNB1 upon knockdown by the three different shRNAs. Overall, the data confirm that KPNB1 plays a key role in the nuclear import of IRF3 and p65 in the rapid establishment of the innate response to prevent the accumulation of viral protein, and in turn subdue viral replication and propagation.

Out of the importins, the paralogous pair IPO7 and IPO8 had an overall negative effect on the translocation of both transcription factors when silenced, which suggests that the similarities between these two can go as far as their effect on cargoes (Figure 6A). Interestingly, KPNB1 and IPO8 were determined to be involved in p65 nuclear import in a NLS-dependent and independent manner, respectively, during a TNF-α stimulation [325]. IPO7 and IPO8 silencing also greatly decreased IFNB1 production, which could be attributed to their effect on nuclear translocation of the transcription factors, especially in the case of shRNA 74 (green) of IPO7 and shRNA 52 of IPO8 (Figure S4). IPO7 is specifically targeted by HIV-1 to facilitate nuclear import of viral DNA for efficient HIV-1 replication [56, 327]. IPO4 silencing specifically decreased IRF3 nuclear transport, and not p65, especially during

the second half of the infection (5 to 10 hours), which suggests that different import carriers can be used at different times of the infection for IRF3 and p65 nuclear transport and may relate to how quick these carriers are in the transport of their cargo. IPO7 and IPO8 silencing does not reduce cell survival because they are not the main import carriers like KPNB1, and their functions could be compensated by other import carriers. The IFNB1 production was reduced in two out of three shRNAs used to silence IPO4, which could be due to the reduced translocation of p65 to the nucleus at 3 hours post-infection and IRF3 at 5 hours post-infection. A possible explanation as to shRNA 89 having a dramatic increase on IFNB1 expression may be due to its minimal negative effect at 3 hours post-infection and greater positive effect at 5 hours post-infection on p65 nuclear translocation, in comparison to shRNA 88 and shRNA 91 (Figure S4).

The transportins, also associated with protein import, also had an effect on IRF3 and p65 nuclear translocation. TNPO1 and TNPO2 were determined to be paralogous pairs, like IPO7 and IPO8 [61]. TNPO1 overall decreased nuclear translocation of both IRF3 and p65 during the entire time course (Figure 6B), which correlates with the reduced expression of IFNB1 (Figure S5). On the other hand, TNPO2 increased IRF3 and p65 nuclear localization during the second half of the infection (Figure 6B), which suggest that it could have a role in export late in the innate immune response or there may be a compensation mechanism for its role in mRNA export by other export factors [50]. The effect of silencing TNPO2 on IFNB1 production is different between the two shRNAs, but do show a correlation with the first 5 hours of the infection as shRNA 70 decreases the nuclear translocation of both transcription factors, hence the decrease in IFNB1 production. The other shRNA 69 shows minimal effect on nuclear translocation with the exception of an increase in p65 nuclear translocation at 5 hours post-infection (Figure S5). TNPO3 is thought to have a role in both import and export [86], but our study reveals that its silencing has an effect on IRF3 nuclear translocation only, similar to TNPO1. This suggests that the involvement of TNPO3 with the nuclear import of the HIV-1 pre-integration complex [52, 53] may have a secondary effect of disrupting IRF3-dependent innate antiviral responses. However, when TNPO3 is silenced, only shRNA 33 shows a correlation between decreased nuclear translocation of transcription factors IRF3 and p65 in the first 5 hours of infection, and a reduction in IFNB1 production (Figure S5). The

other 2 shRNAs have variable negative effects on nuclear translocation, but do not correlate with IFNB1 production, which suggests that further validation is required.

KPNB1 and TNPO1 knockdown have similar effects on the reduction of ISG56 levels (Figures 2 and S3), decrease in IRF3 and p65 nuclear translocation at 5 hours post-infection, and a reduction in IFNB1 expression (Figures 4B and S5). However, TNPO1 knockdown does not increase SeV protein expression, in comparison to KPNB1 knockdown (Figures 2 and S3). It would be interesting to see whether TNPO1 knockdown has a similar phenotype to KPNB1 knockdown on PARP1 cleavage (Figure 4C) to determine whether the induction of apoptosis is due to the reduced activity of the innate antiviral response or the increase in viral protein expression or the combination of both.

Carriers involved in protein export had significant effects in IRF3 and p65 nuclear translocation. The main export carrier, XPO1 increased nuclear translocation of IRF3 early in the infection (1 and 3 hours) when silenced, while this silencing increased nuclear localization of p65 for the entire time course (Figure 6C). Both these transcription factors were shown to be exported by XPO1 through the use of the inhibitor Leptomycin B [328, 329]. The brief effect XPO1 silencing had on IRF3 nuclear localization may explain our preliminary data where the ISG56 promoter remained unchanged in comparison to the control (Figure 3.3). However, IFNB1 production is still reduced (Figure 3.2) upon XPO1 silencing despite the overall increase of p65 in the nucleus, which may be due to p65 transcription of its inhibitor IκBα, which binds to p65 to regulate its expression by exporting it to the cytoplasm for degradation [330-332]. However, IκBα-p65 export is mediated by XPO1, thus XPO1 silencing or inhibition using Leptomycin B blocks this export [329, 333].

The other export carrier is CSE1L, which is involved in the export of Kapα adaptors back to the cytoplasm as a recycling mechanism for the formation of import complexes [44]. Therefore, it is expected that nuclear import of IRF3 and p65 would be decreased when CSE1L is silenced, as these two transcription factors require import adaptors to enter the nucleus (Figure 6C), and explains the decrease in IFNB1 production (Figure S6) and the increase in viral protein expression in SeV in A549 and HEK 293T cells similar to KPNB1 silencing (Figures 2 and S3). However, it does not explain the increase in ISG56 levels in A549 cells at 8 hours and 24 hours post-infection (Figure 2). It has been shown in HEK 293

cells that overexpression of ISG56 reduces the activation of transcription factors induced by a SeV infection such as IRF3, NF-kB p65, and the IFNB1 promoter [334] by negatively regulating TBK1 activation by MAVS [335]. If this evidence is applicable to A549 cells, then CSE1L knockdown, through an unknown mechanism, causes a dramatic increase in ISG56 expression at 8 hours post-infection in comparison to normal levels (Figure 2), which results in a decrease in IRF3 and p65 nuclear translocation, due to lack of activation, and thus the decrease in IFNB1 expression (Figure S6).

The factors involved in mRNA export overall seem to have negative effect on the nuclear translocation of both transcription factors over the time course of the infection (Figure 6D), which could suggest that possibly the mRNA export of these transcription factors are decreased, which by consequence leads to less of these factors in the cytoplasm to be translocated to the nucleus. NXF1 and NXT1 had the greatest effects on the translocation with NXT1 surprisingly having a greater overall effect than by NXF1, the main mRNA export factor. NXT1's main role is to bind to the FG repeats of Nups to mediate the mRNA export by NXF1 [95-97], suggesting that interacting with the NPC is vital for efficient mRNA export through the central channel. A possibility why the NXF1 silencing does not affect the nuclear translocation of IRF3 and p65 as much as NXT1 may be due to NXF2 or even NXF3 compensation for the lack of NXF1, especially since NXF2 can form a heterodimer with NXT1 [103] and NXF3 can utilize XPO1 for mRNA export [104]. NXF1, NXT1 and NXT2 silencing decreased IFNB1 production, which correlates with the decrease in the two transcription factors (Figure S7). However, NXF2 silencing has no effect on IFNB1 production, which suggests the effect of NXF2 silencing on the nuclear translocation of IRF3 and p65 early in the response may be compensating in order for IFNB1 production to remain at normal induction levels.

The RAN gradient is the most important regulator of nucleocytoplasmic transport, so it is not surprising that silencing RAN has a major negative effect on the translocation of both factors (Figure 6E). This may be the reason how EMCV, a virus of the cytoplasmic-replicating picornaviruses, by binding to RAN via its Leader protein, can disrupt nucleocytoplasmic transport, and thus successfully inhibit IFN activity to evade the innate antiviral response [307]. An interesting note is that NUTF2 and RCC1 have similar effects to one another on the

translocation of these transcription factors with IRF3 being less affected by the silencing than p65. NUTF2 is responsible for recycling RanGDP back to the nucleus, and RCC1 is responsible for exchanging the GDP to GTP for the formation of export complexes and the dissociation of import complexes [44], therefore the lack of RanGDP or RanGTP in the nucleus can affect nuclear transport, especially for p65. The silencing of these genes involved in the RAN gradient decrease IFNB1 production to similar levels (Figure S8), suggesting that this process is important for ensuring proper nucleocytoplasmic transport of factors important for IFNB1 production.

The cytoplasmic FG-Nups and filaments overall had a negative effect on the translocation of both transcription when they are silenced, except for NUPL2, whose protein export activity via XPO1 [114, 115] was shown in the nuclear retention of IRF3 in the first hour of infection and p65 during the last half of the infection (Figure 7A). RANBP2 is the main docking site for several import carriers [116-119], and XPO1 and NXF1-mediated export [95, 120]. However, if RANBP2 did play a significant role, its silencing should block all import of these transcription factors, however it seems that RANBP2 acts as a facilitator of nucleocytoplasmic transport. The silencing of cytoplasmic FG-Nups had an overall decrease in IFNB1 production, which correlates with the overall negative effect on nuclear translocation of the transcription factors (Figure S9). Interestingly, HIV-1 targets all of these Nups where NUPL2 aids in the nuclear docking of a viral protein [224], RANBP2 is involved in the nuclear import of the pre-integration complex [222], and NUP214 is recruited by Rev for XPO1-mediated Rev export [227].

The outer-ring Nups tested all belong to the NUP107-160 complex, which are involved in the nuclear import of NLS-containing cargoes [112], as well as regulating the diameter of NPCs [142]. This explains the significant decrease in the nuclear translocation of both transcription factors in the nucleus, especially during the first half (1 to 5 hours) of infection (Figure 7B), which correlates with the decrease in IFNB1 production (Figure S10). These results suggest that not only is nuclear import affected, but the diameter of the pore may not be of adequate size when these Nups are silenced, physically blocking their nuclear entry.

The linker Nup NUP93 is extremely important for the proper assembly of the NPC, especially the recruitment of NUP62 for transport competency in these structures. It is not a

surprise that the silencing of this Nup would decrease the translocation of both transcription factors (Figure 7C), as well as the IFNB1 production (Figure S11) which was previously shown in Baril et al. [336]. Nup88 silencing decreases IRF3 and p65 nuclear translocation early in the response (Figure 7C), which corresponds to the reduction in IFNB1 (Figure S11). Interestingly, NUP88 is known to mediate XPO1 export with NUP214 [128], which previously discussed decrease IFNB1 production when silenced.

The central FG-Nups are extremely important in nucleocytoplasmic transport. The nucleoporins that are part of the NUP62 complex (NUP54, and NUPL1 which encodes NUP58/NUP45) significantly reduce nuclear translocation of both transcription factors when they are silenced, in comparison to NUP35 which does not have such a strong phenotype (Figure 7D). These decreases in nuclear translocation of IRF3 and p65 correspond with the decrease in IFNB1 production for these Nups (Figure S12).

Overall, silencing of Nups reduced the translocation of both transcription factors during the first five hours of infection (Figure 7), while nucleocytoplasmic transporters had differential effects, depending on their function (Figure 6).

3.6 Perspectives

Future works would require validation experiments for the microscopy results, as well as experiments to elucidate the mechanism by which selected hits affect the nuclear transport of IRF3 and p65 and IFNB1 production. This would provide details as to why certain transporters and Nups are targeted by viruses to evade the innate antiviral response and promote their viral replication and growth in the cell.

The validation of the efficacy of the knockdown by shRNAs by measuring mRNA levels via qPCR is essential to making sure that the shRNA is specifically affecting the expression of the gene of interest, and not an off-target effect. Once that is validated, rescue experiments would be performed by overexpressing the gene of interest and see if it rescues the phenotype for IFNB1 expression, as well its effect on IRF3 and/or p65 nuclear translocation, which would confirm that the effect is due to this gene and not an off-target effect by the shRNA. Another experiment would be to determine if there is redundancy between transporters and between nucleoporins in their respective functional and structural groups by knocking down the genes two at a time by shRNA. Also, measuring viral protein and ISG56 expression, which was done on the five main nucleocytoplasmic transporters, would help to isolate key factors like KPNB1 when silenced.

Another important point to determine is if IRF3 and p65 are actually cargoes of certain transporters or Nups to explain their effect on the translocation of these transcription factors. An 10-hour SeV infection time course would be required where co-immunoprecipitations using FLAG-tagged IRF3 and p65, as well as endogenous IPs to measure physiological levels of these transcription factors to determine at which point during the innate antiviral response do these transcription factors interact with Nups or transporters to enter and exit the nucleus. This would also show the dynamics of the transport and elucidate time-sensitive players.

Another experiment would be to validate the microscopy results from the Kapα adaptor proteins, where each one would be silenced and determine whether the other adaptors can compensate for the lack of the other for the nuclear transport of IRF3 and p65.

There was one study that proposed the idea that transporters may be interacting with their cargoes, but not through a NLS or NES, which was the case for a p65 study where it was

determined that IPO8 and XPO7 were involved in the nuclear import of p65 in a NLS-independent manner [325]. This can be done by using peptides containing a NLS or NES which can compete for the binding of transporters to IRF3 or p65. If the NLS or NES peptides do not prevent binding of a transporter to these transcription factors, then it would be plausible that the interaction is not based on these signals, but could be through special structural domains or motifs.

Another experiment of interest would be to use different stimulations to promote the translocation of IRF3 and p65 to the nucleus. In the case of p65, TNF-α stimulation induces nuclear translocation of this factor within an hour [325], in comparison to SeV infection which requires at least five hours for peak p65 translocation into the nucleus in A549 cells. This can provide another layer of transport dynamics and may elucidate transporters which move faster than others in terms of cargo transport.

The understanding of the mechanistic details of these transporters and nucleoporins in how they affect the nucleocytoplasmic transport of IRF3 and p65 during the innate antiviral response can be brought over to other times of viral infections such as in HIV-1 and Influenza A virus (IAV), two RNA viruses which require entry into the nucleus for viral replication. In terms of evading the innate antiviral response by targeting Nups and transporters, this would allow us to identify similarities between RNA viruses in general, and differences between viruses that replicate in the nucleus (HIV-1, IAV) and viruses that replicate in the cytoplasm (HCV, SeV).

In order to come full circle with this study, it is important to validate the relationship between the innate antiviral response and the NPC and its transporters in the context of a HCV infection in liver cells. The composition of the NPC and its transporters differ from one cell line to another [337] and one context to another [338], and therefore the dynamics between this complex and the innate response in A549 cells upon SeV infection cannot be comparable to that in Huh7 cells upon HCV infection. However, the goal of the study is to determine complexes or processes that can be utilized by a wide variety of viruses to circumvent the innate antiviral response, in which the NPC and its transporters are a plausible target based on the results of this study and in the literature.

Conclusion

This project started from the hypothesis that viral-host interactors are playing a role in the evasion of the innate antiviral response as part of a mechanism by the virus for conferring a growth advantage. This led to the identification of proteins involved in nucleocytoplasmic transport, which had a modulatory effect on viral replication as well as on the innate antiviral response.

Further mechanistic studies determined that the effect of these proteins on the innate antiviral response may be due to their effect on the nuclear translocation of key transcription factors. The development of a microscopy-based RNAi screen assessed multiple genes associated with transport, as well as the nuclear pore complex, to determine that indeed these proteins do affect the transport of these factors during a viral infection. This supports the fact this family of proteins is targeted by many types of viruses for the evasion of the immune response.

The research in this Master's thesis has paved a new road in understanding the mechanisms by which transcription factors such as IRF3 and NF-kB p65 enter and exit the nucleus, as part of the first phase of the innate antiviral response, in relation to the nucleoporins and nucleocytoplasmic transporters which mediate trafficking across the nuclear pore complex. These results are a valuable stepping stone in understanding the dynamics of the innate immune response through the trafficking of the nuclear localization of these transcription factors, as well as a starting point to study the trafficking of these factors during the response in the context of other viral infections for the goal of elucidating novel panviral targets for future therapeutics.

Bibliography

1. Messina JP, Humphreys I, Flaxman A, Brown A, Cooke GS, Pybus OG, et al. Global distribution and prevalence of hepatitis C virus genotypes. Hepatology. 2014. doi: 10.1002/hep.27259. PubMed PMID: 25069599.
2. Horner SM. Activation and evasion of antiviral innate immunity by hepatitis C virus. Journal of molecular biology. 2014;426(6):1198-209. doi: 10.1016/j.jmb.2013.10.032. PubMed PMID: 24184198.
3. Kim CW, Chang KM. Hepatitis C virus: virology and life cycle. Clinical and molecular hepatology. 2013;19(1):17-25. doi: 10.3350/cmh.2013.19.1.17. PubMed PMID: 23593605; PubMed Central PMCID: PMC3622851.
4. Lohmann V, Bartenschlager R. On the history of hepatitis C virus cell culture systems. Journal of medicinal chemistry. 2014;57(5):1627-42. doi: 10.1021/jm401401n. PubMed PMID: 24164647.
5. Chevaliez S, Pawlotsky JM. Virology of hepatitis C virus infection. Best practice & research Clinical gastroenterology. 2012;26(4):381-9. doi: 10.1016/j.bpg.2012.09.006. PubMed PMID: 23199498.
6. Foster TL, Belyaeva T, Stonehouse NJ, Pearson AR, Harris M. All three domains of the hepatitis C virus nonstructural NS5A protein contribute to RNA binding. Journal of virology. 2010;84(18):9267-77. doi: 10.1128/JVI.00616-10. PubMed PMID: 20592076; PubMed Central PMCID: PMC2937630.
7. Appel N, Zayas M, Miller S, Krijnse-Locker J, Schaller T, Friebe P, et al. Essential role of domain III of nonstructural protein 5A for hepatitis C virus infectious particle assembly. PLoS pathogens. 2008;4(3):e1000035. doi: 10.1371/journal.ppat.1000035. PubMed PMID: 18369481; PubMed Central PMCID: PMC2268006.
8. Jirasko V, Montserret R, Lee JY, Gouttenoire J, Moradpour D, Penin F, et al. Structural and functional studies of nonstructural protein 2 of the hepatitis C virus reveal its key role as organizer of virion assembly. PLoS pathogens. 2010;6(12):e1001233. doi: 10.1371/journal.ppat.1001233. PubMed PMID: 21187906; PubMed Central PMCID: PMC3002993.
9. Popescu CI, Callens N, Trinel D, Roingeard P, Moradpour D, Descamps V, et al. NS2 protein of hepatitis C virus interacts with structural and non-structural proteins towards virus assembly. PLoS pathogens. 2011;7(2):e1001278. doi: 10.1371/journal.ppat.1001278. PubMed PMID: 21347350; PubMed Central PMCID: PMC3037360.
10. Lindenbach BD, Rice CM. The ins and outs of hepatitis C virus entry and assembly. Nature reviews Microbiology. 2013;11(10):688-700. doi: 10.1038/nrmicro3098. PubMed PMID: 24018384; PubMed Central PMCID: PMC3897199.
11. Blight KJ, McKeating JA, Rice CM. Highly permissive cell lines for subgenomic and genomic hepatitis C virus RNA replication. Journal of virology. 2002;76(24):13001-14. PubMed PMID: 12438626; PubMed Central PMCID: PMC136668.
12. Sumpter R, Jr., Loo YM, Foy E, Li K, Yoneyama M, Fujita T, et al. Regulating intracellular antiviral defense and permissiveness to hepatitis C virus RNA replication through a cellular RNA helicase, RIG-I. Journal of virology. 2005;79(5):2689-99. doi:

10.1128/JVI.79.5.2689-2699.2005. PubMed PMID: 15708988; PubMed Central PMCID: PMC548482.
13. Vercauteren K, de Jong YP, Meuleman P. HCV animal models and liver disease. Journal of hepatology. 2014;61(1 Suppl):S26-33. doi: 10.1016/j.jhep.2014.07.013. PubMed PMID: 25443343.
14. Mercer DF, Schiller DE, Elliott JF, Douglas DN, Hao C, Rinfret A, et al. Hepatitis C virus replication in mice with chimeric human livers. Nat Med. 2001;7(8):927-33. doi: 10.1038/90968. PubMed PMID: 11479625.
15. Bukh J, Meuleman P, Tellier R, Engle RE, Feinstone SM, Eder G, et al. Challenge pools of hepatitis C virus genotypes 1-6 prototype strains: replication fitness and pathogenicity in chimpanzees and human liver-chimeric mouse models. J Infect Dis. 2010;201(9):1381-9. doi: 10.1086/651579. PubMed PMID: 20353362; PubMed Central PMCID: PMC2941994.
16. Li Q, Zhang YY, Chiu S, Hu Z, Lan KH, Cha H, et al. Integrative functional genomics of hepatitis C virus infection identifies host dependencies in complete viral replication cycle. PLoS pathogens. 2014;10(5):e1004163. doi: 10.1371/journal.ppat.1004163. PubMed PMID: 24852294; PubMed Central PMCID: PMC4095987.
17. Ng TI, Mo H, Pilot-Matias T, He Y, Koev G, Krishnan P, et al. Identification of host genes involved in hepatitis C virus replication by small interfering RNA technology. Hepatology. 2007;45(6):1413-21. doi: 10.1002/hep.21608. PubMed PMID: 17518369.
18. Randall G, Panis M, Cooper JD, Tellinghuisen TL, Sukhodolets KE, Pfeffer S, et al. Cellular cofactors affecting hepatitis C virus infection and replication. Proceedings of the National Academy of Sciences of the United States of America. 2007;104(31):12884-9. doi: 10.1073/pnas.0704894104. PubMed PMID: 17616579; PubMed Central PMCID: PMC1937561.
19. Germain MA, Chatel-Chaix L, Gagne B, Bonneil E, Thibault P, Pradezynski F, et al. Elucidating novel hepatitis C virus-host interactions using combined mass spectrometry and functional genomics approaches. Molecular & cellular proteomics : MCP. 2014;13(1):184-203. doi: 10.1074/mcp.M113.030155. PubMed PMID: 24169621; PubMed Central PMCID: PMC3879614.
20. Douam F, Lavillette D, Cosset FL. The mechanism of HCV entry into host cells. Progress in molecular biology and translational science. 2015;129:63-107. doi: 10.1016/bs.pmbts.2014.10.003. PubMed PMID: 25595801.
21. Henke JI, Goergen D, Zheng J, Song Y, Schuttler CG, Fehr C, et al. microRNA-122 stimulates translation of hepatitis C virus RNA. The EMBO journal. 2008;27(24):3300-10. doi: 10.1038/emboj.2008.244. PubMed PMID: 19020517; PubMed Central PMCID: PMC2586803.
22. Jopling CL, Schutz S, Sarnow P. Position-dependent function for a tandem microRNA miR-122-binding site located in the hepatitis C virus RNA genome. Cell host & microbe. 2008;4(1):77-85. doi: 10.1016/j.chom.2008.05.013. PubMed PMID: 18621012; PubMed Central PMCID: PMC3519368.
23. Jopling CL, Yi M, Lancaster AM, Lemon SM, Sarnow P. Modulation of hepatitis C virus RNA abundance by a liver-specific MicroRNA. Science. 2005;309(5740):1577-81. doi: 10.1126/science.1113329. PubMed PMID: 16141076.
24. Chatel-Chaix L, Melancon P, Racine ME, Baril M, Lamarre D. Y-box-binding protein 1 interacts with hepatitis C virus NS3/4A and influences the equilibrium between viral RNA

replication and infectious particle production. Journal of virology. 2011;85(21):11022-37. doi: 10.1128/JVI.00719-11. PubMed PMID: 21849455; PubMed Central PMCID: PMC3194978.
25. Chatel-Chaix L, Germain MA, Motorina A, Bonneil E, Thibault P, Baril M, et al. A host YB-1 ribonucleoprotein complex is hijacked by hepatitis C virus for the control of NS3-dependent particle production. Journal of virology. 2013;87(21):11704-20. doi: 10.1128/JVI.01474-13. PubMed PMID: 23986595; PubMed Central PMCID: PMC3807372.
26. Yang F, Robotham JM, Grise H, Frausto S, Madan V, Zayas M, et al. A major determinant of cyclophilin dependence and cyclosporine susceptibility of hepatitis C virus identified by a genetic approach. PLoS pathogens. 2010;6(9):e1001118. doi: 10.1371/journal.ppat.1001118. PubMed PMID: 20886100; PubMed Central PMCID: PMC2944805.
27. Grise H, Frausto S, Logan T, Tang H. A conserved tandem cyclophilin-binding site in hepatitis C virus nonstructural protein 5A regulates Alisporivir susceptibility. Journal of virology. 2012;86(9):4811-22. doi: 10.1128/JVI.06641-11. PubMed PMID: 22345441; PubMed Central PMCID: PMC3347344.
28. Okamoto T, Nishimura Y, Ichimura T, Suzuki K, Miyamura T, Suzuki T, et al. Hepatitis C virus RNA replication is regulated by FKBP8 and Hsp90. The EMBO journal. 2006;25(20):5015-25. doi: 10.1038/sj.emboj.7601367. PubMed PMID: 17024179; PubMed Central PMCID: PMC1618089.
29. Reiss S, Rebhan I, Backes P, Romero-Brey I, Erfle H, Matula P, et al. Recruitment and activation of a lipid kinase by hepatitis C virus NS5A is essential for integrity of the membranous replication compartment. Cell host & microbe. 2011;9(1):32-45. doi: 10.1016/j.chom.2010.12.002. PubMed PMID: 21238945; PubMed Central PMCID: PMC3433060.
30. Berger KL, Kelly SM, Jordan TX, Tartell MA, Randall G. Hepatitis C virus stimulates the phosphatidylinositol 4-kinase III alpha-dependent phosphatidylinositol 4-phosphate production that is essential for its replication. Journal of virology. 2011;85(17):8870-83. doi: 10.1128/JVI.00059-11. PubMed PMID: 21697487; PubMed Central PMCID: PMC3165839.
31. Tai AW, Salloum S. The role of the phosphatidylinositol 4-kinase PI4KA in hepatitis C virus-induced host membrane rearrangement. PloS one. 2011;6(10):e26300. doi: 10.1371/journal.pone.0026300. PubMed PMID: 22022594; PubMed Central PMCID: PMC3192179.
32. Burckstummer T, Kriegs M, Lupberger J, Pauli EK, Schmittel S, Hildt E. Raf-1 kinase associates with Hepatitis C virus NS5A and regulates viral replication. FEBS letters. 2006;580(2):575-80. doi: 10.1016/j.febslet.2005.12.071. PubMed PMID: 16405965.
33. Vogt DA, Camus G, Herker E, Webster BR, Tsou CL, Greene WC, et al. Lipid droplet-binding protein TIP47 regulates hepatitis C Virus RNA replication through interaction with the viral NS5A protein. PLoS pathogens. 2013;9(4):e1003302. doi: 10.1371/journal.ppat.1003302. PubMed PMID: 23593007; PubMed Central PMCID: PMC3623766.
34. Evans MJ, Rice CM, Goff SP. Phosphorylation of hepatitis C virus nonstructural protein 5A modulates its protein interactions and viral RNA replication. Proceedings of the National Academy of Sciences of the United States of America. 2004;101(35):13038-43. doi: 10.1073/pnas.0405152101. PubMed PMID: 15326295; PubMed Central PMCID: PMC516513.

35. Liu Z, Yang F, Robotham JM, Tang H. Critical role of cyclophilin A and its prolyl-peptidyl isomerase activity in the structure and function of the hepatitis C virus replication complex. Journal of virology. 2009;83(13):6554-65. doi: 10.1128/JVI.02550-08. PubMed PMID: 19386705; PubMed Central PMCID: PMC2698523.
36. Kim CS, Seol SK, Song OK, Park JH, Jang SK. An RNA-binding protein, hnRNP A1, and a scaffold protein, septin 6, facilitate hepatitis C virus replication. Journal of virology. 2007;81(8):3852-65. doi: 10.1128/JVI.01311-06. PubMed PMID: 17229681; PubMed Central PMCID: PMC1866118.
37. Poenisch M, Metz P, Blankenburg H, Ruggieri A, Lee JY, Rupp D, et al. Identification of HNRNPK as regulator of hepatitis C virus particle production. PLoS pathogens. 2015;11(1):e1004573. doi: 10.1371/journal.ppat.1004573. PubMed PMID: 25569684; PubMed Central PMCID: PMC4287573.
38. Salloum S, Wang H, Ferguson C, Parton RG, Tai AW. Rab18 binds to hepatitis C virus NS5A and promotes interaction between sites of viral replication and lipid droplets. PLoS pathogens. 2013;9(8):e1003513. doi: 10.1371/journal.ppat.1003513. PubMed PMID: 23935497; PubMed Central PMCID: PMC3731246.
39. Suzuki R, Sakamoto S, Tsutsumi T, Rikimaru A, Tanaka K, Shimoike T, et al. Molecular determinants for subcellular localization of hepatitis C virus core protein. Journal of virology. 2005;79(2):1271-81. doi: 10.1128/JVI.79.2.1271-1281.2005. PubMed PMID: 15613354; PubMed Central PMCID: PMC538550.
40. Cerutti A, Maillard P, Minisini R, Vidalain PO, Roohvand F, Pecheur EI, et al. Identification of a functional, CRM-1-dependent nuclear export signal in hepatitis C virus core protein. PloS one. 2011;6(10):e25854. doi: 10.1371/journal.pone.0025854. PubMed PMID: 22039426; PubMed Central PMCID: PMC3200325.
41. Neufeldt CJ, Joyce MA, Levin A, Steenbergen RH, Pang D, Shields J, et al. Hepatitis C virus-induced cytoplasmic organelles use the nuclear transport machinery to establish an environment conducive to virus replication. PLoS pathogens. 2013;9(10):e1003744. doi: 10.1371/journal.ppat.1003744. PubMed PMID: 24204278; PubMed Central PMCID: PMC3814334.
42. Levin A, Neufeldt CJ, Pang D, Wilson K, Loewen-Dobler D, Joyce MA, et al. Functional characterization of nuclear localization and export signals in hepatitis C virus proteins and their role in the membranous web. PloS one. 2014;9(12):e114629. doi: 10.1371/journal.pone.0114629. PubMed PMID: 25485706; PubMed Central PMCID: PMC4259358.
43. Allen TD, Cronshaw JM, Bagley S, Kiseleva E, Goldberg MW. The nuclear pore complex: mediator of translocation between nucleus and cytoplasm. Journal of cell science. 2000;113 (Pt 10):1651-9. PubMed PMID: 10769196.
44. Cook A, Bono F, Jinek M, Conti E. Structural biology of nucleocytoplasmic transport. Annu Rev Biochem. 2007;76:647-71. doi: 10.1146/annurev.biochem.76.052705.161529. PubMed PMID: 17506639.
45. Pumroy RA, Cingolani G. Diversification of importin-alpha isoforms in cellular trafficking and disease states. The Biochemical journal. 2015;466(1):13-28. doi: 10.1042/BJ20141186. PubMed PMID: 25656054.
46. Cingolani G, Bednenko J, Gillespie MT, Gerace L. Molecular basis for the recognition of a nonclassical nuclear localization signal by importin beta. Molecular cell. 2002;10(6):1345-53. PubMed PMID: 12504010.

47. Palmeri D, Malim MH. Importin beta can mediate the nuclear import of an arginine-rich nuclear localization signal in the absence of importin alpha. Molecular and cellular biology. 1999;19(2):1218-25. PubMed PMID: 9891056; PubMed Central PMCID: PMC116051.
48. Lee BJ, Cansizoglu AE, Suel KE, Louis TH, Zhang Z, Chook YM. Rules for nuclear localization sequence recognition by karyopherin beta 2. Cell. 2006;126(3):543-58. doi: 10.1016/j.cell.2006.05.049. PubMed PMID: 16901787; PubMed Central PMCID: PMC3442361.
49. Rebane A, Aab A, Steitz JA. Transportins 1 and 2 are redundant nuclear import factors for hnRNP A1 and HuR. Rna. 2004;10(4):590-9. PubMed PMID: 15037768; PubMed Central PMCID: PMC1370549.
50. Shamsher MK, Ploski J, Radu A. Karyopherin beta 2B participates in mRNA export from the nucleus. Proceedings of the National Academy of Sciences of the United States of America. 2002;99(22):14195-9. doi: 10.1073/pnas.212518199. PubMed PMID: 12384575; PubMed Central PMCID: PMC137860.
51. Lai MC, Lin RI, Tarn WY. Transportin-SR2 mediates nuclear import of phosphorylated SR proteins. Proceedings of the National Academy of Sciences of the United States of America. 2001;98(18):10154-9. doi: 10.1073/pnas.181354098. PubMed PMID: 11517331; PubMed Central PMCID: PMC56931.
52. Christ F, Thys W, De Rijck J, Gijsbers R, Albanese A, Arosio D, et al. Transportin-SR2 imports HIV into the nucleus. Current biology : CB. 2008;18(16):1192-202. doi: 10.1016/j.cub.2008.07.079. PubMed PMID: 18722123.
53. Levin A, Hayouka Z, Friedler A, Loyter A. Transportin 3 and importin alpha are required for effective nuclear import of HIV-1 integrase in virus-infected cells. Nucleus. 2010;1(5):422-31. doi: 10.4161/nucl.1.5.12903. PubMed PMID: 21326825; PubMed Central PMCID: PMC3037538.
54. Wang J, Sarkar TR, Zhou M, Sharan S, Ritt DA, Veenstra TD, et al. CCAAT/enhancer binding protein delta (C/EBPdelta, CEBPD)-mediated nuclear import of FANCD2 by IPO4 augments cellular response to DNA damage. Proceedings of the National Academy of Sciences of the United States of America. 2010;107(37):16131-6. doi: 10.1073/pnas.1002603107. PubMed PMID: 20805509; PubMed Central PMCID: PMC2941265.
55. Dhanoya A, Wang T, Keshavarz-Moore E, Fassati A, Chain BM. Importin-7 mediates nuclear trafficking of DNA in mammalian cells. Traffic. 2013;14(2):165-75. doi: 10.1111/tra.12021. PubMed PMID: 23067392; PubMed Central PMCID: PMC3672689.
56. Zaitseva L, Cherepanov P, Leyens L, Wilson SJ, Rasaiyaah J, Fassati A. HIV-1 exploits importin 7 to maximize nuclear import of its DNA genome. Retrovirology. 2009;6:11. doi: 10.1186/1742-4690-6-11. PubMed PMID: 19193229; PubMed Central PMCID: PMC2660290.
57. Jakel S, Albig W, Kutay U, Bischoff FR, Schwamborn K, Doenecke D, et al. The importin beta/importin 7 heterodimer is a functional nuclear import receptor for histone H1. The EMBO journal. 1999;18(9):2411-23. doi: 10.1093/emboj/18.9.2411. PubMed PMID: 10228156; PubMed Central PMCID: PMC1171324.
58. Dean KA, von Ahsen O, Gorlich D, Fried HM. Signal recognition particle protein 19 is imported into the nucleus by importin 8 (RanBP8) and transportin. Journal of cell science. 2001;114(Pt 19):3479-85. PubMed PMID: 11682607.

59. Weinmann L, Hock J, Ivacevic T, Ohrt T, Mutze J, Schwille P, et al. Importin 8 is a gene silencing factor that targets argonaute proteins to distinct mRNAs. Cell. 2009;136(3):496-507. doi: 10.1016/j.cell.2008.12.023. PubMed PMID: 19167051.
60. Wei Y, Li L, Wang D, Zhang CY, Zen K. Importin 8 regulates the transport of mature microRNAs into the cell nucleus. The Journal of biological chemistry. 2014;289(15):10270-5. doi: 10.1074/jbc.C113.541417. PubMed PMID: 24596094; PubMed Central PMCID: PMC4036152.
61. Quan Y, Ji ZL, Wang X, Tartakoff AM, Tao T. Evolutionary and transcriptional analysis of karyopherin beta superfamily proteins. Molecular & cellular proteomics : MCP. 2008;7(7):1254-69. doi: 10.1074/mcp.M700511-MCP200. PubMed PMID: 18353765; PubMed Central PMCID: PMC3837465.
62. Mingot JM, Kostka S, Kraft R, Hartmann E, Gorlich D. Importin 13: a novel mediator of nuclear import and export. The EMBO journal. 2001;20(14):3685-94. doi: 10.1093/emboj/20.14.3685. PubMed PMID: 11447110; PubMed Central PMCID: PMC125545.
63. Grunwald M, Lazzaretti D, Bono F. Structural basis for the nuclear export activity of Importin13. The EMBO journal. 2013;32(6):899-913. doi: 10.1038/emboj.2013.29. PubMed PMID: 23435562; PubMed Central PMCID: PMC3604722.
64. Grunwald M, Bono F. Structure of Importin13-Ubc9 complex: nuclear import and release of a key regulator of sumoylation. The EMBO journal. 2011;30(2):427-38. doi: 10.1038/emboj.2010.320. PubMed PMID: 21139563; PubMed Central PMCID: PMC3025465.
65. Jakel S, Gorlich D. Importin beta, transportin, RanBP5 and RanBP7 mediate nuclear import of ribosomal proteins in mammalian cells. The EMBO journal. 1998;17(15):4491-502. doi: 10.1093/emboj/17.15.4491. PubMed PMID: 9687515; PubMed Central PMCID: PMC1170780.
66. Chou CW, Tai LR, Kirby R, Lee IF, Lin A. Importin beta3 mediates the nuclear import of human ribosomal protein L7 through its interaction with the multifaceted basic clusters of L7. FEBS letters. 2010;584(19):4151-6. doi: 10.1016/j.febslet.2010.08.044. PubMed PMID: 20828572.
67. Plafker SM, Macara IG. Ribosomal protein L12 uses a distinct nuclear import pathway mediated by importin 11. Molecular and cellular biology. 2002;22(4):1266-75. PubMed PMID: 11809816; PubMed Central PMCID: PMC134630.
68. Kose S, Imamoto N, Tachibana T, Yoshida M, Yoneda Y. beta-subunit of nuclear pore-targeting complex (importin-beta) can be exported from the nucleus in a Ran-independent manner. The Journal of biological chemistry. 1999;274(7):3946-52. PubMed PMID: 9933584.
69. Kudo N, Wolff B, Sekimoto T, Schreiner EP, Yoneda Y, Yanagida M, et al. Leptomycin B inhibition of signal-mediated nuclear export by direct binding to CRM1. Exp Cell Res. 1998;242(2):540-7. doi: 10.1006/excr.1998.4136. PubMed PMID: 9683540.
70. Lindsay ME, Holaska JM, Welch K, Paschal BM, Macara IG. Ran-binding protein 3 is a cofactor for Crm1-mediated nuclear protein export. The Journal of cell biology. 2001;153(7):1391-402. PubMed PMID: 11425870; PubMed Central PMCID: PMC2150735.
71. Englmeier L, Fornerod M, Bischoff FR, Petosa C, Mattaj IW, Kutay U. RanBP3 influences interactions between CRM1 and its nuclear protein export substrates. EMBO

reports. 2001;2(10):926-32. doi: 10.1093/embo-reports/kve200. PubMed PMID: 11571268; PubMed Central PMCID: PMC1084078.
72. Nemergut ME, Lindsay ME, Brownawell AM, Macara IG. Ran-binding protein 3 links Crm1 to the Ran guanine nucleotide exchange factor. The Journal of biological chemistry. 2002;277(20):17385-8. doi: 10.1074/jbc.C100620200. PubMed PMID: 11932251.
73. Stuven T, Hartmann E, Gorlich D. Exportin 6: a novel nuclear export receptor that is specific for profilin.actin complexes. The EMBO journal. 2003;22(21):5928-40. doi: 10.1093/emboj/cdg565. PubMed PMID: 14592989; PubMed Central PMCID: PMC275422.
74. Park SH, Park TJ, Lim IK. Reduction of exportin 6 activity leads to actin accumulation via failure of RanGTP restoration and NTF2 sequestration in the nuclei of senescent cells. Exp Cell Res. 2011;317(7):941-54. doi: 10.1016/j.yexcr.2010.12.023. PubMed PMID: 21195711.
75. Mingot JM, Bohnsack MT, Jakle U, Gorlich D. Exportin 7 defines a novel general nuclear export pathway. The EMBO journal. 2004;23(16):3227-36. doi: 10.1038/sj.emboj.7600338. PubMed PMID: 15282546; PubMed Central PMCID: PMC514512.
76. Kutay U, Lipowsky G, Izaurralde E, Bischoff FR, Schwarzmaier P, Hartmann E, et al. Identification of a tRNA-specific nuclear export receptor. Molecular cell. 1998;1(3):359-69. PubMed PMID: 9660920.
77. Kuersten S, Arts GJ, Walther TC, Englmeier L, Mattaj IW. Steady-state nuclear localization of exportin-t involves RanGTP binding and two distinct nuclear pore complex interaction domains. Molecular and cellular biology. 2002;22(16):5708-20. PubMed PMID: 12138183; PubMed Central PMCID: PMC133969.
78. Lipowsky G, Bischoff FR, Schwarzmaier P, Kraft R, Kostka S, Hartmann E, et al. Exportin 4: a mediator of a novel nuclear export pathway in higher eukaryotes. The EMBO journal. 2000;19(16):4362-71. doi: 10.1093/emboj/19.16.4362. PubMed PMID: 10944119; PubMed Central PMCID: PMC302028.
79. Kurisaki A, Kurisaki K, Kowanetz M, Sugino H, Yoneda Y, Heldin CH, et al. The mechanism of nuclear export of Smad3 involves exportin 4 and Ran. Molecular and cellular biology. 2006;26(4):1318-32. doi: 10.1128/MCB.26.4.1318-1332.2006. PubMed PMID: 16449645; PubMed Central PMCID: PMC1367208.
80. Gontan C, Guttler T, Engelen E, Demmers J, Fornerod M, Grosveld FG, et al. Exportin 4 mediates a novel nuclear import pathway for Sox family transcription factors. The Journal of cell biology. 2009;185(1):27-34. doi: 10.1083/jcb.200810106. PubMed PMID: 19349578; PubMed Central PMCID: PMC2700522.
81. Brownawell AM, Macara IG. Exportin-5, a novel karyopherin, mediates nuclear export of double-stranded RNA binding proteins. The Journal of cell biology. 2002;156(1):53-64. doi: 10.1083/jcb.200110082. PubMed PMID: 11777942; PubMed Central PMCID: PMC2173575.
82. Gwizdek C, Ossareh-Nazari B, Brownawell AM, Evers S, Macara IG, Dargemont C. Minihelix-containing RNAs mediate exportin-5-dependent nuclear export of the double-stranded RNA-binding protein ILF3. The Journal of biological chemistry. 2004;279(2):884-91. doi: 10.1074/jbc.M306808200. PubMed PMID: 14570900.
83. Bohnsack MT, Regener K, Schwappach B, Saffrich R, Paraskeva E, Hartmann E, et al. Exp5 exports eEF1A via tRNA from nuclei and synergizes with other transport pathways to confine translation to the cytoplasm. The EMBO journal. 2002;21(22):6205-15. PubMed PMID: 12426392; PubMed Central PMCID: PMC137205.

84. Wild T, Horvath P, Wyler E, Widmann B, Badertscher L, Zemp I, et al. A protein inventory of human ribosome biogenesis reveals an essential function of exportin 5 in 60S subunit export. PLoS Biol. 2010;8(10):e1000522. doi: 10.1371/journal.pbio.1000522. PubMed PMID: 21048991; PubMed Central PMCID: PMC2964341.
85. Bennasser Y, Chable-Bessia C, Triboulet R, Gibbings D, Gwizdek C, Dargemont C, et al. Competition for XPO5 binding between Dicer mRNA, pre-miRNA and viral RNA regulates human Dicer levels. Nature structural & molecular biology. 2011;18(3):323-7. doi: 10.1038/nsmb.1987. PubMed PMID: 21297638; PubMed Central PMCID: PMC3595992.
86. O'Reilly AJ, Dacks JB, Field MC. Evolution of the karyopherin-beta family of nucleocytoplasmic transport factors; ancient origins and continued specialization. PloS one. 2011;6(4):e19308. doi: 10.1371/journal.pone.0019308. PubMed PMID: 21556326; PubMed Central PMCID: PMC3083441.
87. Chook YM, Suel KE. Nuclear import by karyopherin-betas: recognition and inhibition. Biochimica et biophysica acta. 2011;1813(9):1593-606. doi: 10.1016/j.bbamcr.2010.10.014. PubMed PMID: 21029754; PubMed Central PMCID: PMC3135726.
88. Takai Y, Sasaki T, Matozaki T. Small GTP-binding proteins. Physiol Rev. 2001;81(1):153-208. PubMed PMID: 11152757.
89. Wennerberg K, Rossman KL, Der CJ. The Ras superfamily at a glance. Journal of cell science. 2005;118(Pt 5):843-6. doi: 10.1242/jcs.01660. PubMed PMID: 15731001.
90. Weis K. Regulating access to the genome: nucleocytoplasmic transport throughout the cell cycle. Cell. 2003;112(4):441-51. PubMed PMID: 12600309.
91. Bischoff FR, Gorlich D. RanBP1 is crucial for the release of RanGTP from importin beta-related nuclear transport factors. FEBS letters. 1997;419(2-3):249-54. PubMed PMID: 9428644.
92. Matunis MJ, Wu J, Blobel G. SUMO-1 modification and its role in targeting the Ran GTPase-activating protein, RanGAP1, to the nuclear pore complex. The Journal of cell biology. 1998;140(3):499-509. PubMed PMID: 9456312; PubMed Central PMCID: PMC2140169.
93. Plafker K, Macara IG. Facilitated nucleocytoplasmic shuttling of the Ran binding protein RanBP1. Molecular and cellular biology. 2000;20(10):3510-21. PubMed PMID: 10779340; PubMed Central PMCID: PMC85643.
94. Kang Y, Bogerd HP, Yang J, Cullen BR. Analysis of the RNA binding specificity of the human tap protein, a constitutive transport element-specific nuclear RNA export factor. Virology. 1999;262(1):200-9. doi: 10.1006/viro.1999.9906. PubMed PMID: 10489353.
95. Levesque L, Bor YC, Matzat LH, Jin L, Berberoglu S, Rekosh D, et al. Mutations in tap uncouple RNA export activity from translocation through the nuclear pore complex. Molecular biology of the cell. 2006;17(2):931-43. doi: 10.1091/mbc.E04-07-0634. PubMed PMID: 16314397; PubMed Central PMCID: PMC1356601.
96. Matzat LH, Berberoglu S, Levesque L. Formation of a Tap/NXF1 homotypic complex is mediated through the amino-terminal domain of Tap and enhances interaction with nucleoporins. Molecular biology of the cell. 2008;19(1):327-38. doi: 10.1091/mbc.E07-03-0255. PubMed PMID: 17978099; PubMed Central PMCID: PMC2174195.
97. Levesque L, Guzik B, Guan T, Coyle J, Black BE, Rekosh D, et al. RNA export mediated by tap involves NXT1-dependent interactions with the nuclear pore complex. The Journal of biological chemistry. 2001;276(48):44953-62. doi: 10.1074/jbc.M106558200. PubMed PMID: 11579093.

98. Jin L, Guzik BW, Bor YC, Rekosh D, Hammarskjold ML. Tap and NXT promote translation of unspliced mRNA. Genes & development. 2003;17(24):3075-86. doi: 10.1101/gad.1155703. PubMed PMID: 14701875; PubMed Central PMCID: PMC305259.
99. Herold A, Suyama M, Rodrigues JP, Braun IC, Kutay U, Carmo-Fonseca M, et al. TAP (NXF1) belongs to a multigene family of putative RNA export factors with a conserved modular architecture. Molecular and cellular biology. 2000;20(23):8996-9008. PubMed PMID: 11073998; PubMed Central PMCID: PMC86553.
100. Carmody SR, Wente SR. mRNA nuclear export at a glance. Journal of cell science. 2009;122(Pt 12):1933-7. doi: 10.1242/jcs.041236. PubMed PMID: 19494120; PubMed Central PMCID: PMC2723150.
101. Viphakone N, Hautbergue GM, Walsh M, Chang CT, Holland A, Folco EG, et al. TREX exposes the RNA-binding domain of Nxf1 to enable mRNA export. Nat Commun. 2012;3:1006. doi: 10.1038/ncomms2005. PubMed PMID: 22893130; PubMed Central PMCID: PMC3654228.
102. Takano K, Miki T, Katahira J, Yoneda Y. NXF2 is involved in cytoplasmic mRNA dynamics through interactions with motor proteins. Nucleic acids research. 2007;35(8):2513-21. doi: 10.1093/nar/gkm125. PubMed PMID: 17403691; PubMed Central PMCID: PMC1885657.
103. Kerkow DE, Carmel AB, Menichelli E, Ambrus G, Hills RD, Jr., Gerace L, et al. The structure of the NXF2/NXT1 heterodimeric complex reveals the combined specificity and versatility of the NTF2-like fold. Journal of molecular biology. 2012;415(4):649-65. doi: 10.1016/j.jmb.2011.11.027. PubMed PMID: 22123199; PubMed Central PMCID: PMC3265607.
104. Yang J, Bogerd HP, Wang PJ, Page DC, Cullen BR. Two closely related human nuclear export factors utilize entirely distinct export pathways. Molecular cell. 2001;8(2):397-406. PubMed PMID: 11545741.
105. Black BE, Holaska JM, Levesque L, Ossareh-Nazari B, Gwizdek C, Dargemont C, et al. NXT1 is necessary for the terminal step of Crm1-mediated nuclear export. The Journal of cell biology. 2001;152(1):141-55. PubMed PMID: 11149927; PubMed Central PMCID: PMC2193657.
106. Alcazar-Roman AR, Tran EJ, Guo S, Wente SR. Inositol hexakisphosphate and Gle1 activate the DEAD-box protein Dbp5 for nuclear mRNA export. Nature cell biology. 2006;8(7):711-6. doi: 10.1038/ncb1427. PubMed PMID: 16783363.
107. Weirich CS, Erzberger JP, Flick JS, Berger JM, Thorner J, Weis K. Activation of the DExD/H-box protein Dbp5 by the nuclear-pore protein Gle1 and its coactivator InsP6 is required for mRNA export. Nature cell biology. 2006;8(7):668-76. doi: 10.1038/ncb1424. PubMed PMID: 16783364.
108. von Moeller H, Basquin C, Conti E. The mRNA export protein DBP5 binds RNA and the cytoplasmic nucleoporin NUP214 in a mutually exclusive manner. Nature structural & molecular biology. 2009;16(3):247-54. doi: 10.1038/nsmb.1561. PubMed PMID: 19219046.
109. Rayala HJ, Kendirgi F, Barry DM, Majerus PW, Wente SR. The mRNA export factor human Gle1 interacts with the nuclear pore complex protein Nup155. Molecular & cellular proteomics : MCP. 2004;3(2):145-55. doi: 10.1074/mcp.M300106-MCP200. PubMed PMID: 14645504.
110. Kendirgi F, Rexer DJ, Alcazar-Roman AR, Onishko HM, Wente SR. Interaction between the shuttling mRNA export factor Gle1 and the nucleoporin hCG1: a conserved

mechanism in the export of Hsp70 mRNA. Molecular biology of the cell. 2005;16(9):4304-15. doi: 10.1091/mbc.E04-11-0998. PubMed PMID: 16000379; PubMed Central PMCID: PMC1196339.
111. Hoelz A, Debler EW, Blobel G. The structure of the nuclear pore complex. Annu Rev Biochem. 2011;80:613-43. doi: 10.1146/annurev-biochem-060109-151030. PubMed PMID: 21495847.
112. Grossman E, Medalia O, Zwerger M. Functional architecture of the nuclear pore complex. Annu Rev Biophys. 2012;41:557-84. doi: 10.1146/annurev-biophys-050511-102328. PubMed PMID: 22577827.
113. Cautain B, Hill R, de Pedro N, Link W. Components and regulation of nuclear transport processes. The FEBS journal. 2015;282(3):445-62. doi: 10.1111/febs.13163. PubMed PMID: 25429850.
114. Waldmann I, Spillner C, Kehlenbach RH. The nucleoporin-like protein NLP1 (hCG1) promotes CRM1-dependent nuclear protein export. Journal of cell science. 2012;125(Pt 1):144-54. doi: 10.1242/jcs.090316. PubMed PMID: 22250199.
115. Farjot G, Sergeant A, Mikaelian I. A new nucleoporin-like protein interacts with both HIV-1 Rev nuclear export signal and CRM-1. The Journal of biological chemistry. 1999;274(24):17309-17. PubMed PMID: 10358091.
116. Walde S, Thakar K, Hutten S, Spillner C, Nath A, Rothbauer U, et al. The nucleoporin Nup358/RanBP2 promotes nuclear import in a cargo- and transport receptor-specific manner. Traffic. 2012;13(2):218-33. doi: 10.1111/j.1600-0854.2011.01302.x. PubMed PMID: 21995724.
117. Hutten S, Walde S, Spillner C, Hauber J, Kehlenbach RH. The nuclear pore component Nup358 promotes transportin-dependent nuclear import. Journal of cell science. 2009;122(Pt 8):1100-10. doi: 10.1242/jcs.040154. PubMed PMID: 19299463.
118. Hamada M, Haeger A, Jeganathan KB, van Ree JH, Malureanu L, Walde S, et al. Ran-dependent docking of importin-beta to RanBP2/Nup358 filaments is essential for protein import and cell viability. The Journal of cell biology. 2011;194(4):597-612. doi: 10.1083/jcb.201102018. PubMed PMID: 21859863; PubMed Central PMCID: PMC3160583.
119. Delphin C, Guan T, Melchior F, Gerace L. RanGTP targets p97 to RanBP2, a filamentous protein localized at the cytoplasmic periphery of the nuclear pore complex. Molecular biology of the cell. 1997;8(12):2379-90. PubMed PMID: 9398662; PubMed Central PMCID: PMC25714.
120. Singh BB, Patel HH, Roepman R, Schick D, Ferreira PA. The zinc finger cluster domain of RanBP2 is a specific docking site for the nuclear export factor, exportin-1. The Journal of biological chemistry. 1999;274(52):37370-8. PubMed PMID: 10601307.
121. Mahadevan K, Zhang H, Akef A, Cui XA, Gueroussov S, Cenik C, et al. RanBP2/Nup358 potentiates the translation of a subset of mRNAs encoding secretory proteins. PLoS Biol. 2013;11(4):e1001545. doi: 10.1371/journal.pbio.1001545. PubMed PMID: 23630457; PubMed Central PMCID: PMC3635865.
122. Ferreira PA, Yunfei C, Schick D, Roepman R. The cyclophilin-like domain mediates the association of Ran-binding protein 2 with subunits of the 19 S regulatory complex of the proteasome. The Journal of biological chemistry. 1998;273(38):24676-82. PubMed PMID: 9733766.
123. Yi H, Friedman JL, Ferreira PA. The cyclophilin-like domain of Ran-binding protein-2 modulates selectively the activity of the ubiquitin-proteasome system and protein biogenesis.

The Journal of biological chemistry. 2007;282(48):34770-8. doi: 10.1074/jbc.M706903200. PubMed PMID: 17911097.
124. Bernad R, van der Velde H, Fornerod M, Pickersgill H. Nup358/RanBP2 attaches to the nuclear pore complex via association with Nup88 and Nup214/CAN and plays a supporting role in CRM1-mediated nuclear protein export. Molecular and cellular biology. 2004;24(6):2373-84. PubMed PMID: 14993277; PubMed Central PMCID: PMC355853.
125. Walther TC, Pickersgill HS, Cordes VC, Goldberg MW, Allen TD, Mattaj IW, et al. The cytoplasmic filaments of the nuclear pore complex are dispensable for selective nuclear protein import. The Journal of cell biology. 2002;158(1):63-77. doi: 10.1083/jcb.200202088. PubMed PMID: 12105182; PubMed Central PMCID: PMC2173022.
126. Boer J, Bonten-Surtel J, Grosveld G. Overexpression of the nucleoporin CAN/NUP214 induces growth arrest, nucleocytoplasmic transport defects, and apoptosis. Molecular and cellular biology. 1998;18(3):1236-47. PubMed PMID: 9488438; PubMed Central PMCID: PMC108836.
127. Roloff S, Spillner C, Kehlenbach RH. Several phenylalanine-glycine motives in the nucleoporin Nup214 are essential for binding of the nuclear export receptor CRM1. The Journal of biological chemistry. 2013;288(6):3952-63. doi: 10.1074/jbc.M112.433243. PubMed PMID: 23264634; PubMed Central PMCID: PMC3567648.
128. Hutten S, Kehlenbach RH. Nup214 is required for CRM1-dependent nuclear protein export in vivo. Molecular and cellular biology. 2006;26(18):6772-85. doi: 10.1128/MCB.00342-06. PubMed PMID: 16943420; PubMed Central PMCID: PMC1592874.
129. Bernad R, Engelsma D, Sanderson H, Pickersgill H, Fornerod M. Nup214-Nup88 nucleoporin subcomplex is required for CRM1-mediated 60 S preribosomal nuclear export. The Journal of biological chemistry. 2006;281(28):19378-86. doi: 10.1074/jbc.M512585200. PubMed PMID: 16675447.
130. Stavru F, Nautrup-Pedersen G, Cordes VC, Gorlich D. Nuclear pore complex assembly and maintenance in POM121- and gp210-deficient cells. The Journal of cell biology. 2006;173(4):477-83. doi: 10.1083/jcb.200601002. PubMed PMID: 16702234; PubMed Central PMCID: PMC2063858.
131. Hallberg E, Wozniak RW, Blobel G. An integral membrane protein of the pore membrane domain of the nuclear envelope contains a nucleoporin-like region. The Journal of cell biology. 1993;122(3):513-21. PubMed PMID: 8335683; PubMed Central PMCID: PMC2119659.
132. Mansfeld J, Guttinger S, Hawryluk-Gara LA, Pante N, Mall M, Galy V, et al. The conserved transmembrane nucleoporin NDC1 is required for nuclear pore complex assembly in vertebrate cells. Molecular cell. 2006;22(1):93-103. doi: 10.1016/j.molcel.2006.02.015. PubMed PMID: 16600873.
133. Eisenhardt N, Redolfi J, Antonin W. Interaction of Nup53 with Ndc1 and Nup155 is required for nuclear pore complex assembly. Journal of cell science. 2014;127(Pt 4):908-21. doi: 10.1242/jcs.141739. PubMed PMID: 24363447.
134. Yamazumi Y, Kamiya A, Nishida A, Nishihara A, Iemura S, Natsume T, et al. The transmembrane nucleoporin NDC1 is required for targeting of ALADIN to nuclear pore complexes. Biochemical and biophysical research communications. 2009;389(1):100-4. doi: 10.1016/j.bbrc.2009.08.096. PubMed PMID: 19703420.
135. Kind B, Koehler K, Lorenz M, Huebner A. The nuclear pore complex protein ALADIN is anchored via NDC1 but not via POM121 and GP210 in the nuclear envelope.

Biochemical and biophysical research communications. 2009;390(2):205-10. doi: 10.1016/j.bbrc.2009.09.080. PubMed PMID: 19782045.
136. Antonin W, Franz C, Haselmann U, Antony C, Mattaj IW. The integral membrane nucleoporin pom121 functionally links nuclear pore complex assembly and nuclear envelope formation. Molecular cell. 2005;17(1):83-92. doi: 10.1016/j.molcel.2004.12.010. PubMed PMID: 15629719.
137. Bodoor K, Shaikh S, Enarson P, Chowdhury S, Salina D, Raharjo WH, et al. Function and assembly of nuclear pore complex proteins. Biochemistry and cell biology = Biochimie et biologie cellulaire. 1999;77(4):321-9. PubMed PMID: 10546895.
138. Funakoshi T, Maeshima K, Yahata K, Sugano S, Imamoto F, Imamoto N. Two distinct human POM121 genes: requirement for the formation of nuclear pore complexes. FEBS letters. 2007;581(25):4910-6. doi: 10.1016/j.febslet.2007.09.021. PubMed PMID: 17900573.
139. Mitchell JM, Mansfeld J, Capitanio J, Kutay U, Wozniak RW. Pom121 links two essential subcomplexes of the nuclear pore complex core to the membrane. The Journal of cell biology. 2010;191(3):505-21. doi: 10.1083/jcb.201007098. PubMed PMID: 20974814; PubMed Central PMCID: PMC3003318.
140. Yavuz S, Santarella-Mellwig R, Koch B, Jaedicke A, Mattaj IW, Antonin W. NLS-mediated NPC functions of the nucleoporin Pom121. FEBS letters. 2010;584(15):3292-8. doi: 10.1016/j.febslet.2010.07.008. PubMed PMID: 20624389.
141. Harel A, Orjalo AV, Vincent T, Lachish-Zalait A, Vasu S, Shah S, et al. Removal of a single pore subcomplex results in vertebrate nuclei devoid of nuclear pores. Molecular cell. 2003;11(4):853-64. PubMed PMID: 12718872.
142. Bui KH, von Appen A, DiGuilio AL, Ori A, Sparks L, Mackmull MT, et al. Integrated structural analysis of the human nuclear pore complex scaffold. Cell. 2013;155(6):1233-43. doi: 10.1016/j.cell.2013.10.055. PubMed PMID: 24315095.
143. Boehmer T, Enninga J, Dales S, Blobel G, Zhong H. Depletion of a single nucleoporin, Nup107, prevents the assembly of a subset of nucleoporins into the nuclear pore complex. Proceedings of the National Academy of Sciences of the United States of America. 2003;100(3):981-5. doi: 10.1073/pnas.252749899. PubMed PMID: 12552102; PubMed Central PMCID: PMC298712.
144. Boehmer T, Jeudy S, Berke IC, Schwartz TU. Structural and functional studies of Nup107/Nup133 interaction and its implications for the architecture of the nuclear pore complex. Molecular cell. 2008;30(6):721-31. doi: 10.1016/j.molcel.2008.04.022. PubMed PMID: 18570875; PubMed Central PMCID: PMC2446439.
145. Lussi YC, Hugi I, Laurell E, Kutay U, Fahrenkrog B. The nucleoporin Nup88 is interacting with nuclear lamin A. Molecular biology of the cell. 2011;22(7):1080-90. doi: 10.1091/mbc.E10-05-0463. PubMed PMID: 21289091; PubMed Central PMCID: PMC3069011.
146. Grandi P, Dang T, Pane N, Shevchenko A, Mann M, Forbes D, et al. Nup93, a vertebrate homologue of yeast Nic96p, forms a complex with a novel 205-kDa protein and is required for correct nuclear pore assembly. Molecular biology of the cell. 1997;8(10):2017-38. PubMed PMID: 9348540; PubMed Central PMCID: PMC25664.
147. Sachdev R, Sieverding C, Flotenmeyer M, Antonin W. The C-terminal domain of Nup93 is essential for assembly of the structural backbone of nuclear pore complexes. Molecular biology of the cell. 2012;23(4):740-9. doi: 10.1091/mbc.E11-09-0761. PubMed PMID: 22171326; PubMed Central PMCID: PMC3279400.

148. Hawryluk-Gara LA, Shibuya EK, Wozniak RW. Vertebrate Nup53 interacts with the nuclear lamina and is required for the assembly of a Nup93-containing complex. Molecular biology of the cell. 2005;16(5):2382-94. doi: 10.1091/mbc.E04-10-0857. PubMed PMID: 15703211; PubMed Central PMCID: PMC1087243.
149. Hawryluk-Gara LA, Platani M, Santarella R, Wozniak RW, Mattaj IW. Nup53 is required for nuclear envelope and nuclear pore complex assembly. Molecular biology of the cell. 2008;19(4):1753-62. doi: 10.1091/mbc.E07-08-0820. PubMed PMID: 18256286; PubMed Central PMCID: PMC2291426.
150. Theerthagiri G, Eisenhardt N, Schwarz H, Antonin W. The nucleoporin Nup188 controls passage of membrane proteins across the nuclear pore complex. The Journal of cell biology. 2010;189(7):1129-42. doi: 10.1083/jcb.200912045. PubMed PMID: 20566687; PubMed Central PMCID: PMC2894445.
151. Andersen KR, Onischenko E, Tang JH, Kumar P, Chen JZ, Ulrich A, et al. Scaffold nucleoporins Nup188 and Nup192 share structural and functional properties with nuclear transport receptors. eLife. 2013;2:e00745. doi: 10.7554/eLife.00745. PubMed PMID: 23795296; PubMed Central PMCID: PMC3679522.
152. Griffis ER, Xu S, Powers MA. Nup98 localizes to both nuclear and cytoplasmic sides of the nuclear pore and binds to two distinct nucleoporin subcomplexes. Molecular biology of the cell. 2003;14(2):600-10. doi: 10.1091/mbc.E02-09-0582. PubMed PMID: 12589057; PubMed Central PMCID: PMC149995.
153. Griffis ER, Altan N, Lippincott-Schwartz J, Powers MA. Nup98 is a mobile nucleoporin with transcription-dependent dynamics. Molecular biology of the cell. 2002;13(4):1282-97. doi: 10.1091/mbc.01-11-0538. PubMed PMID: 11950939; PubMed Central PMCID: PMC102269.
154. Pritchard CE, Fornerod M, Kasper LH, van Deursen JM. RAE1 is a shuttling mRNA export factor that binds to a GLEBS-like NUP98 motif at the nuclear pore complex through multiple domains. The Journal of cell biology. 1999;145(2):237-54. PubMed PMID: 10209021; PubMed Central PMCID: PMC2133102.
155. Ren Y, Seo HS, Blobel G, Hoelz A. Structural and functional analysis of the interaction between the nucleoporin Nup98 and the mRNA export factor Rae1. Proceedings of the National Academy of Sciences of the United States of America. 2010;107(23):10406-11. doi: 10.1073/pnas.1005389107. PubMed PMID: 20498086; PubMed Central PMCID: PMC2890840.
156. Fontoura BM, Blobel G, Yaseen NR. The nucleoporin Nup98 is a site for GDP/GTP exchange on ran and termination of karyopherin beta 2-mediated nuclear import. The Journal of biological chemistry. 2000;275(40):31289-96. doi: 10.1074/jbc.M004651200. PubMed PMID: 10875935.
157. Oka M, Asally M, Yasuda Y, Ogawa Y, Tachibana T, Yoneda Y. The mobile FG nucleoporin Nup98 is a cofactor for Crm1-dependent protein export. Molecular biology of the cell. 2010;21(11):1885-96. doi: 10.1091/mbc.E09-12-1041. PubMed PMID: 20375145; PubMed Central PMCID: PMC2877646.
158. Melcak I, Hoelz A, Blobel G. Structure of Nup58/45 suggests flexible nuclear pore diameter by intermolecular sliding. Science. 2007;315(5819):1729-32. doi: 10.1126/science.1135730. PubMed PMID: 17379812.
159. Solmaz SR, Blobel G, Melcak I. Ring cycle for dilating and constricting the nuclear pore. Proceedings of the National Academy of Sciences of the United States of America.

2013;110(15):5858-63. doi: 10.1073/pnas.1302655110. PubMed PMID: 23479651; PubMed Central PMCID: PMC3625290.
160. Hu T, Guan T, Gerace L. Molecular and functional characterization of the p62 complex, an assembly of nuclear pore complex glycoproteins. The Journal of cell biology. 1996;134(3):589-601. PubMed PMID: 8707840; PubMed Central PMCID: PMC2120945.
161. Paschal BM, Gerace L. Identification of NTF2, a cytosolic factor for nuclear import that interacts with nuclear pore complex protein p62. The Journal of cell biology. 1995;129(4):925-37. PubMed PMID: 7744965; PubMed Central PMCID: PMC2120498.
162. Ribbeck K, Lipowsky G, Kent HM, Stewart M, Gorlich D. NTF2 mediates nuclear import of Ran. The EMBO journal. 1998;17(22):6587-98. doi: 10.1093/emboj/17.22.6587. PubMed PMID: 9822603; PubMed Central PMCID: PMC1171005.
163. Bayliss R, Ribbeck K, Akin D, Kent HM, Feldherr CM, Gorlich D, et al. Interaction between NTF2 and xFxFG-containing nucleoporins is required to mediate nuclear import of RanGDP. Journal of molecular biology. 1999;293(3):579-93. doi: 10.1006/jmbi.1999.3166. PubMed PMID: 10543952.
164. Guan T, Kehlenbach RH, Schirmer EC, Kehlenbach A, Fan F, Clurman BE, et al. Nup50, a nucleoplasmically oriented nucleoporin with a role in nuclear protein export. Molecular and cellular biology. 2000;20(15):5619-30. PubMed PMID: 10891499; PubMed Central PMCID: PMC86026.
165. Ogawa Y, Miyamoto Y, Asally M, Oka M, Yasuda Y, Yoneda Y. Two isoforms of Npap60 (Nup50) differentially regulate nuclear protein import. Molecular biology of the cell. 2010;21(4):630-8. doi: 10.1091/mbc.E09-05-0374. PubMed PMID: 20016008; PubMed Central PMCID: PMC2820426.
166. Matsuura Y, Stewart M. Nup50/Npap60 function in nuclear protein import complex disassembly and importin recycling. The EMBO journal. 2005;24(21):3681-9. doi: 10.1038/sj.emboj.7600843. PubMed PMID: 16222336; PubMed Central PMCID: PMC1276725.
167. Pumroy RA, Nardozzi JD, Hart DJ, Root MJ, Cingolani G. Nucleoporin Nup50 stabilizes closed conformation of armadillo repeat 10 in importin alpha5. The Journal of biological chemistry. 2012;287(3):2022-31. doi: 10.1074/jbc.M111.315838. PubMed PMID: 22130666; PubMed Central PMCID: PMC3265882.
168. Makise M, Mackay DR, Elgort S, Shankaran SS, Adam SA, Ullman KS. The Nup153-Nup50 protein interface and its role in nuclear import. The Journal of biological chemistry. 2012;287(46):38515-22. doi: 10.1074/jbc.M112.378893. PubMed PMID: 23007389; PubMed Central PMCID: PMC3493896.
169. Moroianu J, Blobel G, Radu A. RanGTP-mediated nuclear export of karyopherin alpha involves its interaction with the nucleoporin Nup153. Proceedings of the National Academy of Sciences of the United States of America. 1997;94(18):9699-704. PubMed PMID: 9275187; PubMed Central PMCID: PMC23253.
170. Ullman KS, Shah S, Powers MA, Forbes DJ. The nucleoporin nup153 plays a critical role in multiple types of nuclear export. Molecular biology of the cell. 1999;10(3):649-64. PubMed PMID: 10069809; PubMed Central PMCID: PMC25193.
171. Nakielny S, Shaikh S, Burke B, Dreyfuss G. Nup153 is an M9-containing mobile nucleoporin with a novel Ran-binding domain. The EMBO journal. 1999;18(7):1982-95. doi: 10.1093/emboj/18.7.1982. PubMed PMID: 10202161; PubMed Central PMCID: PMC1171283.

172. Ogawa Y, Miyamoto Y, Oka M, Yoneda Y. The interaction between importin-alpha and Nup153 promotes importin-alpha/beta-mediated nuclear import. Traffic. 2012;13(7):934-46. doi: 10.1111/j.1600-0854.2012.01367.x. PubMed PMID: 22510057.
173. Hase ME, Cordes VC. Direct interaction with nup153 mediates binding of Tpr to the periphery of the nuclear pore complex. Molecular biology of the cell. 2003;14(5):1923-40. doi: 10.1091/mbc.E02-09-0620. PubMed PMID: 12802065; PubMed Central PMCID: PMC165087.
174. Krull S, Thyberg J, Bjorkroth B, Rackwitz HR, Cordes VC. Nucleoporins as components of the nuclear pore complex core structure and Tpr as the architectural element of the nuclear basket. Molecular biology of the cell. 2004;15(9):4261-77. doi: 10.1091/mbc.E04-03-0165. PubMed PMID: 15229283; PubMed Central PMCID: PMC515357.
175. Coyle JH, Bor YC, Rekosh D, Hammarskjold ML. The Tpr protein regulates export of mRNAs with retained introns that traffic through the Nxf1 pathway. Rna. 2011;17(7):1344-56. doi: 10.1261/rna.2616111. PubMed PMID: 21613532; PubMed Central PMCID: PMC3138570.
176. Rajanala K, Nandicoori VK. Localization of nucleoporin Tpr to the nuclear pore complex is essential for Tpr mediated regulation of the export of unspliced RNA. PloS one. 2012;7(1):e29921. doi: 10.1371/journal.pone.0029921. PubMed PMID: 22253824; PubMed Central PMCID: PMC3258255.
177. Frosst P, Guan T, Subauste C, Hahn K, Gerace L. Tpr is localized within the nuclear basket of the pore complex and has a role in nuclear protein export. The Journal of cell biology. 2002;156(4):617-30. doi: 10.1083/jcb.200106046. PubMed PMID: 11839768; PubMed Central PMCID: PMC2174070.
178. Henaff D, Radtke K, Lippe R. Herpesviruses exploit several host compartments for envelopment. Traffic. 2012;13(11):1443-9. doi: 10.1111/j.1600-0854.2012.01399.x. PubMed PMID: 22805610.
179. Boehmer PE, Nimonkar AV. Herpes virus replication. IUBMB Life. 2003;55(1):13-22. doi: 10.1080/1521654031000070645. PubMed PMID: 12716057.
180. Pasdeloup D, Blondel D, Isidro AL, Rixon FJ. Herpesvirus capsid association with the nuclear pore complex and viral DNA release involve the nucleoporin CAN/Nup214 and the capsid protein pUL25. Journal of virology. 2009;83(13):6610-23. doi: 10.1128/JVI.02655-08. PubMed PMID: 19386703; PubMed Central PMCID: PMC2698519.
181. Koffa MD, Clements JB, Izaurralde E, Wadd S, Wilson SA, Mattaj IW, et al. Herpes simplex virus ICP27 protein provides viral mRNAs with access to the cellular mRNA export pathway. The EMBO journal. 2001;20(20):5769-78. doi: 10.1093/emboj/20.20.5769. PubMed PMID: 11598019; PubMed Central PMCID: PMC125682.
182. Chen IH, Sciabica KS, Sandri-Goldin RM. ICP27 interacts with the RNA export factor Aly/REF to direct herpes simplex virus type 1 intronless mRNAs to the TAP export pathway. Journal of virology. 2002;76(24):12877-89. PubMed PMID: 12438613; PubMed Central PMCID: PMC136725.
183. Chen IH, Li L, Silva L, Sandri-Goldin RM. ICP27 recruits Aly/REF but not TAP/NXF1 to herpes simplex virus type 1 transcription sites although TAP/NXF1 is required for ICP27 export. Journal of virology. 2005;79(7):3949-61. doi: 10.1128/JVI.79.7.3949-3961.2005. PubMed PMID: 15767397; PubMed Central PMCID: PMC1061567.
184. Tian X, Devi-Rao G, Golovanov AP, Sandri-Goldin RM. The interaction of the cellular export adaptor protein Aly/REF with ICP27 contributes to the efficiency of herpes simplex

virus 1 mRNA export. Journal of virology. 2013;87(13):7210-7. doi: 10.1128/JVI.00738-13. PubMed PMID: 23637401; PubMed Central PMCID: PMC3700301.
185. Soliman TM, Silverstein SJ. Herpesvirus mRNAs are sorted for export via Crm1-dependent and -independent pathways. Journal of virology. 2000;74(6):2814-25. PubMed PMID: 10684298; PubMed Central PMCID: PMC111772.
186. Malik P, Tabarraei A, Kehlenbach RH, Korfali N, Iwasawa R, Graham SV, et al. Herpes simplex virus ICP27 protein directly interacts with the nuclear pore complex through Nup62, inhibiting host nucleocytoplasmic transport pathways. The Journal of biological chemistry. 2012;287(15):12277-92. doi: 10.1074/jbc.M111.331777. PubMed PMID: 22334672; PubMed Central PMCID: PMC3320978.
187. Ote I, Lebrun M, Vandevenne P, Bontems S, Medina-Palazon C, Manet E, et al. Varicella-zoster virus IE4 protein interacts with SR proteins and exports mRNAs through the TAP/NXF1 pathway. PloS one. 2009;4(11):e7882. doi: 10.1371/journal.pone.0007882. PubMed PMID: 19924249; PubMed Central PMCID: PMC2775670.
188. Cai M, Wang S, Xing J, Zheng C. Characterization of the nuclear import and export signals, and subcellular transport mechanism of varicella-zoster virus ORF9. The Journal of general virology. 2011;92(Pt 3):621-6. doi: 10.1099/vir.0.027029-0. PubMed PMID: 21106804.
189. Chang CW, Lee CP, Su MT, Tsai CH, Chen MR. BGLF4 kinase modulates the structure and transport preference of the nuclear pore complex to facilitate nuclear import of Epstein-Barr virus lytic proteins. Journal of virology. 2015;89(3):1703-18. doi: 10.1128/JVI.02880-14. PubMed PMID: 25410863; PubMed Central PMCID: PMC4300756.
190. Boyle SM, Ruvolo V, Gupta AK, Swaminathan S. Association with the cellular export receptor CRM 1 mediates function and intracellular localization of Epstein-Barr virus SM protein, a regulator of gene expression. Journal of virology. 1999;73(8):6872-81. PubMed PMID: 10400785; PubMed Central PMCID: PMC112772.
191. Lischka P, Sorg G, Kann M, Winkler M, Stamminger T. A nonconventional nuclear localization signal within the UL84 protein of human cytomegalovirus mediates nuclear import via the importin alpha/beta pathway. Journal of virology. 2003;77(6):3734-48. PubMed PMID: 12610148; PubMed Central PMCID: PMC149505.
192. Wang L, Li M, Cai M, Xing J, Wang S, Zheng C. A PY-nuclear localization signal is required for nuclear accumulation of HCMV UL79 protein. Medical microbiology and immunology. 2012;201(3):381-7. doi: 10.1007/s00430-012-0243-4. PubMed PMID: 22628116.
193. Doorbar J, Quint W, Banks L, Bravo IG, Stoler M, Broker TR, et al. The biology and life-cycle of human papillomaviruses. Vaccine. 2012;30 Suppl 5:F55-70. doi: 10.1016/j.vaccine.2012.06.083. PubMed PMID: 23199966.
194. Doorbar J. Molecular biology of human papillomavirus infection and cervical cancer. Clin Sci (Lond). 2006;110(5):525-41. doi: 10.1042/CS20050369. PubMed PMID: 16597322.
195. Bordeaux J, Forte S, Harding E, Darshan MS, Klucevsek K, Moroianu J. The l2 minor capsid protein of low-risk human papillomavirus type 11 interacts with host nuclear import receptors and viral DNA. Journal of virology. 2006;80(16):8259-62. doi: 10.1128/JVI.00776-06. PubMed PMID: 16873281; PubMed Central PMCID: PMC1563822.
196. Darshan MS, Lucchi J, Harding E, Moroianu J. The l2 minor capsid protein of human papillomavirus type 16 interacts with a network of nuclear import receptors. Journal of

virology. 2004;78(22):12179-88. doi: 10.1128/JVI.78.22.12179-12188.2004. PubMed PMID: 15507604; PubMed Central PMCID: PMC525100.
197. Bian XL, Wilson VG. Common importin alpha specificity for papillomavirus E2 proteins. Virus research. 2010;150(1-2):135-7. doi: 10.1016/j.virusres.2010.02.011. PubMed PMID: 20193720; PubMed Central PMCID: PMC2859985.
198. Le Roux LG, Moroianu J. Nuclear entry of high-risk human papillomavirus type 16 E6 oncoprotein occurs via several pathways. Journal of virology. 2003;77(4):2330-7. PubMed PMID: 12551970; PubMed Central PMCID: PMC141087.
199. Onder Z, Moroianu J. Nuclear import of cutaneous beta genus HPV8 E7 oncoprotein is mediated by hydrophobic interactions between its zinc-binding domain and FG nucleoporins. Virology. 2014;449:150-62. doi: 10.1016/j.virol.2013.11.020. PubMed PMID: 24418548; PubMed Central PMCID: PMC3894589.
200. McKee CH, Onder Z, Ashok A, Cardoso R, Moroianu J. Characterization of the transport signals that mediate the nucleocytoplasmic traffic of low risk HPV11 E7. Virology. 2013;443(1):113-22. doi: 10.1016/j.virol.2013.04.031. PubMed PMID: 23725695; PubMed Central PMCID: PMC3758764.
201. Eberhard J, Onder Z, Moroianu J. Nuclear import of high risk HPV16 E7 oncoprotein is mediated by its zinc-binding domain via hydrophobic interactions with Nup62. Virology. 2013;446(1-2):334-45. doi: 10.1016/j.virol.2013.08.017. PubMed PMID: 24074597; PubMed Central PMCID: PMC3789256.
202. Summers J, Mason WS. Replication of the genome of a hepatitis B--like virus by reverse transcription of an RNA intermediate. Cell. 1982;29(2):403-15. PubMed PMID: 6180831.
203. Li HC, Huang EY, Su PY, Wu SY, Yang CC, Lin YS, et al. Nuclear export and import of human hepatitis B virus capsid protein and particles. PLoS pathogens. 2010;6(10):e1001162. doi: 10.1371/journal.ppat.1001162. PubMed PMID: 21060813; PubMed Central PMCID: PMC2965763.
204. Forgues M, Marrogi AJ, Spillare EA, Wu CG, Yang Q, Yoshida M, et al. Interaction of the hepatitis B virus X protein with the Crm1-dependent nuclear export pathway. The Journal of biological chemistry. 2001;276(25):22797-803. doi: 10.1074/jbc.M101259200. PubMed PMID: 11287420.
205. Schmitz A, Schwarz A, Foss M, Zhou L, Rabe B, Hoellenriegel J, et al. Nucleoporin 153 arrests the nuclear import of hepatitis B virus capsids in the nuclear basket. PLoS pathogens. 2010;6(1):e1000741. doi: 10.1371/journal.ppat.1000741. PubMed PMID: 20126445; PubMed Central PMCID: PMC2813275.
206. Deng T, Engelhardt OG, Thomas B, Akoulitchev AV, Brownlee GG, Fodor E. Role of ran binding protein 5 in nuclear import and assembly of the influenza virus RNA polymerase complex. Journal of virology. 2006;80(24):11911-9. doi: 10.1128/JVI.01565-06. PubMed PMID: 17005651; PubMed Central PMCID: PMC1676300.
207. Hutchinson EC, Orr OE, Man Liu S, Engelhardt OG, Fodor E. Characterization of the interaction between the influenza A virus polymerase subunit PB1 and the host nuclear import factor Ran-binding protein 5. The Journal of general virology. 2011;92(Pt 8):1859-69. doi: 10.1099/vir.0.032813-0. PubMed PMID: 21562121.
208. Tafforeau L, Chantier T, Pradezynski F, Pellet J, Mangeot PE, Vidalain PO, et al. Generation and comprehensive analysis of an influenza virus polymerase cellular interaction

network. Journal of virology. 2011;85(24):13010-8. doi: 10.1128/JVI.02651-10. PubMed PMID: 21994455; PubMed Central PMCID: PMC3233135.
209. Tarendeau F, Boudet J, Guilligay D, Mas PJ, Bougault CM, Boulo S, et al. Structure and nuclear import function of the C-terminal domain of influenza virus polymerase PB2 subunit. Nature structural & molecular biology. 2007;14(3):229-33. doi: 10.1038/nsmb1212. PubMed PMID: 17310249.
210. Gabriel G, Herwig A, Klenk HD. Interaction of polymerase subunit PB2 and NP with importin alpha1 is a determinant of host range of influenza A virus. PLoS pathogens. 2008;4(2):e11. doi: 10.1371/journal.ppat.0040011. PubMed PMID: 18248089; PubMed Central PMCID: PMC2222953.
211. Sasaki Y, Hagiwara K, Kakisaka M, Yamada K, Murakami T, Aida Y. Importin alpha3/Qip1 is involved in multiplication of mutant influenza virus with alanine mutation at amino acid 9 independently of nuclear transport function. PloS one. 2013;8(1):e55765. doi: 10.1371/journal.pone.0055765. PubMed PMID: 23383277; PubMed Central PMCID: PMC3559588.
212. Satterly N, Tsai PL, van Deursen J, Nussenzveig DR, Wang Y, Faria PA, et al. Influenza virus targets the mRNA export machinery and the nuclear pore complex. Proceedings of the National Academy of Sciences of the United States of America. 2007;104(6):1853-8. doi: 10.1073/pnas.0610977104. PubMed PMID: 17267598; PubMed Central PMCID: PMC1794296.
213. Elton D, Simpson-Holley M, Archer K, Medcalf L, Hallam R, McCauley J, et al. Interaction of the influenza virus nucleoprotein with the cellular CRM1-mediated nuclear export pathway. Journal of virology. 2001;75(1):408-19. doi: 10.1128/JVI.75.1.408-419.2001. PubMed PMID: 11119609; PubMed Central PMCID: PMC113933.
214. Neumann G, Hughes MT, Kawaoka Y. Influenza A virus NS2 protein mediates vRNP nuclear export through NES-independent interaction with hCRM1. The EMBO journal. 2000;19(24):6751-8. doi: 10.1093/emboj/19.24.6751. PubMed PMID: 11118210; PubMed Central PMCID: PMC305902.
215. Chase GP, Rameix-Welti MA, Zvirbliene A, Zvirblis G, Gotz V, Wolff T, et al. Influenza virus ribonucleoprotein complexes gain preferential access to cellular export machinery through chromatin targeting. PLoS pathogens. 2011;7(9):e1002187. doi: 10.1371/journal.ppat.1002187. PubMed PMID: 21909257; PubMed Central PMCID: PMC3164630.
216. Yu M, Liu X, Cao S, Zhao Z, Zhang K, Xie Q, et al. Identification and characterization of three novel nuclear export signals in the influenza A virus nucleoprotein. Journal of virology. 2012;86(9):4970-80. doi: 10.1128/JVI.06159-11. PubMed PMID: 22345439; PubMed Central PMCID: PMC3347336.
217. Read EK, Digard P. Individual influenza A virus mRNAs show differential dependence on cellular NXF1/TAP for their nuclear export. The Journal of general virology. 2010;91(Pt 5):1290-301. doi: 10.1099/vir.0.018564-0. PubMed PMID: 20071484; PubMed Central PMCID: PMC3052562.
218. Predicala R, Zhou Y. The role of Ran-binding protein 3 during influenza A virus replication. The Journal of general virology. 2013;94(Pt 5):977-84. doi: 10.1099/vir.0.049395-0. PubMed PMID: 23303829.

219. Matreyek KA, Engelman A. Viral and cellular requirements for the nuclear entry of retroviral preintegration nucleoprotein complexes. Viruses. 2013;5(10):2483-511. doi: 10.3390/v5102483. PubMed PMID: 24103892; PubMed Central PMCID: PMC3814599.
220. Gallay P, Hope T, Chin D, Trono D. HIV-1 infection of nondividing cells through the recognition of integrase by the importin/karyopherin pathway. Proceedings of the National Academy of Sciences of the United States of America. 1997;94(18):9825-30. PubMed PMID: 9275210; PubMed Central PMCID: PMC23276.
221. Ao Z, Danappa Jayappa K, Wang B, Zheng Y, Kung S, Rassart E, et al. Importin alpha3 interacts with HIV-1 integrase and contributes to HIV-1 nuclear import and replication. Journal of virology. 2010;84(17):8650-63. doi: 10.1128/JVI.00508-10. PubMed PMID: 20554775; PubMed Central PMCID: PMC2919037.
222. Zhang R, Mehla R, Chauhan A. Perturbation of host nuclear membrane component RanBP2 impairs the nuclear import of human immunodeficiency virus -1 preintegration complex (DNA). PloS one. 2010;5(12):e15620. doi: 10.1371/journal.pone.0015620. PubMed PMID: 21179483; PubMed Central PMCID: PMC3001881.
223. Popov S, Rexach M, Ratner L, Blobel G, Bukrinsky M. Viral protein R regulates docking of the HIV-1 preintegration complex to the nuclear pore complex. The Journal of biological chemistry. 1998;273(21):13347-52. PubMed PMID: 9582382.
224. Le Rouzic E, Mousnier A, Rustum C, Stutz F, Hallberg E, Dargemont C, et al. Docking of HIV-1 Vpr to the nuclear envelope is mediated by the interaction with the nucleoporin hCG1. The Journal of biological chemistry. 2002;277(47):45091-8. doi: 10.1074/jbc.M207439200. PubMed PMID: 12228227.
225. Ebina H, Aoki J, Hatta S, Yoshida T, Koyanagi Y. Role of Nup98 in nuclear entry of human immunodeficiency virus type 1 cDNA. Microbes and infection / Institut Pasteur. 2004;6(8):715-24. doi: 10.1016/j.micinf.2004.04.002. PubMed PMID: 15207818.
226. Askjaer P, Jensen TH, Nilsson J, Englmeier L, Kjems J. The specificity of the CRM1-Rev nuclear export signal interaction is mediated by RanGTP. The Journal of biological chemistry. 1998;273(50):33414-22. PubMed PMID: 9837918.
227. Zolotukhin AS, Felber BK. Nucleoporins nup98 and nup214 participate in nuclear export of human immunodeficiency virus type 1 Rev. Journal of virology. 1999;73(1):120-7. PubMed PMID: 9847314; PubMed Central PMCID: PMC103815.
228. Taniguchi I, Mabuchi N, Ohno M. HIV-1 Rev protein specifies the viral RNA export pathway by suppressing TAP/NXF1 recruitment. Nucleic acids research. 2014;42(10):6645-58. doi: 10.1093/nar/gku304. PubMed PMID: 24753416; PubMed Central PMCID: PMC4041468.
229. Sivan G, Martin SE, Myers TG, Buehler E, Szymczyk KH, Ormanoglu P, et al. Human genome-wide RNAi screen reveals a role for nuclear pore proteins in poxvirus morphogenesis. Proceedings of the National Academy of Sciences of the United States of America. 2013;110(9):3519-24. doi: 10.1073/pnas.1300708110. PubMed PMID: 23401514; PubMed Central PMCID: PMC3587217.
230. Porter FW, Palmenberg AC. Leader-induced phosphorylation of nucleoporins correlates with nuclear trafficking inhibition by cardioviruses. Journal of virology. 2009;83(4):1941-51. doi: 10.1128/JVI.01752-08. PubMed PMID: 19073724; PubMed Central PMCID: PMC2643766.
231. Bardina MV, Lidsky PV, Sheval EV, Fominykh KV, van Kuppeveld FJ, Polyakov VY, et al. Mengovirus-induced rearrangement of the nuclear pore complex: hijacking cellular

phosphorylation machinery. Journal of virology. 2009;83(7):3150-61. doi: 10.1128/JVI.01456-08. PubMed PMID: 19144712; PubMed Central PMCID: PMC2655543.
232. Park N, Skern T, Gustin KE. Specific cleavage of the nuclear pore complex protein Nup62 by a viral protease. The Journal of biological chemistry. 2010;285(37):28796-805. doi: 10.1074/jbc.M110.143404. PubMed PMID: 20622012; PubMed Central PMCID: PMC2937907.
233. Park N, Katikaneni P, Skern T, Gustin KE. Differential targeting of nuclear pore complex proteins in poliovirus-infected cells. Journal of virology. 2008;82(4):1647-55. doi: 10.1128/JVI.01670-07. PubMed PMID: 18045934; PubMed Central PMCID: PMC2258732.
234. Castello A, Izquierdo JM, Welnowska E, Carrasco L. RNA nuclear export is blocked by poliovirus 2A protease and is concomitant with nucleoporin cleavage. Journal of cell science. 2009;122(Pt 20):3799-809. doi: 10.1242/jcs.055988. PubMed PMID: 19789179.
235. Johansson M, Brooks AJ, Jans DA, Vasudevan SG. A small region of the dengue virus-encoded RNA-dependent RNA polymerase, NS5, confers interaction with both the nuclear transport receptor importin-beta and the viral helicase, NS3. The Journal of general virology. 2001;82(Pt 4):735-45. PubMed PMID: 11257177.
236. Rawlinson SM, Pryor MJ, Wright PJ, Jans DA. CRM1-mediated nuclear export of dengue virus RNA polymerase NS5 modulates interleukin-8 induction and virus production. The Journal of biological chemistry. 2009;284(23):15589-97. doi: 10.1074/jbc.M808271200. PubMed PMID: 19297323; PubMed Central PMCID: PMC2708855.
237. Zhang LK, Chai F, Li HY, Xiao G, Guo L. Identification of host proteins involved in Japanese encephalitis virus infection by quantitative proteomics analysis. Journal of proteome research. 2013;12(6):2666-78. doi: 10.1021/pr400011k. PubMed PMID: 23647205.
238. Ghildyal R, Ho A, Wagstaff KM, Dias MM, Barton CL, Jans P, et al. Nuclear import of the respiratory syncytial virus matrix protein is mediated by importin beta1 independent of importin alpha. Biochemistry. 2005;44(38):12887-95. doi: 10.1021/bi050701e. PubMed PMID: 16171404.
239. Ghildyal R, Ho A, Dias M, Soegiyono L, Bardin PG, Tran KC, et al. The respiratory syncytial virus matrix protein possesses a Crm1-mediated nuclear export mechanism. Journal of virology. 2009;83(11):5353-62. doi: 10.1128/JVI.02374-08. PubMed PMID: 19297465; PubMed Central PMCID: PMC2681974.
240. von Kobbe C, van Deursen JM, Rodrigues JP, Sitterlin D, Bachi A, Wu X, et al. Vesicular stomatitis virus matrix protein inhibits host cell gene expression by targeting the nucleoporin Nup98. Molecular cell. 2000;6(5):1243-52. PubMed PMID: 11106761.
241. Rajani KR, Pettit Kneller EL, McKenzie MO, Horita DA, Chou JW, Lyles DS. Complexes of vesicular stomatitis virus matrix protein with host Rae1 and Nup98 involved in inhibition of host transcription. PLoS pathogens. 2012;8(9):e1002929. doi: 10.1371/journal.ppat.1002929. PubMed PMID: 23028327; PubMed Central PMCID: PMC3460625.
242. Faria PA, Chakraborty P, Levay A, Barber GN, Ezelle HJ, Enninga J, et al. VSV disrupts the Rae1/mrnp41 mRNA nuclear export pathway. Molecular cell. 2005;17(1):93-102. doi: 10.1016/j.molcel.2004.11.023. PubMed PMID: 15629720.
243. Her LS, Lund E, Dahlberg JE. Inhibition of Ran guanosine triphosphatase-dependent nuclear transport by the matrix protein of vesicular stomatitis virus. Science. 1997;276(5320):1845-8. PubMed PMID: 9188527.

244. Takeuchi O, Akira S. Pattern recognition receptors and inflammation. Cell. 2010;140(6):805-20. doi: 10.1016/j.cell.2010.01.022. PubMed PMID: 20303872.
245. Takeuchi O, Akira S. Innate immunity to virus infection. Immunol Rev. 2009;227(1):75-86. doi: 10.1111/j.1600-065X.2008.00737.x. PubMed PMID: 19120477.
246. Chow J, Franz KM, Kagan JC. PRRs are watching you: Localization of innate sensing and signaling regulators. Virology. 2015. doi: 10.1016/j.virol.2015.02.051. PubMed PMID: 25800355.
247. Seth RB, Sun L, Chen ZJ. Antiviral innate immunity pathways. Cell research. 2006;16(2):141-7. doi: 10.1038/sj.cr.7310019. PubMed PMID: 16474426.
248. Cai X, Chiu YH, Chen ZJ. The cGAS-cGAMP-STING pathway of cytosolic DNA sensing and signaling. Molecular cell. 2014;54(2):289-96. doi: 10.1016/j.molcel.2014.03.040. PubMed PMID: 24766893.
249. Chiang JJ, Davis ME, Gack MU. Regulation of RIG-I-like receptor signaling by host and viral proteins. Cytokine & growth factor reviews. 2014;25(5):491-505. doi: 10.1016/j.cytogfr.2014.06.005. PubMed PMID: 25023063.
250. Taniguchi T, Ogasawara K, Takaoka A, Tanaka N. IRF family of transcription factors as regulators of host defense. Annu Rev Immunol. 2001;19:623-55. doi: 10.1146/annurev.immunol.19.1.623. PubMed PMID: 11244049.
251. Taniguchi T, Takaoka A. The interferon-alpha/beta system in antiviral responses: a multimodal machinery of gene regulation by the IRF family of transcription factors. Current opinion in immunology. 2002;14(1):111-6. PubMed PMID: 11790540.
252. Honda K, Yanai H, Takaoka A, Taniguchi T. Regulation of the type I IFN induction: a current view. Int Immunol. 2005;17(11):1367-78. doi: 10.1093/intimm/dxh318. PubMed PMID: 16214811.
253. Fujita T, Sakakibara J, Sudo Y, Miyamoto M, Kimura Y, Taniguchi T. Evidence for a nuclear factor(s), IRF-1, mediating induction and silencing properties to human IFN-beta gene regulatory elements. The EMBO journal. 1988;7(11):3397-405. PubMed PMID: 2850164; PubMed Central PMCID: PMC454838.
254. Miyamoto M, Fujita T, Kimura Y, Maruyama M, Harada H, Sudo Y, et al. Regulated expression of a gene encoding a nuclear factor, IRF-1, that specifically binds to IFN-beta gene regulatory elements. Cell. 1988;54(6):903-13. PubMed PMID: 3409321.
255. Kirchhoff S, Koromilas AE, Schaper F, Grashoff M, Sonenberg N, Hauser H. IRF-1 induced cell growth inhibition and interferon induction requires the activity of the protein kinase PKR. Oncogene. 1995;11(3):439-45. PubMed PMID: 7543195.
256. Benech P, Vigneron M, Peretz D, Revel M, Chebath J. Interferon-responsive regulatory elements in the promoter of the human 2',5'-oligo(A) synthetase gene. Molecular and cellular biology. 1987;7(12):4498-504. PubMed PMID: 2830497; PubMed Central PMCID: PMC368134.
257. Schafer SL, Lin R, Moore PA, Hiscott J, Pitha PM. Regulation of type I interferon gene expression by interferon regulatory factor-3. The Journal of biological chemistry. 1998;273(5):2714-20. PubMed PMID: 9446577.
258. Harada H, Fujita T, Miyamoto M, Kimura Y, Maruyama M, Furia A, et al. Structurally similar but functionally distinct factors, IRF-1 and IRF-2, bind to the same regulatory elements of IFN and IFN-inducible genes. Cell. 1989;58(4):729-39. PubMed PMID: 2475256.
259. Tanaka N, Kawakami T, Taniguchi T. Recognition DNA sequences of interferon regulatory factor 1 (IRF-1) and IRF-2, regulators of cell growth and the interferon system.

Molecular and cellular biology. 1993;13(8):4531-8. PubMed PMID: 7687740; PubMed Central PMCID: PMC360068.
260. Weaver BK, Kumar KP, Reich NC. Interferon regulatory factor 3 and CREB-binding protein/p300 are subunits of double-stranded RNA-activated transcription factor DRAF1. Molecular and cellular biology. 1998;18(3):1359-68. PubMed PMID: 9488451; PubMed Central PMCID: PMC108849.
261. Eisenbeis CF, Singh H, Storb U. Pip, a novel IRF family member, is a lymphoid-specific, PU.1-dependent transcriptional activator. Genes & development. 1995;9(11):1377-87. PubMed PMID: 7797077.
262. Matsuyama T, Grossman A, Mittrucker HW, Siderovski DP, Kiefer F, Kawakami T, et al. Molecular cloning of LSIRF, a lymphoid-specific member of the interferon regulatory factor family that binds the interferon-stimulated response element (ISRE). Nucleic acids research. 1995;23(12):2127-36. PubMed PMID: 7541907; PubMed Central PMCID: PMC306999.
263. Yamagata T, Nishida J, Tanaka S, Sakai R, Mitani K, Yoshida M, et al. A novel interferon regulatory factor family transcription factor, ICSAT/Pip/LSIRF, that negatively regulates the activity of interferon-regulated genes. Molecular and cellular biology. 1996;16(4):1283-94. PubMed PMID: 8657101; PubMed Central PMCID: PMC231112.
264. Takaoka A, Yanai H, Kondo S, Duncan G, Negishi H, Mizutani T, et al. Integral role of IRF-5 in the gene induction programme activated by Toll-like receptors. Nature. 2005;434(7030):243-9. doi: 10.1038/nature03308. PubMed PMID: 15665823.
265. Barnes B, Lubyova B, Pitha PM. On the role of IRF in host defense. J Interferon Cytokine Res. 2002;22(1):59-71. doi: 10.1089/107999002753452665. PubMed PMID: 11846976.
266. Ratovitski EA. DeltaNp63alpha/IRF6 interplay activates NOS2 transcription and induces autophagy upon tobacco exposure. Arch Biochem Biophys. 2011;506(2):208-15. doi: 10.1016/j.abb.2010.11.020. PubMed PMID: 21129360.
267. Driggers PH, Ennist DL, Gleason SL, Mak WH, Marks MS, Levi BZ, et al. An interferon gamma-regulated protein that binds the interferon-inducible enhancer element of major histocompatibility complex class I genes. Proceedings of the National Academy of Sciences of the United States of America. 1990;87(10):3743-7. PubMed PMID: 2111015; PubMed Central PMCID: PMC53979.
268. Nelson N, Kanno Y, Hong C, Contursi C, Fujita T, Fowlkes BJ, et al. Expression of IFN regulatory factor family proteins in lymphocytes. Induction of Stat-1 and IFN consensus sequence binding protein expression by T cell activation. Journal of immunology. 1996;156(10):3711-20. PubMed PMID: 8621906.
269. Bovolenta C, Driggers PH, Marks MS, Medin JA, Politis AD, Vogel SN, et al. Molecular interactions between interferon consensus sequence binding protein and members of the interferon regulatory factor family. Proceedings of the National Academy of Sciences of the United States of America. 1994;91(11):5046-50. PubMed PMID: 8197182; PubMed Central PMCID: PMC43928.
270. Fagerlund R, Melen K, Cao X, Julkunen I. NF-kappaB p52, RelB and c-Rel are transported into the nucleus via a subset of importin alpha molecules. Cellular signalling. 2008;20(8):1442-51. doi: 10.1016/j.cellsig.2008.03.012. PubMed PMID: 18462924.
271. Mercurio F, Manning AM. Multiple signals converging on NF-kappaB. Curr Opin Cell Biol. 1999;11(2):226-32. PubMed PMID: 10209157.

272. Ivashkiv LB, Donlin LT. Regulation of type I interferon responses. Nature reviews Immunology. 2014;14(1):36-49. doi: 10.1038/nri3581. PubMed PMID: 24362405; PubMed Central PMCID: PMC4084561.
273. Levy DE, Darnell JE, Jr. Stats: transcriptional control and biological impact. Nature reviews Molecular cell biology. 2002;3(9):651-62. doi: 10.1038/nrm909. PubMed PMID: 12209125.
274. Takaoka A, Yanai H. Interferon signalling network in innate defence. Cellular microbiology. 2006;8(6):907-22. doi: 10.1111/j.1462-5822.2006.00716.x. PubMed PMID: 16681834.
275. Chawla-Sarkar M, Lindner DJ, Liu YF, Williams BR, Sen GC, Silverman RH, et al. Apoptosis and interferons: role of interferon-stimulated genes as mediators of apoptosis. Apoptosis. 2003;8(3):237-49. PubMed PMID: 12766484.
276. Yoshimura A, Naka T, Kubo M. SOCS proteins, cytokine signalling and immune regulation. Nature reviews Immunology. 2007;7(6):454-65. doi: 10.1038/nri2093. PubMed PMID: 17525754.
277. Khabar KS, Young HA. Post-transcriptional control of the interferon system. Biochimie. 2007;89(6-7):761-9. doi: 10.1016/j.biochi.2007.02.008. PubMed PMID: 17408842; PubMed Central PMCID: PMC1994070.
278. Curtsinger JM, Valenzuela JO, Agarwal P, Lins D, Mescher MF. Type I IFNs provide a third signal to CD8 T cells to stimulate clonal expansion and differentiation. Journal of immunology. 2005;174(8):4465-9. PubMed PMID: 15814665.
279. Kolumam GA, Thomas S, Thompson LJ, Sprent J, Murali-Krishna K. Type I interferons act directly on CD8 T cells to allow clonal expansion and memory formation in response to viral infection. J Exp Med. 2005;202(5):637-50. doi: 10.1084/jem.20050821. PubMed PMID: 16129706; PubMed Central PMCID: PMC2212878.
280. Thompson LJ, Kolumam GA, Thomas S, Murali-Krishna K. Innate inflammatory signals induced by various pathogens differentially dictate the IFN-I dependence of CD8 T cells for clonal expansion and memory formation. Journal of immunology. 2006;177(3):1746-54. PubMed PMID: 16849484.
281. Jungo F, Dayer JM, Modoux C, Hyka N, Burger D. IFN-beta inhibits the ability of T lymphocytes to induce TNF-alpha and IL-1beta production in monocytes upon direct cell-cell contact. Cytokine. 2001;14(5):272-82. doi: 10.1006/cyto.2001.0884. PubMed PMID: 11444907.
282. Garoufalis E, Kwan I, Lin R, Mustafa A, Pepin N, Roulston A, et al. Viral induction of the human beta interferon promoter: modulation of transcription by NF-kappa B/rel proteins and interferon regulatory factors. Journal of virology. 1994;68(8):4707-15. PubMed PMID: 8035474; PubMed Central PMCID: PMC236410.
283. Du W, Maniatis T. An ATF/CREB binding site is required for virus induction of the human interferon beta gene [corrected]. Proceedings of the National Academy of Sciences of the United States of America. 1992;89(6):2150-4. PubMed PMID: 1532252; PubMed Central PMCID: PMC48614.
284. Panne D, Maniatis T, Harrison SC. Crystal structure of ATF-2/c-Jun and IRF-3 bound to the interferon-beta enhancer. The EMBO journal. 2004;23(22):4384-93. doi: 10.1038/sj.emboj.7600453. PubMed PMID: 15510218; PubMed Central PMCID: PMC526468.

285. Zhang L, Pagano JS. Structure and function of IRF-7. J Interferon Cytokine Res. 2002;22(1):95-101. doi: 10.1089/107999002753452700. PubMed PMID: 11846980.
286. Zhang M, Wu X, Lee AJ, Jin W, Chang M, Wright A, et al. Regulation of IkappaB kinase-related kinases and antiviral responses by tumor suppressor CYLD. The Journal of biological chemistry. 2008;283(27):18621-6. doi: 10.1074/jbc.M801451200. PubMed PMID: 18467330; PubMed Central PMCID: PMC2441564.
287. Friedman CS, O'Donnell MA, Legarda-Addison D, Ng A, Cardenas WB, Yount JS, et al. The tumour suppressor CYLD is a negative regulator of RIG-I-mediated antiviral response. EMBO reports. 2008;9(9):930-6. doi: 10.1038/embor.2008.136. PubMed PMID: 18636086; PubMed Central PMCID: PMC2529351.
288. Zhang M, Wang L, Zhao X, Zhao K, Meng H, Zhao W, et al. TRAF-interacting protein (TRIP) negatively regulates IFN-beta production and antiviral response by promoting proteasomal degradation of TANK-binding kinase 1. J Exp Med. 2012;209(10):1703-11. doi: 10.1084/jem.20120024. PubMed PMID: 22945920; PubMed Central PMCID: PMC3457734.
289. Lin R, Heylbroeck C, Pitha PM, Hiscott J. Virus-dependent phosphorylation of the IRF-3 transcription factor regulates nuclear translocation, transactivation potential, and proteasome-mediated degradation. Molecular and cellular biology. 1998;18(5):2986-96. PubMed PMID: 9566918; PubMed Central PMCID: PMC110678.
290. O'Dea E, Hoffmann A. The regulatory logic of the NF-kappaB signaling system. Cold Spring Harb Perspect Biol. 2010;2(1):a000216. doi: 10.1101/cshperspect.a000216. PubMed PMID: 20182598; PubMed Central PMCID: PMC2827908.
291. Algarte M, Nguyen H, Heylbroeck C, Lin R, Hiscott J. IkappaB-mediated inhibition of virus-induced beta interferon transcription. Journal of virology. 1999;73(4):2694-702. PubMed PMID: 10074115; PubMed Central PMCID: PMC104025.
292. Rodriguez MS, Thompson J, Hay RT, Dargemont C. Nuclear retention of IkappaBalpha protects it from signal-induced degradation and inhibits nuclear factor kappaB transcriptional activation. The Journal of biological chemistry. 1999;274(13):9108-15. PubMed PMID: 10085161.
293. Huang TT, Miyamoto S. Postrepression activation of NF-kappaB requires the amino-terminal nuclear export signal specific to IkappaBalpha. Molecular and cellular biology. 2001;21(14):4737-47. doi: 10.1128/MCB.21.14.4737-4747.2001. PubMed PMID: 11416149; PubMed Central PMCID: PMC87155.
294. Arenzana-Seisdedos F, Turpin P, Rodriguez M, Thomas D, Hay RT, Virelizier JL, et al. Nuclear localization of I kappa B alpha promotes active transport of NF-kappa B from the nucleus to the cytoplasm. Journal of cell science. 1997;110 (Pt 3):369-78. PubMed PMID: 9057089.
295. Odendall C, Kagan JC. The unique regulation and functions of type III interferons in antiviral immunity. Curr Opin Virol. 2015;12:47-52. doi: 10.1016/j.coviro.2015.02.003. PubMed PMID: 25771505.
296. Odendall C, Dixit E, Stavru F, Bierne H, Franz KM, Durbin AF, et al. Diverse intracellular pathogens activate type III interferon expression from peroxisomes. Nat Immunol. 2014;15(8):717-26. doi: 10.1038/ni.2915. PubMed PMID: 24952503; PubMed Central PMCID: PMC4106986.
297. Seth RB, Sun L, Ea CK, Chen ZJ. Identification and characterization of MAVS, a mitochondrial antiviral signaling protein that activates NF-kappaB and IRF 3. Cell. 2005;122(5):669-82. doi: 10.1016/j.cell.2005.08.012. PubMed PMID: 16125763.

298. Onoguchi K, Yoneyama M, Takemura A, Akira S, Taniguchi T, Namiki H, et al. Viral infections activate types I and III interferon genes through a common mechanism. The Journal of biological chemistry. 2007;282(10):7576-81. doi: 10.1074/jbc.M608618200. PubMed PMID: 17204473.
299. Osterlund P, Veckman V, Siren J, Klucher KM, Hiscott J, Matikainen S, et al. Gene expression and antiviral activity of alpha/beta interferons and interleukin-29 in virus-infected human myeloid dendritic cells. Journal of virology. 2005;79(15):9608-17. doi: 10.1128/JVI.79.15.9608-9617.2005. PubMed PMID: 16014923; PubMed Central PMCID: PMC1181545.
300. Dumoutier L, Tounsi A, Michiels T, Sommereyns C, Kotenko SV, Renauld JC. Role of the interleukin (IL)-28 receptor tyrosine residues for antiviral and antiproliferative activity of IL-29/interferon-lambda 1: similarities with type I interferon signaling. The Journal of biological chemistry. 2004;279(31):32269-74. doi: 10.1074/jbc.M404789200. PubMed PMID: 15166220.
301. Doyle SE, Schreckhise H, Khuu-Duong K, Henderson K, Rosler R, Storey H, et al. Interleukin-29 uses a type 1 interferon-like program to promote antiviral responses in human hepatocytes. Hepatology. 2006;44(4):896-906. doi: 10.1002/hep.21312. PubMed PMID: 17006906.
302. Olagnier D, Hiscott J. Type I and type III interferon-induced immune response: it's a matter of kinetics and magnitude. Hepatology. 2014;59(4):1225-8. doi: 10.1002/hep.26959. PubMed PMID: 24677190.
303. Wang R, Nan Y, Yu Y, Zhang YJ. Porcine reproductive and respiratory syndrome virus Nsp1beta inhibits interferon-activated JAK/STAT signal transduction by inducing karyopherin-alpha1 degradation. Journal of virology. 2013;87(9):5219-28. doi: 10.1128/JVI.02643-12. PubMed PMID: 23449802; PubMed Central PMCID: PMC3624296.
304. Frieman M, Yount B, Heise M, Kopecky-Bromberg SA, Palese P, Baric RS. Severe acute respiratory syndrome coronavirus ORF6 antagonizes STAT1 function by sequestering nuclear import factors on the rough endoplasmic reticulum/Golgi membrane. Journal of virology. 2007;81(18):9812-24. doi: 10.1128/JVI.01012-07. PubMed PMID: 17596301; PubMed Central PMCID: PMC2045396.
305. Pryor MJ, Rawlinson SM, Butcher RE, Barton CL, Waterhouse TA, Vasudevan SG, et al. Nuclear localization of dengue virus nonstructural protein 5 through its importin alpha/beta-recognized nuclear localization sequences is integral to viral infection. Traffic. 2007;8(7):795-807. doi: 10.1111/j.1600-0854.2007.00579.x. PubMed PMID: 17537211.
306. Du Y, Bi J, Liu J, Liu X, Wu X, Jiang P, et al. 3Cpro of foot-and-mouth disease virus antagonizes the interferon signaling pathway by blocking STAT1/STAT2 nuclear translocation. Journal of virology. 2014;88(9):4908-20. doi: 10.1128/JVI.03668-13. PubMed PMID: 24554650; PubMed Central PMCID: PMC3993825.
307. Porter FW, Bochkov YA, Albee AJ, Wiese C, Palmenberg AC. A picornavirus protein interacts with Ran-GTPase and disrupts nucleocytoplasmic transport. Proceedings of the National Academy of Sciences of the United States of America. 2006;103(33):12417-22. doi: 10.1073/pnas.0605375103. PubMed PMID: 16888036; PubMed Central PMCID: PMC1567894.
308. Shaw ML, Cardenas WB, Zamarin D, Palese P, Basler CF. Nuclear localization of the Nipah virus W protein allows for inhibition of both virus- and toll-like receptor 3-triggered

signaling pathways. Journal of virology. 2005;79(10):6078-88. doi: 10.1128/JVI.79.10.6078-6088.2005. PubMed PMID: 15857993; PubMed Central PMCID: PMC1091709.
309. Reid SP, Valmas C, Martinez O, Sanchez FM, Basler CF. Ebola virus VP24 proteins inhibit the interaction of NPI-1 subfamily karyopherin alpha proteins with activated STAT1. Journal of virology. 2007;81(24):13469-77. doi: 10.1128/JVI.01097-07. PubMed PMID: 17928350; PubMed Central PMCID: PMC2168840.
310. Xu W, Edwards MR, Borek DM, Feagins AR, Mittal A, Alinger JB, et al. Ebola virus VP24 targets a unique NLS binding site on karyopherin alpha 5 to selectively compete with nuclear import of phosphorylated STAT1. Cell host & microbe. 2014;16(2):187-200. doi: 10.1016/j.chom.2014.07.008. PubMed PMID: 25121748; PubMed Central PMCID: PMC4188415.
311. Irie T, Yoshida A, Sakaguchi T. Clustered basic amino acids of the small sendai virus C protein Y1 are critical to its RAN GTPase-mediated nuclear localization. PloS one. 2013;8(8):e73740. doi: 10.1371/journal.pone.0073740. PubMed PMID: 23951363; PubMed Central PMCID: PMC3739745.
312. Fontoura BM, Blobel G, Matunis MJ. A conserved biogenesis pathway for nucleoporins: proteolytic processing of a 186-kilodalton precursor generates Nup98 and the novel nucleoporin, Nup96. The Journal of cell biology. 1999;144(6):1097-112. PubMed PMID: 10087256; PubMed Central PMCID: PMC2150585.
313. Enninga J, Levy DE, Blobel G, Fontoura BM. Role of nucleoporin induction in releasing an mRNA nuclear export block. Science. 2002;295(5559):1523-5. doi: 10.1126/science.1067861. PubMed PMID: 11809937.
314. Faria AM, Levay A, Wang Y, Kamphorst AO, Rosa ML, Nussenzveig DR, et al. The nucleoporin Nup96 is required for proper expression of interferon-regulated proteins and functions. Immunity. 2006;24(3):295-304. doi: 10.1016/j.immuni.2006.01.014. PubMed PMID: 16546098.
315. Baril M, Racine ME, Penin F, Lamarre D. MAVS dimer is a crucial signaling component of innate immunity and the target of hepatitis C virus NS3/4A protease. Journal of virology. 2009;83(3):1299-311. Epub 2008/11/28. doi: 10.1128/JVI.01659-08. PubMed PMID: 19036819; PubMed Central PMCID: PMC2620913.
316. Li K, Foy E, Ferreon JC, Nakamura M, Ferreon AC, Ikeda M, et al. Immune evasion by hepatitis C virus NS3/4A protease-mediated cleavage of the Toll-like receptor 3 adaptor protein TRIF. Proceedings of the National Academy of Sciences of the United States of America. 2005;102(8):2992-7. doi: 10.1073/pnas.0408824102. PubMed PMID: 15710891; PubMed Central PMCID: PMC548795.
317. Tamassia N, Le Moigne V, Rossato M, Donini M, McCartney S, Calzetti F, et al. Activation of an immunoregulatory and antiviral gene expression program in poly(I:C)-transfected human neutrophils. Journal of immunology. 2008;181(9):6563-73. PubMed PMID: 18941247.
318. Fensterl V, Sen GC. The ISG56/IFIT1 gene family. J Interferon Cytokine Res. 2011;31(1):71-8. doi: 10.1089/jir.2010.0101. PubMed PMID: 20950130; PubMed Central PMCID: PMC3021354.
319. Schoenenberger CA, Buchmeier S, Boerries M, Sutterlin R, Aebi U, Jockusch BM. Conformation-specific antibodies reveal distinct actin structures in the nucleus and the cytoplasm. J Struct Biol. 2005;152(3):157-68. doi: 10.1016/j.jsb.2005.09.003. PubMed PMID: 16297639.

320. Theiss AL, Jenkins AK, Okoro NI, Klapproth JM, Merlin D, Sitaraman SV. Prohibitin inhibits tumor necrosis factor alpha-induced nuclear factor-kappa B nuclear translocation via the novel mechanism of decreasing importin alpha3 expression. Molecular biology of the cell. 2009;20(20):4412-23. doi: 10.1091/mbc.E09-05-0361. PubMed PMID: 19710421; PubMed Central PMCID: PMC2762146.
321. Agrawal T, Gupta GK, Agrawal DK. Calcitriol decreases expression of importin alpha3 and attenuates RelA translocation in human bronchial smooth muscle cells. Journal of clinical immunology. 2012;32(5):1093-103. doi: 10.1007/s10875-012-9696-x. PubMed PMID: 22526597; PubMed Central PMCID: PMC3444658.
322. Perez M, Soler-Torronteras R, Collado JA, Limones CG, Hellsten R, Johansson M, et al. The fungal metabolite galiellalactone interferes with the nuclear import of NF-kappaB and inhibits HIV-1 replication. Chem Biol Interact. 2014;214:69-76. doi: 10.1016/j.cbi.2014.02.012. PubMed PMID: 24631022.
323. Taylor SL, Frias-Staheli N, Garcia-Sastre A, Schmaljohn CS. Hantaan virus nucleocapsid protein binds to importin alpha proteins and inhibits tumor necrosis factor alpha-induced activation of nuclear factor kappa B. Journal of virology. 2009;83(3):1271-9. doi: 10.1128/JVI.00986-08. PubMed PMID: 19019947; PubMed Central PMCID: PMC2620888.
324. Fagerlund R, Kinnunen L, Kohler M, Julkunen I, Melen K. NF-{kappa}B is transported into the nucleus by importin {alpha}3 and importin {alpha}4. The Journal of biological chemistry. 2005;280(16):15942-51. doi: 10.1074/jbc.M500814200. PubMed PMID: 15677444.
325. Liang P, Zhang H, Wang G, Li S, Cong S, Luo Y, et al. KPNB1, XPO7 and IPO8 mediate the translocation ofNF-kappaB/p65 into the nucleus. Traffic. 2013;14(11):1132-43. doi: 10.1111/tra.12097. PubMed PMID: 23906023.
326. Cunningham MD, Cleaveland J, Nadler SG. An intracellular targeted NLS peptide inhibitor of karyopherin alpha:NF-kappa B interactions. Biochemical and biophysical research communications. 2003;300(2):403-7. PubMed PMID: 12504098.
327. Ao Z, Huang G, Yao H, Xu Z, Labine M, Cochrane AW, et al. Interaction of human immunodeficiency virus type 1 integrase with cellular nuclear import receptor importin 7 and its impact on viral replication. The Journal of biological chemistry. 2007;282(18):13456-67. doi: 10.1074/jbc.M610546200. PubMed PMID: 17360709.
328. Kumar KP, McBride KM, Weaver BK, Dingwall C, Reich NC. Regulated nuclear-cytoplasmic localization of interferon regulatory factor 3, a subunit of double-stranded RNA-activated factor 1. Molecular and cellular biology. 2000;20(11):4159-68. PubMed PMID: 10805757; PubMed Central PMCID: PMC85785.
329. Tam WF, Lee LH, Davis L, Sen R. Cytoplasmic sequestration of rel proteins by IkappaBalpha requires CRM1-dependent nuclear export. Molecular and cellular biology. 2000;20(6):2269-84. PubMed PMID: 10688673; PubMed Central PMCID: PMC110843.
330. Scott ML, Fujita T, Liou HC, Nolan GP, Baltimore D. The p65 subunit of NF-kappa B regulates I kappa B by two distinct mechanisms. Genes & development. 1993;7(7A):1266-76. PubMed PMID: 8319912.
331. Chiao PJ, Miyamoto S, Verma IM. Autoregulation of I kappa B alpha activity. Proceedings of the National Academy of Sciences of the United States of America. 1994;91(1):28-32. PubMed PMID: 8278379; PubMed Central PMCID: PMC42879.
332. Saccani S, Marazzi I, Beg AA, Natoli G. Degradation of promoter-bound p65/RelA is essential for the prompt termination of the nuclear factor kappaB response. J Exp Med.

2004;200(1):107-13. doi: 10.1084/jem.20040196. PubMed PMID: 15226358; PubMed Central PMCID: PMC2213320.
333. Johnson C, Van Antwerp D, Hope TJ. An N-terminal nuclear export signal is required for the nucleocytoplasmic shuttling of IkappaBalpha. The EMBO journal. 1999;18(23):6682-93. doi: 10.1093/emboj/18.23.6682. PubMed PMID: 10581242; PubMed Central PMCID: PMC1171731.
334. Li Y, Li C, Xue P, Zhong B, Mao AP, Ran Y, et al. ISG56 is a negative-feedback regulator of virus-triggered signaling and cellular antiviral response. Proceedings of the National Academy of Sciences of the United States of America. 2009;106(19):7945-50. doi: 10.1073/pnas.0900818106. PubMed PMID: 19416887; PubMed Central PMCID: PMC2683125.
335. Zhou X, Michal JJ, Zhang L, Ding B, Lunney JK, Liu B, et al. Interferon induced IFIT family genes in host antiviral defense. Int J Biol Sci. 2013;9(2):200-8. doi: 10.7150/ijbs.5613. PubMed PMID: 23459883; PubMed Central PMCID: PMC3584916.
336. Baril M, Es-Saad S, Chatel-Chaix L, Fink K, Pham T, Raymond VA, et al. Genome-wide RNAi screen reveals a new role of a WNT/CTNNB1 signaling pathway as negative regulator of virus-induced innate immune responses. PLoS pathogens. 2013;9(6):e1003416. doi: 10.1371/journal.ppat.1003416. PubMed PMID: 23785285; PubMed Central PMCID: PMC3681753.
337. Ori A, Banterle N, Iskar M, Andres-Pons A, Escher C, Khanh Bui H, et al. Cell type-specific nuclear pores: a case in point for context-dependent stoichiometry of molecular machines. Mol Syst Biol. 2013;9:648. doi: 10.1038/msb.2013.4. PubMed PMID: 23511206; PubMed Central PMCID: PMC3619942.
338. Culjkovic-Kraljacic B, Baguet A, Volpon L, Amri A, Borden KL. The oncogene eIF4E reprograms the nuclear pore complex to promote mRNA export and oncogenic transformation. Cell Rep. 2012;2(2):207-15. doi: 10.1016/j.celrep.2012.07.007. PubMed PMID: 22902403; PubMed Central PMCID: PMC3463940.

Annex 1: Elucidating novel hepatitis C virus-host interactions using combined mass spectrometry and functional genomics approaches.

This annex is to state that I contributed to the paper "**Elucidating novel hepatitis C virus-host interactions using combined mass spectrometry and functional genomics approaches."** by Germain et al., published in the peer-review journal "Molecular & Cellular Proteomics" in 2014. As second co-author, I performed the experiments and contributed to the explanation for the results shown in Figure 9 and Figure S4.